A BIOPHYSICAL STUDY OF THE PLANT CELL MEMBRANE

By

IVÁN ORTEGA BLAKE, B.Sc., M.Sc.

A Thesis presented for the degree of Doctor of Philosophy of the University of Edinburgh in the Faculty of Science.

MARCH, 1978.

ABSTRACT

The current theories of the membrane electrical properties of the giant algal cells of the Characeae are reviewed. The experimental techniques for the determination of such properties are discussed and a comparison between these techniques, for both the D.C. and A.C. case, are made. In the latter case it was necessary to obtain the time dependent solution of the A.C. cable theory and the numerical behaviour of this solution. From this comparison it is proposed that symmetric external current injection together with the 0.42L technique is a very suitable method for these studies.

Using this method the membrane electric parameters of Nitella translucens were determined. The effects of external pH, 2, 4-dinitrophenol and A.C. of different frequencies on these parameters were studied. The effects of external pH and the presence of DNP on the vacuolar pH were also determined.

It was found that the experimental observations favoured the Spanswick theory for the Characean membrane electric properties, but modified to account for the membrane resistance being pH independent. The observed effects of DNP favoured the mechanism for the action of DNP proposed by Duncan and Croghan. The observed A.C. frequency dependence of the membrane resistance and experiments on the punch-through effect are inconsistent with the Coster double fixed charge model of membrane structure.

C O N T E N T S

C O N T E N T S (Contd.)

C O N T E N T S (Contd.)

CHAPTER I

INTRODUCTION

It is well established that the internal ionic composition of any biological cell is quite different from that of its environment and that there is a continuous flow of these ions between the two phases. Most cell biophysicists consider that it is the cell membrane which rate-limits this ionic transport. This thesis is concerned with some aspects of the ionic transport in the giant algal cells of the Characeae. Ionic transport will occur by means of simple or complex diffusion processes. It is therefore necessary to begin by considering the physical basis of these processes.

1.1 Diffusion Processes

a) The Nernst-Planck Equation

In any diffusion process a convenient thermodynamic function to consider is the Gibbs free energy. The change in this energy function occurring during the process can be expressed as:

$$dG = ((\bar{\mu}_j)_i - (\bar{\mu}_j)_o)dn_j \qquad (1.1)$$

where $\bar{\mu}_j$ is the electrochemical potential, o and i denote the two sides of the diffusion barrier and dn_j is the mumber of moles of the jth component diffusing across the interphase.

If μ_j changes continuously from region o to region i, equation (1.1) can be expressed as:

$$\frac{dG}{dn_j} = \int_o^i \frac{\partial \mu_j}{\partial x} dx$$

which can be identified as an energy change $\int -Xdx$ produced by the action of the force X, where $X = -\frac{\partial \mu_j}{\partial x}$, the electrochemical potential gradient.

In general the system will contain m diffusing constituents and the flux (in mol. cm^{-2} s^{-1}) for each component will be given by the Onsager equations:

$$J_j = L_{ij} X_i + \ldots + L_{mj} X_m \quad .$$

The terms $L_{ij} X_i$ for $i = j$ represent the flux of the ion produced by its own electrochemical gradient. The terms $L_{ij} X_i$ for $i \neq j$ represent the flux of the ion j produced by the electrochemical gradient of ion i. It is usually assumed that cross-coupling coefficients, L_{ij} for $i \neq j$, are near zero. Schwartz (1) shows that such an approximation is valid only in dilute solutions.

Using the above assumption the velocity of the ion will be proportional to its driving force and is given by:

$$\nu_i = -u_i \frac{\partial \bar{\mu}_i}{\partial x}$$

where the proportionality constant u_i is the ion mobility. If C_i is the concentration in moles per unit volume then the flux will be given by:

$$J_i = -u_i C_i \frac{\partial \bar{\mu}_i}{\partial x} \qquad (1.2)$$

An expression for the electrochemical potential can be obtained from thermodynamic considerations, e.g. Plonsey (2), and it is

$$\bar{\mu}_i = \mu_i^o(P,T) + RT\ \ell n(a_i) + z_i F\phi \qquad (1.3)$$

where μ_i^o is the chemical potential in a reference state at pressure P and temperature T, R is the gas constant, a_i is the ion activity, z_i is the valency of the ion, F is the Faraday constant and ϕ the electrical potential. The activity a_i is expressed as $\gamma_i C_i$ where γ_i is the activity coefficient. If it is assumed that $\gamma_i = 1$ substitution of equation (1.3) in equation (1.2) gives

$$J_i = -D_i\left(\frac{\partial C_i}{\partial x} + \frac{z_i C_i F}{RT}\ \frac{\partial \phi}{\partial x}\right) \qquad (1.4)$$

where $D_i = \dfrac{u_i RT}{(z_i)F}$ is the diffusion constant. This is known as the Nernst-Planck equation. Plonsey (2) shows that a more rigorous expression for the flux, i.e. with $\gamma \neq 1$, will have the same form as equation (1.4) but the diffusion coefficient will now be given by

$$D_i = \frac{u_i RT}{|z_i|F}\left[1 + \frac{\partial \ell n \gamma_i}{\partial x} \Big/ \frac{\partial \ell n C_i}{\partial x}\right]$$

He also presents a Debye-Huckel analysis which indicates that the assumption of $\gamma_i = 1$ is only valid for dilute solutions.

b) Simple Solutions of the Nernst-Planck Equation

The simplest diffusion process that can occur is the free movement of ions through a liquid interphase in which there are variations of ionic composition or concentration. The ions can diffuse freely in such a region but they have to satisfy the condition of electroneutrality, i.e. there must be no charge separation in a solution volume, except of microscopic dimensions. Thus

$$\Sigma C_k z_k = \Sigma C_a |z_a| \tag{1.5}$$

where a and k denotes anion and cation. Plonsey (2), showed that in the range of biological concentrations electroneutrality has to be maintained in volumes larger than that of a sphere of 8 Å diameter. He concluded that in spite of the approximations in the computation electroneutrality can be assumed in the 100 Å thick biological membranes.

Using equation (1.4) and equation (1.5) together with the condition that in free diffusion no net charge transfer can occur, i.e. $z_k F J_k = |z_a| F J_a$, the following equation is obtained:

$$\frac{\partial \phi}{\partial x} = \frac{u_k - u_a}{u_k z_k + u_a |z_a|} \frac{RT}{F} \frac{\partial \ell n C_s}{\partial x} \tag{1.6}$$

where C_s is the salt concentration. Equation (1.6) can be integrated to give the potential across the interphase if it is assumed that the mobilities are independent of x. In the general case, where more than one salt is diffusing across the interphase, equation (1.6) can be integrated with the additional

condition of a linear variation of concentration, i.e. $C_i = (C_i)_i + ((C_i)_o - (C_i)_i)x/d$, where d is the thickness of the interphase. This is called the Henderson integration and the resulting equation is:

$$\phi = \frac{RT}{F} \sum_j \frac{(u_j/z_j)((C_j)_p - (C_j)_i)}{\Sigma u_j((C_j)_o - (C_j)_i)} \ln \sum \frac{(C_j)_i u_j}{(C_j)_o u_j} .$$

In Chapter IV this equation is applied to the liquid interphase occurring at the tip of a glass microelectrode and some of its consequences are discussed. Free diffusion is a transient phenomenon which will reach equilibrium when both regions have the same concentration. However, if there were a selective membrane at the interphase the system could reach equilibrium with different salt concentrations at each region. For instance:

$$(NaCl)_o \quad \Big| \quad (NaCl)_o + NaP$$

where NaP is a sodium proteinate and P^{-n} is a protein of valency n to which the membrane is impermeable. When such a system is in equilibrium all ionic fluxes must be zero. Integration of the Nernst-Planck equation under these conditions and with the assumption that $(\partial u/\partial x) = 0$ yields:

$$\phi = \frac{RT}{F} \ln \frac{(C_{Na^+})_i}{(C_{Na^+})_o} = \frac{RT}{F} \ln \frac{(C_{Cl^-})_o}{(C_{Cl^-})_i} . \qquad (1.7)$$

Applying the electroneutrality condition to regions i and o gives

$$\phi = \frac{-RT}{F} \ln \frac{nP^{-n} + \left[n(P^{-n})^2 + 4(C_{Na^+})_i^2\right]}{2(C_{Na^+})_o} .$$

A system which satisfies equation (1.7) is said to be in a Donnan equilibrium. Such a system is not usually representative of biological membranes, though Donnan potentials are sometimes assumed to exist between the membrane and the adjacent solution.

A less severe restriction than that of assuming all the ion fluxes to be zero is to assume that only some of the ion fluxes are zero. In this case the potential across the membrane is given by:

$$\phi = \frac{RT}{zF} \ln \frac{(C_i)_i}{(C_i)_o} \quad .$$

This is the Nernst equation and will be satisfied by any ionic species for which $J_i = 0$; such ions are said to be at their Nernst equilibrium potential.

In most cases the potential across a biological membrane does not correspond to the Nernst potential of any of the ions present. The Nernst-Planck equation has then to be solved with even less severe restrictions.

1.2 Physical Membrane Models

Membrane models will differ according to the physical properties which are assigned to them. However, all models will share the following features:

1) the membrane is of constant thickness, homogeneous and infinite in extent in the transverse plane;
2) the cross-coupled coefficients in the Onsager equations are negligible;
3) the solutions on both sides of the membrane are uniform

and large in extent so that changes in ionic concentration due to the transit of permeable ions can be ignored;

4) there is no net flow of solvent and ion transport due to convection is negligible.

If it is also assumed that:

5) the membrane is neutral;

6) the ion mobilities are the same within and without the membrane;

7) the activity coefficient γ is unity,

then the resulting model represents a porous membrane, such as cellophane, in dilute solutions. This model is known as the Planck membrane.

a) The Planck Membrane

The Planck membrane model has not been particularly successful when applied to biological systems and this is undoubtedly due to its very restrictive assumptions. It is however the basis for other models which are more relevant to the biological situation and it is therefore convenient to outline its solution.

The Nernst-Planck equation can be solved using the following conditions:

a) the membrane is in the steady state, i.e.

$$\frac{\partial J_i}{\partial x} = 0 \quad \text{for all} \quad J_i \tag{1.8}$$

b) there is electroneutrality inside the membrane, i.e.

$$\Sigma z_i C_i^+ = \Sigma |z_i| C_i^- \tag{1.9}$$

c) there is no net current flowing, i.e.,

$$\Sigma z_i F J_i^+ + \Sigma z_i F J_i^- = 0 \quad . \tag{1.10}$$

The exact solution for the Planck membrane for univalent ions shows (see Plonsey (2)) that the total ionic concentration varies linearly within the membrane and the electric field is logarithmic. The solution is:

$$\frac{\zeta U_i - U_o}{W_i - \zeta W_o} = \frac{\ell n(C_o/C_i) - \ell n(\zeta) C_o - C_i}{\ell n(C_o/C_i) + \ell n(\zeta) C_o - C_i}$$

where C is the total concentration, $U = \Sigma u_i^+ C_i^+$, $W = \Sigma u_i^- C_i^-$ and $\zeta = e^{(FE/RT)}$ where E is the membrane potential. This is a very complicated transcendental equation which has to be solved by iterative procedures. An approximated solution can be obtained, without invoking condition (1.10), if the following identity is satisfied:

$$\frac{C_o - C_i}{C_i} = \delta << 1 \; .$$

In this case the potential within the membrane is given by:

$$\phi(x) = \phi(i) + \frac{E}{\ell n(1+\delta)} \ell n(1 + \frac{\delta}{d} x)$$

where d is the width of the membrane. If the first term only of a Taylor expansion of the logarithm is taken, $\phi(x)$ has the following form:

$$\phi(x) = \phi_i + \frac{E \cdot x}{d} \tag{1.11}$$

In other words, if the total ionic concentrations are nearly equal on both sides of a Planck membrane a constant field will exist across the membrane. This is valid even if

a net current flows through the membrane.

An alternative approach would be to make the arbitrary assumption of a constant field in which case the integration of the Nernst-Planck equations is particularly straightforward. This approach is the basis of the Goldman membrane model.

b) The Goldman Membrane

The Goldman equations are obtained by making use of assumptions (6) and (7). When the concentrations C_i and C_o are equal, assumption (5) can also be made and the Goldman membrane will be simply a particular case of the Planck membrane. However if $C_i \neq C_o$ then the assumption of a linear potential is inconsistent with that of a neutral membrane in which the field is logarithmic. Moreover, as Hogg (3) showed, the electroneutrality condition, as defined by equation (1.9), can only be satisfied when the constant field assumption is made if $C_i \simeq C_o$. Since electroneutrality has to be maintained, equation (1.9) would have to be modified to include an extra charge term for the case of constant field and $C_i \neq C_o$. It is not usually realized that in this case the Goldman equations imply a charged membrane.

The Nernst-Planck equation can be written as:

$$\frac{J_i}{u_i} e^{(Z_i F/RT)\phi} = - RT \frac{\partial}{\partial x} (\overline{C}_i e^{(Z_i F/RT)\phi})$$

where $\overline{C}_i$ indicates the ion concentration inside the membrane. Using the steady state condition this equation can be solved to give:

$$J_i = - RT \frac{\left[(\bar{C}_i)_o e^{(Z_i F/RT)\Delta\phi} - (\bar{C}_i)_i\right]}{e^{(Z_i F/RT)\phi_i} \int_i^o \frac{1}{u_i} e^{(Z_i F/RT)\phi} dx} \qquad (1.12)$$

If the assumptions of a constant field and constant ion mobilities are made, the integration can be performed and equation (1.12) yields the well known Goldman flux equation:

$$J_i = \frac{Z_i u_i FE}{d} \left(\frac{(\bar{C}_i)_o e^{(Z_i F/RT)E} - (\bar{C}_i)_i}{1 - e^{-(Z_i F/RT)E}} \right) \qquad (1.13)$$

This equation, however, involves the ionic concentrations inside the membrane, which are not known. To overcome this problem Hodgkin and Katz (4) assumed that the internal concentrations were proportional to the external concentrations, i.e. $\bar{C}_i = {}^{\beta}C_i$, where β is called the partition coefficient. They also defined the permeability coefficients P_i as

$$P_i = \frac{u_i \beta_i RT}{d} \qquad (1.14)$$

Equation (1.13) can then be written as:

$$J_i = \frac{Z_i P_i FE}{RT} \left[\frac{(C_i)_o e^{-(Z_i FE/RT)} - (C_i)_i}{1 - e^{-(Z_i FE/RT)}} \right] \qquad (1.15)$$

If the condition of no net current is used an expression for E is obtained

$$E = \frac{RT}{F} \left[\frac{\Sigma P_k (C_k)_o + \Sigma P_a (C_a)_i}{\Sigma P_k (C_k)_i + \Sigma P_a (C_a)_o} \right] \qquad (1.16)$$

This is the Goldman potential equation. The equation has been used extensively in electrophysiological studies and is frequently identified with the constant field assumption. However, it has been pointed out that the assumption of other forms for the electric field will lead to the same equation. This was done in the following way by Schwartz (1).

Writing $\phi' = \phi - \frac{(\phi_o - \phi_i)}{2}$ the following expressions are obtained

$$\phi - \phi_i = \frac{\Delta\phi}{2} + \phi'$$

and

$$\phi_o - \phi = \frac{\Delta\phi}{2} - \phi' \quad .$$

If these expressions are substituted into equation (1.12) the flux equations for cations, J_k, and anions, J_a, have the following form

$$J_k = RT \left[\frac{(\bar{C}_k)_o \, e^{(F/RT)\Delta\phi} - (\bar{C}_k)_i}{Q_k} \right]$$

$$J_a = RT \left[\frac{(\bar{C}_a)_o - (\bar{C}_a)_i \, e^{(F/RT)\Delta\phi}}{Q_a} \right]$$

where $Q_k = \frac{1}{u_k} e^{(F/2RT)\Delta\phi} \int_i^o e^{(F/RT)\phi'} dx = \frac{1}{u_k} e^{(F/2RT)\Delta\phi} N_+$

$$Q_a = \frac{1}{u_a} e^{(F/2RT)} \int_i^o e^{-(F/RT)\phi'} dx = \frac{1}{u_a} e^{(F/2RT)\Delta\phi} N_-$$

If the condition of no net current flow is now used the membrane potential is given by

$$E = RT \ln \left[\frac{(1/N_+)\Sigma u_k (\bar{C}_k)_i + (1/N_-)\Sigma u_a (\bar{C}_a)_o}{(1/N_+)\Sigma u_k (\bar{C}_k)_o + (1/N_-)\Sigma u_a (\bar{C}_a)_i} \right] \qquad (1.17)$$

From this equation it can be seen that the Goldman potential equation will be obtained, without any assumption about the membrane field, if the membrane is permeable only to ions of the same charge. A particular form of equation (1.17), when the only ions involved are K^+ and Na^+, is called the Hodgkin-Katz equation.

The Goldman equation will also be obtained if $N_+ = N_-$, i.e. if the following identity is satisfied:

$$\int_i^o \left[e^{(F/RT)\phi'} - e^{(F/RT)\phi'} \right] dx = 0 \quad .$$

Thus

$$\int_i^o \sinh((F/RT)\phi')dx = 0 \qquad (1.18)$$

is the only constraint on the electric field. A large group of functions $\phi(x)$ satisfy equation (1.18), including the functions having odd symmetry about the midplane through the membrane; a constant field is just one of such functions. The same conclusion was reached by Hogg (3) from a kinetic treatment of ion transport across the membrane.

Yet another approach to the solution of the Nernst-Planck equation is to use empirical methods to determine the integrals N_+ and N_- in equation (1.17); this was the approach of Kimizuka and Koketzu (5).

c) The Kimizuka and Koketzu Membrane

From equation (1.12) Kimizuka and Koketzu defined their permeability coefficients to be

$$\frac{1}{P_\alpha'} = e^{-(Z_\alpha/2RT)E} \int_i^o \frac{1}{D_\alpha} e^{(Z_\alpha F/FT) + (\eta_\alpha/RT)} dx \qquad (1.19)$$

where D_α is the diffusion coefficient and the extra energy term η_α is included to account for any excess free energy, e.g. the partition energy. There is no necessity to define D_α since the integration is not performed. Thus assumptions (6) and (7) are not used and this is particularly convenient since the assumption that mobilities are independent of x is not trivial and is probably invalid in most biological membranes.

Integration of equation (1.19) with the assumption of constant field, constant D_α, and constant η_α gives a relation between the Hodgkin-Katz and Kimizuka-Koketzu permeability coefficients:

$$P_\alpha' = P_\alpha \frac{Z_\alpha FE/2RT}{\sinh(Z_\alpha FE/2RT)} \qquad (1.20)$$

where the Hodgkin-Katz partition coefficients have been identified with $\exp(-\eta_\alpha/RT)$.

Equation (1.20) was obtained with the assumptions of constant field, constant D_α and constant η_α. In this case the Hodgkin-Katz and Kimizuka-Koketzu permeabilities should be identical and this will only occur if $(Z_\alpha FE/2RT)^2 << 1$. It is interesting to mention that Hogg (3) found from kinetic considerations that a similar condition $\pm(Z_\alpha FE/nRT) << 1$, where n is the number of jumping

processes] must be satisfied for the assumption of a constant field to be valid.

Equation (1.20) can also be obtained simply as the ratio between the Goldman flux equation (1.15) and the Kimisuka-Koketzu flux equation

$$J_\alpha = P_\alpha'((C_\alpha)_o e^{-(FE/2RT)} - (C_\alpha)_i e^{(FE/2RT)}) \qquad (1.20)$$

Equation (1.20) can therefore be used for computing the Kimizuka-Koketzu permeabilities from the values of the Hodgkin-Katz permeabilities without making any assumptions about the nature of the field, the diffusion coefficient D_α or the extra energy term η_α.

By invoking the zero net current condition and assuming the permeable ions to be univalent an expression for the membrane potential can be obtained from equation (1.21). The resulting expression has the same form as the Goldman potential equation but the permeability coefficients are now P_α'. However substitution of (1.21) into this expression gives the Goldman potential equation. Thus the Goldman equation can be obtained without the assumption of a constant diffusion coefficient and with no assumption whatsoever about the form of the membrane field, providing the permeable ions are univalent.

It has been stated that the assumption of constant ionic mobilities and a membrane field which is other than logarithmic when $C_i \neq C_o$ implies a charged membrane. The assumption of a charged membrane in biological systems is a valid one since complex proteins and lipoids can present groups with fixed charges and it is worthwhile considering such models.

d) Fixed Charge Membranes

Fixed charge membranes can be dealt with in a similar way to the Planck membranes, e.g. Plonsey (2). The electroneutrality condition is now expressed as $\Sigma Z_i C_i + Z_q q$ where q is the concentration of the fixed charge and Z_q is its valency. Without going into detail let it be said that the solutions of the Nernst-Planck equations in this case are semi-empirical but the empirical parameters, varied to fit the experiments, can be identified with microscopic membrane properties. They do not include partition coefficients and the ions are in Donnan equilibrium across the membrane boundaries. A fixed charge membrane model which is relevant to the present work has been proposed by Coster (6) and it will be discussed in a later section.

1.3 The Predictions of the Membrane Models

Due to its complexity the equation corresponding to the Planck membrane has seldom been used. On the other hand, the Goldman potential equation has been extensively used in the description of the membrane potential. It can be said that the Goldman potential equation has been, in general, successful. This is not surprising, despite the severity of the constant field assumption, since it has been shown that the equation is quite general for univalent ions. The equation does not depend on the form of the field, the form of the mobilities inside the membrane and it can even account for partition energy contributions. This is a consequence of the experimental determination of the permeability coefficients.

Unfortunately this is not commonly realized and the success of the Goldman equation is usually taken as an indication of the validity of the constant field approximation.

The assumption of a constant field is, however, an absolute requirement for the derivation of both the Goldman flux equation and the expression for the membrane conductance. The membrane conductance G_m is defined as

$$G_m = d(\Sigma zFJ_i)/dE$$

and its expression is characteristic of each membrane model. For instance, for the Goldman membrane (Hope and Walker (7)) G_m is given by:

$$G_m = \frac{F^2}{RT^2} \frac{AB}{A-B} \ell n \frac{A}{B} \qquad (1.22)$$

where $A = P_K(K)_o + P_{Na}(Na)_o + P_{C\ell}(C\ell)_i$

and $B = P_K(K)_i + P_{Na}(Na)_i + P_{C\ell}(C\ell)_o$

whereas for the Kimizuka-Koketzu membrane (Duncan and Croghan, (8)) the conductance is:

$$G_m = \frac{F^2}{RT} \sqrt{A'B'} \qquad (1.23)$$

where A' and B' are given in terms of the Kimizuka-Koketzu permeabilities.

Equations (1.22) and (1.23) are only valid near the resting state of the membrane. In general the conductances are functions of the membrane potential so they will exhibit electric rectification. Hope (9) compared the rectification curves predicted by the Planck membrane and the Goldman membrane. He found that the experimental results for Chara cells were better fitted to the Goldman curve though both models predicted

the same conductances for the resting state. Duncan and Croghan (8) compared the resting conductances predicted by the Goldman and the Kimizuka and Koketzu membranes with the experimental values obtained for toad lens membranes. Their results show a better agreement with the second model.

When biological membranes are displaced far away from their resting state several rectification effects are observed, some of which cannot be explained by the simple dependence of G_m on E, e.g. the action potential of excitable membranes. In this case there is the need to postulate empirical membrane mechanisms. In the giant algae cells of the Characeae a wide variety of anomalous responses have been observed, and a consequent profusion of empirical models have arisen. This work is concerned with the studies of such responses and some of the models proposed are now described.

1.4 Empirical Models for the Characeae

The responses of Nitella translucens to the application of current are shown in Figure 1.1. There are four types of responses: rectification near the resting state; the action potential for depolarizing currents; a transient response to large hyperpolarizing currents and an action potential resulting from the switching off of the large hyperpolarizing currents (anode break excitation). A model in which the membrane properties are considered to arise exclusively from passive diffusional processes was advanced to explain the first two types of response (Hope (9) and Hope and Walker (10)).

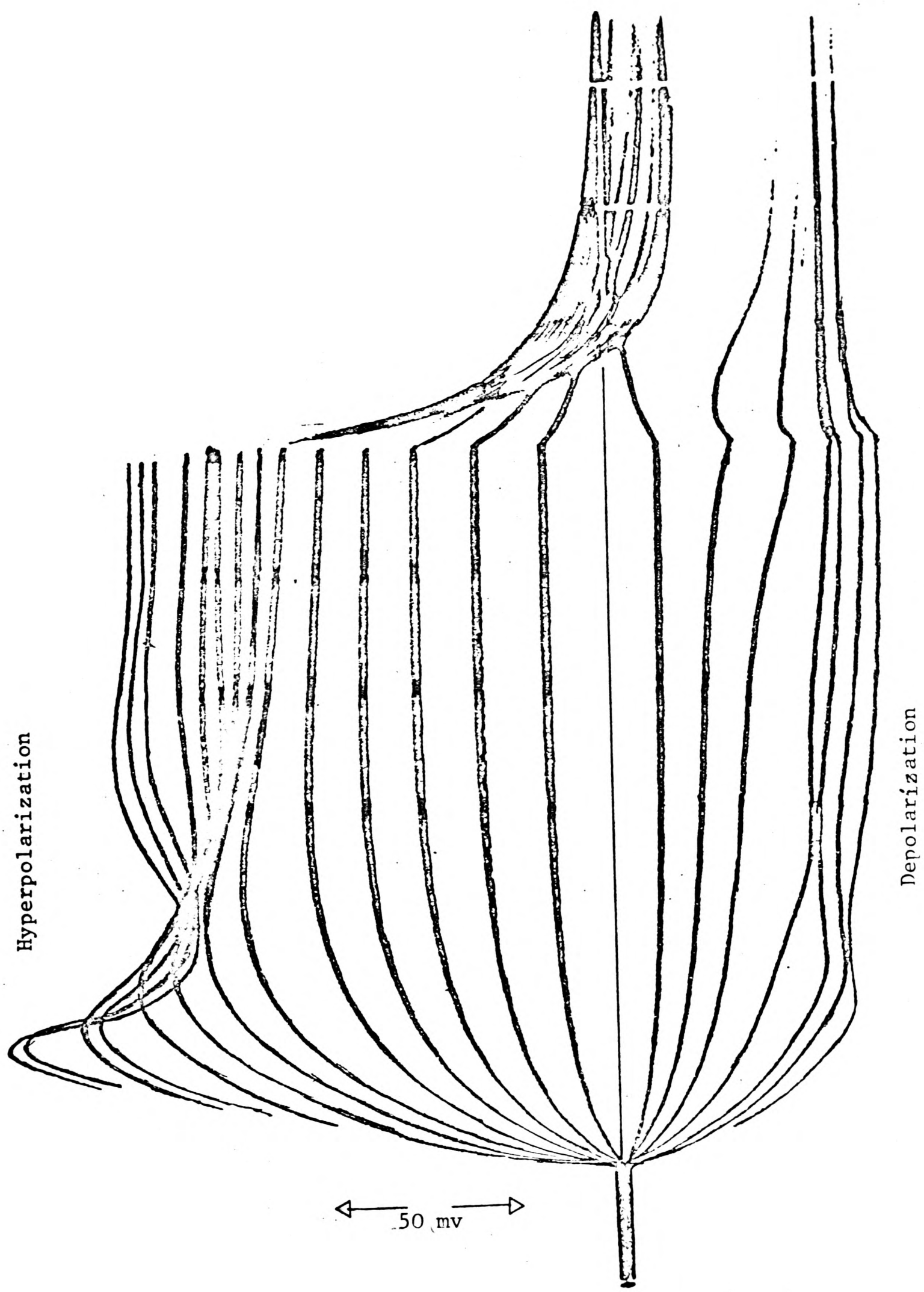

Fig. 1.1 The voltage response to current pulses of fixed duration (·5 sec) and of equal increments of ·5μA/cm starting at ·5μA/cm .

a) The passive diffusion model

In this model the membrane potential and conductance were explained in terms of the passive diffusion of K^+ and Na^+ in the resting state and of the passive diffusion of $C\ell^-$ and K^+ in the excited state. However it was observed that the resting state, particularly in the case of Nitella translucens (Spanswick, Stolarek and Williams (11)), could be described by the Hodgkin-Katz equation only after the cells had been presoaked for long periods in $NaC\ell$ and if the experiments were carried out in calcium-free solutions. In the presence of calcium the excursions of the resting potential in response to changes in the Na^+, K^+ and Ca^{++} concentrations could not be fitted to a Goldman-type potential equation involving these three ions. It was proposed that the principal effects of calcium were associated with the cell wall. However the presence of calcium is necessary for the initiation of an action potential (Hope, (12)). This led Findlay and Hope (13) to propose that the action potential was due to a passive Ca^{++} influx and a passive K^+ efflux, though earlier Gaffey and Mullins (14) had proposed that the phenomena was due to the passive efflux of $C\ell^-$ followed by K^+. This is now generally accepted. The role of Ca^{++} in the action potential has therefore to be explained by a mechanism other than that of simple diffusion.

The biggest cause for concern was the finding that the directly measured membrane conductance (G_e) was larger by an order of magnitude than G_f, the conductance predicted from the passive influxes of Na^+ and K^+ (MacRobbie (15), and Williams, Johnston and Dainty (16)). The basis for the calculation of the membrane conductance from these ionic fluxes is the Ussing-Teorell equation:

$$RT \ \ell n((J_i)_{in}/(J_j)_{out}) = (\bar{\mu}_j)_o - (\bar{\mu}_j)_i$$

which is valid for passive, independent ion transport.

This equation can be differentiated and rearranged to give an expression for the conductance:

$$G_m = \frac{F^2}{RT} \sum_j z_j^2 (J_j)_{in} - \sum_j (J_j^o) \frac{\Delta \ell n (J_j)_{out}}{\Delta E} \qquad (1.24)$$

where (J_j^o) is the flux of ion j in the resting state. If ions of the same sign only are permeable and the total current is zero in the resting state, the second term in (1.24) vanishes (Hogg, Williams and Johnston, (17)) and this is what was assumed in the attempt to correlate the two values of resistance. The observed lack of correlation could arise from (a) coupled ion transport, (b) an extra passive ionic flux or (c) a net current in the resting state. One form of coupled ion transport involves a single file of ions (Hodgkin and Keynes, (18)). In the case of Nitella the number of ions in the file would have to be at least ten and this seems inconceivable.

The possibility of an extra passive flux being overlooked in equation (1.24) was explored by Kitasato (19) who focussed his attention on the known effects of pH in the membrane potential of the Characeae, (Kishimoto, (20)). As a result of his observations he proposed the existence of a H^+ electrogenic pump.

b) The H^+ electrogenic pump

1) Kitasato (19) proposed that the main current carrying ion is H^+ in which case the Goldman equation has to be modified:

$$E = \frac{RT}{F} \ell n \left[\frac{P_K (K)_o + P_{Na} (Na)_o + P_H (H)_o + P_{C\ell} (C\ell)_i}{P_K (K)_i + P_{Na} (Na)_i + P_H (H)_i + P_{C\ell} (C\ell)_o} \right] \qquad (1.25)$$

Since $P_H >> P_K, P_{Na}, P_{C\ell}$

$$E \approx \frac{RT}{F} \ell n \frac{(H)_o}{(H)_i} = E_H \, . \qquad (1.26)$$

This equation, however, did not describe the membrane potential and Kitasato invoked the existence of a H^+ extrusion mechanism which would maintain constant internal pH and produce the observed potential. This gives a modified form of (1.26):

$$E = E_H - \frac{F J_{extrusion}}{G_m} \qquad (1.27)$$

where the second term is the ohmic potential produced by the passive H^+ influx which, in the absence of an external current, is equal to the H^+ extrusion. If the H^+ pump were to stop the membrane should move to E_H. Kitasato claimed that his experiments with 2, 4 dinitrophenol (DNP) support the existence of an electrogenic pump. He also proposed that the discrepancy between the electrically measured conductance and that obtained from flux measurements was due to the neglect of the passive H^+ flux. He estimated this flux from measurements of the current required to clamp the membrane potential at the K^+ Nernst potential in solutions of different pH. He found that the conductance associated with such changes agreed with the electrically measured conductance.

Criticism of this model has been expressed by Walker and Hope [10] (21) but have been discounted by Spanswick (22-25) who supports the concept of an electrogenic pump but with a different operating mechanism.

2) In the Spanswick model the passive H^+ fluxes are regarded as being negligible compared with the electrogenic H^+ flux; this is considered to be due to a very low H^+ permeability. The equivalent circuit in this case is:

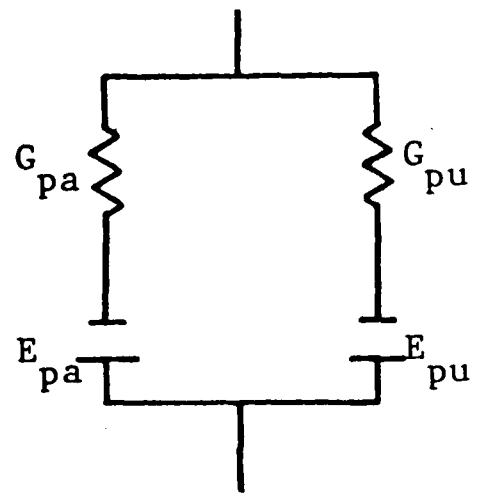

where G_{pa} and E_{pa} are the passive membrane conductance and potential and G_{pu} and E_{pu} the conductance and e.m.f. of the pump. Spanswick (24) assumes that G_{pa} is much smaller than G_{pu}. In this case the hydrogen extrusion will continue until halted by the resting membrane potential, i.e., when $E = E_{pu}$. In this case E can be expressed as:

$$E = \frac{\Delta\bar{\mu}_p}{F\nu_H} - \frac{RT}{F} \ell n \left(\frac{H_i^+}{H_o^+} \right) = E_{pu} \qquad (1.28)$$

where $\Delta\bar{\mu}_p$ is the change in free energy of the non-transported components involved in the extrusion reaction and ν_H is the stoichiometric coefficient of the reaction. The equation for the conductance is then

$$G_m = G_{pu} + G_{pa} \simeq G_{pu} = F^2 L \nu_H^2$$

where L is a thermodynamic conductance coefficient. Spanswick contends that the conductance computed from flux measurements, i.e. at zero current, will be G_{pa} whereas in the electrical measurements the applied current, carried by H^+, is shunted through the pump and the measured conductance is G_{pu}. He reinterpreted Kitasato's H^+ flux data as being a H^+ flux through the pump.

The Spanswick model is consistent with the hypothesis, proposed by Smith and Walker (26), that $C\ell^-$ is transported

into the cell as a result of the H^+ potential gradient produced by H^+ extrusion. This gradient would be large enough to drive chloride inwards either by co-transport with H^+ or by a $C\ell^-/OH^-$ exchange. The Spanswick model can also rationalize the observed changes in membrane potential and resistance when the illumination of the cell is varied. This response to light-dark changes, which is the strongest evidence against a passive diffusion model, attracted the attention of Vredenberg (27-30) who proposed a third electrogenic model.

3) Vredenberg's observations of the responses of the membrane potential and conductance of Nitella to varying periods of illumination, following prolonged preconditioning of the cells in the dark, led him to propose that these parameters characterize the energy state of the membrane. The membrane can be transferred to a different energy state by changes in pH or illumination or applied current. He further proposed that the different energy states would always follow the rectification curves because all changes in E and R_m produced by changes in pH or illumination are a consequence of current flow through the membrane, the current being supplied by the electrogenic pump. The neglect of this current when G_e is being determined would lead to the observed discrepancy between G_f and G_e.

The pH responses of the membrane potential and resistance of the Characeae have also been explained in terms of changes in the structure of a doubly fixed charge membrane, Coster (6, 31-33).

c) The Coster fixed charge membrane model

In this model the membrane is considered to consist of a lipid structure presenting a double lattice in which one side of the membrane has fixed positive charges and the other side has fixed negative charges. This polarization between the two regions forms a depletion layer with a high resistivity because the ion concentration is very low. The equivalent circuit in this case is:

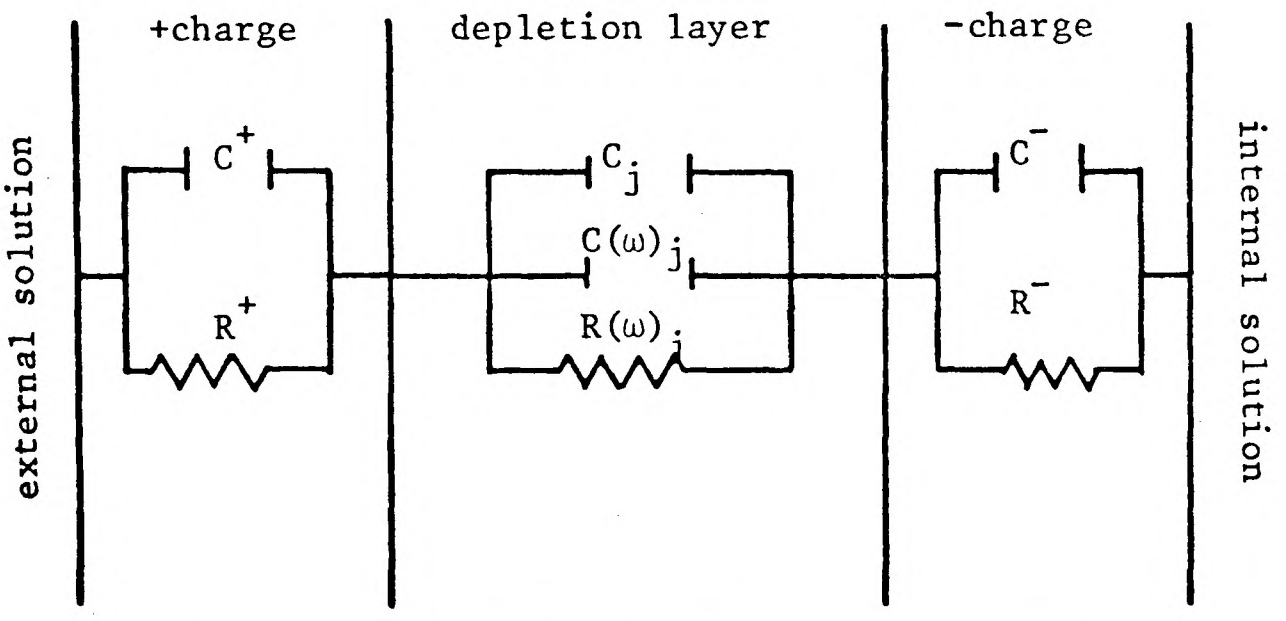

It can be seen that in addition to the resistance and capacitance associated with the lipid membrane structure the resistance and capacitance of the depletion layer are introduced. The effects of pH on the membrane parameters are then explicable in terms of changes in the fixed charge regions. In biological membranes the charged regions could arise from the ionisation of the NH_2 and COOH groups of the membrane proteins. It is therefore to be expected that changes in the H^+ concentration, i.e. in the hydrogen bonding rate, will produce changes in this ionization. The theory can also account for changes in the observed resistance and capacitance, a largely overlooked parameter, when A.C.

is applied to the membrane. However the strongest experimental basis for the theory is a phenomenon which appears when very large hyperpolarizing currents are applied. In this case (see Figure 1.2), the slope resistance of an I/V curve goes through a region of very low and even negative values. The depletion layer width depends on the membrane potential. It increases with increasing potential but at sufficiently large potentials the depletion layer will occupy the whole membrane and an avalanche of current will flow in the same way as in a Zenner diode.

In a recent paper Okhawa and Kishimoto (34) presented experimental evidence which contradicts the Coster hypothesis. These results are interpreted as supporting the hypothesis that changes in the membrane e.m.f. are the prime causes of the transient phenomena observed in the Characeæ (Kishimoto (35, 36) and Ohkawa and Kishimoto (34, 37, 38)).

d) The Kishimoto model

It has already been mentioned that the generally accepted mechanism of the action potential in the Characeae involves an efflux of Cl followed by an efflux of K. However Kishimoto points out that time separated ion currents require the capacitative discharge of the membrane, $C_m \frac{\partial E}{\partial t}$. With the long duration of the action potential this would imply unrealistically large values for C_m. Kishimoto therefore considered that the two effluxes take place simultaneously and this led him to propose the following equivalent circuit:

Figure 1.2 The voltage response to a current ramp showing the punch-through effect.

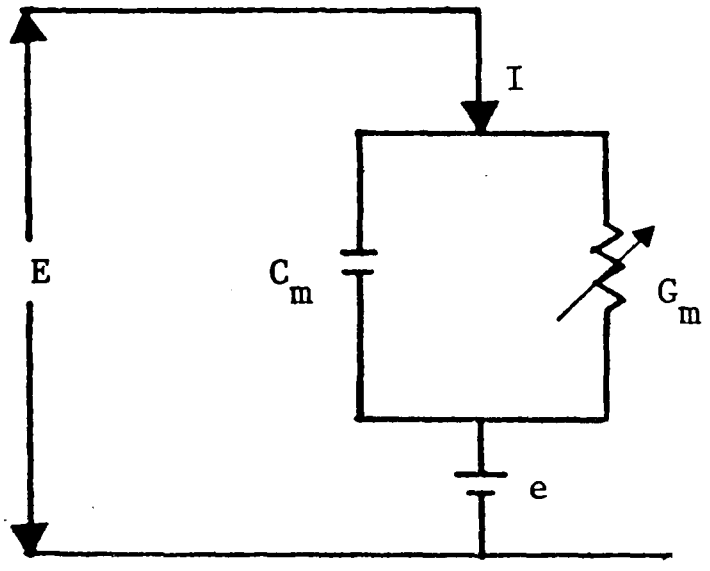

where e is the membrane e.m.f. and I the current. Both G_m and e are functions of E and time. The membrane potential is then given by

$$E = I/G_m(E,t) + e(E,t) \quad . \qquad (1.30)$$

Kishimoto (35) was able to determine the values of E, I and G_m; G_m was computed from the response to small fast signals superimposed on I. He found that the behaviour of $G_m(E,t)$ did not explain the observed changes in $E(t)$ and so he proposed that the action potential was caused mainly by a transient change in the e.m.f.

Kishimoto and Okhawa (34, 36-38) found support for this hypothesis in observations of the other transients of the Characeae. For instance in some cases anode break excitation could occur without a prior decrease in membrane conductance, i.e., the observed change in $E(t)$ would have to be due to changes in the e.m.f. (see equation (1.30)). Similarly measurements of the conductance in the punch-through region showed a small decrease, contrary to the Coster model which predicts an extremely large decrease. The observed decrease in potential in this region is then explained as an excursion

of the e.m.f. in the direction of depolarization.

The present work is concerned with an electrophysiological study of the membrane impedance of Nitella translucens and the significance of this impedance on ion transport phenomena. As a preamble it is necessary to consider the cable like properties of the cells of Nitella translucens.

REFERENCES (CHAPTER 1)

1) Schwartz, T.L., The thermodynamic foundations of membrane physiology. Biophysics and Physiology of Excitable Membranes, Edit. Aldeman, W.J., Van Nostrand Reinhold Company (1971).

2) Plonsey, R., Bioelectric Phenomena, McGraw-Hill, (1969).

3) Hogg, J., Ph.D. Thesis, University of Edinburgh (1966).

4) Hodgkin, A.L. & Katz, B., J. Physiol. 108, 37 (1949).

5) Kimizuka, h. & Koketzu, K., J. Theoret. Biol. 6, 290 (1964).

6) Coster, H.G.L., Biophys. J. 5, 669 (1965).

7) Walker, N.A. & Hope, A.B., Aust. J. Biol. Sci. 22, 1179 (1969).

8) Duncan, G. & Croghan, P.C., Expt. Eye. Res. 10, 192 (1970).

9) Hope, A.B., Ion Transport and Membranes, Butterworths London (1971).

10) Hope, A.B. & Walker, N.A., The Physiology of Giant Algal Cells. Cambridge University Press (1975).

11) Spanswick, R.M., Stolarek, J. & Williams, E.J., J. Expt. Bot. 15, 193 (1967).

12) Hope, A.B., Aust. J. Biol. Sci. 14, 26 (1961).

13) Hope, A.B. & Findlay, G.P., Pl. Cell. Physiol. 5, 377 (1964).

14) Gaffey, C.T. & Mullins, L.J., J. Physiol., 144, 505 (1958).

15) MacRobbie, E.A.C., J. Gen. Physiol. 45, 861 (1962).

16) Williams, E.J., Johnston, R.J. & Dainty, J., J. Expt. Bot. 15, 1 (1964).

17) Hogg, J., Williams, E.J. & Johnston, R.J., J. Theoret. Biol. 24, 317 (1969).

18) Hodgkin, A.L. & Keynes, R.D., J. Physiol. 128, 61 (1955).

19) Kitasato, H., J. Gen. Physiol. 52, 60 (1968).

20) Kishimoto, U., Ann. Rep. Sci. Works. Fac. Sci, Osaka Univ. 7, 115 (1959).

~~21) Walker, N.A. & Hope, A.B., Aust. J. Biol. Sci., 22, 1179 (1969).~~

22) Spanswick, R.M., Biochim. Biophys. Acta 288, 73 (1972).

23) Spanswick, R.M., J. Membrane Biol. 2, 59 (1970).

24) Spanswick, R.M., Biochim. Biophys. Acta 332, 387 (1974).

25) Spanswick, R.M., Electrogenesis in Photosynthetic Tissues. Ion Transport in Plants. Edit. Anderson, W.P., Academic Press (1973).

26) Smith, F.A. & Walker, N.A., J. Exp. Bot. 27, 45 (1976).

27) Vredenberg, W.J., Biochem. Biophys. Res. Comm. 37, 785 (1969).

28) Vredenberg, W.J., Biochem. Biophys. Res. Comm. 42-1, 111 (1971).

29) Vredenberg, W.J. & Tonk, W.J., Biochim. et. Biophys. Acta 298, 354 (1973).

30) Vredenberg, W.J., Energy Control of Ion fluxes, Ion Transport in Plants, Edit. Anderson, W.P., Academic Press. (1973)

31) Coster, H.G.L., Aust. J. Biol. Sci. 21, 243 (1969).

32) Coster, H.G.L., Biophys. J. 9, 666 (1969).

33) Coster, H.G.L. & Smith, J.R., The effect of pH on the low frequency capacitance of the membranes of Chara corallina, Membrane Transport in Plants, Edit. Zimmermann, U. and Dainty, J., Springer-Verlag (1974).

34) Okhawa, T. & Kishimoto, U., Plant and Cell Physiol. 18, 67 (1977).

35) Kishimoto, U., Plant and Cell Physiol. 7, 429 (1966).

36) Kishimoto, U., Plant and Cell Physiol. 9, 539 (1968).

37) Okhawa, T. & Kishimoto, U., Plant and Cell Physiol. 15, 1039 (1974).

38) Okhawa, T. & Kishimoto, U., Plant and Cell Physiol. 16, 83 (1975).

CHAPTER II

D.C. CABLE THEORY AND MEMBRANE IMPEDANCE MEASUREMENTS

The cylindrical geometry of the single cells of the Characeae endows these cells with the electrical properties of a core conductor. Classical core conductor theory is therefore applicable and the resistance and capacitance of the membranes of these cells can be determined. In general, however, the numerical computations are tedious and it is desirable that these be circumvented by suitable design of the experimental arrangement. This has been done in a number of ways for D.C. experiments and these techniques are reviewed in the present chapter. Additionally, the D.C. method developed in the present work is described and critically assessed. In a subsequent chapter it will be shown how it has been applied in A.C. experiments. As a preamble to this chapter it is worth considering the problems that arise because of the cable effects.

2.1 The Core Conductor Model

This is represented in Figure 2.1:

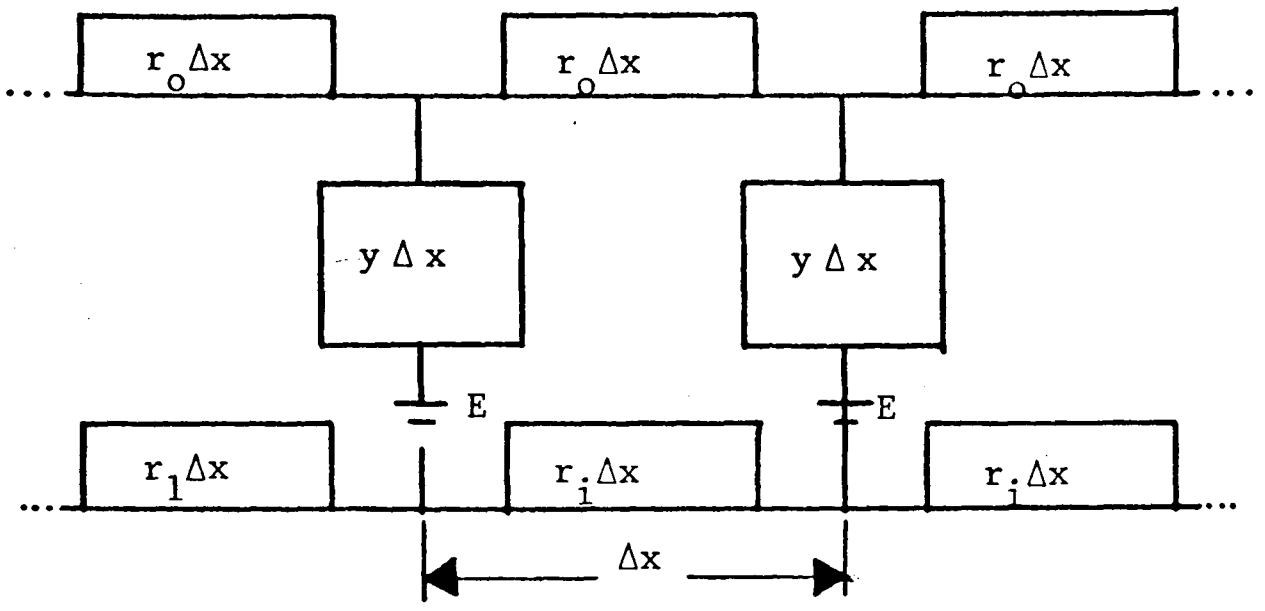

Figure 2.1

---

where:

r_o = resistance per unit length (Ω/cm) of the external solution.

r_i = resistance per unit length (Ω/cm) of the cell sap.

Y = complex admittance of the cell membrane.

E = membrane potential (mv).

Δ_x = a small section of the cable length.

Y is assumed to have the form

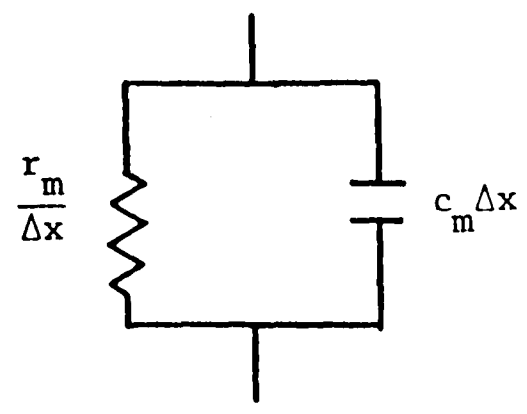

Figure 2.2

where:

r_m = resistance × unit length (Ω.cm) of cell membrane.

c_m = capacitance/unit length (f/cm) of cell membrane.

The electrical behaviour of this cable is determined by the values of the parameters r_m, c_m, r_o, r_i and the type of termination at the end points of the cable. r_o and r_i can be computed from the conductivities of the two solutions. The determination of the values of r_m and c_m is complicated by the particular behaviour of leaky cables in which there is attenuation and distortion of the voltage response with increasing distance from the point of current injection. It is therefore not possible to obtain for instance, the resistance value by a simple Ohm's law calculation unless short cell techniques are used. In this case a short segment of the cell is isolated and it is then only necessary to consider a single element $y\Delta x$ (see, for example, Cole and Curtis (1)). In the general case, however, the exact solution of the equation for the core-conductor model has to be obtained.

2.2 Solutions of the Cable Equations for the D.C. Case

Figure 2.3 is a detailed diagram of a small section Δx of a co-axial cable. In this figure i denotes the current flowing in the two solutions and V denotes the change in potential difference arising from the leakage current through the membrane.

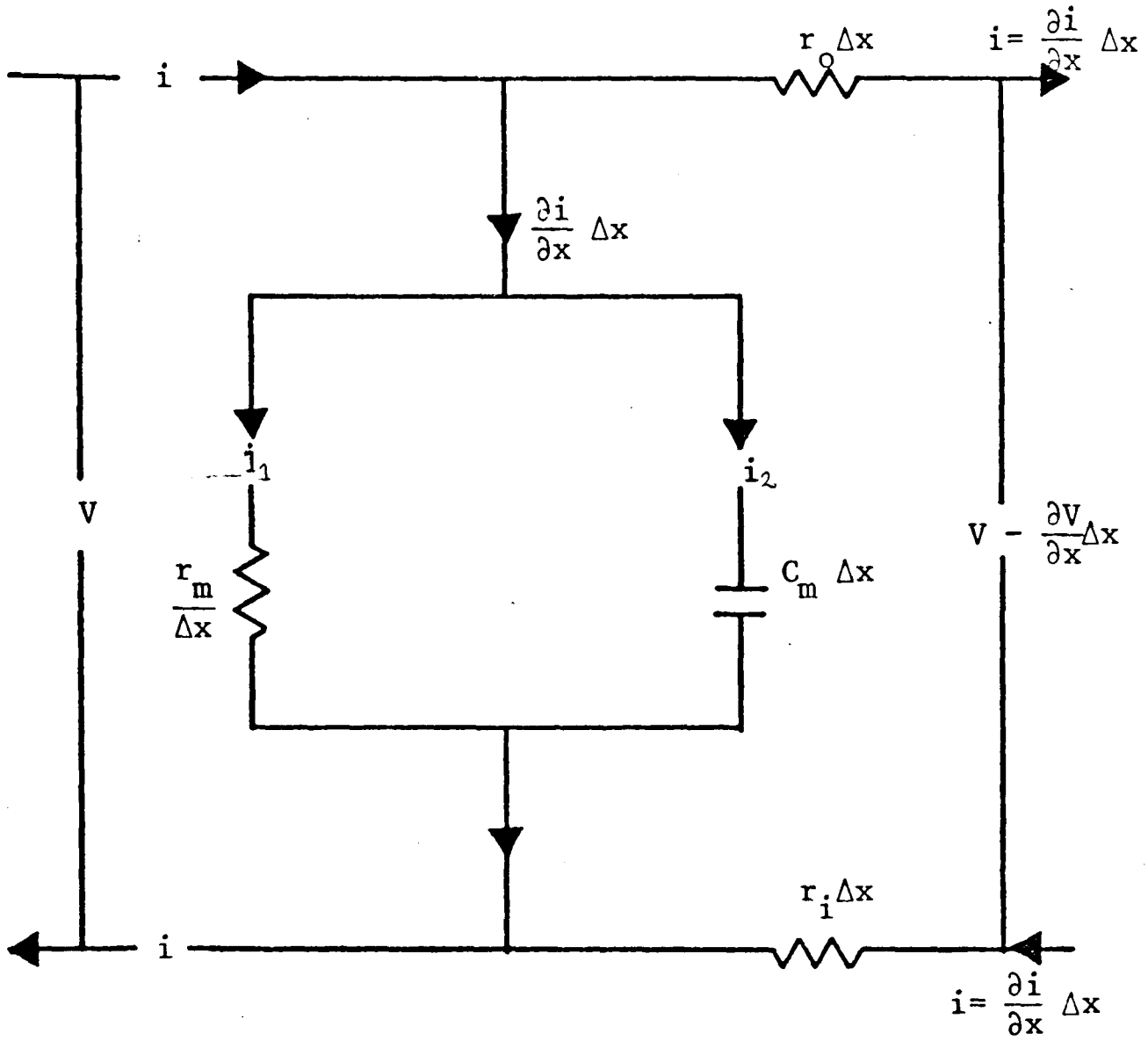

Figure 2.3

Analysis of this circuit yields the following:

$$-V + i(r_o\Delta x) + V - \frac{\partial V}{\partial x}\Delta x + i(r_i\Delta x) = 0$$

$$\therefore \quad i(r_o + r_i) = \frac{\partial V}{\partial x} \tag{2.1}$$

and

$$\frac{\partial i}{\partial x}\Delta x = i_1 + i_2 = \frac{V\Delta x}{r_m} + c_m\Delta x \frac{\partial V}{\partial t}$$

$$\therefore \quad \frac{\partial i}{\partial x} = \frac{V}{r_m} + c_m \frac{\partial V}{\partial t} \quad . \tag{2.2}$$

Introducing the parameters $\lambda^2 = \frac{r_m}{r_i+r_o}$, $r_o+r_i = r_{oi}$ and $\tau = c_m r_m$ and the dimensionless variables $X = \frac{x}{\lambda}$ and $T = \frac{t}{\tau}$, equations (2.1) and (2.2) become:

$$(r_{oi})i = \frac{1}{\lambda}\frac{\partial V}{\partial X} \tag{2.3}$$

$$\frac{c_m V}{\tau \partial T} + \frac{V}{r_m} = \frac{1}{\lambda}\frac{\partial i}{\partial X} \quad . \tag{2.4}$$

The steady state solution, $V(X,\infty)$, for these equations i.e. for $t >> \tau$, when a current of amplitude I is applied to an infinite line is:

$$V(X,\infty) = \frac{I}{2}\lambda r_{oi} e^{-X} \quad . \tag{2.5}$$

For the case of a short cable of length 2ℓ terminated by infinite impedances and where the current is injected at the midpoint, the solution is:

$$V(X,\infty) = \frac{I}{2}\lambda r_{oi} \frac{\cosh(L-X)}{\sinh(L)} \quad . \tag{2.6}$$

The time-dependent solutions for these two cases are respectively:

$$V(X,T) = \frac{I\lambda}{4} r_{oi}\left[e^{-X}\operatorname{erfc}\left\{\frac{X}{2\sqrt{T}} - \sqrt{T}\right\} - e^{X}\operatorname{erfc}\left\{\frac{X}{2\sqrt{T}} + \sqrt{T}\right\}\right] \tag{2.7}$$

where $\operatorname{erfc} Z = 1 - \operatorname{erf} Z$ and erf, the error function is defined by

$$\operatorname{erf} Z = \frac{2}{\sqrt{\pi}}\int_0^Z e^{-\omega^2}\, d\omega$$

(see Hodgkin and Rushton (2))

and

$$\begin{aligned} V(X,T) = {} & \frac{I\lambda}{4} r_{oi} \sum_0^\infty \left[e^{-(2nL+X)}\operatorname{erfc}\left\{\frac{(2nL-X)}{2\sqrt{T}} - \sqrt{T}\right\}\right] \\ & - \frac{I\lambda}{4} r_{oi} \sum_0^\infty \left[e^{-(2nL+X)}\operatorname{erfc}\left\{\frac{(2nL+X)}{2\sqrt{T}} + \sqrt{T}\right\}\right] \\ & + \frac{I\lambda}{4} r_{oi} \sum_0^\infty \left[e^{-(2nL-X)}\operatorname{erfc}\left\{\frac{(2nL-x)}{2\sqrt{T}} - \sqrt{T}\right\}\right] \\ & - \frac{I\lambda}{4} r_{oi} \sum_0^\infty \left[e^{(2nL-X)}\operatorname{erfc}\left\{\frac{(2nL-X)}{2\sqrt{T}} + \sqrt{T}\right\}\right] \end{aligned} \tag{2.8}$$

(see Hogg, Williams and Johnston (3)).

In Figure 2.4 the profiles of the voltage responses along non-inductive leaky cables for different L values (equations (2.5) and (2.6)) are shown. It can be seen that the attenuation of the voltage response is strongly dependent on the value of L. The physical basis for this behaviour was presented by Hogg et al. (3). They considered the case in which the finite line is terminated at $X = \pm L$ by infinite impedances, i.e. the cell nodes. Any power incident on these terminations is reflected with a phase change of π and no power is absorbed. Thus at any time the resultant voltage response at any point X can be found by summing up the contributions arising from these doubly infinite reflections. The reflection patterns are shown in Figure 2.7*. From these it can be seen that a reflected signal will be identical in all respects to the signal in an infinite line which has passed through a distance equal to the path length of the reflected signal. Hence V(X,T) will be the summation of the values of V(X,T) for an infinite line at distances X, 2L-X, 2L+X, 4L-X, 4L+X, ..., . These distances can be arranged in two sets:

$$\text{set A} = S(2nL + X) \qquad n = 0,1,2,.... \qquad (2.9)$$

$$\text{set B} = S(2nL - X) \qquad n = 1,2,3,.... \qquad (2.10)$$

where S indicates a succession. Any one term of set A will contribute to the potential an amount $V_n = f|(2nL+X),T|$ and similarly for set B $V_n = f|(2nL-X),T|$ where f(X,T) is the value of V(X,T) for the infinite line.

The total voltage response at X is then

$$V(X,T) = \sum_{o}^{\infty} f|(2nL+X),T| + \sum_{o}^{\infty} f|(2nL-X),T|$$

which on substitution of the known value of $f(X,T)$, from equation (2.5), becomes equation (2.8). It should be noted that the same result can be obtained by using operational calculus to solve equations (2.3) and (2.4) (Hogg (4)).

2.3 The Cable Model for the Characeae

In the previous section it was shown that the electrical behaviour of an infinite line differs from that of a short cable. In the former the steady state voltage response decreases exponentially whereas in the latter the attenuation is much less marked. The factor which determines whether a cable can be regarded as infinite or otherwise is the ratio $\ell/\lambda = L$. For nerve fibres λ is only a few mm. in the resting state and the assumption of an infinite cable model is valid even for fibre segments of a few cm. In the Characeae λ in the resting state is about 3 cm. and even 12 cm. long cells will behave as short cables.

Thus the signal response to an applied current will differ between a nerve fibre and a characean cell. The differences in the steady state value, i.e. $V(X,\infty)$ are shown in Figure 2.4. It is also to be expected that the time dependent solution, $V(X,T)$, will be different for the two cases. The ratio $\alpha = V(X,1)/V(X,\infty)$ which is the fraction of $V(X,\infty)$ reached by $V(X)$ at time $t = \tau$ gives an indication of the time dependency and can be used for

the computation of τ. Hodgkin and Rushton (2) computed this ratio for nerve fibres. They found that this ratio has the value of 0.824 at $X = 0$. Hogg et al. (3) computed the same ratio when both X and L are varied (see Figure 2.5). From this figure it can be seen that (i) as $L \to \infty$ and $X \to 0$, $\alpha \to 0.824$, (ii) as $L \to \infty$ and $X \to L$, $\alpha \to 0$ and (iii) as $L \to 0$, $\alpha \to 0.632$ for any value of X. Thus, whereas for nerve fibre α depends only on X, in the Characeae this ratio is a function of both X and L.

The above conclusions are based on computations made on the assumption that the characean cells have terminations of infinite impedance. This, however, is not the only possibility. If the cells were finite cables terminated by their characteristic impedances, all the incident power would be absorbed by these terminations and the cells would behave in an exactly similar manner to nerve fibres. In order to elucidate which of the two models is valid Hogg et al. (3) compared the predicted $V(X,T)$ for both models with the experimentally recorded $V(X,T)$. There is a remarkable fit between the experimental curve and the theoretical curve for the infinite impedance termination model but a poor fit for the model in which cells are terminated by their characteristic impedance. However, direct measurements of the trasnodal impedance (Spanswick and Costerton (5), Bostrom and Walker (6) and Skierczyńska (7)) predict low values for this parameter. This agrees with the observed translocation of $C\ell^-$ through the cell node, Williams and Fensom (8), Bostrom and Walker (6). However, it has to be emphasised that these experiments were performed on nodes with intact cells on both sides. It might be expected that

the nodal resistance would increase substantially when one of the cells is removed. This promise has however never been directly tested hitherto. Part of the present work was devoted to these particular measurements and this is discussed in Chapter VI. Briefly, these experiments support the model in which the terminations present infinite impedance to the flow of current.

2.4 D.C. Experimental Techniques

Broadly speaking there exist three different techniques for the measurement of the membrane electrical parameters of the Characeae. The differences are mainly centred on the method of supplying current to the cell; current can be supplied intracellularly, extracellularly or through an open vacuole. But whichever method is used it is usually possible to devise an experimental arrangement in which cable effects are largely minimised. This of course ensures more speedy computation of the results.

a) Intracellularly applied current

If current I is injected through a point microelectrode inserted at the midpoint of the cell, then equation (2.6) gives the expression for the recorded voltage response. Williams, Johnston and Dainty (9), computed the membrane resistance and capacitance of Nitella transluceus using this equation and, as they showed, there are two unknowns λ and r_{oi}. Thus it was necessary to record the voltage response at two values of X in order to determine r_m. The membrane capacitance was computed from the voltage response recorded at a point X close to the current electrode. As shown in Figure 2.5 the

Figure 2.4 The voltage response profile along the half-length of cells of various lengths.

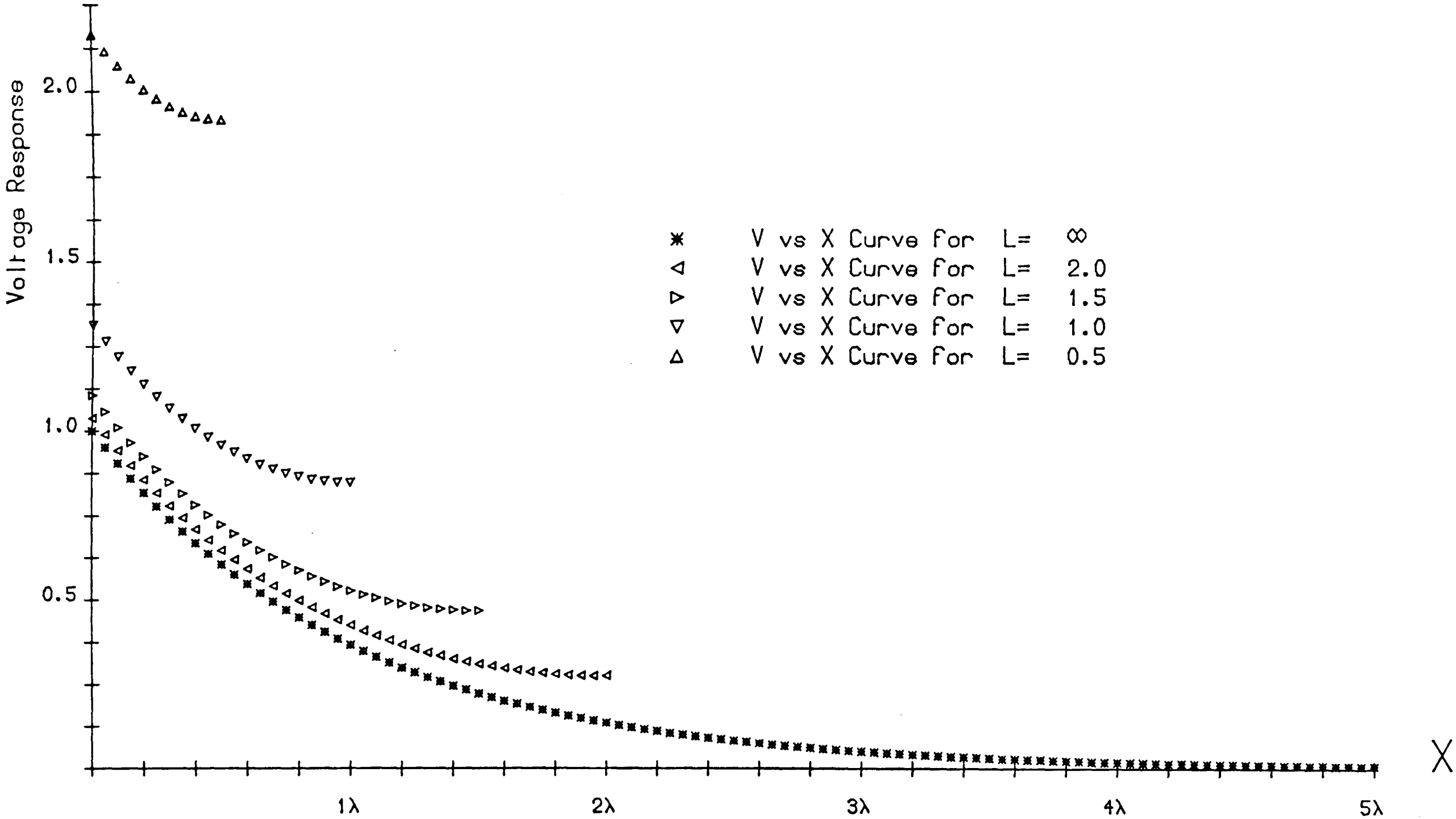

value of α in this particular case will be between 0.632 and 0.824. An estimation of C_m was therefore obtained. But C_m can be determined as accurately as required if the values of r_m and λ are previously known. The exact value of α at a particular point X can be found from Figure 2.5. The technique has however certain disadvantages:
i) two voltage recording electrodes are required, ii) λ has to be computed by a tedious trial and error method and iii) the injection of current through a point microelectrode introduces several problems which are discussed in Chapter V.

The shortcomings i) and ii) were circumvented by Hogg, Williams and Johnston (10) who showed how the computation of the membrane resistance could be achieved with a single voltage recording electrode:

Rewriting equation (2.6)

$$V(X) \times \frac{2\pi d\ell}{I} = \frac{r_m 2\pi d\ell}{2\lambda} \frac{\cosh(L-X)}{\sinh(L)} \quad \text{where} \quad d = \text{cell diameter}$$

then it can be seen that

$$R'_m = \frac{V(X)}{I} 2\pi d\ell = R_m \left[\frac{L \cosh(L-X)}{\sinh(L)} \right] \qquad (2.9)$$

where $R_m = r_m \pi d$, the membrane resistance ($\Omega.cm^2$).

R'_m, the membrane resistance (also in $\Omega.cm^2$) uncorrected for the space constant, is equal to the uncorrected resistance value R_m, times a factor K, where $K = \left[\frac{L \cosh(L-X)}{\sinh(L)} \right]$
Hogg et al.[10] computed this factor for several values of X and L. It can be seen from Figure 2.6 that K is unity at the particular distance X = 0.42L from the current injecting electrode. Hence a single voltage recording electrode

Figure 2.5.

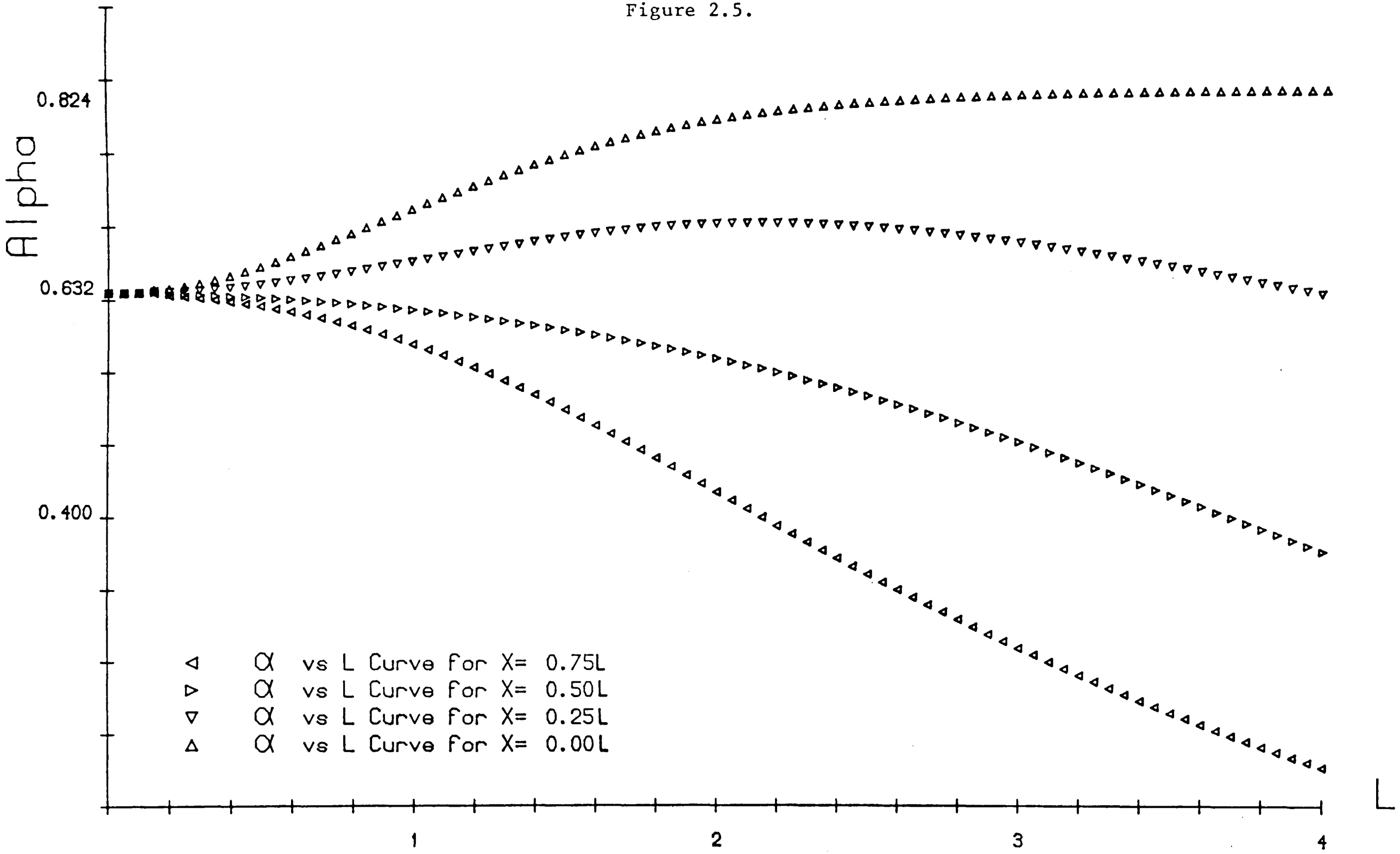
Alpha
0.824
0.632
0.400
1
2
3
4
L
◁ α vs L Curve for X= 0.75L
▷ α vs L Curve for X= 0.50L
▽ α vs L Curve for X= 0.25L
△ α vs L Curve for X= 0.00L

Figure 2.6.

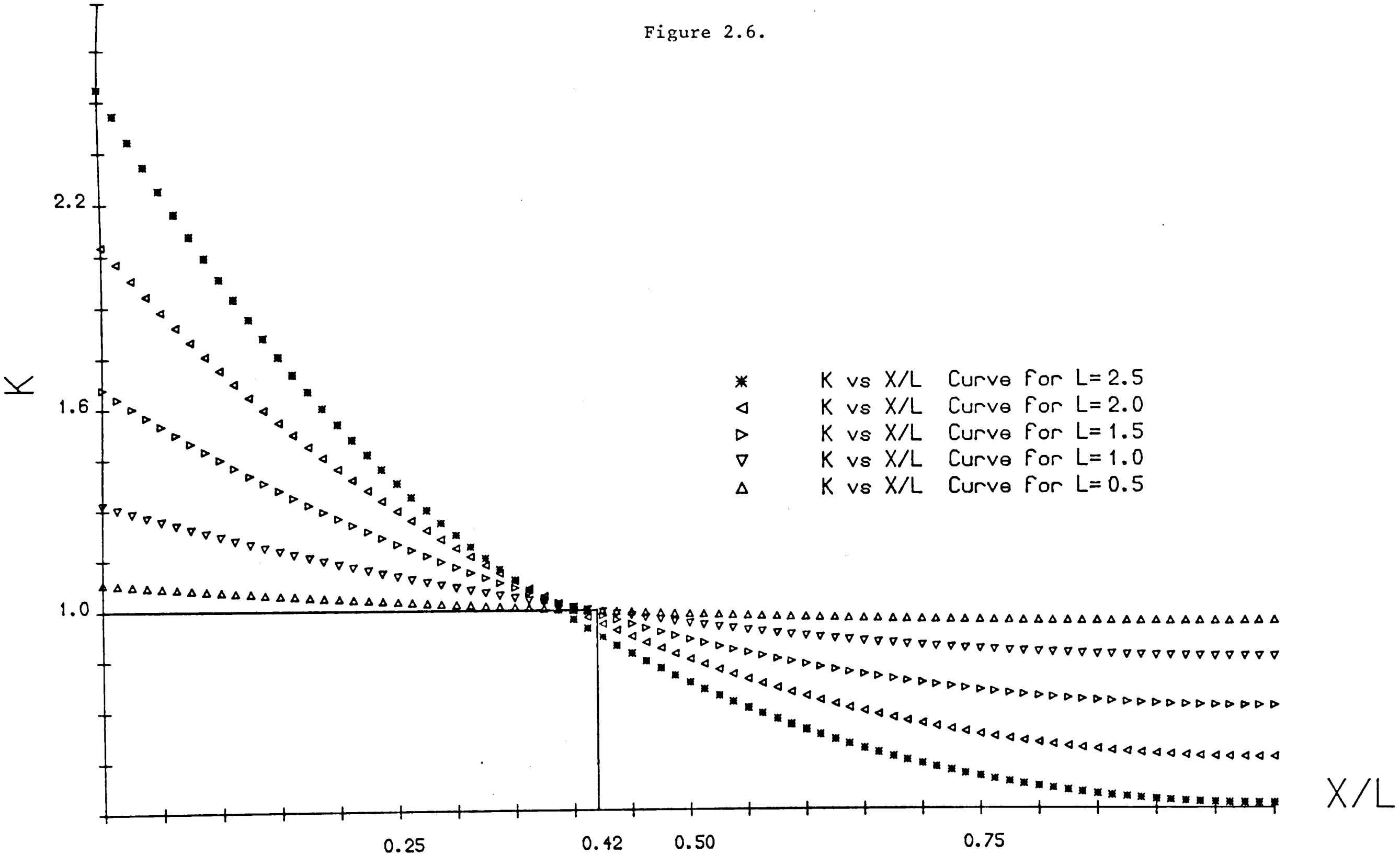
K
2.2
1.6
1.0
0.25
0.42
0.50
0.75
X/L
* K vs X/L Curve for L= 2.5
◁ K vs X/L Curve for L= 2.0
▷ K vs X/L Curve for L= 1.5
▽ K vs X/L Curve for L= 1.0
△ K vs X/L Curve for L= 0.5

inserted at this point will permit the computation of the corrected membrane resistance, R_m, by a simple Ohm's law calculation.

For the computation of the membrane capacitance prior knowledge of the space constant λ is necessary. But λ can only be computed with the use of two voltage recording electrodes and so the 0.42L method provides only an estimate of C_m. However computation of α for $X = 0.42L$ (Figure 2.7) shows that α has a constant value of 0.632 for L ranging from 0.0 to 1.3. Moreover it shows that recording of the voltage response at a distance $X = (0.42 \pm 0.02)L$ ensures that the value of α can be taken as 0.632 for any Nitella cell whose length is less than 5 cm.

Another method, using intracellular current of injection, involves the use of a long axial electrode (Kishimoto (11), and Findlay (12)). In this case a long (≃1 cm.) fine metal microelectrode is inserted through the cell node and along the axis of the isolated cell segment; the cell segment has the same length as the microelectrode. This effectively space clamps the membrane potential and reduces the whole isolated segment to a single $Y\Delta x$ circuit.

b) Open vacuole technique

Recently the perfusion technique used in animal physiology has been used in plant physiology by Tazawa, Kikayama and Nagakawa (13). A cell is mounted in a three compartment bath (see Chapter V for details) and the nodes of the turgorless cell are cut off so that the cell vacuole is open to the lateral compartments. In this way external

Figure 2.7.

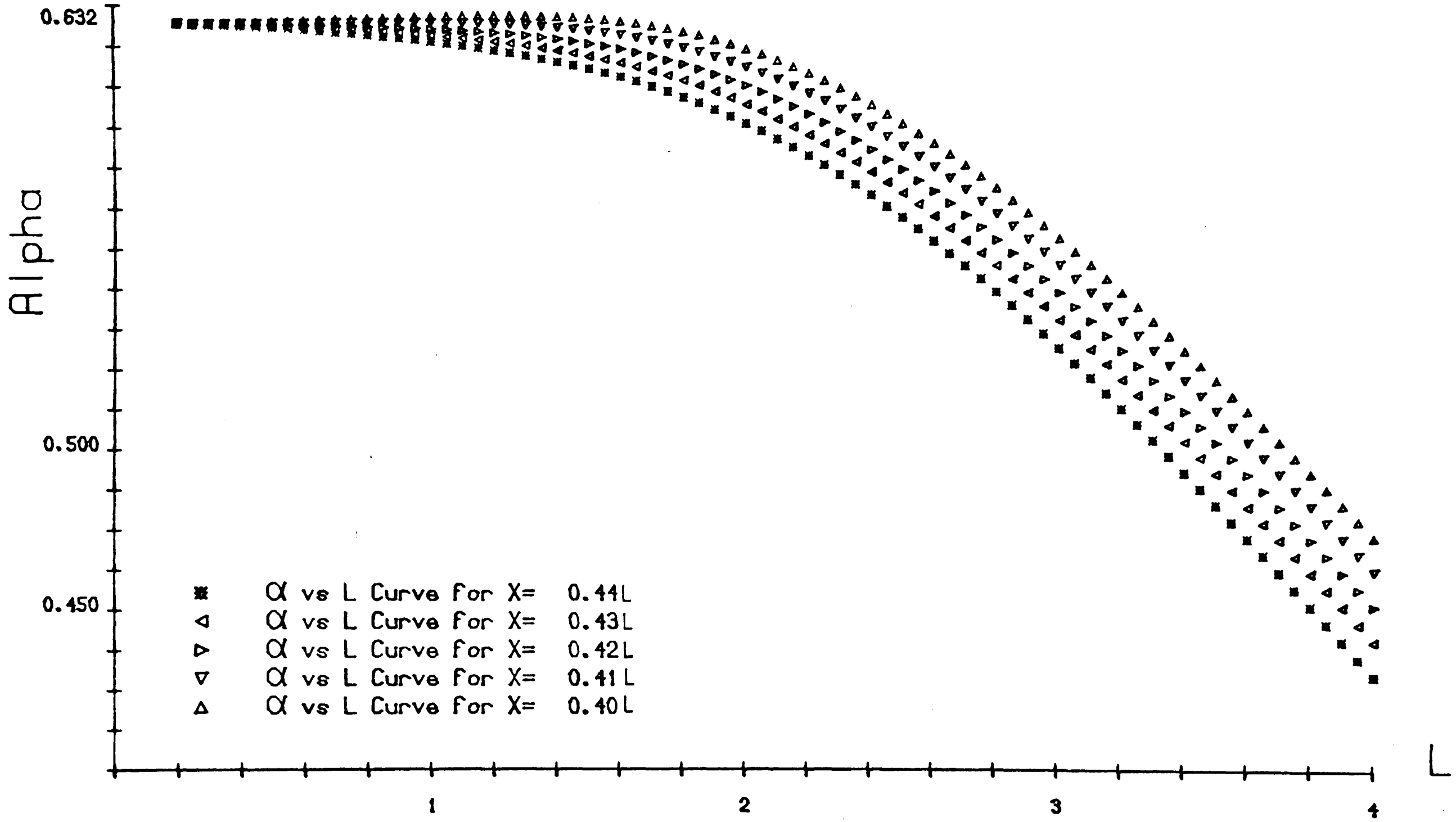
0.632
Alpha
0.500
0.450
α vs L Curve for X= 0.44L
α vs L Curve for X= 0.43L
α vs L Curve for X= 0.42L
α vs L Curve for X= 0.41L
α vs L Curve for X= 0.40L
1
2
3
4
L

electrodes located in the lateral compartments will also be located in the cell vacuole. If the central compartment is short enough the assumption of a single RC circuit will be valid. The electrical constants can then be determined from the response to a square pulse of current flowing between the lateral and the central compartments. Thus in this technique there is no microelectrode perforating the membrane. This could of course give a value for the membrane resistance which is different from that obtained in the methods using a perforating microelectrode. This is discussed further in Section 2.6.

c) Extracellularly applied current

In this case the cell is mounted in a multicompartment cell bath and the current is then made to flow from one segment to another, through the cell membrane and the cell sap. The method, which is a short cell method, was devised so that the cable effects could be minimised. Initially the membrane resistance was determined by a Wheatstone bridge arrangement and without any internal voltage recording electrodes, e.g. Kishimoto (14). Later Oda (15) used a three compartment cell bath and internal voltage recording microelectrodes. He assumed that the central cell segment was short enough to be considered as a single RC circuit but the actual dimensions of this segment were not reported. He supplied a steady current from one of the side compartments and a train of square current pulses from the other. In this way he computed R_m and C_m for different values of the membrane potential. However Kitasato (16) stressed

the need for symmetry in the current supply, i.e. the same current should be fed from the two lateral compartments. This ensures a better space clamping of the membrane potential.

It is now necessary to discuss the form of the change in membrane potential, $V(X,T)$, obtained in the different modes of current injection. It should be noted that the form of $V(X,T)$ will be the same for both the open vacuole technique and for the techniques of external current injection.

2.5 The Forms of $V(X,T)$ for the Different Modes of Current Injection

(1) Point current injection.

This was the case considered by Hogg et al. (3).and shown in Figure 2.7*. The algebra required for writing $V(X,\infty)$ in the form of equation (2.6) is now reproduced:

For $T = \infty$ $\operatorname{erfc}(\infty) = 0$ and $\operatorname{erfc}(-\infty) = 1$.

Thus $V(X,\infty)$ has the following form:

$$V(X,\infty) = \frac{I\lambda}{4} r_{oi} \left| \sum_{o}^{\infty} e^{-(2nL+X)} + \sum_{o}^{\infty} e^{-(2nL-X)} \right| .$$

If $n = n+1$ in the second summation, $V(X,\infty)$ becomes

$$V(X,\infty) = \frac{I\lambda}{4} r_{oi} \left| \sum_{o}^{\infty} e^{-(2nL+X)} + \sum_{o}^{\infty} e^{-(2(n+1)L-X)} \right|$$

$$= \frac{I\lambda}{4} r_{oi} \left| \sum_{o}^{\infty} e^{(-2nL+L-L-X)} + e^{(-2n-L-L+X)} \right|$$

$$= \frac{I\lambda}{4} r_{oi} \left[(e^{(L-X)} + e^{-(L-X)}) \sum_{o}^{\infty} e^{-(2n+1)L} \right] .$$

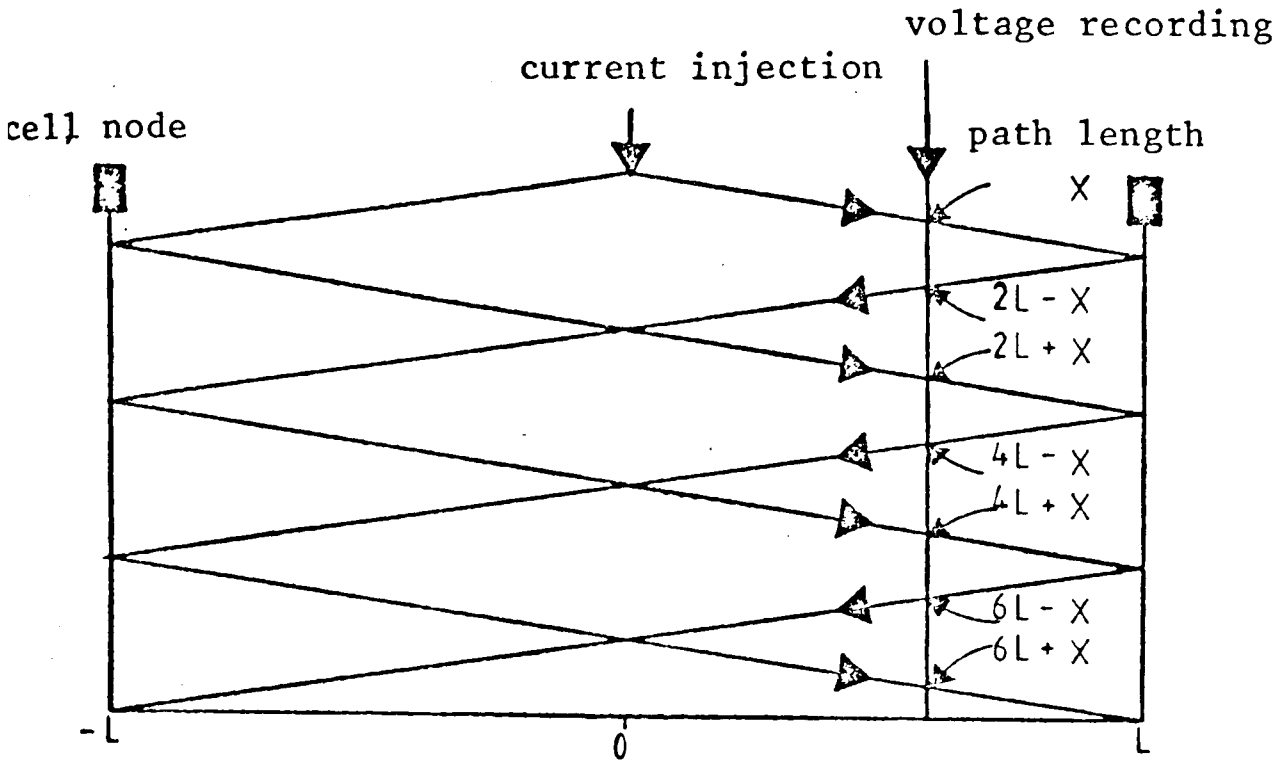

Figure 2.7*. Voltage reflections pattern in midpoint current injection.

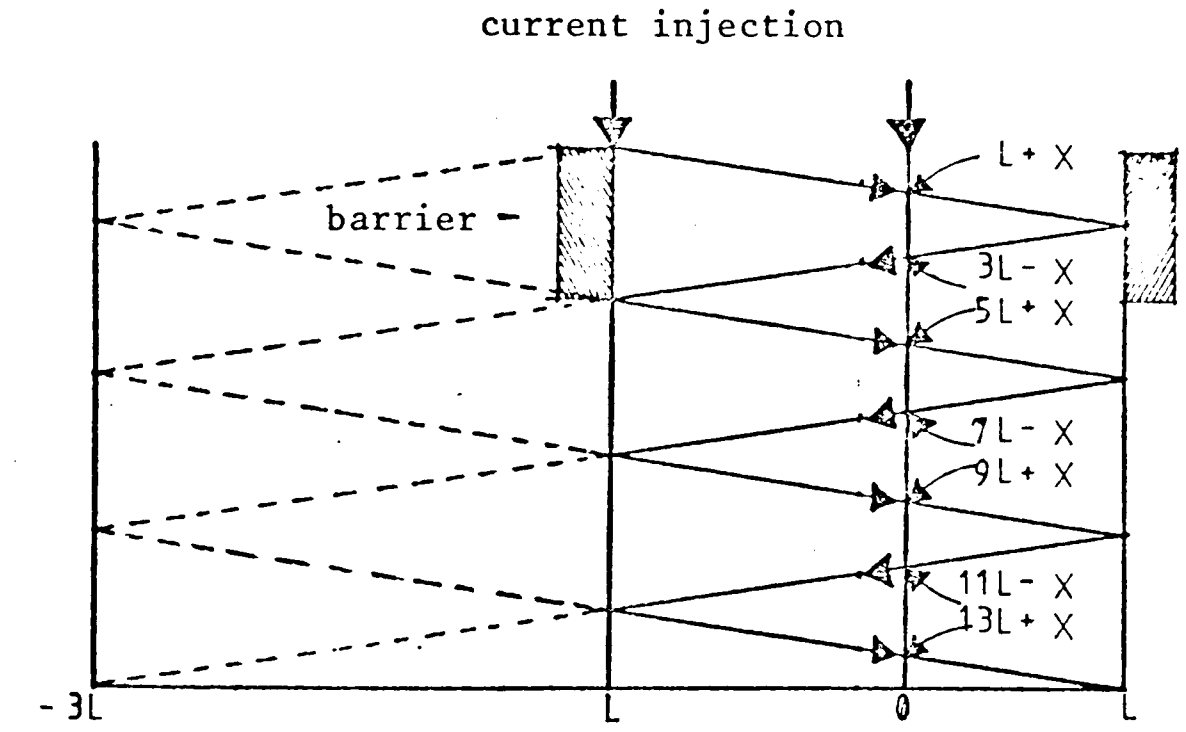

Figure 2.8. Voltage reflection pattern in asymmetric current injection. The broken lines represent the virtual reflections, i.e. those which would occur in a midpoint current injection in a cell of half length = 2λL.

ent injection current injection

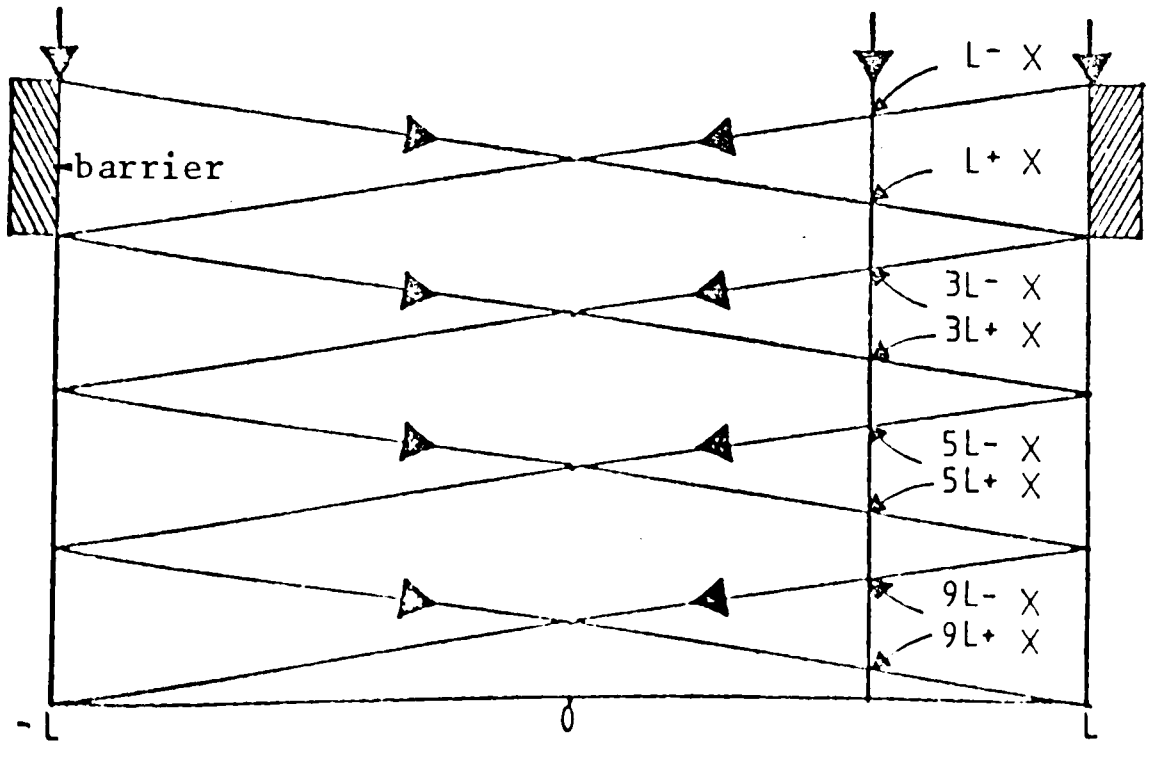

Figure 2.9. Voltage reflection pattern in a symmetric current injection.

Using the fact that $\frac{1}{1-e^{-2L}} = \sum_{o}^{\infty} e^{-2nL}$

then

$$\sum_{o}^{\infty} e^{-(2n+1)L} = \frac{1}{e^{L}-e^{-L}} = \frac{2}{\sinh(L)}$$

and $V(X,\infty)$ becomes

$$V(X,\infty) = \frac{I\lambda}{2} r_{oi} \frac{\cosh(L-X)}{\sinh(L)}$$

which is equation (2.6).

(2) Asymmetric external current injection

This was the technique used by Oda (15) and the patterns of the voltage reflections are shown in Figure 2.8. From this figure it can be seen that the path lengths of the reflections can be grouped in the following successions:

Set A = L+X, 5L+X, 9L+X, ... = $S(4nL+L+X)$ $n = 0,1,2,...$

Set B = 3L-X, 7L-X, 11L-X, .. = $S(4nL-L-X)$ $n = 1,2,3,...$

If the substitutions $\chi = X+L$ and $\zeta = 2L$ are now made then:

Set A = $S(2n\,\zeta+\chi)$ $n = 0,1,2,...$

Set B = $S(2n\,\zeta-\chi)$ $n = 1,2,3,...$.

These two equations are exactly the same as equations (2.9) and (2.10). Thus $V(\chi,T)$ for asymmetric current injection can be obtained from substituting X by $\chi-L$ and L by $\frac{\zeta}{2}$ in (2.8). For instance:

$$V(\chi,\infty) = \frac{I\lambda}{2} r_{oi} \frac{\cosh(\zeta-\chi)}{\sinh(\zeta)}$$

or

$$V(X,\infty) = \frac{I\lambda}{2} r_{oi} \frac{\cosh(L-X)}{\sinh(2L)} \quad . \qquad (2.11)$$

This expression corresponds to the case of a midpoint current injection in a cell of half length $2\lambda L$ and centred at $X = -L$ (see Figure 2.8).

(3) Symmetric external current injection

In this form of current application the magnitude of the current is exactly the same from the two side compartments to the central one (Kitasato, (16)). The voltage reflections for this case are shown in Figure 2.9. It can be seen that the path lengths of the reflections can be grouped as follows:

Set A = $L+X, 3L+X, 5L+X, \ldots = S((2n+1)L+X)$ $\quad n = 0,1,2\ldots$

Set B = $L-X, 3L-X, 5L-X, \ldots = S((2n+1)L-X)$ $\quad n = 0,1,2\ldots$.

Substituting $\chi = X+L$

Set A = $S(2nL+\chi)$ $\quad n = 0,1,2,\ldots$

Set B = $S(2nL-\chi)$ $\quad n = 1,2,3,\ldots$

which are again equations (2.9) and (2.10). The voltage response is then

$$V(\chi,\infty) = \frac{I\lambda}{2} r_{oi} \frac{\cosh(L-\chi)}{\sinh(L)}$$

or $$V(X,\infty) = \frac{I\lambda\, r_{oi}}{2} \frac{\cosh(X)}{\sinh(L)} \quad . \qquad (2.12)$$

Thus symmetric external current injection is equivalent to two point current injections in a cell of half length λL, one injection being made at $+L$ and the other at $-L$.

Note: Equations (2.6), (2.11) and (2.12) can also be obtained by appropriate solution of the cable equations (2.1) and (2.2). Differentiating equations (2.1) and (2.2) and considering steady state conditions, i.e. $\partial V/\partial T = 0$, gives:

$$\frac{\lambda^2 \partial^2 V}{\partial X^2} - V = 0 \quad \text{and} \quad \frac{\lambda^2 \partial^2 I}{\partial X} - I = 0 \ .$$

The solution of these equations are:

$$V(X) = A \cosh(X) + B(\sinh(X)) \tag{2.13}$$

$$I(X) = \frac{-B\lambda}{r_m} \cosh(X) - \frac{A\lambda}{r_m} \sinh(X) \ . \tag{2.14}$$

For case (1) the following boundary conditions apply:

At $X = 0$ $I(0) = I/2$, I being the injected current.

At $X = \pm L$ $I(-L) = I(+L) = 0$.

Hence $B = -\frac{Ir_m}{2\lambda}$ and $A = -B/\tanh(L)$ which upon substitution in equations (2.13) and (2.14) give:

$$V(X) = \frac{I\lambda}{2} r_{oi} \frac{\cosh(L-X)}{\sinh(L)} = \frac{V(0)\cosh(L-X)}{\cosh(L)} \text{ for } 0<X<L$$

or

$$V(X) = V(0) \frac{\cosh(L+X)}{\cosh(L)} \text{ for } -L<X<0 \ .$$

Similarly for case (2) the boundary conditions are

$$I(L) = 0 \quad \text{and} \quad I(-L) = I.$$

Thus $A = Ir_m/2\lambda\sinh(L)$ and $B = -A \tanh(L)$ which upon substitution into (2.13) and (2.14) gives:

$$V(X) = \frac{I\lambda}{2} r_{oi} \frac{\cosh(L-X)}{\sinh(2L)} = V(-L) \frac{\cosh(L-X)}{\cosh(2L)} \ .$$

For (3) the boundary conditions are: $I(0) = 0$ and $I(\pm L) = \pm I/2$. Thus $B = 0$ and $A = Ir_m/2$ and

$$V(X) = \frac{I\lambda}{2} r_{oi} \frac{\cosh(X)}{\sinh(L)} = V(-L) \frac{\cosh(X)}{\cosh(L)} .$$

The profiles of the membrane voltage response in each case are shown in Figure 2.10. Symmetrical current injection (V_1 and V_3) produces a better space clamping of the membrane potential than asymmetric current injection (curve V_2). The actual numerical values reproduced in the figure correspond to a cell segment of length 1 cm and $\lambda = 2$ cm.

2.6 The Measurements of R_m and C_m

With efficient space clamping the membrane resistance and capacitance can readily be computed. This is also true in the point current injection method, where the clamping is poor, provided the 0.42L technique is used. It will now be shown that this same technique can also be used with symmetric external current injection.

Equation (2.12) can be rewritten as

$$2\pi d\ell \frac{V(L-X)}{I} = 2\pi d\ell \frac{r_m}{2\lambda} \frac{\cosh(L-X)}{\sinh(L)}$$

thus $$R_m'(L-X) = KR_m$$

where $R_m'(L-X)$ is the resistance measured when the voltage is recorded at the point $L-X$ and K is the factor shown in Figure 2.6. Thus the uncorrected resistance R_m' will be equal to the corrected resistance if the voltage response is recorded at the point $L-X = 0.42L$, i.e. $X = 0.58L$.

The membrane capacitance can be computed from the values of the time constant $\tau_m = R_m C_m$. τ_m can be obtained by measuring the time required for $V(X,T)$ to acquire a value

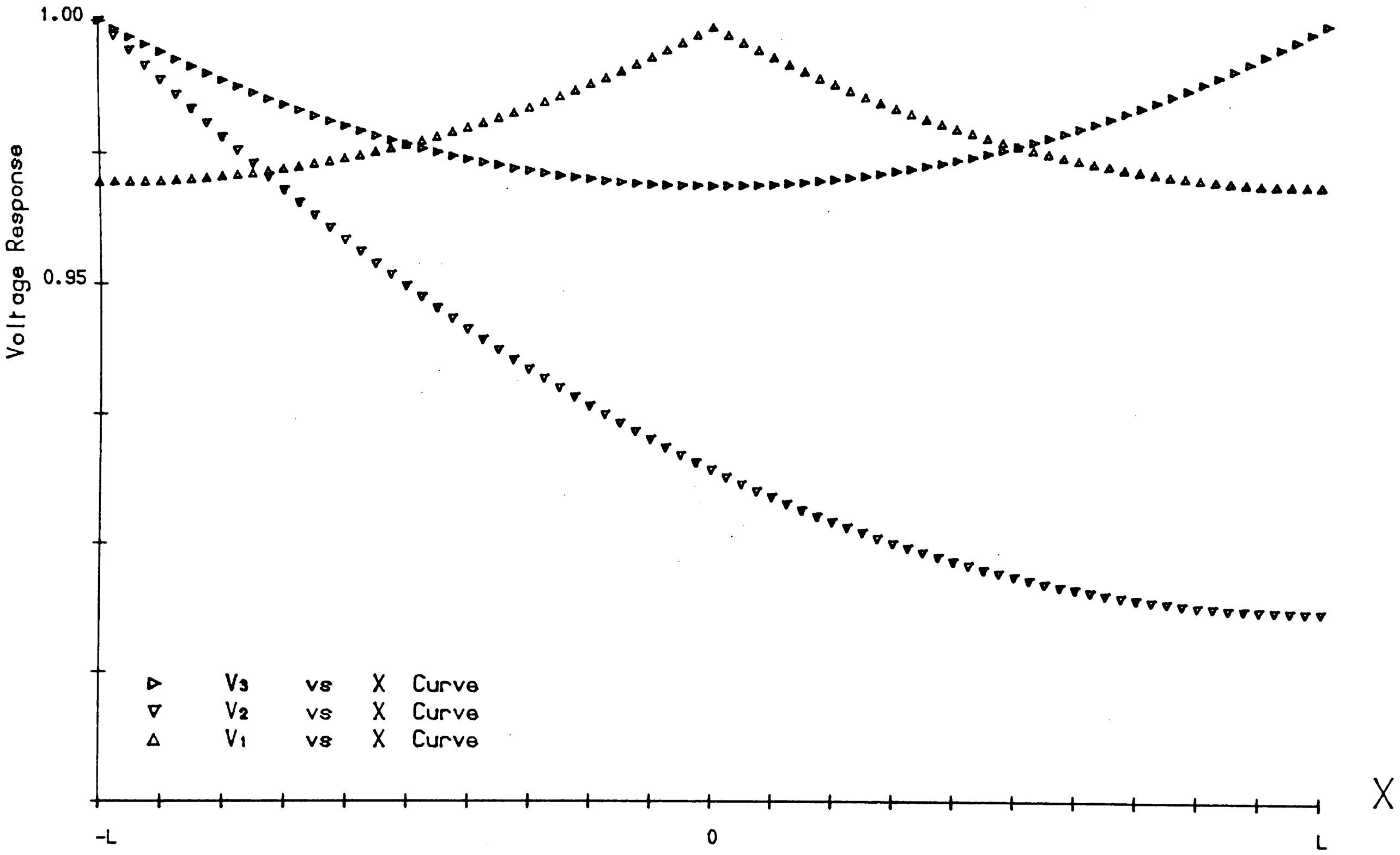

Figure 2.10 The voltage response profiles along the cells for the three different modes of current injection.

of $(\alpha.V(X,\infty))$. It is now convenient to consider the error that is introduced in the value of C_m by assuming $\alpha = 0.632$ at the points $X = (0.42 \pm 0.02)L$.

In Figure 2.11 the values of the ratios $\frac{V(0.44,T)}{V(0.44,\infty)}$, $\frac{V(0.42,T)}{V(0.42,\infty)}$ and $\frac{V(0.40,T)}{V(0.40,\infty)}$ are shown as functions of T and L. It can be seen that for $L = 1$ these ratios have values very close to 0.632 for $T = 1$. The third ratio acquires this value at $T = 1.01$. Thus the error in the C_m measurement will be less than 1%. For $L = 2$, $\frac{V(0.44,T)}{V(0.44,\infty)}$ has a value of 0.632 at $T = 1.07$. That is, an error of 7% would be introduced into the evaluation of the time constant if it is assumed that $\alpha = 0.632$. A similar analysis for $L = 3$ indicates that the error in the estimate of the capacitance will be 23%.

2.7 Comparison of the Different Techniques

It has been shown that good space clamping can be obtained in a short segment of Nitella cell when symmetric current injection is used. The effectiveness of the space clamping will be reduced if larger segments are considered or if, for some reason (e.g. membrane excitation), the membrane resistance decreases. When a long axial electrode is used there is a complete space clamping of the cell segment for any value of the membrane resistance. For this reason the axial electrode method has been regarded as a better technique than external current injection. It will be shown here that this is not necessarily the case for the Characeae. The axial electrode technique was originally developed for studies on nerve fibres. In this case it is

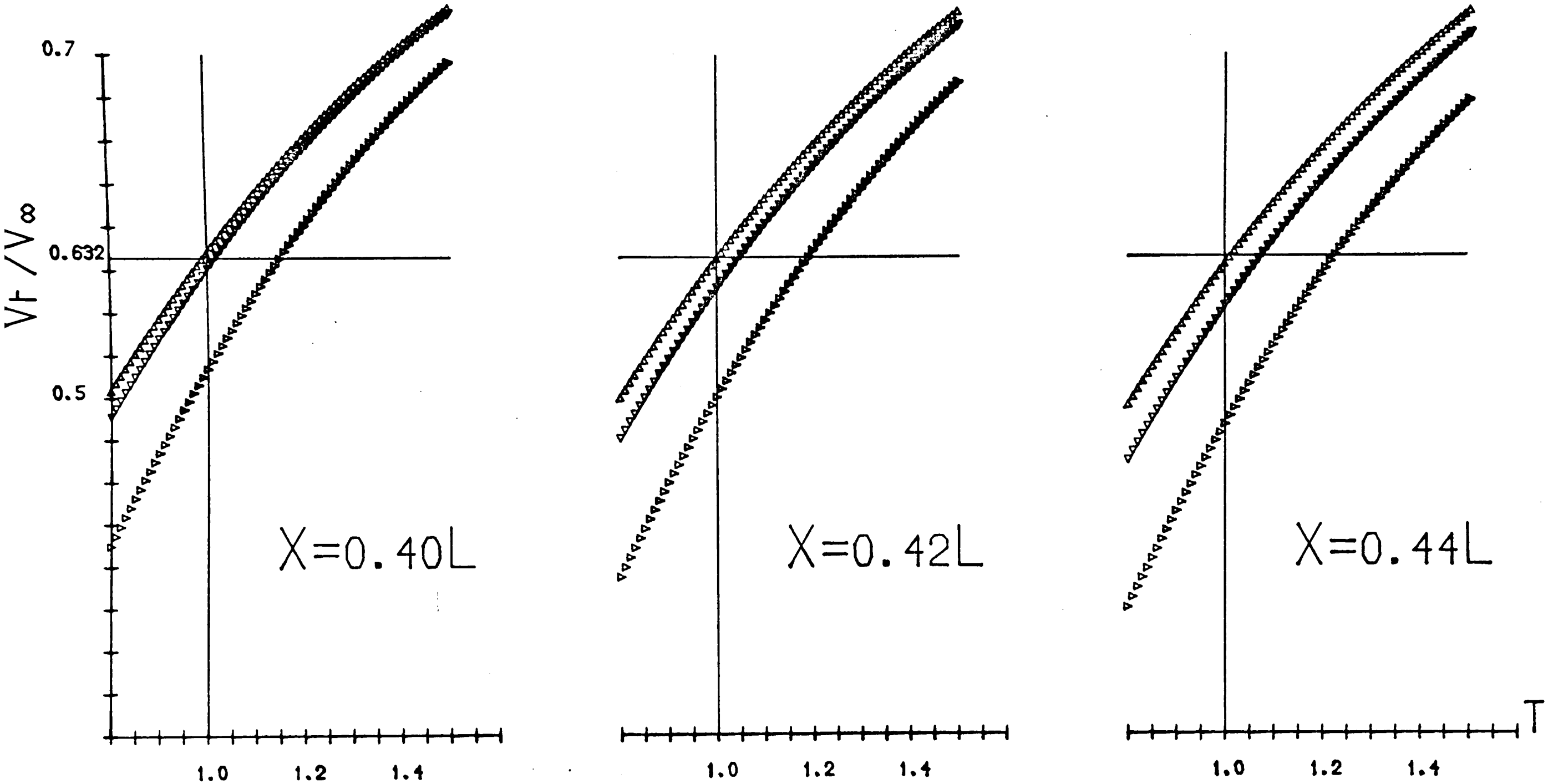
0.7
0.632
0.5
Vt /V∞
X=0.40L
X=0.42L
X=0.44L
1.0
1.2
1.4
T
▵ Vt/V∞ vs T Curve for L= 3.0
▽ Vt/V∞ vs T Curve for L= 2.0
△ Vt/V∞ vs T Curve for L= 1.0

Figure 2.11.

an indispensable tool since a λ value of 2 mm. would require extremely small cell segments to achieve reasonably efficient space clamping by any other method. On balance it is probably a more satisfactory method than the use of a point electrode. There are however some disadvantages:

a) The insertion of the long axial electrode is a major interference with the system. Considerable skill is required to avoid damaging the cell when such an electrode is inserted into the cell.

b) In intracellular current application the chemical reaction at the electrode surface occurs inside the cell. This reaction could produce unwarranted modifications to the cell sap. A quantitative estimation of the magnitude of these effects for the currents normally used with these experiments, is now presented.

1 μA of current is equivalent to 10^{-6} coulombs/sec or 0.623×10^{13} electrons/sec. Since there are N electrons in one mole (N is the Avogadro's number)

$$I = \frac{0.623 \times 10^{13}}{N} \text{ Moles/sec.}$$

for a univalent ion reaction.

In a cell of 10 cm. length and 1 mm. diameter this current will produce a change in the concentration of the ion involved at the rate of 3×10^{-7} moles/sec.

If the internal electrode is an Ag/AgCℓ wire with a good coating the only reaction occurring at its surface will be:

$$AgC\ell + e^- \rightleftarrows Ag + C\ell^- \quad .$$

Any reasonable current would have to be flowing for very long periods in order to affect the ≃100 mM chloride concentration of the cell sap. However, as Kitasato (18) suggests, the

situation will be rather different when platinum, iridium or tungsten electrodes are used. The reactions occurring at these electrodes are:

$$OH^- + OH^- \rightarrow \frac{1}{2}O_2 + 2e^- + H_2O$$

$$e^- + H^+ \rightarrow \frac{1}{2}H_2 \quad .$$

Thus changes in H^+ or OH^- concentrations at the rate of 3×10^{-7} moles/sec. will have strong effects on the cell pH, since this pH is $\simeq 5$ (Chapter VI). This effect will be very marked in voltage clamping experiments. In this case high currents are injected for relatively long periods. For instance, the clamping current required to balance the action potential is $\simeq 20\mu A$ and lasts for $\simeq 1$ sec. (Findlay (19)). This problem does not arise in nerve because its action potential is 10^4 times faster than in the Characeae.

The open vacuole technique has some more obvious disadvantages since substantial modifications of the system are involved:

a) The open cell is turgorless and there is a need for an osmoticum in the external solution and it has been shown (Rueskin (20)) that osmoticums can affect the ionic uptake.

b) The open cell has an open cytoplasm short circuited to the cell vacuole and probably no cytoplasmic streaming. This however does not seem to be very critical since the cells can survive for long periods.

The advantage of measuring the resistance of a non-perforated membrane was stressed by Tazawa et al. (13).

They compared the values of the resistance obtained by this method and the values obtained by the conventional microelectrode technique. The resistance of Nitella flexilis was higher when measured with the open vacuole technique In some cases the open vacuole resistance was twice the value of the resistances obtained by conventional microelectrodes. They point out that external recording electrode methods predict higher resistance values than microelectrode methods. They conclude that the open vacuole technique measures more faithfully the membrane resistance of the Characeae.

In order to assess the effect of perforation on the membrane resistance, part of this work is devoted to the determination of the ratio

$$\frac{R_a}{R_b} = \frac{\text{resistance before perforation}}{\text{resistance after perforation}}$$

in Nitella translucens. Such experiments are described in detail in Chapter 7. Their results indicate that the resistance recovers its original value one hour after insertion.

Asymmetric external current injection does not have the advantage of a complete space clamping, but a virtual space clamping can be obtained for reasonably short cell segments. There is of course the necessity for one perforating microelectrode but the perforation by such an electrode is unlikely to cause irreversible damage of the cell membrane. It is indeed the simplest technique of all, requiring no metal microelectrodes (see Chapter V) or special bathing solutions.

Kishimoto (21) states that it is convenient to use an internal electrode in order to eliminate the tangential flow of current along the membrane. Cole (22) had suggested that such a current flow might possibly introduce a surface capacitance. Taylor (23), however, stated that this possibility has been ruled out by the results of Taylor and Chandler in their measurements on squid axon membrane where both internal and external electrode methods predicted the same kind of membrane behaviour.

The limitation to the use of symmetric external current injection depends on the value of λ. A decrease in the value of λ reduces the effectiveness of the technique and such a reduction occurs during the action potential. However, it has been shown that for Nitella (Kishimoto (24, 25)) and Nitella translucens (Bradley (26)) the membrane resistance decreases by not more than a fivefold and the space constant will therefore decrease by not more than $\sqrt{5}$ of its resting value. Thus the external current injection technique will still be perfectly adequate if used in conjunction with the 0.42L technique. For Chara Brauni (Oda, (27)) the space constant decreases to one tenth of its resting value. In this case external current injection can still be used but shorter cell segments would be required. It should be mentioned that there could be states of the Nitella membrane where its resistance attains very low values, e.g., Coster (28) observed that when the Chara membrane is hyperpolarized it goes through a region of very low resistance. This is the punch-through effect.

2.8 Conclusions

The electrical models representing long cylindrical cells can be either an infinite leaky coaxial cable, e.g. nerve, or a short leaky coaxial cable terminated by infinite impedances, e.g. the Characeae. The solution of the cable equations appropriate to each model allows for the computation of the membrane parameters R_m and C_m. For the Characeae the assumption of a simple RC circuit can be made for short cell segments ($\simeq$ 1 cm. length). Furthermore, recording the voltage response at the particular point $X = 0.42L$ allows for the extension of the use of a simple Ohm's law calculation to longer cell segments. These conclusions were originally deduced for the case of current injection at the mid point of the cell. In the present work it has been shown that all current injection modes share the same mathematical solution but differ only in their boundary conditions. As a result the 0.42L technique can be extended to methods using external current injection. It has also been shown that this technique not only allows for easy and accurate computations of R_m but also of C_m.

Comparison of the different techniques indicates that symmetric external current injection in conjunction with the 0.42L technique seems to be the most adequate for studies on the Characeae. It involves the simplest of manipulative techniques and cell impalement and R_m and C_m can be computed as readily as in more sophisticated techniques. It provides a high degree of accuracy in measurements of the resting state parameters and is reasonably accurate for studies of the excited state. The error in R_m measurements

has been assumed to be small because of the closeness of the factor K to unity at $X = 0.42L$ for most values of L. A quantitative estimate of this error is presented in the next chapter, where the possibility of extending this technique to A.C. measurements is considered.

REFERENCES (CHAPTER II)

1) Cole, K.S. & Curtis, H.J., J. Gen. Physiol. 21, 189 (1938)

2) Hodgkin, A.L. & Rushton, W.A., Proc. Roy. Soc. B133, 444, (1946).

3) Hogg, J., Williams, E.J. & Johnston, R.J., J. Theoret. Biol. 24, 317 (1969).

4) Hogg, J., Ph.D. Thesis, Edinburgh University (1966).

5) Spanswick, R.M. & Costerton, J.W.F., J. Cell. Sci. 2, 451 (1967).

6) Bostrom, T.E. & Walker, N.A., J. Expt. Bot. 27, 97, 347 (1976).

7) Skierczyńska, J., J. Expt. Bot. 19, 59, 389 (1968).

8) Williams, E.J. & Fensom, D.S., J. Expt. Bot. 26, 95, 783 (1975).

9) Williams, E.J., Johnston, R.J. & Dainty, J., J. Expt. Bot. 15, 43, 1 (1964).

10) Hogg, J., Williams, E.J. & Johnston, R.J., Biochim. Biophys. Acta 150, 518 (1968).

11) Kishimoto, U., J. Gen. Physiol. 40, 5, 663 (1957).

12) Findlay, G.P., Nature (London) 191, 812 (1961).

13) Tazawa, M., Kikayama, M. & Nagakura, S., Plant and Cell Physiol. 16, 611 (1975).

14) Kishimoto, U., Biol. Bull. 121, 370 (1961).

15) Oda, K., The Science Reports of Tonoku University, Biology 26, 2 (1960).

16) Kitasato, H., J. Gen. Physiol. 52, 60, (1968).

17) Findlay, G.P., Aust. J. Biol. Sci. 17-2, 388 (1969).

18) Kitasato, H., Private oommunication.

19) Findlay, G.P., Aust. J. Biol. Sci. 17-2, 388 (1969).

20) Rueskin, A., Protoplastes et fusion des cellules somatiques végetales. Versailles (1972). Editions de l'Institute Nationale de la Recherche Agronomique (1973).

21) Kishimoto, U., Jap. J. Physiol. 24, 403 (1974).

22) Cole, K.S., Membranes, Ions and Impulses, University of California Press (1968).

23) Taylor, E.R., J. Cell. and Comp. Physiol., Suppl. 2, 66, 21 (1965).

24) Kishimoto, U., Plant & Cell Physiol. 7, 559 (1966).

25) Kishimoto, U., Ibid. 9, 559 (1968).

26) Bradley, J., Ph.D. thesis, Edinburgh University (1966).

27) Oda, K., The Science Reports of Tonoku University, Biology, 27, 187 (1961).

28) Coster, H.G.L., Biophys. J. 5, 6 (1965).

CHAPTER III

A.C. CABLE THEORY AND MEMBRANE IMPEDANCE MEASUREMENTS

In the previous chapter it was shown how measurements of the membrane resistance and capacitance can be made with the use of direct current (D.C.) It was also shown that without very good space clamping of the membrane the C_m values will be less accurate than those of R_m. This was first pointed out by Cole and Curtis (1). The difficulty that arises is in V(X,T) which has a form given by the error function and which is almost indistinguishable in the oscilloscope trace from a simple exponential form; thus the rise time of the simple RC circuit is easily confused with that due to cable effects. Cole and Curtis (1) advocated the use of A.C. methods for the determination of the membrane capacitance as a better alternative to D.C. methods. Since then A.C. methods have been used to advantage in many instances. Taylor (2) studied the behaviour of the membrane dielectric constant and went on to consider its implications for membrane structure. Kishimoto (3) and Skierczyńska, Żokniercznk and Bulanda (4) found that the membrane impedance measurements could not be explained by assuming a simple RC circuit model for the element $Y\Delta x$ and proposed a combination of parallel or series RC circuits. Coster and Smith (5) studied the membrane impedance responses to A.C. of low frequency. They concluded that R_m and C_m are both frequency dependent. If C_m is frequency dependent then A.C. methods would be the only means of providing meaningful measurements of this parameter.

In A.C. studies the cable behaviour of the cell has again to be taken into account in any experimental technique which is developed. Of the A.C. techniques which have been employed to date the one using a long axial electrode has been most favoured and this has allowed for the simple computation of $R_m(\omega)^{\dagger}$ and $C_m(\omega)$. An analysis of A.C. cable theory shows that the 0.42L and external current injection technique can be used to advantage in A.C. studies. This analysis involves the time dependent solution of the A.C. cable equations.

[$\dagger\omega = 2\pi f$, f being the A.C. frequency.]

3.1 The A.C. Time Dependent Solution of the Cable Equations

From Figure 2.3 it can be seen that equation (2.1) can be written as

$$\bar{I}(r_o + r_i) = \frac{\partial \bar{V}}{\partial x} \qquad (3.1)$$

where $\bar{I}$ is the A.C. current input and $\bar{V}$ the corresponding voltage response. Similarly equation (2.2) becomes:

$$\frac{\partial \bar{I}}{\partial x} = \frac{\bar{V}}{z} \qquad (3.2)$$

where $z = r_m/(1 + j\omega c_m r_m)$ is the impedance times unit length length of the membrane and $j = \sqrt{-1}$.

The complex space constant, λ_c, is given by

$$\lambda_c^2 = \lambda^2(1 + j\omega\tau_m)^{-1} = \frac{z}{r_{oi}} .$$

Defining $X_c = x/\lambda_c$ and $L_c = \ell/\lambda_c$ and differentiating equations (3.1) and (3.2) gives:

$$\frac{\partial^2 \bar{V}}{\partial X_c^2} = \bar{V} \quad \text{and} \quad \frac{\partial^2 \bar{I}}{\partial X_c^2} = \bar{I} .$$

The solutions of these equations are

$$\bar{V} = Ae^{-X_c} + Be^{X_c} \tag{3.3}$$

$$\bar{I} = Ce^{-X_c} + De^{X_c} \quad . \tag{3.4}$$

Using the condition

$$\frac{\partial \bar{I}}{\partial X_c} = \bar{V} \frac{\lambda_c}{z}$$

then $-C = A\lambda_c/z$ and $D = B\lambda_c/z$.

Thus

$$\bar{I} = -A \frac{\lambda_c}{z} e^{-X_c} + B \frac{\lambda_c}{z} e^{X_c} \quad .$$

For the case of midpoint current injection the boundary conditions are:

At $x = 0$ $\bar{I}(X_c) = \bar{I}/2$ and at $x = \ell$ $I(X_c) = 0$.

Thus $A = \frac{\bar{I}}{2} \frac{z}{\lambda_c} \frac{e^{2L_c}}{(1-e^{2L_c})}$

and $B = \frac{\bar{I}}{2} \frac{z}{\lambda_c} (1 - e^{2L_c})^{-1}$.

Substitution in equation (3.3) gives

$$\bar{V} = \frac{\bar{I}}{2} \frac{z}{\lambda_c} \left(\frac{e^{2L_c - X_c} + e^{X_c}}{1 - e^{2L_c}} \right)$$

$$\therefore \quad \bar{V} = \frac{\bar{I}}{2} \lambda_c r_{oi} \frac{\cosh(L_c - X_c)}{\sinh(L_c)} \tag{3.5}$$

where I can be expressed in the form $\bar{I} = Ie^{j\omega t}$.

3.2 A.C. Time Independent Case

If it is assumed, as did Williams, Johnston and Dainty (6), that R_m is independent of frequency then C_m can be computed from the expression for the amplitude of the voltage response V. This amplitude can be obtained as follows:

Rewriting equation (3.5) as

$$\bar{V} = \frac{\bar{I}\, e^{j\omega t}\lambda r_{oi}}{2p} \quad \frac{\cosh(p(L-X))}{\sinh(pL)} \tag{3.6}$$

where $p = (1 + j\omega\tau)^{\frac{1}{2}} = ce^{jd}$

and $c = (1 + \omega^2\tau^2)^{\frac{1}{4}}$ and $d = \frac{1}{2}\tan^{-1}(\omega\tau)$. (3.7)

Thus

$$\bar{V} = \frac{I}{2}\frac{\lambda r_{oi}}{c} \quad \frac{\cosh(ce^{jd}(L-X))}{\sinh(ce^{jd}L)}\, e^{j(\omega t-d)}$$

$$= \frac{I}{2}\frac{r_{oi}}{c}\left[\frac{\left[\cosh\left[c(L-X)(\cos d + j\sin d)\right]\right]}{\sinh\left[cL(\cos d + j\sin d)\right]}\right] e^{j(\omega t-d)} .$$

Writing

$$\left.\begin{aligned} c(L-X)\cos d &= q, \quad c(L-X)\sin d = s \\ cL\cos d &= m \quad \text{and} \quad cL\sin d = n \end{aligned}\right\} \tag{3.8}$$

then

$$\frac{\left[\cosh\, c(L-X)(\cos d + j\, \sin d)\right]}{\left[\sinh\, cL(\cos d + j\, \sin d)\right]} = \frac{\cosh(q + js)}{\sinh(m + jn)}$$

$$= \frac{\cosh q \cosh js + \sinh q \sinh js}{\sinh m \cosh jn + \cosh m \sinh jn}$$

$$= \frac{\cosh q \cos s + j \sinh q \sin s}{\sinh m \cos n + j \cosh m \sin n}$$

which on multiplying both numerator and denominator by

(sinh m cos n - j cosh m sin n) becomes

$$\frac{\cosh q \sinh m \cos n \cos s + \sinh q \cosh m \sin n \sin s + j(\sinh q \sinh m \sin s \cos n - \cosh q \cosh m \sin n \sin s)}{\sinh^2 m \cos^2 n + \cosh^2 m \sin^2 n}$$

which has the form $Ae^{j\theta}$ where

$$\theta = \tan^{-1}\left\{\frac{\sinh q \sinh m \sin s \cos n - \cosh q \cosh m \sin n \cos s}{\cosh q \sinh m \cos n \cos s + \sinh q \cosh m \sin n \sin s}\right\} \quad (3.9)$$

and

$$A = \frac{\left[(\cosh q \sinh m \cos n \cos s + \sinh q \cosh m \sin n \sin s)^2 + (\sinh q \sinh m \sin s \cos n - \cosh q \cosh m \sin n \cos s)^2\right]^{\frac{1}{2}}}{\sinh^2 m + \sin^2 n}$$

$$\therefore \quad A = \left(\frac{\sinh^2 q + \cos^2 s}{\sinh^2 m + \sin^2 n}\right)^{\frac{1}{2}}$$

Finally equation (3.5) can be written as

$$\bar{V} = \frac{I}{2}\left[\frac{\lambda r_{oi}}{c} \frac{\sinh^2 q + \cos^2 s}{\sinh^2 m + \sin^2 n}\right]^{\frac{1}{2}} \cos(\omega t - d - \theta) \; . \quad (3.10)$$

The amplitude of equation (3.8) is then

$$V = \frac{I\lambda r_{oi}}{2(1+\omega^2\tau^2)^{\frac{1}{4}}} \left[\frac{\sinh^2 q + \cos^2 s}{\sinh^2 m + \sin^2 n}\right]^{\frac{1}{2}} \quad (3.11)$$

This expression was used by Williams et al. (6) to compute the value of C_m. They measured the amplitudes of the voltage responses at two known distances from the current injecting electrode. From the ratio of these amplitudes and the values of R_m and λ, obtained from D.C. measurements on the same cell, they calculated the membrane capacitance.

There are some obvious disadvantages in this approach:

(a) two internal voltage recording electrodes are required,

(b) it is necessary to compute the values of R_m and λ from D.C. experiments, (c) equation (3.11) has to be solved

numerically by a tedious trial and error method. These disadvantages can be circumvented by short cell methods. The length of the cell segment for which A.C. cable effects can be safely ignored can be computed with the aid of equation (3.11). This was first done by Śkierczinska et al. (4) who considered the voltage response at $x = 0$ in which case equation (3.11) becomes

$$\bar{V} = \frac{I}{2} \lambda_c r_{oi} (\coth(L_c) \quad .$$

These authors stated that $\coth(L_c) \simeq 1$ for a 1 cm. segment of Nitellopsis obtusa when used in a frequency range from 20 to 1000 Hz. The numerical behaviour of this factor is not however reported. It will be recalled that Hogg, Williams and Johnston (7) found a similar factor in their D.C. measurements and its numerical behaviour allowed for the development of the 0.42L technique. It should be possible to adopt a similar approach in A.C. studies. However, it must be noted that in the event of R_m being frequency dependent the D.C. value of R_m and λ can no longer be used for solving equation (3.11). Moreover equation (3.11) cannot be solved alone since it involves two unknowns, R_m and C_m. A second physical condition relating R_m and C_m is therefore required. The most obvious relationship comes through the phase angle.

3.3 The Phase Angle of the A.C. response

Equation (3. 11) is of the form

$$\bar{V}(X,t) = V \cos(\omega t + \phi)$$

where the phase angle $\phi = \theta - d$ and θ is given by expression

(3.9). This can be rewritten as:

$$\theta = \tan^{-1}\left[-\frac{\left[\cosh(q+m)\sin(n-s) + \cosh(q-m)\sin(n+s)\right]}{\sinh(m+q)\cos(n-s) - \sinh(q-m)\cos(n+s)}\right] .$$

Defining $L' = cL$ and $X' = cX$ and using equations (3.8)

$$-\theta = \tan^{-1}\left[\frac{\cosh(2L'-X')\cos d)\sin(X'\sin d) + \cosh(X'\cos d)\sin(2L'-X')\sin d)}{\sinh(2L'-X')\cos d)\cos(X\sin d) + \sin R(X'\cos d)\cos(2L'-X')\sin d)}\right] \tag{3.12}$$

Similarly equation (3.11) becomes

$$V = \frac{I}{2}\frac{\lambda r_{oi}}{(1+\omega^2\tau^2)^{\frac{1}{4}}}\left[\frac{\sinh^2((L'-X')\cos d + \cos^2(L'-X')\sin d}{\sinh^2(L'\cos d) + \sin^2(L'\sin d)}\right]^{\frac{1}{2}} \tag{3.13}$$

Finally

$$\bar{V}(X',t) = V(\cos(\omega t - (\tfrac{1}{2}\tan^{-1}(\omega\tau) - \theta)) . \tag{3.14}$$

3.4 Special Cases of $\bar{V}(X',t)$

It is of intrinsic interest to consider the effect on $V(X',t)$ of imposing limiting values on the various parameters because it allows comparison of $V(X',t)$ with known solutions and thus corroborates the general expression.

a) The D.C. steady state case ($\omega = 0$)

In this case equation (3.14) becomes

$$V = \frac{I}{2}\lambda r_{oi}\left(\frac{\sinh^2(L-X) + 1}{\sinh^2 L}\right)^{\frac{1}{2}}\cos(\theta)$$

$$= \frac{I}{2}\lambda r_{oi}\frac{\cosh(L-X)}{\sinh L}\cos(\theta) .$$

But $\theta = 0$ in this case and the above equation is then the same as equation (2.6).

b) The A.C. case for an infinite line $(L \to \infty)$

It is the parameter L' rather than the actual cell length 2ℓ which determines whether the cable approaches an infinite line; L' will increase its value when either $\lambda \to 0$ or $\omega \to \infty$.

Equation (3.13) can be written as:

$$V = \frac{I}{2} \frac{\lambda r_{oi}}{(1+\omega^2\tau^2)^{\frac{1}{4}}} \times \left[\frac{(e^{(L'-X')\cos d} - e^{-(L'-X')\cos d})^2 + \cos^2((L'-X')\sin d)}{(e^{L'\cos d} - e^{-L'\cos d})^2 + \sin^2(L'\sin d)} \right]^{\frac{1}{2}}$$

$$= \frac{I}{2} \frac{\lambda r_{oi}}{(1+\omega^2\tau^2)^{\frac{1}{4}}} \times \left[\frac{e^{-2X'\cos d} + e^{-2L'\cos d} + e^{-2L'\cos d} \cos^2((L'-X')\sin d)}{1 + e^{-4L'\cos d} + e^{-2L'\cos d} \sin^2(L'\sin d)} \right]^{\frac{1}{2}}$$

If $L \to \infty$ then

$$V = \frac{I}{2} \frac{\lambda r_{oi}}{(1+\omega^2\tau^2)^{\frac{1}{2}}} e^{-X'\cos d} .$$

Similarly writing

$$\theta = -\tan^{-1} \left[\frac{(e^{(2L'-X')\cos d} + e^{(-2L'-X')\cos d})\sin(X'\sin d) + (e^{X'\cos d} + e^{-X'\cos d})\sin((2L'X')\sin d)}{(e^{(2L'-X')\cos d} - e^{-(2L'-X'\cos d})\cos(X'\sin d) + (e^{X'\cos d} - e^{-X'\cos d})\cos((2L'-X')\sin d)} \right]$$

Thus as L' and $L'-X' \to \infty$

$$\theta = \tan^{-1}(\tan X' \sin d) = X' \sin d .$$

Thus the time dependent solution for A.C. in an infinite line is:

$$V(X',t) = \frac{\lambda r_{oi}}{(1+\omega^2\tau^2)^{\frac{1}{4}}} e^{-X'\cos d}\cos(\omega t - \tfrac{1}{2}\tan^{-1}(\omega\tau) - X'\sin(\tfrac{1}{2}\tan^{-1}(\omega\tau)) .$$

c) The A.C. case for a short cell ($L' \to 0$)

Equations (3.12) and (3.13) are the expressions from which the numerical values of R_m and C_m have to be computed. These expressions are formidable and do not allow for ready and easy estimation of R_m and C_m. Clearly it is desirable to avoid such cumbersome computations and this can be achieved by using a short cell method. For this method to be a viable proposition it is necessary, as it was in the D.C. case, to examine the numerical behaviour of $V(X',t)$ in order to determine the optimum length of the cell segment. For a short cell $L' \to 0$ and $V(X',t)$ should approximate in some way to the equivalent expression which would be obtained for the circuit

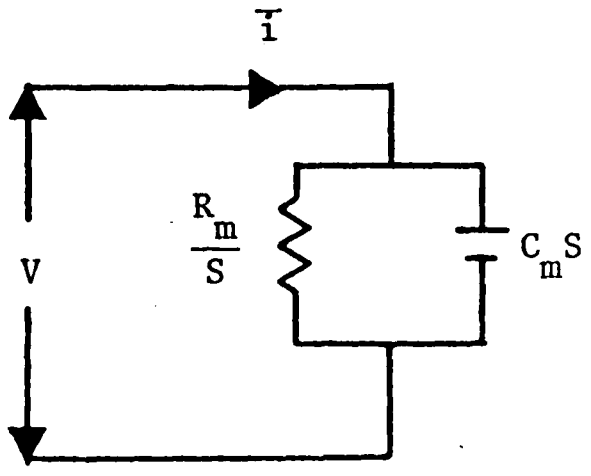

where S = area of segment.

For such a circuit the impedance is given by

$$\frac{1}{Z} = \frac{S}{R_m} + j\ C_m S$$

or $$Z = \frac{R_m}{S}(1+\omega^2\tau^2)^{-\frac{1}{2}} e^{-j\tan^{-1}(\omega\tau)} .$$

$$\bar{V} = \bar{I}Z = \frac{I}{S} R_m (1+\omega^2\tau^2)^{-\frac{1}{2}} e^{j(\omega t-\tan^{-1}(\omega\tau)}$$

$$\therefore \quad V(X,t) = \mathrm{Re}(\bar{V})$$

$$\text{and} \quad V(X,t) = \frac{I R_m}{S}(1+\omega^2\tau^2)^{-\frac{1}{2}}\cos(\omega\tau - \tan^{-1}(\omega\tau)). \qquad (3.15)$$

It is now necessary to express equation (3.14) in a form similar to equation (3.15) and to see if it becomes equation (3.15) as $L' \to 0$.

Equation (3.13) can be rewritten as

$$V4\pi r\ell = \frac{r_m I 4\pi r}{2\lambda(1+\omega^2\tau^2)^{\frac{1}{2}}} \times \left(\frac{(1+\omega^2\tau^2)^{\frac{1}{4}}}{\lambda}\right)\ell\left(\frac{\sinh^2((L'-X')\cos d)+\cos^2((L'-X')\sin d)}{\sinh^2(L'\cos d)+\sin(L'\sin d)}\right)$$

$$\therefore \quad V = \frac{R_m}{S(1+\omega^2\tau^2)^{\frac{1}{2}}} \; Kl$$

$$\text{where} \quad Kl = L'\left(\frac{\sinh^2((L'-X')\cos d + \cos((L'-X')\sin d)}{\sinh^2(L'\cos d) + \sin(L'\sin d)}\right) \qquad (3.16)$$

$$\text{Similarly} \quad -\phi = \tfrac{1}{2}\tan^{-1}(\omega\tau) + \theta = \tan^{-1}(\omega\tau)K2 \qquad (3.17)$$

$$\text{where} \quad K2 = \frac{\tan^{-1}(\omega\tau) + 2\theta}{2\tan^{-1}(\omega\tau)} \; . \qquad (3.18)$$

Thus

$$V(X',t) = \frac{I R_m Kl}{S(1+\omega^2\tau^2)^{\frac{1}{2}}}\cos(\omega\tau - \tan^{-1}(\omega\tau)K2) \; .$$

Hence equation (3.14) becomes equation (3.15) as Kl and $K2 \to 1$. Rewriting Kl as

$$Kl = \left(\frac{\sinh^2((L'-X')\cos d + \cos^2((L'-X')\sin d}{\cos^2 d\,\frac{\sinh^2(L'\cos d)}{L'^2\cos^2 d} + \sin^2 d\,\frac{\sin^2(L'\sin d)}{L'^2\sin^2 d}}\right)$$

it can be seen that $Kl \to 1$ as $L' \to 0$. Similarly from

$$\theta = \tan^{-1}\left(\frac{X'\sin d + 2L'\sin d - X'\sin d}{2L'\cos d - X'\cos d + X'\cos d}\right)$$

it can be seen that $K2 \rightarrow 1$ as $L' \rightarrow 0$.

Thus $V(X',t)$ approaches the form corresponding to a simple RC circuit when the cell length is reduced. The approximation of a short cell segment to a single RC circuit depends ultimately on the numerical values of factors K1 and K2. It should then be possible to obtain a quantitative estimate of the accuracy in the R_m and C_m values when a given segment is treated as a short cell. It is also convenient to see if the factors K1 and K2 behave in a similar way to the factor K in the D.C. case. This would allow for the extension of the 0.42L technique to A.C. studies.

3.5 The Numerical Behaviour of $\bar{V}(X',t) = V\cos(\omega t+\phi)$

In this work external current injection is used and the numerical computations were performed on the equations corresponding to this case. In Chapter II it was shown that the equations corresponding to symmetric external current injection can be obtained from the equations derived for midpoint current injection by the simple expedient of substituting $X = X+L$; in the present A.C. case the appropriate substitution is $X' = X' + L'$. Thus equations (3.12), (3.13), (3.16) and (3.18) become

$$V = \frac{I\lambda r_{oi}}{2(1+\omega^2\tau^2)^{\frac{1}{4}}} \left[\frac{\sinh^2(X'\cos d) + \cos^2(X'\sin d)}{\sinh^2(L'\cos d) + \sin^2(L'\sin d)}\right]^{\frac{1}{2}} \qquad (3.19)$$

$$\theta = -\tan^{-1}\left[\frac{\cosh((L'-X')\cos d)\sin((X'+L')\sin d) + \cosh((X'+L')\cos d)\sin((L'-X')\sin d)}{\sinh((L'-X')\cos d)\cos((X'+L')\sin d) + \sinh((X'+L')\cos d)\cos((L'-X')\sin d)}\right] \qquad (3.20)$$

$$K1 = L' \left[\frac{\sinh^2(X'\cos d) + \cos^2(X'\sin d)}{\sinh^2(L'\cos d) + \sin^2(L'\sin d)} \right] \tag{3.21}$$

$$K2 = \frac{\tan^{-1}(\omega\tau) + 2\theta}{2\tan^{-1}(\omega\tau)} \tag{3.22}$$

In the following computations the numerical values of $R_{m_{cm}}$, C_m and λ are assumed to be 20 KΩ × cm², 1 μf/cm² and 2λ respectively. These are typical resting state values for Nitella translucens.

a) The space clamping behaviour

The profile of the amplitude of the voltage response (equation (3.19)) along the length of the cell can be expressed in terms of the response at points $X' = \pm L'$, in a similar way to that shown in Figure 2.10.

Substituting $X'=L'$ in equation (3.19)

$$V_{L'} = \frac{I}{2} \frac{\lambda r_{oi}}{(1+\omega^2\tau^2)^{\frac{1}{4}}} \left[\frac{\sinh^2(L'\cos d) + \cos^2(L'\sin d)}{\sinh^2(L'\cos d) + \sin^2(L'\sin d)} \right]^{\frac{1}{2}}$$

$$\therefore \quad V = V_{L'} \left[\frac{\sinh^2(X'\cos d) + \cos^2(X \sin d)}{\sinh^2(L'\cos d) + \cos^2(L'\sin d)} \right]^{\frac{1}{2}} \tag{3.23}$$

The profile of the voltage response $\bar{V}(X',t)$ can be expressed in terms of the amplitude $V_{L'}$ and the time $t' = \phi(L')/\omega$, this being the time at which $V_{L'}$ is attained:

$$\bar{V}(X',t'=\phi(L')/\omega) = V_{L'} \left[\frac{\sinh^2(X'\cosd + \cos^2(X'\sind)}{\sinh^2(L'\cosd) + \cos^2(L'\sind)} \right]^{\frac{1}{2}} \cos(\phi-\phi(L'))$$

or, substituting for $\phi(L')$,

$$\bar{V}(X',\phi(L')/\omega) = V_{L'} \left[\frac{\sinh(X'\cosd) + \cos(X'\sind)}{\sinh(L'\cosd) + \cos(L'\sind)} \right]^{\frac{1}{2}} \times$$

$$\cos\left[\theta - \tan^{-1}\left[\frac{\sin(2L'\sind)}{\sinh(2L'\cos d} \right] \right] \tag{3.24}$$

The profiles of $V(X')$ and $\bar{V}(X',t')$ are shown in Figures 3.1 and 3.2. They show the space clamping for a cell segment of length 1 cm. and for different values of the frequency f. Figures 3.3 and 3.4 show the same profiles for f = 10 Hz and different values of ℓ, the cell segment length.

The actual space clamping of the cell is given by $\bar{V}(X',t')$ since $V(X')$ will be attained at different times for different values of X'. $\bar{V}(X',t')$ decreases with X' more quickly than does $V(X')$. This is because, in addition to the decrease in amplitude, $\bar{V}(X',t')$ shows also the dependence of the phase angle on X', i.e., in the term $\cos(\theta-\theta(L'))$. This cosine dependence will produce a space wave in addition to the time wave produced by A.C. Numerical computation shows that this effect, characteristic of transmission lines, would appear in Nitella translucens only at very high frequencies (>100 K Hz).

b) The phase angle behaviour

The numerical behaviour of the phase angle is shown in Figures 3.5 and 3.6. (In Figure 3.5 ℓ=1 cm and in Figure 3.6 f = 10 Hz.) It can be seen that there is a strong dependence of ϕ on X' when ℓ is increased. However there is a region around 0.58L where this dependence is very small. This suggests that the 0.42L technique can be extended to A.C. studies. (Note: In Chapter II it was shown that the particular behaviour occurring at 0.42L for midpoint current injection occurs at 0.58L for symmetric external current injection.)

c) The behaviour of the factors K1 and K3

An assessment of the validity of the assumption of a single RC circuit for a given segment can be obtained from the numerical

Figure 3.1.

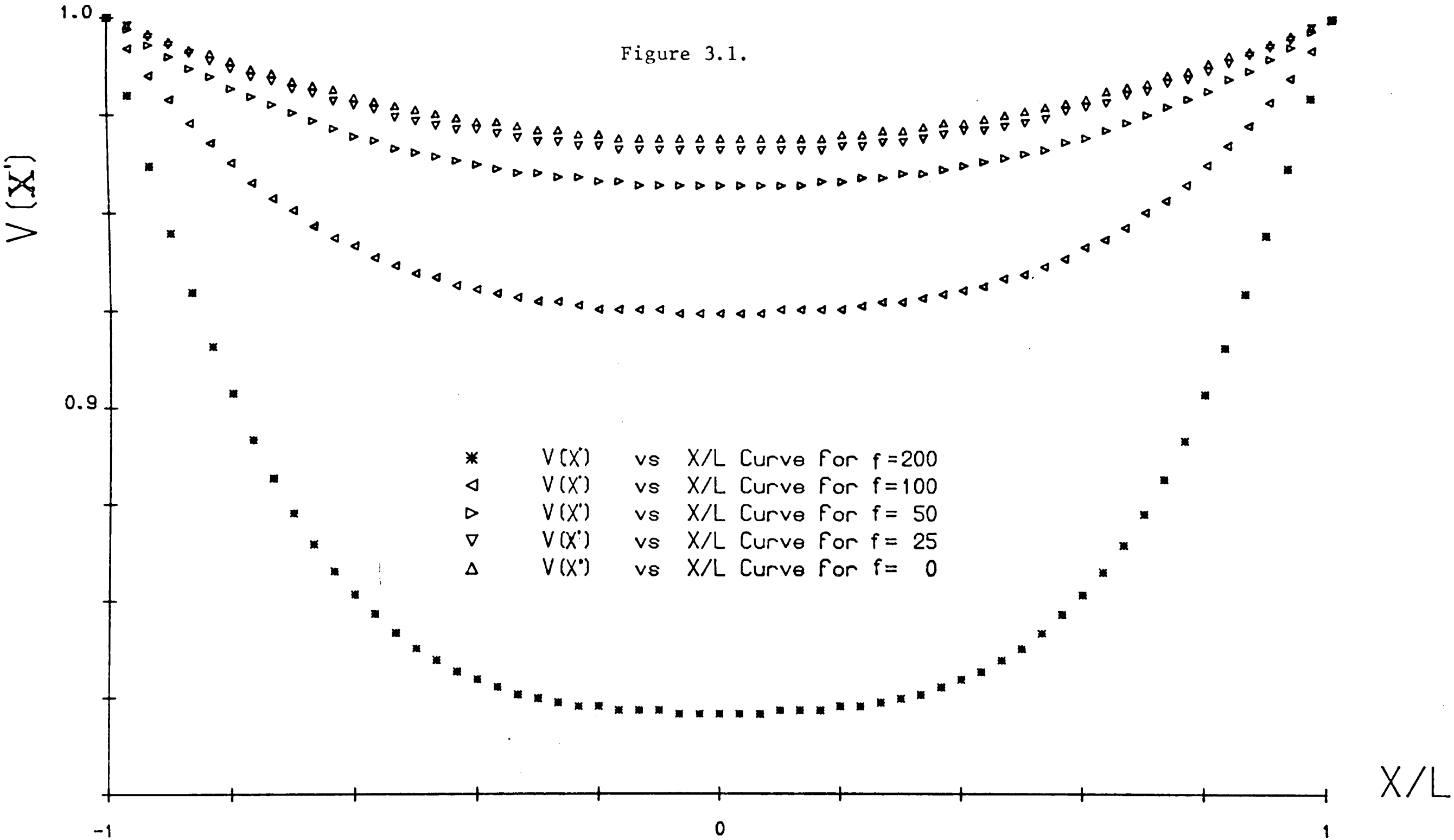
1.0
0.9
V(X')
X/L
-1
0
1
* V(X') vs X/L Curve for f=200
◁ V(X') vs X/L Curve for f=100
▷ V(X') vs X/L Curve for f= 50
▽ V(X') vs X/L Curve for f= 25
△ V(X') vs X/L Curve for f= 0

Figure 3.2.

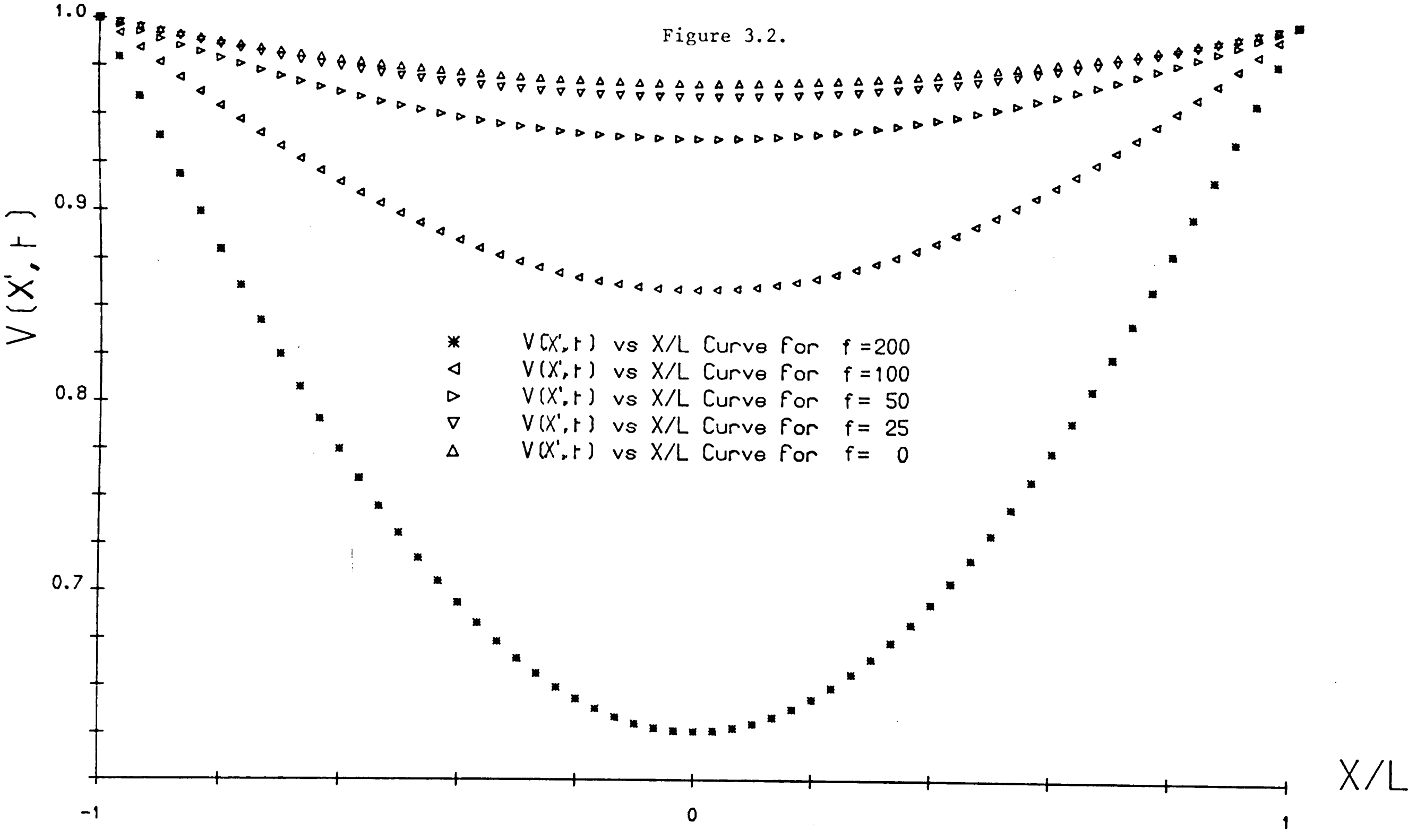
1.0
0.9
0.8
0.7
V(X',f)
X/L
-1
0
1
V(X',f) vs X/L Curve for f =200
V(X',f) vs X/L Curve for f =100
V(X',f) vs X/L Curve for f= 50
V(X',f) vs X/L Curve for f= 25
V(X',f) vs X/L Curve for f= 0

Figure 3.3.

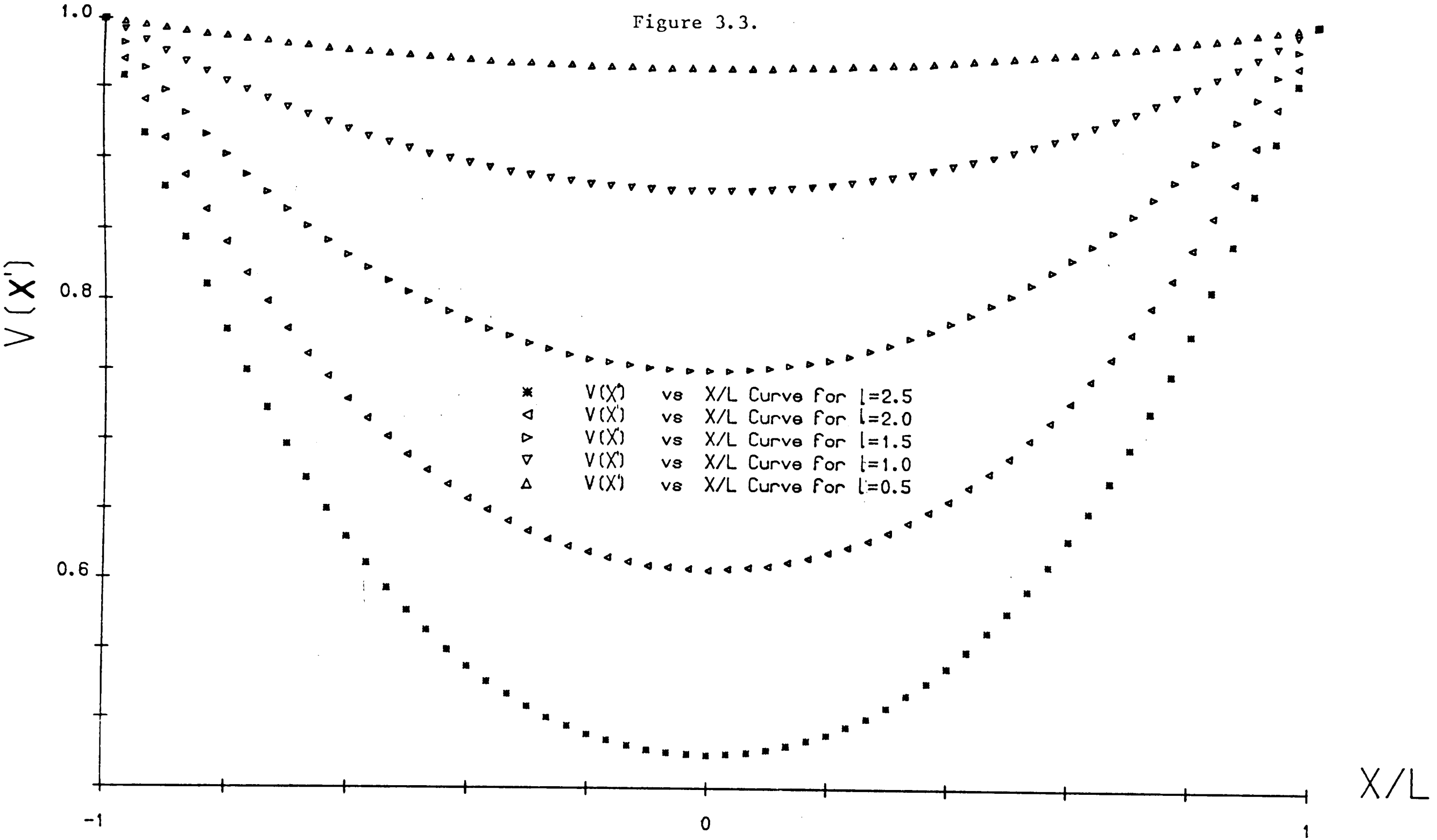
1.0
0.8
0.6
V(X')
X/L
-1
0
1
V(X') vs X/L Curve for l=2.5
V(X') vs X/L Curve for l=2.0
V(X') vs X/L Curve for l=1.5
V(X') vs X/L Curve for l=1.0
V(X') vs X/L Curve for l=0.5

Figure 3.4.

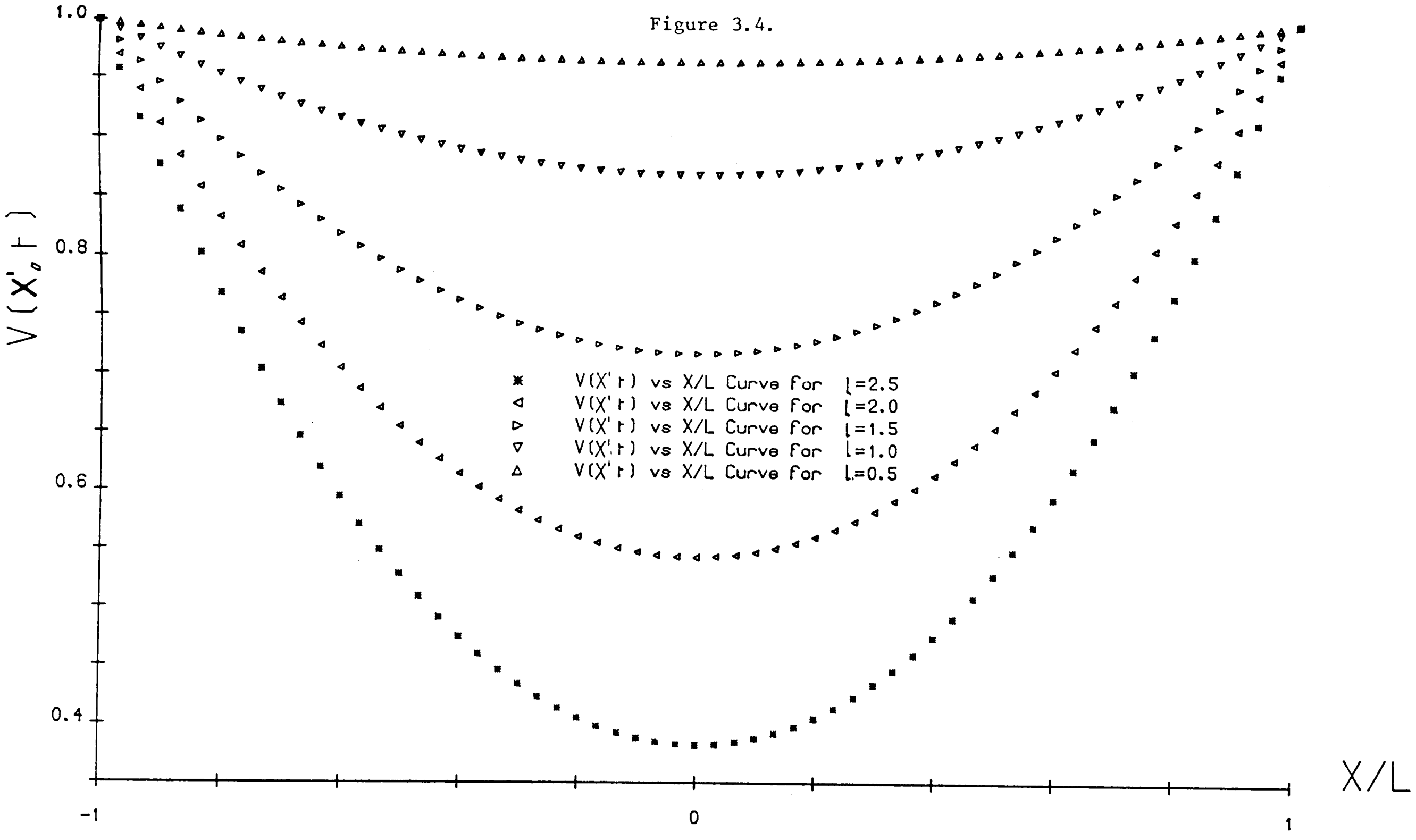
1.0
0.8
0.6
0.4
V(X',f)
-1
0
1
X/L
V(X',f) vs X/L Curve for L=2.5
V(X',f) vs X/L Curve for L=2.0
V(X',f) vs X/L Curve for L=1.5
V(X',f) vs X/L Curve for L=1.0
V(X',f) vs X/L Curve for L=0.5

Figure 3.5.

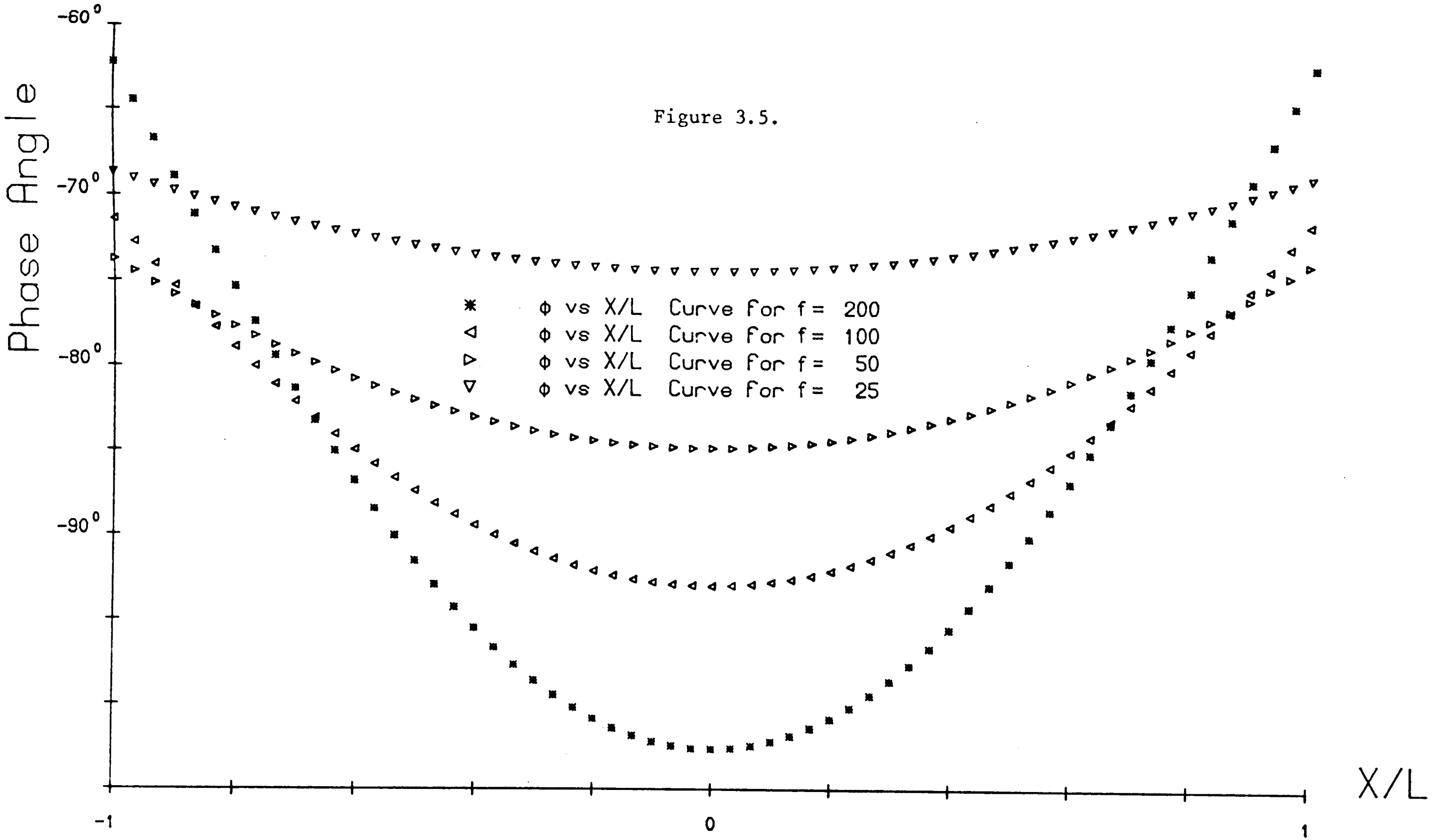
Phase Angle
-60°
-70°
-80°
-90°
* Φ vs X/L Curve for f = 200
◁ Φ vs X/L Curve for f = 100
▷ Φ vs X/L Curve for f = 50
▽ Φ vs X/L Curve for f = 25
-1
0
1
X/L

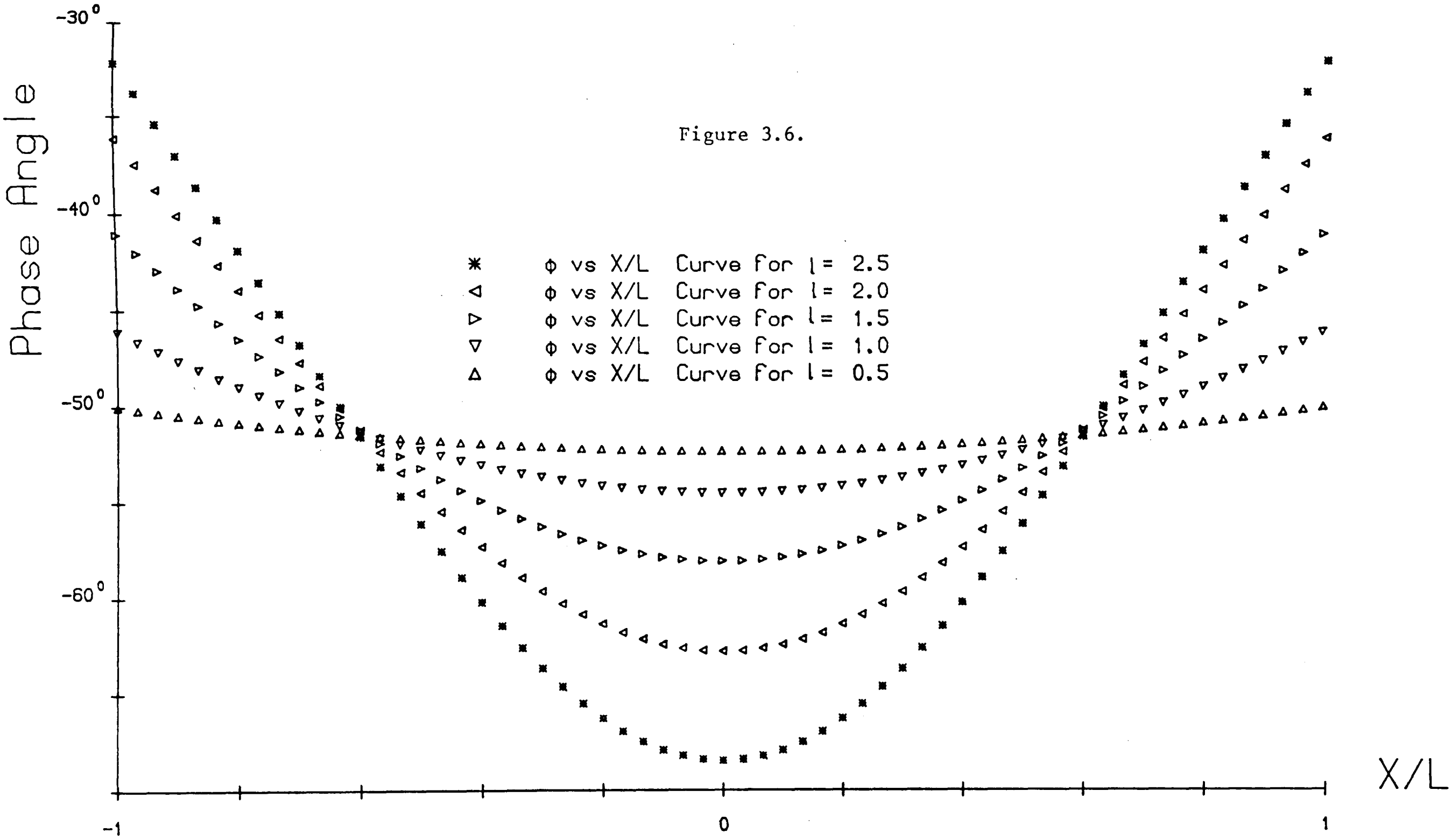
Phase Angle
-30°
-40°
-50°
-60°
X/L
-1
0
1
* φ vs X/L Curve for l = 2.5
◁ φ vs X/L Curve for l = 2.0
▷ φ vs X/L Curve for l = 1.5
▽ φ vs X/L Curve for l = 1.0
△ φ vs X/L Curve for l = 0.5

Figure 3.6.

behaviour of factors K1 and K2 defined in Section 3.4. The behaviour of K1 is reproduced in Figures 3.7 and 3.8. Figure 3.7 shows that for a given segment length (1 cm) K1 behaves in a similar manner to the factor K in D.C. studies (f = 0 in this figure). Figure 3.8 shows that for a given frequency (10 Hz) and different ℓ values, K1 is again close to unity at X = 0.58L. This indicates that the 0.42L technique can be extended to measurement of the amplitude of the voltage response to A.C., with its accuracy being a function of the A.C. frequency.

Since the phase angle $-\phi = \tan^{-1}(\omega\tau)K2$ it seems reasonable to perform a similar analysis of the behaviour of K2. However the main interest is not the phase angle but rather the membrane time constant τ. Thus an expression of the form

$$-\tan\phi = \omega\tau\ K3$$

will be considered, i.e. the relationship between the experimentally measured value of $\tan\phi$ and the corresponding membrane parameter τ.

Equation (3.17) can be written as $-(\phi+\phi') = \tan^{-1}(\omega\tau)$

where $\phi' = \phi\left(\frac{1}{K2} - 1\right)$. (3.25)

Thus $\omega\tau = -\tan\left[\frac{1 + \tan\phi'/\tan\phi}{1 - \tan\phi\ \tan\phi'}\right]$.

Therefore K3 can be defined as:

$$K3 = \left[\frac{1 - \tan\phi\ \tan\phi'}{1 + \tan\phi'/\tan\phi}\right] . \qquad (3.26)$$

From equations (3.17) and (3.23)

$$-\phi = \tan^{-1}(\omega\tau)\left[\frac{\tan^{-1}(\omega\tau) + 2\theta}{2\tan^{-1}(\omega\tau)}\right] \qquad (3.27)$$

Figure 3.7.

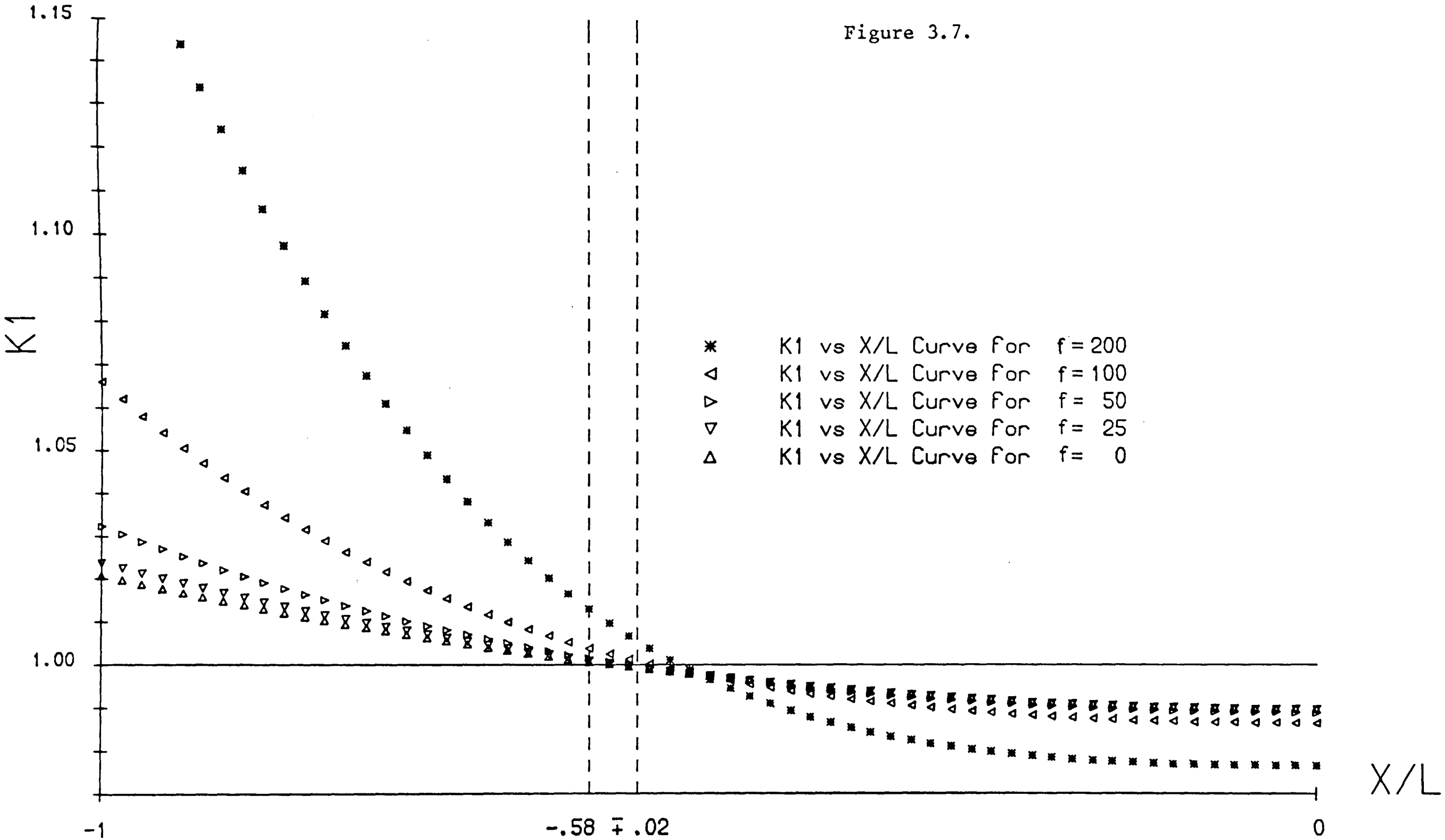
1.15
1.10
1.05
1.00
K1
X/L
-1
-.58 ∓ .02
0
✱ K1 vs X/L Curve for f = 200
◁ K1 vs X/L Curve for f = 100
▷ K1 vs X/L Curve for f = 50
▽ K1 vs X/L Curve for f = 25
△ K1 vs X/L Curve for f = 0

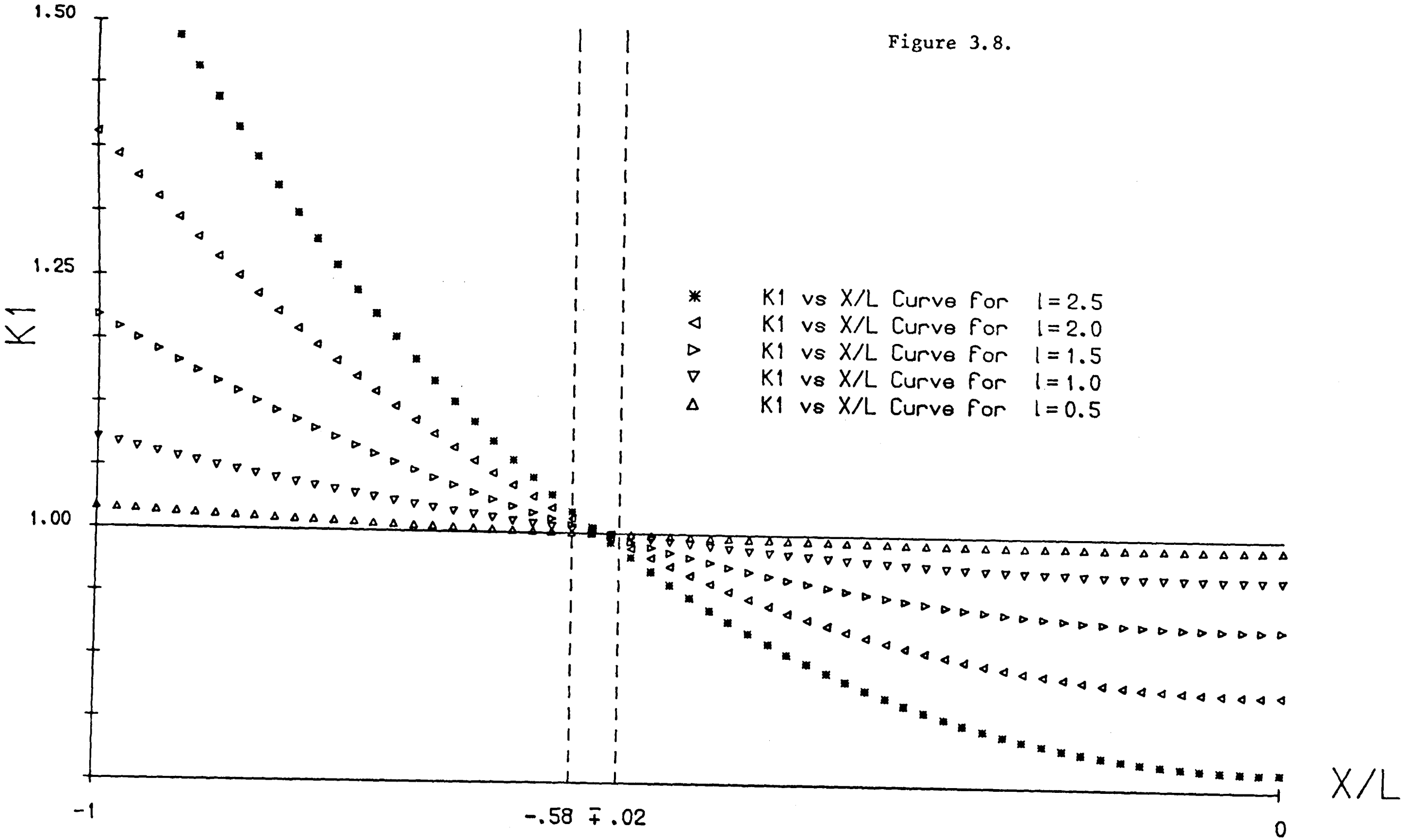
1.50
1.25
1.00
K1
-1
-.58 ∓ .02
0
X/L
* K1 vs X/L Curve for l=2.5
◁ K1 vs X/L Curve for l=2.0
▷ K1 vs X/L Curve for l=1.5
▽ K1 vs X/L Curve for l=1.0
△ K1 vs X/L Curve for l=0.5

Figure 3.8.

and from equations (3.25) and (3.22)

$$-\phi' = \phi \left(\frac{\tan^{-1}(\omega\tau) - 2\theta}{\tan^{-1}(\omega\tau) + 2\theta} \right) . \qquad (3.28)$$

Substitution of equations (3.27) and (3.28) into equation (3.26) gives:

$$K3 = \frac{1-\tan((\tan^{-1}(\omega\tau))/2) + \theta)\tan((\tan^{-1}(\omega\tau))/2 - \theta)}{1+(\tan((\tan^{-1}(\omega\tau))/2 -\theta))/\tan((\tan^{-1}(\omega\tau))/2 + \theta)} .$$

To check the validity of this definition of K3 the value $\theta = \frac{\tan^{-1}(\omega\tau)}{2}$, i.e., the value of θ when L' = O, can be substituted into this expression. In this case the expression becomes unity which is what would be expected for a single RC circuit.

The numerical behaviour of K3 is shown in Figures 3.9, where ℓ = 1.0 cm and 3.10, where f = 10 Hz. It will be noted that the behaviour of K3 is more complex than that of K1. As frequency increases a singularity appears just ahead of X = O.58L. Nevertheless it is clear that around X = O.58L K3 has a value near unity.

The behaviour of K1 and K3 in the vicinity of X = O.58L shows that the O.42L technique can be used for measurements of both the amplitude of the A.C. voltage response and its time constant. The accuracy of these measurements for a given segment length, range of frequencies, and point of recording can be estimated from the departure of the numerical values of K1 and K3 from unity. However the accuracy in the computed values of $R_m(\omega)$ and $C_m(\omega)$ is not so readily obtained. In this case

Figure 3.9.

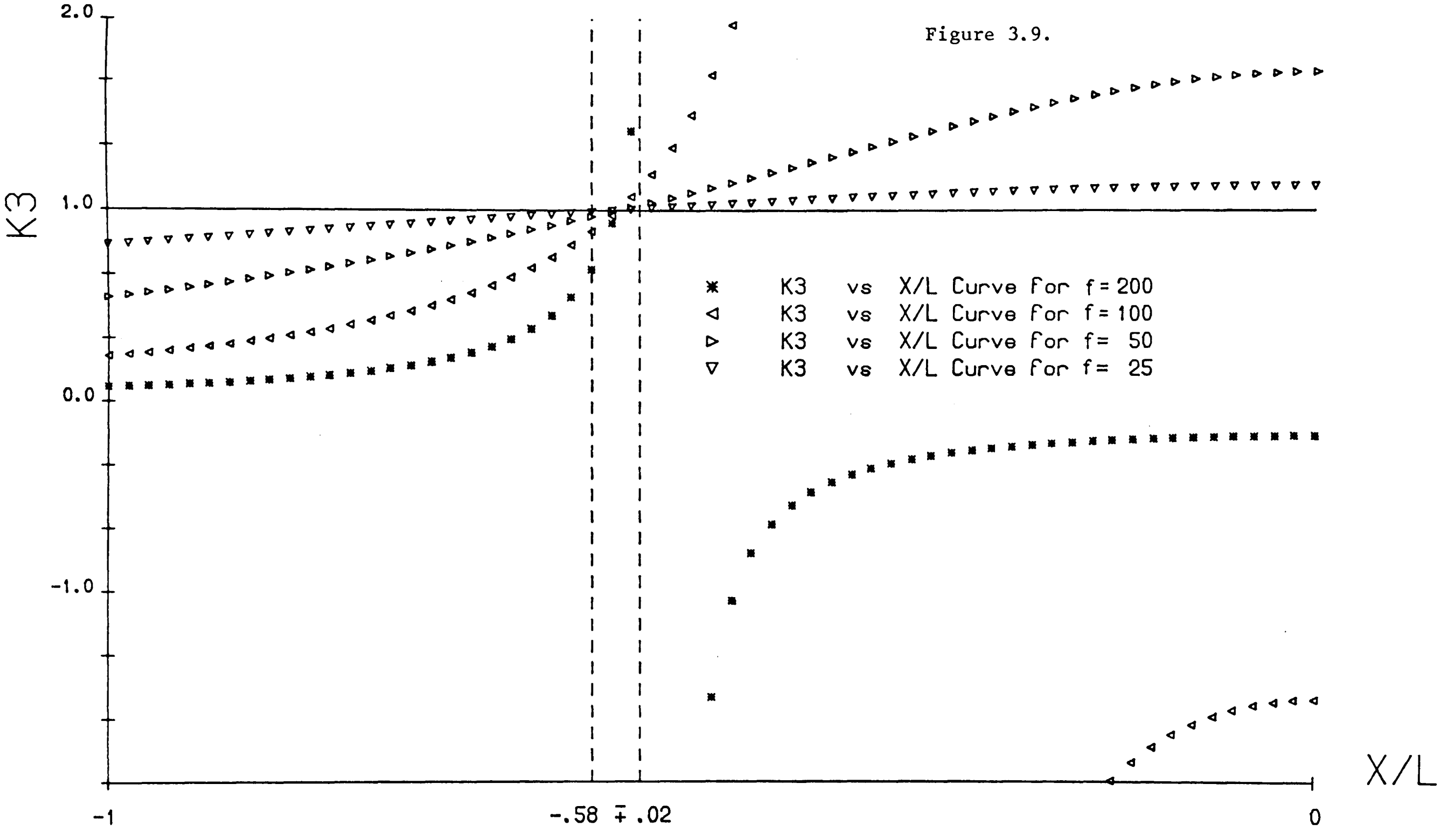
2.0
1.0
0.0
-1.0
K3
X/L
-1
-.58 ∓ .02
0
K3 vs X/L Curve for f = 200
K3 vs X/L Curve for f = 100
K3 vs X/L Curve for f = 50
K3 vs X/L Curve for f = 25

Figure 3.10.

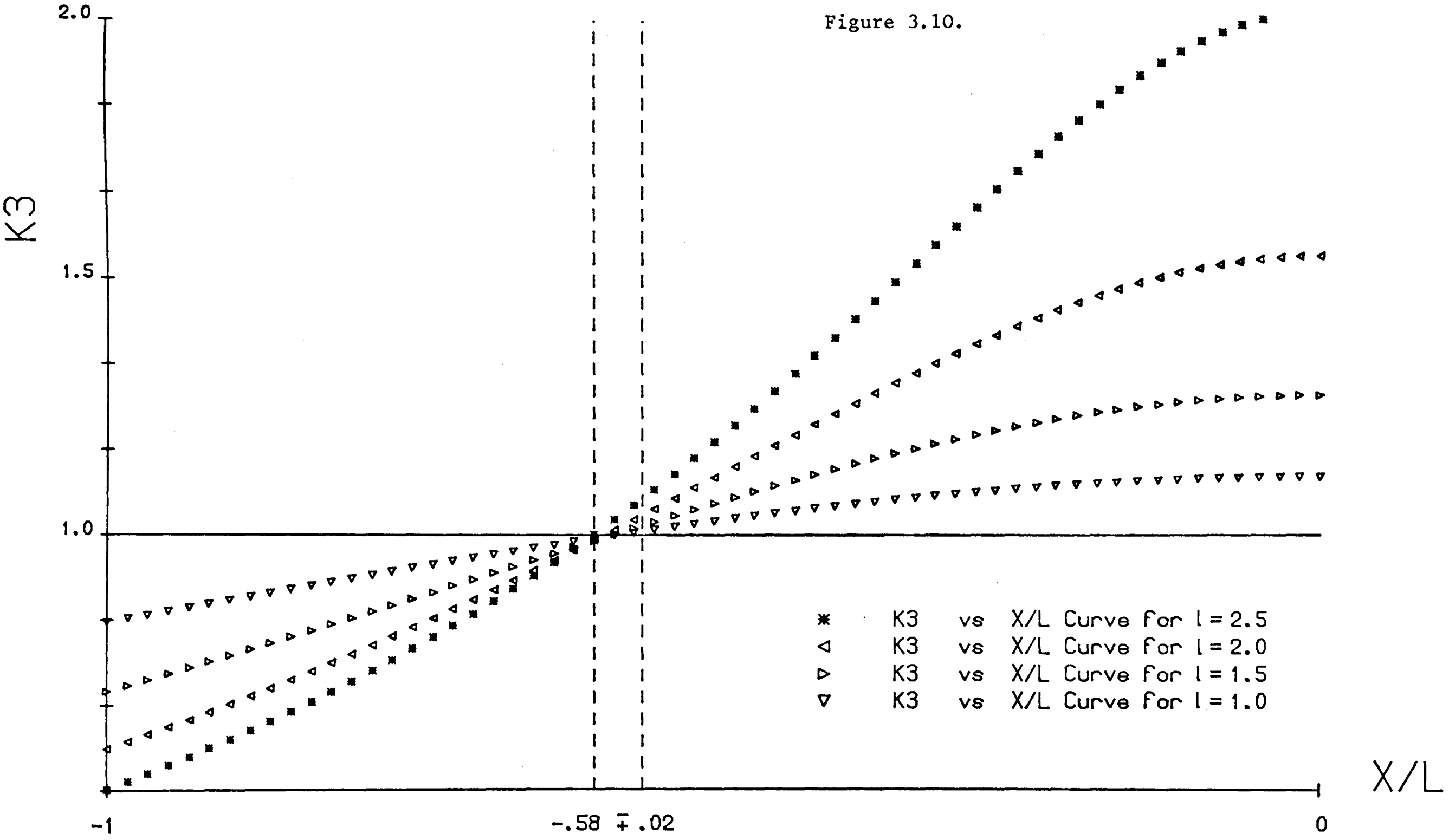
2.0
1.5
1.0
K3
X/L
-1
-.58 ∓ .02
0
* K3 vs X/L Curve for l = 2.5
◁ K3 vs X/L Curve for l = 2.0
▷ K3 vs X/L Curve for l = 1.5
▽ K3 vs X/L Curve for l = 1.0

both K1 and K3 have to be used for the computation of each parameter.

3.6 The Accuracy of the Computed Values of R_m and C_m

$R_m(\omega)$ and $C_m(\omega)$ can be computed from the following expressions:

$$A = \frac{\text{Resistance of the cell segment}}{\text{Area of the cell segment}} = \frac{R_m K1}{(1+\omega^2\tau^2)^{\frac{1}{2}}}$$

and

$$B = -\tan^{-1}(\text{phase angle}) = \omega R_m C_m K3$$

where A and B are experimentally measured quantities. Writing

$$\frac{A}{K1} = A + \delta A = \frac{R_m}{(1+\omega^2\tau^2)^{\frac{1}{2}}} \quad \text{and} \quad \frac{B}{K3} = B + \delta B = \omega\tau$$

where $\delta A = A(\frac{1}{K1} - 1)$ and $\delta B = B(\frac{1}{K3} - 1)$ it can be seen that the deviation of K1 and K3 from unity is reflected as an error in the values of A and B. δA and δB arise from cable effects. They will be zero for a single RC circuit or for cases in which cable effects can be neglected, i.e., K1 = K3 = 1. In these cases

$$R_m = A(1 + B^2)^{\frac{1}{2}} \quad \text{and} \quad C_m = B/R_m\omega \; . \qquad (3.29)$$

The deviations in the values of R_m and C_m produced by cable effects are then given:

$$\delta R_m = \frac{\partial R_m}{\partial(\text{cable effects})} = (1+B^2)^{\frac{1}{2}}\delta A + \frac{A}{2}(1+B^2)^{-\frac{1}{2}}2B\delta B$$

$$\therefore \quad \delta R_m = R_m\left[(\frac{1}{K1} - 1) + \frac{(\omega\tau)^2}{(1+(\omega\tau)^2)}(\frac{1}{K3} - 1)\right] \; .$$

Similarly

$$\delta C_m = \frac{\partial C_m}{\partial(\text{cable effects})} = \frac{\delta B}{\omega R_m} - \frac{B}{\omega R_m^2}\,\delta R_m$$

$$= \frac{B}{\omega R_m}\left(\frac{1}{K3} - 1\right) - \frac{B}{\omega R_m}\left(\frac{\delta R_m}{R_m}\right)$$

$$\therefore \quad \delta C_m = C_m \left[\left(\frac{1}{K3} - 1\right)\left(\frac{1}{1+(\omega\tau)^2}\right) - \left(\frac{1}{K1} - 1\right)\right]$$

The quantities $\frac{\delta R_m}{R_m} \times 100 = e_R$ and $\frac{\delta C_m}{C_m} \times 100 = e_C$

are the percentage errors introduced by the assumption of a single RC circuit. Their values will be a function of the segment length, point of voltage recording and the A.C. frequency. The values of e_R and e_C along the cell segment for different values of ℓ and $f = 10$ Hz are shown in Figures 3.11 and 3.12. It can be seen that, as expected, e_R and e_C attain near zero values in the vicinity of 0.58L. The values of e_R and e_C along the cell segment for different values of f and a cell segment length of 1 cm. are shown in Figures 3.13 and 3.14. Again both parameters are near zero at $X = 0.58L$. e_R is strongly dependent on frequency, as indicated by the increasing slopes in the curves with increasing frequency. At 0.58L e_R is zero for any frequency but because of the very steep slopes of the curves for frequencies bigger than 100 Hz it is imperative that the point of recording be precisely located at such frequencies. On the other hand the values of e_C around 0.58L are remarkably small over a wide region around 0.58L and a wide range of frequencies.

In conclusion it can be said that using symmetric current injection in a short segment of Nitella translucens introduces

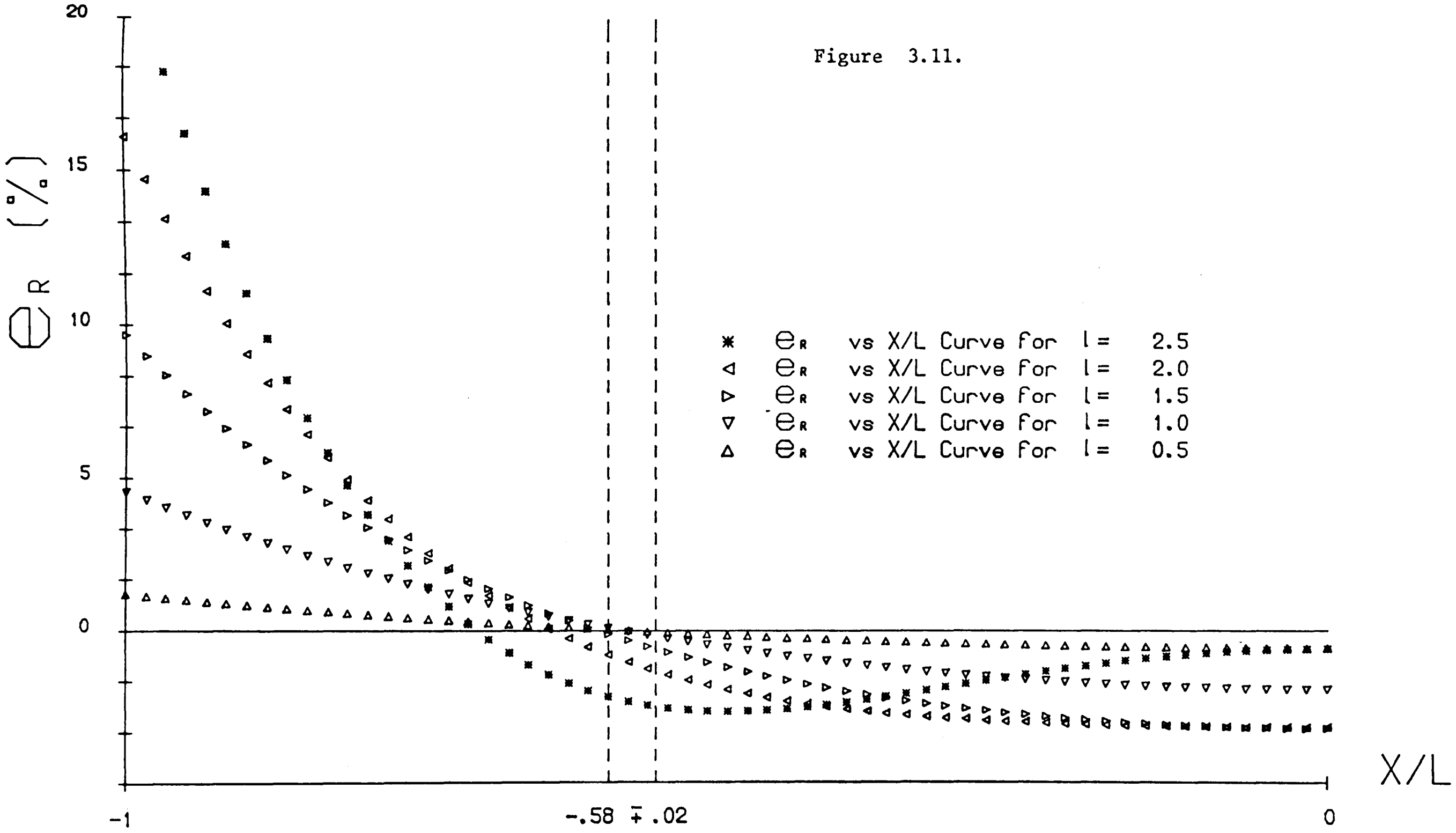
20
15
10
5
0
e_R (%)
-1
-.58 ∓ .02
0
X/L
* e_R vs X/L Curve for l = 2.5
◁ e_R vs X/L Curve for l = 2.0
▷ e_R vs X/L Curve for l = 1.5
▽ e_R vs X/L Curve for l = 1.0
△ e_R vs X/L Curve for l = 0.5

Figure 3.11.

Figure 3.12.

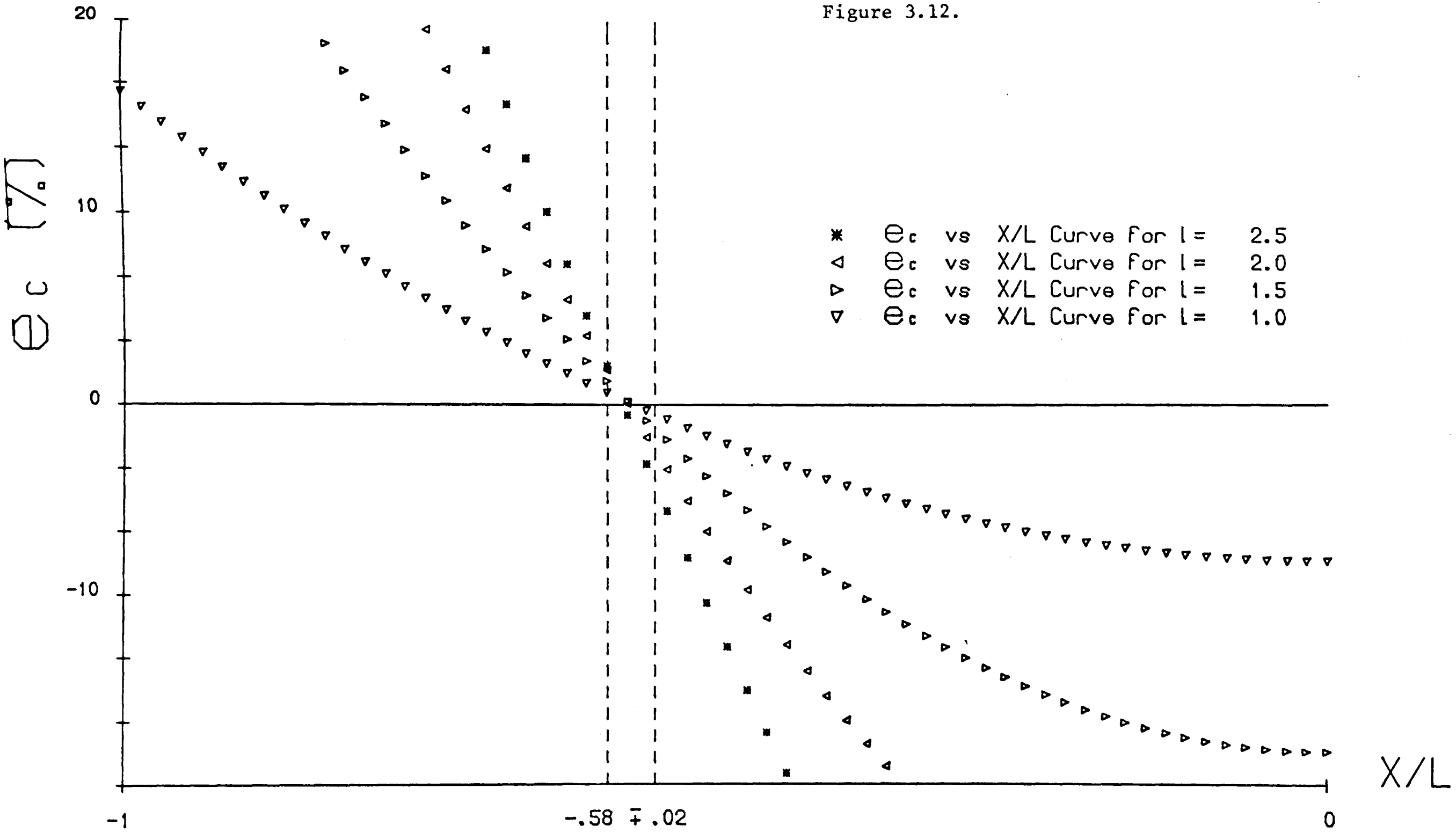

✱ ϵ_c vs X/L Curve for l = 2.5
◁ ϵ_c vs X/L Curve for l = 2.0
▷ ϵ_c vs X/L Curve for l = 1.5
▽ ϵ_c vs X/L Curve for l = 1.0

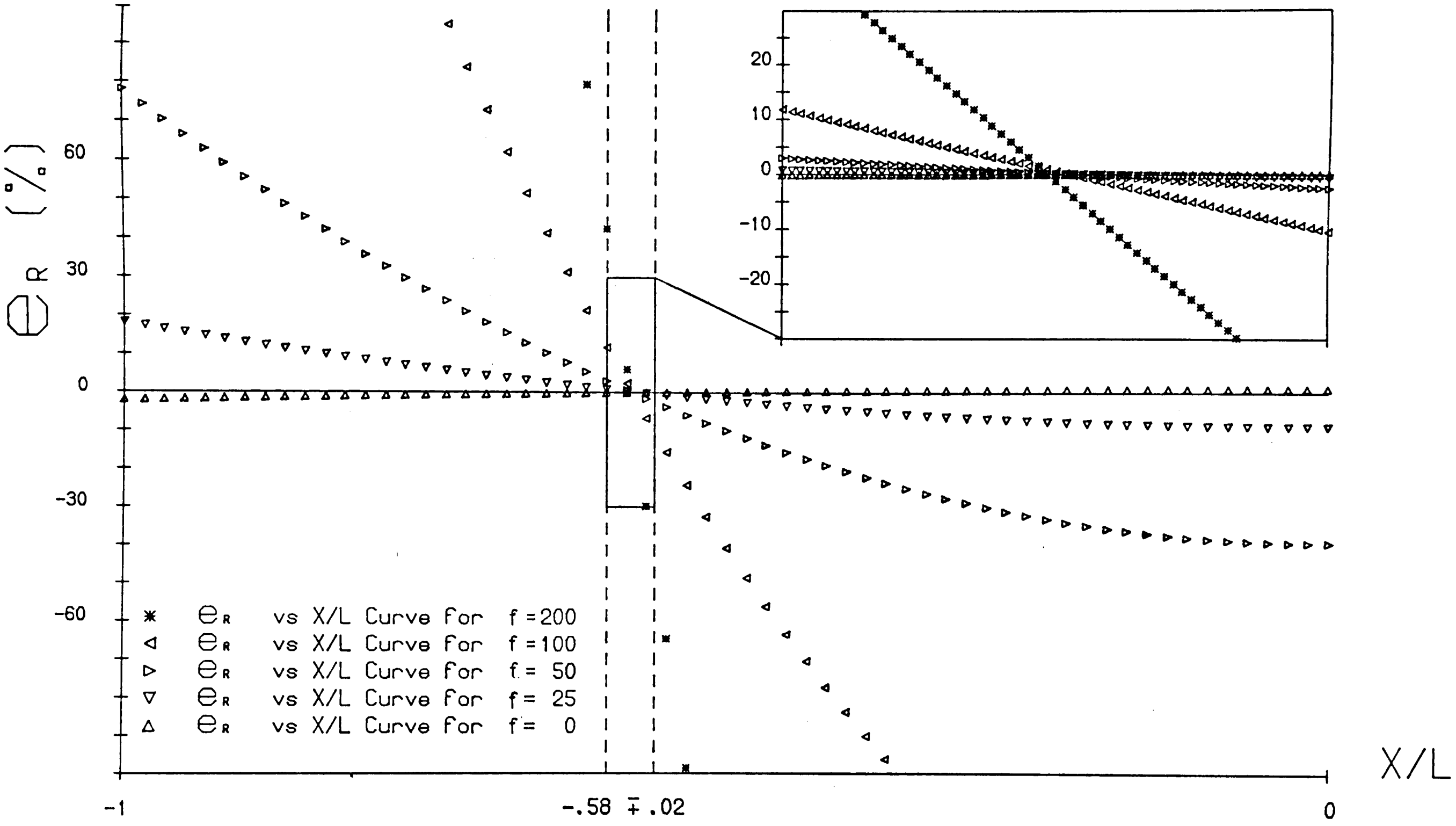
e_R (%)
60
30
0
-30
-60
20
10
0
-10
-20
* e_R vs X/L Curve for f = 200
◁ e_R vs X/L Curve for f = 100
▷ e_R vs X/L Curve for f = 50
▽ e_R vs X/L Curve for f = 25
△ e_R vs X/L Curve for f = 0
-1
-.58 ∓ .02
0
X/L

Figure 3.13.

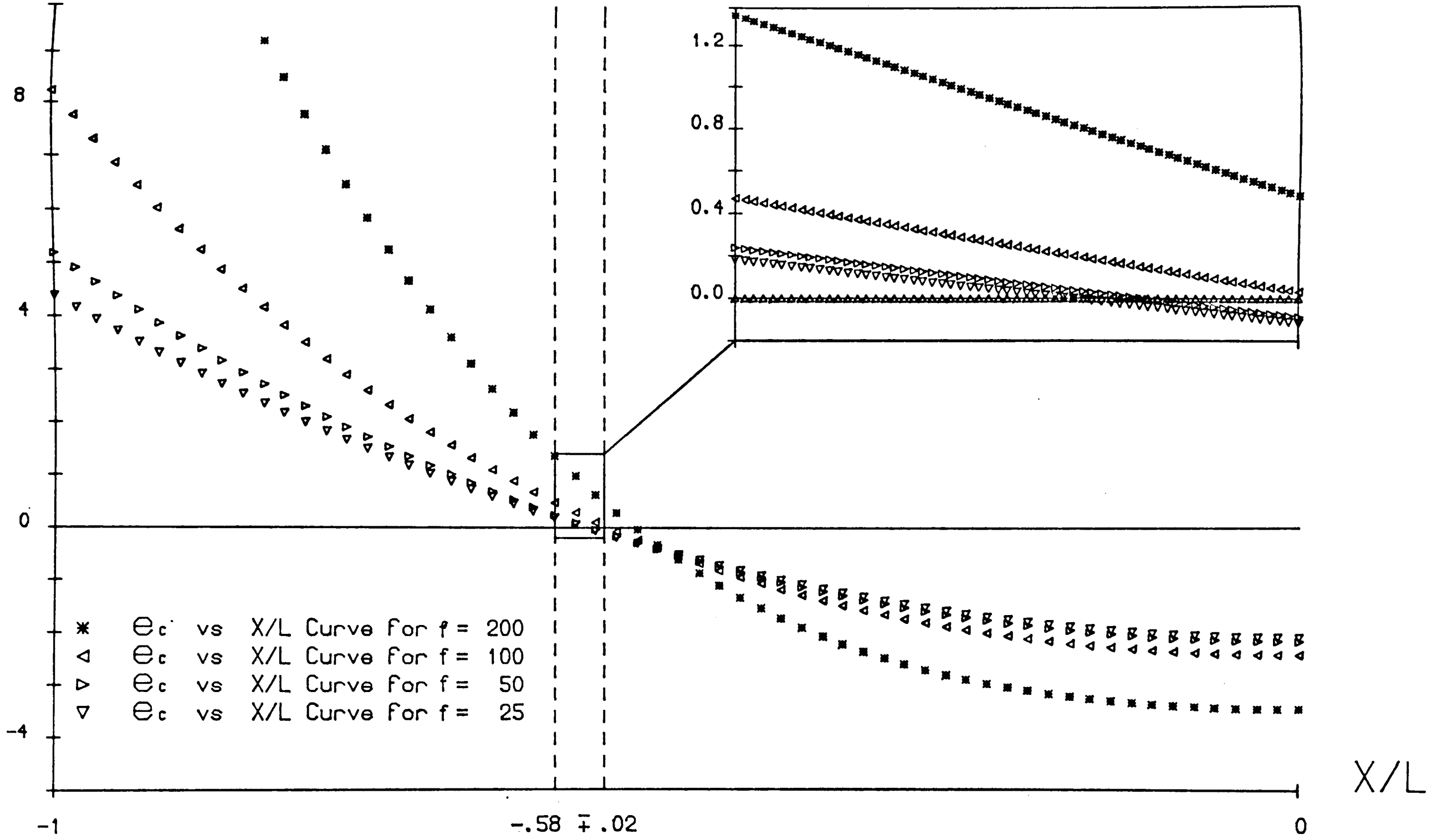
e_c (%)
8
4
0
-4
1.2
0.8
0.4
0.0
e_c vs X/L Curve for f = 200
e_c vs X/L Curve for f = 100
e_c vs X/L Curve for f = 50
e_c vs X/L Curve for f = 25
-1
-.58 ∓ .02
0
X/L

Figure 3.14.

remarkably small errors in the computation of R_m and C_m for a frequency range of 0 to 100 Hz if the 0.42L technique is used. This latter technique also allows for the use of larger segment lengths at low frequencies.

The above computations and conclusions were made assuming the values $R_m = 20\ k\Omega\ cm^2$, and $C_m = 1\ \mu f/cm^2$ for any value of the A.C. frequency. Coster and Smith (5) reported that in Chara C_m can increase its value twofold at low frequencies. They also reported that R_m can decrease to one quarter of its value at $f \simeq 100$ Hz.

All the expressions considered above depend on C_m though the factor $(1+\omega^2\tau^2)^{-\frac{1}{4}}$. Since changes in the values of C_m occur only at low frequencies the factor $1+(\omega\tau)^2$ will be only very slightly affected by this C_m dependence. For instance, the more marked ω dependence of C_m reported by Coster and Smith occurs at 5 Hz. In this case $\omega\tau \simeq 0.1$ and $(1+\omega^2\tau^2)^{-\frac{1}{4}} \simeq 1$. The dependence on C_m of the terms sin d and cos d, where $d = \frac{1}{2}\tan^{-1}(\omega\tau)$ is also very small for the range of frequencies in which C_m varies.

Changes in the values of R_m will affect the above computations not only through the value of τ but also through the value of $\lambda = \sqrt{r_m/r_{oi}}$. Decreases in the value of R_m occur over a wide range of frequencies and also during the excited state of the membrane. The values of e_R and e_C in these two cases could be different from the values shown in the previous figures.

The effectiveness of space clamping in A.C. studies depends on the value of $L' = \frac{\ell\sqrt{r_{oi}}}{\sqrt{r_m}}(1+\omega^2\tau^2)^{-\frac{1}{4}}$. Reductions

in the value of r_m will decrease L' but this will be compensated by increases in $(1+\omega^2\tau^2)^{-\frac{1}{4}}$. For instance for $\omega\tau > 1$ $L = \ell\sqrt{r_{oi}}\,(\omega\tau)^{\frac{1}{2}}$ which is completely independent of the value of r_m.

The effect of the reduction of a resistance value R_a to a resistance value R_b on $e_R((0.58 \pm 0.02)L')$ and $e_C(0.58 \pm 0.02)L')$ are shown in Figures 3.15 and 3.16. It can be seen that even for a tenfold decrease in the membrane resistance and an A.C. frequency of 100 Hz these errors are still acceptably small. This indicates that external current injection plus the 0.42L technique is perfectly adequate for A.C. studies in the frequency range 0 to 100 Hz. Furthermore it can be extended to A.C. studies of the excited state in the same range of frequencies.

3.7 Discussion

Coster and Smith (5) have pointed out that $C_m(\omega)$ measurements require the use of a long axial electrode, an independent voltage recording electrode and very accurate recording equipment. These authors could resolve amplitude values to 0.1% and phase angles of 0.01°. It is interesting to compare the error in the R_m and C_m values introduced by this technique with the errors introduced by cable effects in the technique used in this present work.

Differentiation of (3.29) yields

$$dR_m = R_m \frac{dA}{A} + R_m \frac{B^3}{1+B^2} \frac{dB}{B}$$

and

$$dC_m = C_m \frac{dB}{B} + C_m \frac{dR_m}{R_m} \quad .$$

Figure 3.15.

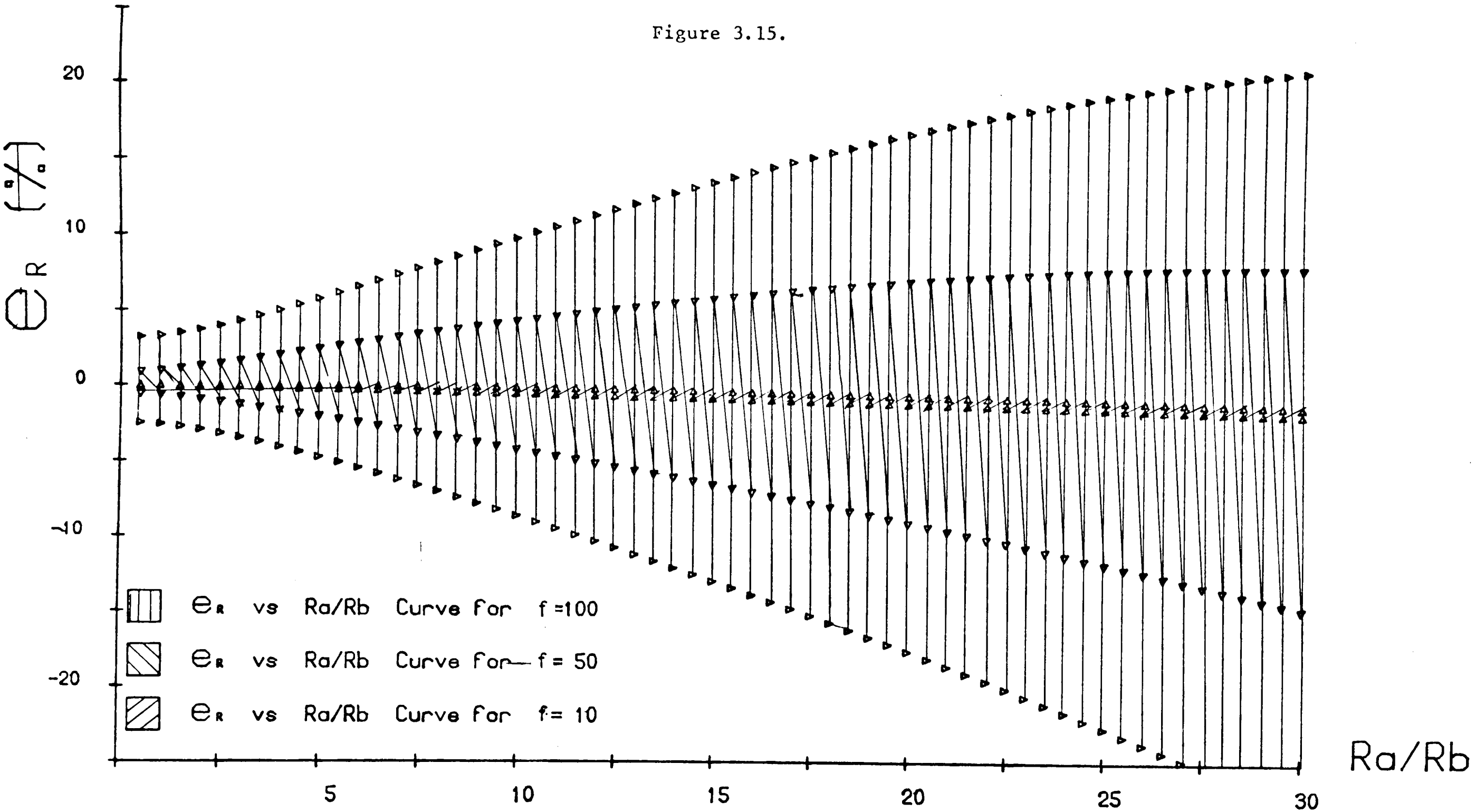
20
10
0
-10
-20
e_R (%)
e_R vs Ra/Rb Curve for f =100
e_R vs Ra/Rb Curve for f = 50
e_R vs Ra/Rb Curve for f= 10
5
10
15
20
25
30
Ra/Rb

Figure 3.16.

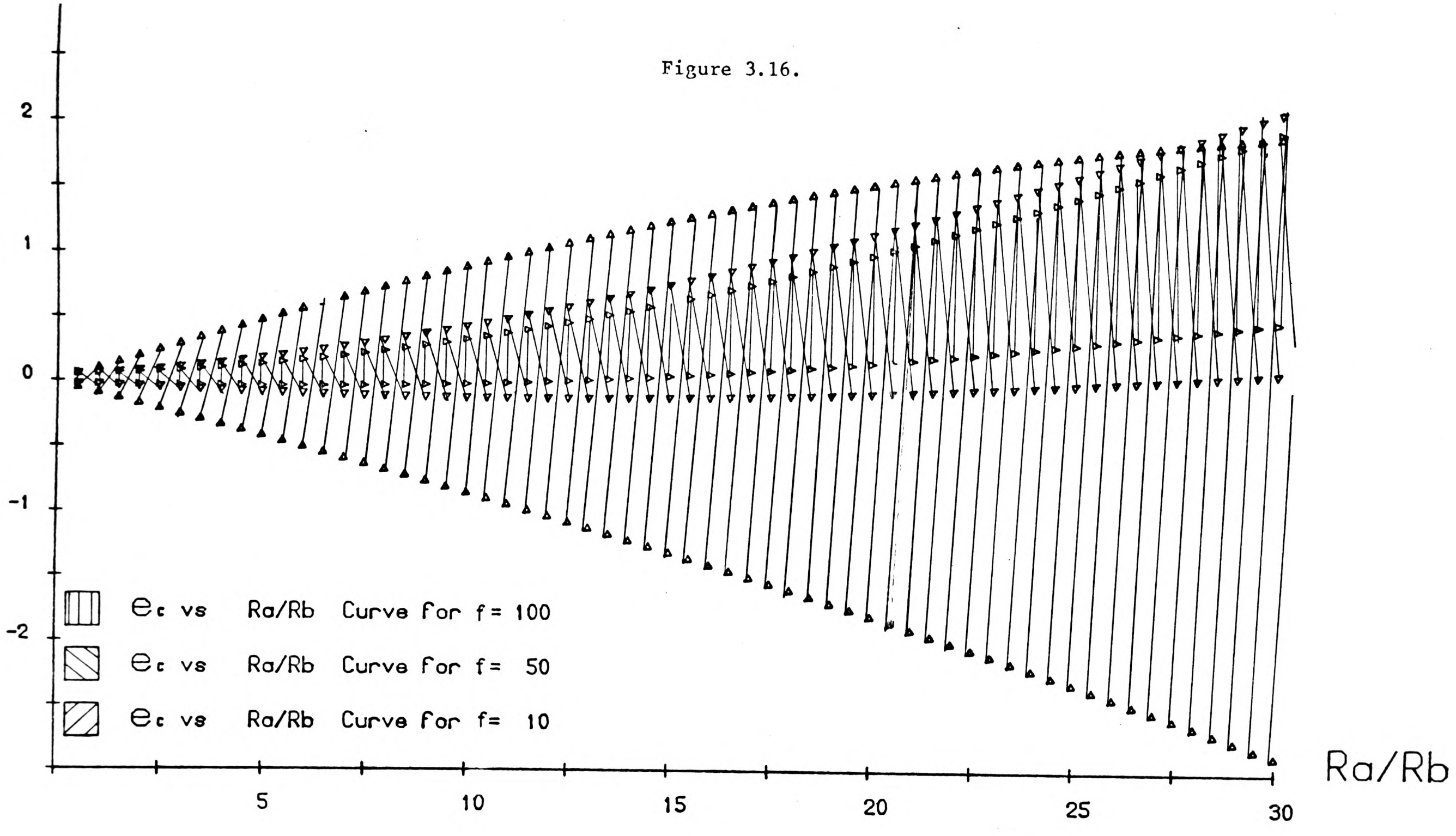
ec (%)
2
1
0
-1
-2
ec vs Ra/Rb Curve for f= 100
ec vs Ra/Rb Curve for f= 50
ec vs Ra/Rb Curve for f= 10
5
10
15
20
25
30
Ra/Rb

In this case $\frac{dA}{A}$ and $\frac{dB}{B}$ are the recording errors in A and B. In the work of Coster and Smith $dA/A = .001$ and $dB/B \simeq \tan(.0001)/\tan(0.04)$ for $1 < f < 10$ Hz. Substitution of these values in the above equations show that $\frac{dR_m}{R_m} \times 100 \simeq 0.1\%$ and $\frac{dC_m}{C_m} \times 100 \simeq 0.1\%$ which are of similar magnitude to e_R and e_C. Hence there is insufficient experimental resolution to distinguish between measurements performed with the long axial electrode and those employing the present technique in the frequency range 0 to 10 Hz.

3.8 Conclusions

The solution of the cable equations for A.C. current has been presented. It was found that the exact solution can be expressed as the solution for a single RC circuit multiplied by certain factors. The numerical behaviour of these factors indicates that the 0.42L technique can be extended to A.C. studies.

A quantitative estimate of the errors in the R_m and C_m values introduced by neglecting cable behaviour in Nitella translucens has been presented. These errors are reasonably small if the 0.42L technique is used. If, in addition, a short cell segment is considered these errors are in the range of the experimental resolution at low frequencies.

It should be pointed out that the method favoured in this work could be used in A.C. studies of the excited state of the membrane. A.C. methods should be particularly useful

for determining the excited state resistance of the first part of the action potential since it has a duration of less than 40 ms and for D.C. work square pulses of at least 100 ms duration are required in order for the voltage response to reach a steady value.

REFERENCES (CHAPTER III)

1) Curtis, J.H. & Cole, K.J., J. Gen. Physiol. 21, 189 (1938).

2) Kishimoto, U., Jap. J. Physiol., 24, 403 (1974).

3) Taylor, R.E., J. Cell. Comp. Physiol., Suppl. 2, 66 (1965)

4) Skierczyńska, J., Żoknierczenk R. & Bulanda, W., J. Expt. Bot. 24, 78, 38 (1973).

5) Coster, H.G.L. & Smith, J.R., Membrane Transport in Plants. Edited by Zimmermann and Dainty, Springer-Verlag (1974).

6) Williams, E.J., Johnston, J. & Dainty. J., J. Expt. Botany 15 43, 1, (1964).

7) Hogg, J., Williams, E.J. & Johnston, J., Biochim. Biophys. Acta 150, 640 (1968).

CHAPTER IV

EXPERIMENTAL CONSIDERATIONS

The measurement of the standing potential between the interior of a biological cell and its bathing medium - the membrane resting potential - together with the measurements of the membrane impedance contributes towards the understanding of the ion transport processes through the membrane. In these measurements the basic experimental technique involves the insertion of an electric probe into the cell and the connection of this probe through a suitable measuring device to another electric probe located outside the cell. Certain electrochemical considerations arise in the selection of these probes and this in turn has a bearing on the electronics of the measuring devices to be used.

Whilst there are several texts available (e.g. references 1-6) which deal with certain specific problems in the measurement of the membrane electric parameters, the tendency has been to concentrate exclusively either on the practical side or on the theoretical side. Furthermore the most recent advances cited in the literature have not yet been incorporated into reference books.

As far as I am aware there is no single reference book which gives a general overall account of the problems encountered in membrane electric measurements, the understanding of such problems and practical ways of coping with them. This has encouraged the preparation of this chapter in which some of these problems are reviewed.

4.1 The Electrophysiological Electrodes

It was Galvani who first observed the twitching of a frog's legs when the animal was touched simultaneously with the ends of two different pieces of metal, e.g. iron and zinc, joined together. He suggested that this effect was produced entirely by the living tissue. This interpretation was challenged by Volta, who showed that the electromotive force in most of the Galvani experiments was of an electrochemical nature and originated at the contact points between metal and tissue. This type of controversy occurs even today. For instance, Plonsey (5), mentions the different results obtained by Chandler and Hodgkin[17] and by Tasaki, Luxoro and Ruarte[18] when measuring the action potential of squid axon at equal external and internal potassium concentrations with different electrode systems. What emerges from this controversy is that it is important to determine what exactly is being measured by any given electrode arrangement. It is convenient to consider in detail the processes which occur at any electrode system and their possible effects on the recorded observations.

i) Metal electrodes

When two pieces of wire are connected through an electrolytic solution and the potential between them is measured it will be observed that the electric potential has a value of a few hundred millivolts which is subject to continuous drifting. This behaviour is clearly undesirable in a system which is intended to be used as a reference point. This

liquid-metal junction, the metal electrode, is an unavoidable stage in the electronic circuitry which is used for measuring the membrane electrical properties. The behaviour of this interphase is now considered. (See, for example, Plonsey (5), Bockriøs and Reddy (6) and Sawyer and Roberts (7)).

The Galvanic Cell: When a silver wire is connected through a solution of HCℓ to a platinum wire an e.m.f. is developed in the circuit. This arises because two different reactions occur at each electrode:

$$H_2 = 2H^+ + 2e^- \quad \text{at the platinum terminal}$$

and $$AgC\ell + e^- = Ag^+ + C\ell^- \quad \text{at the silver terminal.}$$

The net result is an exothermic reaction when the circuit is completed: $H_2 + 2AgC \overset{\Delta}{\rightleftarrows} 2HC + 2Ag$. This reaction can supply current and the system is known as a Galvanic Cell.

When the circuit is open the e.m.f. will manifest itself as a standing potential between the electrodes. It is convenient to think of this potential as the sum of two potentials associated with each electrode respectively. This is called the half cell potential. The platinum half cell potential is defined to be zero and all other metal half cell potentials are then obtained from the galvanic potential of a platinum-metal cell.

Half cell potentials range from hundreds to thousands of millivolts, i.e., several times larger than cell membrane potentials. In spite of these large values galvanic potentials should not in principle present any problem to the measurement of the membrane potential. They could be subtracted from the actual reading or cancelled out

by the use of two identical half cells in opposition. However, in practice a residual potential is observed even when identical wires are used. This residual potential arises because of the chemical reactions occurring at the electrodes; these reactions can give rise to changes in the concentrations and composition of the solutions in the vicinity of the electrodes. Half cell e.m.f's are determined under standard conditions by placing a battery in the external circuit to oppose almost exactly the cell reaction. The difference between the e.m.f. values corresponding to zero current in the circuit (ideal case) and non-zero current (practical case) can be expressed as:

$$\eta = E(i) - E(i=0) . \qquad (4.1)$$

η is called the electrode polarization.

Electrode Polarization: The principal forms of electrode polarization are a) concentration polarization and b) transition polarization.

a) Concentration polarization arises because the concentration of the ion involved in the chemical reaction decreases in the electrode vicinity. As a result a diffusion potential appears between this region and the bulk of the solution. This will happen when high current densities are used and the electrode reaction occurs freely. The current limiting step is the flux of ions towards the electrode. This flux is expressed by Fick's law:

$$\phi_x = -D \frac{dC}{dx} = D \frac{C_b - C_e}{\delta} \qquad (4.2)$$

where D is Fick's diffusion constant, δ the thickness of the depletion layer and C_b and C_e are respectively the concentrations of the bulk solution and the solution in the vicinity of the electrode.

Using equation (4.2) the current density J can be expressed as:

$$J = zF\phi_x = \frac{zFDC_b}{\delta}\left(1 - \frac{C_e}{C_b}\right) \tag{4.3}$$

where z is the ion valency and F is the Faraday constant.

Diffusion potentials have the form

$$\eta_C = \frac{RI}{ZF} \ln \frac{C_e}{C_b} \tag{4.4}$$

where η_C is the concentration polarization.

Substituting equation (4.4) into equation (4.3) gives

$$J = \frac{zFD}{\delta} C_b\left(1 - \exp\left(\frac{zF\eta_C}{Rt}\right)\right) \tag{4.5}$$

From equation (4.4) it can be seen that when $\frac{C_e}{C_b} \to 0$, i.e. when the concentration around the electrode is negligible compared with that of the bulk solution, the current reaches a limiting value:

$$J_{lim} = \frac{zFD}{\delta} C_b \tag{4.6}$$

The concentration polarization can then be expressed in terms of this limiting current

$$\frac{J}{J_{lim}} = 1 - \exp\left(\frac{zF\eta_C}{Rt}\right)$$

$$\therefore \eta_c = \frac{RT}{zF} \ln\left(1 - \frac{J}{J_{lim}}\right) \tag{4.7}$$

for $J < J_{lim}$ equation (4.7) becomes

$$\eta_c = \frac{RT}{zF} \frac{J}{J_{lim}} = \frac{\delta RT}{z^2F^2DC_b} J \qquad (4.8)$$

The concentration polarization depends not only on the constants F, D and C_b but also on δ and J. δ, the thickness of the depleted layer, is a function of time and current and it is the cause of the drift observed in the standing potential measured between two wires immersed in the same solution. The dependence of η_c on $(1/C_b)$ emphasises that polarization effects are more pronounced in dilute solutions, such as often occur in plant systems.

b) Transition polarization arises in systems where there is difficulty in the charge transfer reaction occurring at the electrode-solution interphase. Charge transfer will occur at both electrodes as a result of the reaction $O + 2e^- \rightleftarrows R$, where O and R are soluble substances reduced at the cathode and oxidised at the anode. The resultant current can be expressed as the sum of the corresponding cathodic current, J_c, and the anodic current, J_a.

$$J = J_a - |J_c| . \qquad (4.9)$$

To a first approximation the reaction rates are a function of the concentration of the reactants and the activation energy of the process. This can be expressed with the use of the Arrhenius equation

$$-J_c = zF\ K_c\ C_o \exp(-\frac{\Delta G_c}{RT}) \qquad (4.10)$$

and

$$-J_a = zF\ K_a\ C_R \exp(-\frac{\Delta G_a}{RT}) \qquad (4.11)$$

where K and ΔG are respectively the reaction constant and the activation energy.

When there is a potential difference, E_i, between the electrodes the reaction will be favoured in one direction and inhibited in the opposite direction. For instance if, ΔG_a is reduced by a fraction αzFE_i then ΔG_c will be increased by $(1 - \alpha)zFE_i$. The resultant partial currents are:

$$J_a = zF\ K_a\ C_R \exp\left(\frac{-\Delta G_a + \alpha zFE_i}{RT}\right) \tag{4.12}$$

and

$$J_c = -zF\ K_c\ C_o \exp\left(\frac{-\Delta G_c - (1-\alpha)zFE_i}{RT}\right) . \tag{4.13}$$

When the electrodes are at equilibrium E_i is the reversible potential difference E_{rev} and both currents J_a and $|J_c|$ are equal. This particular value of the total current is called the exchange current J_o. The constant term in equations (4.12) and (4.13) can then be expressed as

$$zF\ K_a\ C_R = J_o \exp\left(\frac{\Delta G_a - \alpha zFE_{rev}}{RT}\right)$$

and (4.14)

$$zF\ K_c\ C_o = J_o \exp\left(\frac{\Delta G_c + (1-\alpha)zFE_{rev}}{RT}\right)$$

Utilizing equations (4.12), (4.13) and (4.14) together with the fact that in the absence of concentration polarization transition polarization is defined as $\eta_t = E_i - E_{rev}$, the net current can be expressed as :

$$J = J_o\left\{\exp\left(\frac{\alpha zF\eta_t}{RT}\right) - \exp\left(\frac{-(1-\alpha)zF\eta_t}{RT}\right)\right\} \tag{4.15}$$

This expression is known as the Bultler-Volmer equation, relating the circuit current and the driving e.m.f. For small arguments of the exponential terms, i.e. for small values of the transition polarization, equation (4.15) can be expressed approximately as:

$$J = \frac{J_o z F \eta_t}{RT}$$

$$\therefore \quad \eta_t = \frac{zF}{RT} \frac{J}{J_o} \tag{4.16}$$

The onset of the transition polarization can now be explained. Initially, at time = 0, both the metal and the solution are at an equal potential since they are conductors and there is no potential difference at the interphase. However spontaneous reactions will occur and even at zero field the reaction will be favoured in one direction, thus producing spontaneous charge transfer. The interphase will become charged and a potential will develop until the system reaches equilibrium. The transition polarization depends essentially on $(1/J_o)$, i.e., on the rate of electron transfer. A potential difference at the interphase arises because the charge transfer is not fast enough to cope with the current in the circuit. This bottleneck is the opposite of the phenomena occurring with concentration polarization. At one time it was thought that the rate of electron transfer was always very high so that $J_o \to 0$ and the interphase was at equilibrium. It was thought that only ill-conditioned electrode systems would present strong polarization effects. However recent measurements show that this is but the norm.

Different metals have very different exchange currents for a given reaction. For instance H_2 evolution occurs readily at platinum and rhodium whereas in other metals, such

as silver and gold, it requires a few volts. That is, silver and gold electrodes will show strong transition polarization effects whereas the effects with platinum and rhodium are minimal.

Adsorption layers: In addition to the potentials introduced by electrode polarization a further extraneous potential can arise if adsorbed layers are formed on the electrode surface. These layers can be of the form of a non-conducting film, an oxide film or an ion-conducting film.

a) Non-conducting films are formed as a reaction of the biological cell to the inserted electrode, e.g. Walker (8). In this case a coating of organic material insulates the electrode and this will produce spurious results.

b) Oxide films, or oxygen layers, form at the anode of an electrolytic reaction. This happens when a certain threshold potential between the electrodes is reached. The value of this voltage depends on the metal used. The resistance of the oxide film introduces an ohmic potential.

c) Ionic-conducting films are formed when reactions other than electrolysis occur at the electrode surface, e.g. Ag Cℓ formation on a silver wire. Again an ohmic potential is introduced which steadily increases as the coating of the electrode progresses.

The reduction of electrode polarization: For accurate measurements electrode polarization must be minimised. The common cause of all types of polarization is high current density. It is therefore essential to reduce the current as much as possible. Current densities can reach high values if metal

microelectrodes are used since the area over which charge transfer is effected is very small. For this and other reasons metal micro-electrodes must be connected to high impedance recorders. This electronic stage will be described later. With the use of the high impedance probes the requirement of minimal current density can be satisfied for recording electrodes but not for current injecting electrodes. Hence two different sets of electrodes must be used for potential recording and current injection.

Another source of polarization is the existence of a stagnant layer in the electrode vicinity where the ionic concentration is low. In biological systems the concentration cannot in general be altered and the stagnant phase cannot be reduced by stirring. There is, however, a way of increasing the ionic concentration around the electrode and at the same time favouring charge transfer. This involves the formation of a chemical coating on the electrode surface to produce the so-called non-polarizable electrode. For instance silver and mercury can be treated to behave like non-polarizable electrodes. They are coated with a sparingly soluble salt of the metal, i.e., Ag Cℓ or Hg Cℓ (calomel). In the case of a silver wire coated with Ag Cℓ the reaction $Ag\,C\ell + e^- \rightleftharpoons Ag\,C\ell^-$ takes place. This reaction occurs readily so that the transition polarization is reduced considerably. Furthermore the Ag Cℓ being sparingly soluble remains close to the electrode surface and the limiting current increases considerably thereby reducing concentration polarization.

Platinum gives high exchange current values for both cathodic and anodic electrolysis and so transition polarization will be small. If small current densities are used it is

unlikely that a depletion of H^+ or OH^- will occur and so concentration polarization will also be small. The oxide adsorption layer occurs in platinum at a potential difference of a few volts and so in the range of biological potentials adsorption layer effects will be small. For these reasons platinum is considered to be non-polarizable at small current densities. It is extensively used for microelectrodes since it has also the advantage of strength and stiffness.

Non-polarizable electrodes, or reversible electrodes, show little rectification, indicating that the system is near equilibrium. Polarization effects are then minimal except when the electrode area is reduced to very small dimensions. Frank and Becker (2) state that no metallic electrode with a recording surface of less than a few square microns is effective for the recording of steady potentials. Polarization is less critical if A.C. is used because during the brief period of the half cycle there is a smaller change in concentration at the interphase. The stagnant layer behaves as a capacitor and the reactance of the electrode varies inversely with the frequency.

Summarizing, it can be said that metal electrodes will always present polarization effects which will interfere with the recording of electric potentials. When the current density is small this polarization potential is approximately:

$$\eta = \eta_t + \eta_c = \left| \frac{\delta RT}{z^2F^2DC_b} + \frac{zF}{RTJ_o} \right| J$$

differentiating this expression gives

$$\frac{\partial \eta}{\partial J} = \frac{\delta RT}{z^2F^2DC_b} + \frac{zF}{RTJ_o} = R_e$$

where R_e is the electrode resistance. It can be seen that the electrode resistance depends on several factors: a) the frequency of A.C. (through δ), b) the concentration and composition of the solution (through $1/C_b$ and $1/J_o$) and c) the voltage at which the electrode is recording (through $1/J_o$). Thus to associate a resistance value to an electrode of certain area, as is common practice, is invalid. Each electrode should be tested under the particular experimental conditions under which it will be used.

ii) Glass microelectrodes.

All polarization effects are minimized as the metal area is increased. It is therefore convenient to make the liquid-metal interphase as large as possible and to connect it to the cell interior through some form of electrolytic bridge. This is the basis of glass microelectrodes which are filled with concentrated electrolyte. These electrodes are made from glass tubes ($\sim$ 1 mm o.d.) which have been drawn to very fine tips at one end. Electric connection with the recording instrument is then made with the use of a large coated wire (Ag Cl or Hg Cl) immersed in the concentrated chloride solution.

There will however be a liquid-liquid junction at the tip of the micropipette. In other words, there is a region where the composition varies from that in the pipette to that of the cell interior. An electric field thus arises in this region and an additional e.m.f. is introduced into the measuring system. It is therefore necessary to look at the behaviour of the liquid-liquid junctions so that this e.m.f. can be accounted for when electrical measurements are being interpreted. In Chapter I it was shown that the liquid-liquid junction

potential, E_L, is given by

$$E_L = \frac{RT}{F} \sum_j \frac{(u_j/z_i)((C_j)_o - (C_j)_i)}{\sum u_j((C_j)_o - (C_j)_i)} \ln \left[\frac{\sum (C_j)_i u_j}{\sum (C_j)_o u_j}\right] \qquad (4.17)$$

At the tip of a microelectrode a junction exists in which there is a variation of both composition and concentration, e.g.

$HC\ell(C_1) + KC\ell(C_2) + NaC\ell(C_3) : KC\ell(C_4)$. In this case equation (4.17) has the form

$$E_L = \frac{RT}{F}\left\{\frac{C_1(u_{H^+}-u_{C\ell^-}) + C_2(u_{K^+}-u_{C\ell^-}) + C_3(u_{Na^+}-u_{C\ell^-}) - C_4(u_{K^+}-u_{C\ell^-})}{C_1(u_{H^+}+u_{C\ell^-}) + C_2(u_{K^+}+u_{C\ell^-}) + C_3(u_{Na^+}+u_{C\ell^-}) - C_4(u_{K^+}+u_{C\ell^-})}\right\}$$

$$\times \ln\left\{\frac{C_1(u_{H^+} + u_{C\ell^-}) + C_2(u_{K^+} + u_{C\ell^-}) + C_3(u_{Na^+} + u_{C\ell^-})}{C_4(u_{K^+} + u_{C\ell^-})}\right\}$$

The ionic concentration in the microelectrode, C_4, is usually much higher than the concentrations outside, i.e. $C_4 >> C_1+C_2+C_3$. Since the ion mobilities of K^+ and $C\ell^-$ are very nearly equal, equation (4.18) can be written approximately as

$$E_L \simeq \frac{(u_{K^+}-u_{C\ell^-})}{(u_{K^+}+u_{C\ell^-})} \ln\left\{\frac{C_1(u_{H^+}+u_{C\ell^-}) + C_2(u_{K^+}+u_{C\ell^-}) + C_3(u_{Na^+}+u_{C\ell^-})}{C_4(u_{K^+} + u_{C\ell^-})}\right\}$$

The coefficient of the logarithm is very small.and therefore it is to be expected that E_L is also small. It is for this reason that micropipettes are normally filled with 3 or 4M $KC\ell$ solutions. However it should be noted that for $C_4 > C_1+C_2+C_3$ the argument of the logarithm is very small and therefore E_L could have large negative values. As a

result some workers prefer to use an electrolytic filling of a composition approximating to that of the cell interior. The liquid junction is minimized and there is little contamination of the cell interior, but the electrode resistance increases considerably.

Whichever solution is used for filling the bridge a few mv. potential is unavoidable. When the bridge is taken to microscopic dimensions the potential developed at the junction cannot be accounted for simply by a diffusion potential. Originally it was assumed that this extra potential arose from contamination of the electrode tip, e.g. Adrian (9). Later it was suggested that this potential was caused by the negative charges on the glass wall, Agin et al. (10). However no experimental evidence supporting either of these assumptions was presented and the tip potential was simply ignored.

There is now an extensive study of the tip potential by Okada and Indye (11) which makes the situation clearer. They found that there is a relation between the soaking time of the electrodes and the tip potentials developed. They also found that the electrode resistance decreases with soaking time, which is in contrast with the common view that high tip potentials imply high electrode resistances. To check this they measured the resistance of the glass wall near the tip. They found that this resistance decreased with increasing soaking time, suggesting an extensive hydration of the glass wall near the tip. This was further confirmed by the fact that in freshly prepared electrodes the resistance of the glass wall in a narrow tip region, about 15μ , increased steeply with increasing distance from the tip. In

contrast, in electrodes soaked for seven days, this increase was less steep over a wider region, about 100μ. Okada and Indye (11) then proposed the following model of the glass electrode:

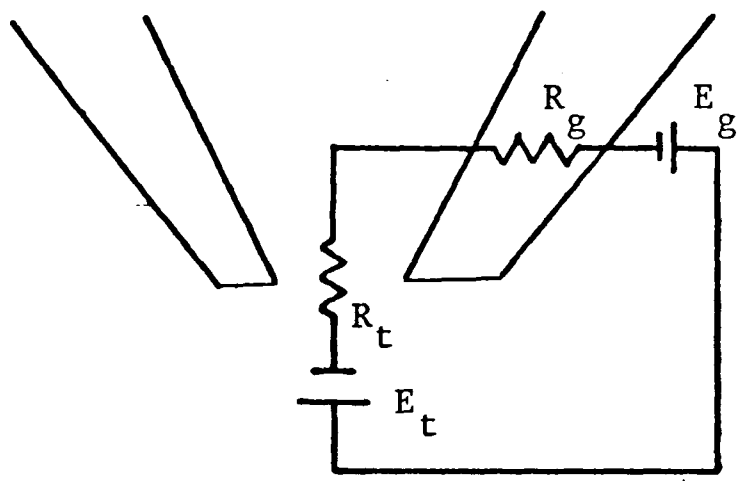

$$E = \frac{R_t}{R_g+R_t} E_g + \frac{R_g}{R_g+R_t} E_t$$

The complete tip potential consists of a potential occurring at the tip pore (E_t), mainly a diffusion potential, and a potential occurring across the thin glass wall near the electrode tip (E_g). In freshly prepared electrodes E_g will be very small but its value will increase during the time the electrode remains inserted in the cell.

The graphs of Okada and Inoye indicate that the tip potential might treble its value after a day's soaking. It is therefore necessary to use electrodes having small tip potentials when freshly prepared so that their incremented values are also small.

The glass microelectrode can be connected to a metal terminal, leading to the electronic equipment, in two ways: a) directly by introducing an Ag/AgCℓ wire into the glass tube, b) through an electrolytic bridge which would join the glass microelectrode to some stabilized liquid-metal junction, e.g. a calomel half cell. The first method is simpler and has the advantage of keeping the signal path

as short as possible. However an Ag/AgCℓ wire immersed in a concentrated KCℓ solution will soon be stripped of its coating. It is therefore necessary to recoat the wire frequently. If fast response recordings only are required the slow drift in the potential produced by the uncoating of the wire is unimportant. On the other hand, if prolonged recording of steady potentials is required, it is better to use a stabilized liquid metal junction, e.g. an Ag/AgCℓ electrode immersed in a saturated AgCℓ solution. The disadvantage of this connection is that a longer signal path is introduced. Connection from the microelectrode to the stabilized half cell can be made by means of an agar bridge, which facilitates the electrode manipulation. In this case a colloid-liquid junction appears. If both regions have the same composition and concentration no additional e.m.f. will arise, but some time is required for the junction to stabilize.

Glass electrodes are now widely used for recording and sometimes also for current injection. However these electrodes have very high impedances (>5 MΩ) and the passage of current is thus very restricted. Another consequence of the high impedance is that the electrodes cannot be connected to recording equipment with the usual input impedance of 1 MΩ. An intermediate electronic stage, the high impedance probe, has to be used.

4.2 The High Impedance Probe

The following diagram shows the basic circuit with the recording instrument connected to the microelectrode,

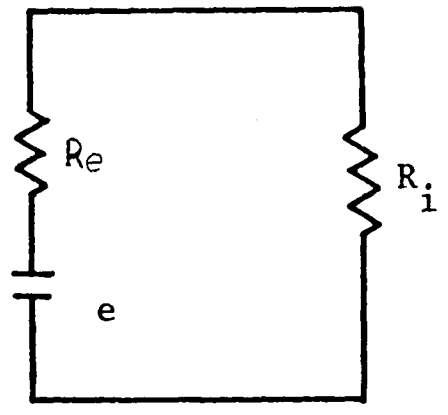

where R_i is the input resistance of the recording instrument and R_e is the microelectrode resistance plus the membrane resistance. It can be seen that the e.m.f. appearing at the recording instrument is given by $E_i = \frac{R_i e}{R_e + R_i}$. If $R_i << R_e$ this e.m.f. will be very small and difficult to measure. Furthermore there is also a stray capacitance effect because of the high impedance of the electrode and so a small signal across R_i will be severely distorted. It is therefore necessary to have a high impedance stage between the electrode terminal and the recording instrument. The most common solution to this problem is the use of a cathode follower or, better still, a differential amplifier.

(a) The cathode follower has been used extensively in electrophysiology. It has been reviewed (Hogg (12)) and will be described here because of its importance and also because it is the basis for more sophisticated alternatives.

The cathode follower consists of a value amplifier connected in the following way

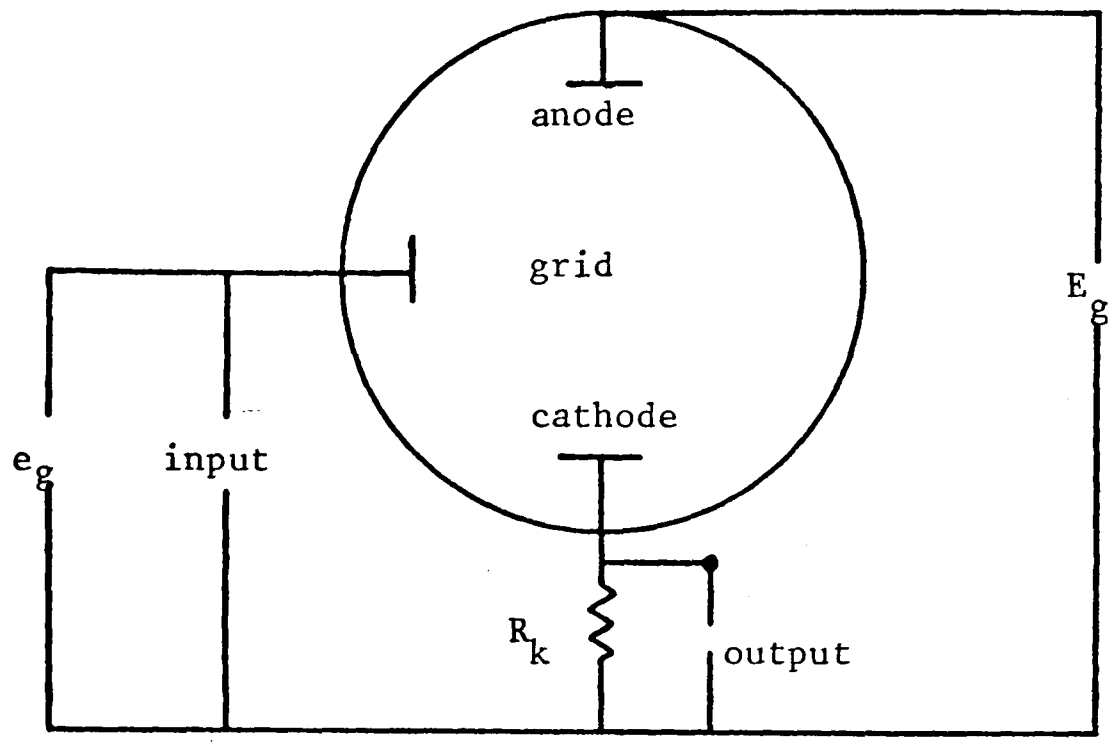

From the figure:

$$e_g = e_{gk} + i_k R_k \tag{4.19}$$

and

$$E_g = i_k R_k + e_{ak}$$

where e_{gk} is the grid-cathode voltage, e_{ak} is the anode-cathode voltage and i_k is the cathode current.

Solving the above equations by differentiation it can be shown that the gain of the stage defined as $G = \frac{\Delta i_k R_k}{\Delta E_g}$, can be expressed as

$$G = \frac{\mu R_k}{\mu/g_m + R_k + \mu R_k}$$

where $1/g_m = \frac{\partial e_{gk}}{\partial i_k}$ is the mutual conductance and $1/\mu = -\frac{\partial e_{gk}}{\partial e_{ak}}$ is the amplification factor.

$\mu/g_m = r_a$, the anode resistance and hence

$$G = \frac{\mu R_k/(r_a+R_k)}{1+\mu R_k/(r_a+R_k)} = \frac{A}{1+A} .$$

For typical values of A, the constants of the value,

G is very close to unity.

Equation (4.19) can now be written as

$$\Delta e_g = \Delta e_{gk} + G\,\Delta e_g$$

$$\therefore \quad \Delta e_{gk} = \Delta e_g(1-G) \quad .$$

This relation indicates that the cathode follower provides an excellent coupling between the electrodes and the recording instrument because:

a) Large changes in e_g, the input voltage, produce only small changes in e_{gk}, the operational state of the amplifier.

b) In a normal amplifier the input is connected between grid and cathode, i.e. $e_{gk} = e_g$, and the charge on the stray capacitance between grid and cathode, C_{gk}, is given by $e_g C_{gk}$. In a cathode follower however the charge on the stray capacitance is given by $e_{gk} C_{gk}$ and this can be written as $e_g(1-G)C_{gk}$, as if the capacitance were reduced by $1/(1-G)$. This reduction will diminish the distortion of the signal and increase the turnover frequency, i.e. the A.C. frequency at which the signal is attenuated to half its value.

c) In a normal amplifier the input resistance is given by $R_i = \frac{\partial e_g}{\partial i_k}$ whereas in a cathode follower $R_i = \frac{\partial e_g}{\partial i_k (1-G)}$, thus the cathode follower input resistance is effectively $(1/(1-G))$ times bigger. $\frac{R_i}{R_e+R_i} \simeq 1$ and so the e.m.f. across R_i is almost the whole membrane signal.

d) The output voltage of the cathode follower is given by

$$\Delta i_k R_k = \Delta e_g G = \frac{\mu}{1+\mu}\,\Delta e_g\,\frac{R_k}{R_k + r_a/(1+\mu)}$$

which is equivalent to

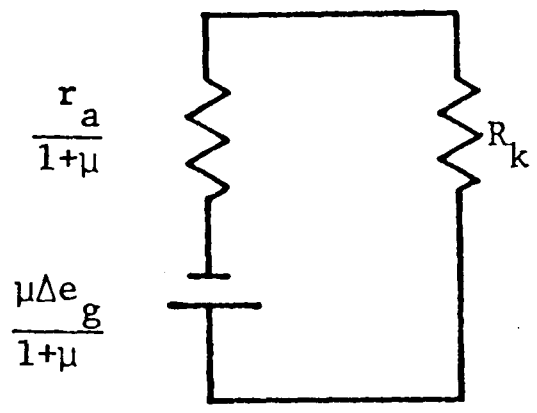

Thus the cathode follower output impedance R_o can be expressed as $r_a/(1+\mu)$ and since $\mu >> 1$ $R_o \simeq r_a/\mu = {}^1/g_m$ which is always small. As a result the cathode follower can be coupled easily to any succeeding stage.

(b) <u>The differential amplifier</u> involves the use of operational amplifier as voltage followers with feedback (Young (13)). An operational amplifier is an integrated circuit which can amplify the input signal many times. The simplest diagram of this circuit is represented in Figure 4.1. In this circuit the input signal will be amplified and collected at the output terminal. However if one of the input terminals is connected to the output and the earth connection is made to the power supply then the resulting circuit will behave as a voltage follower.

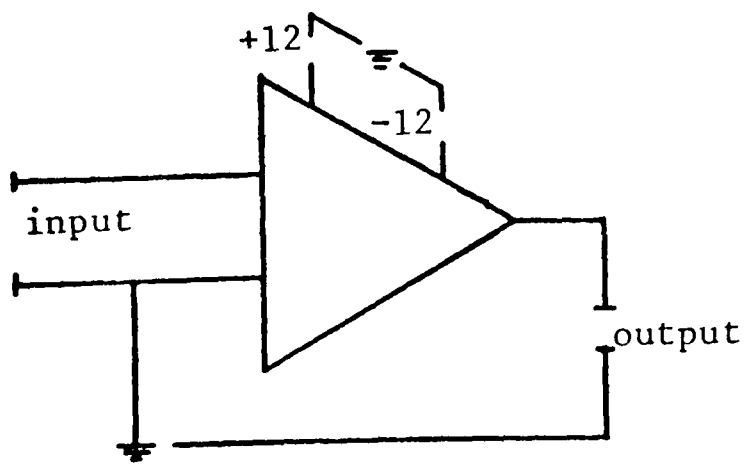

Figure 4.1 Operational Amplifier

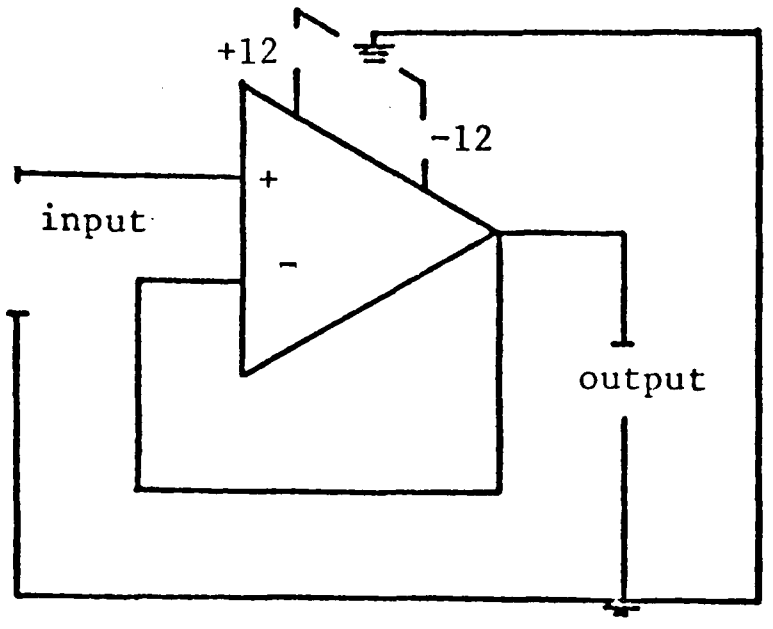

Figure 4.2 Voltage Follower

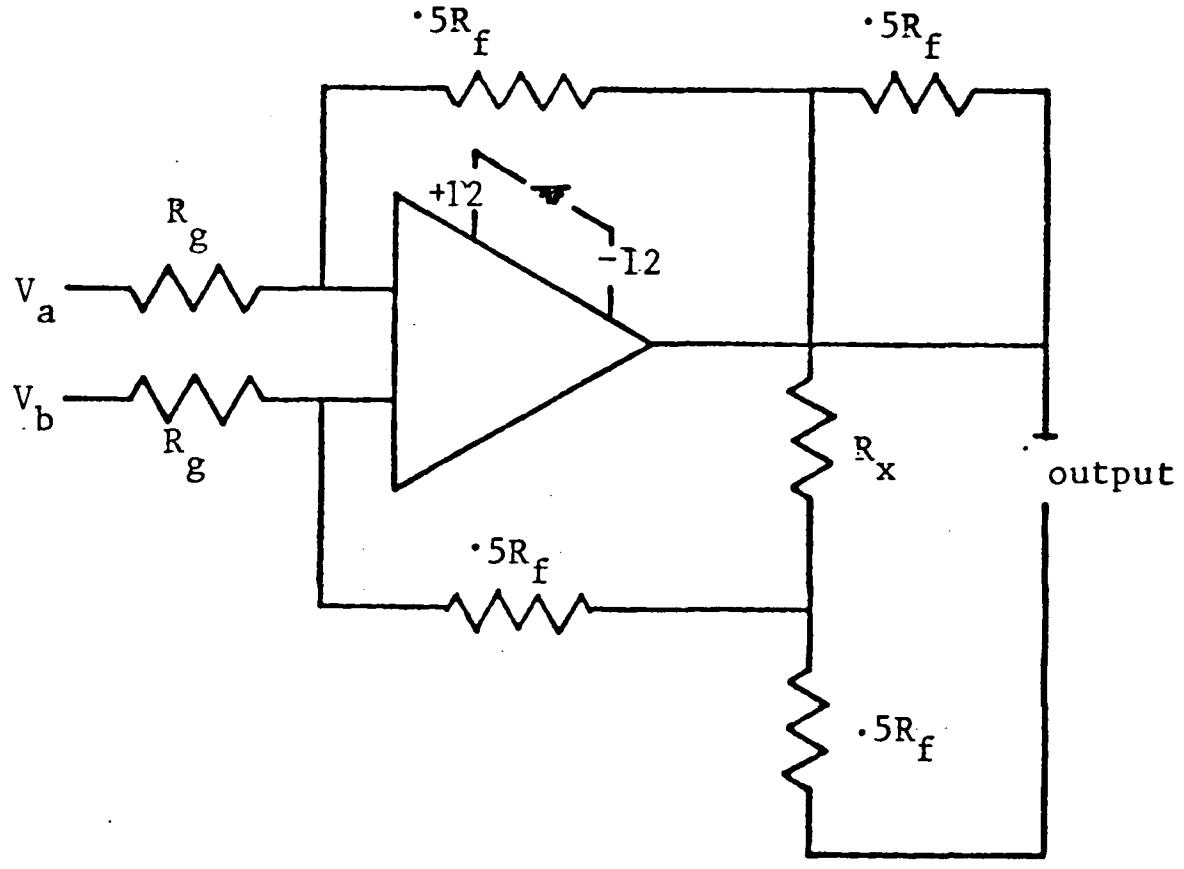

Figure 4.3 Differential Amplifier.

In the circuit represented in Figure 4.2 the input current, i_1, flowing into the positive terminal will emerge amplified at the output, but the output is short circuited to the negative input terminal and so a current i_2 will flow back to the amplifier. i_2 will emerge at the positive terminal thus working against the initial current i_1. The output voltage increases from its initial zero value until the current i_2 attains the same value as current i_1 and the signal cannot be further amplified. As a result the output voltage has the same value as the input voltage and the stage has a gain of unity. The important point is that since i_2 opposes i_1, virtually no current flows out of the input terminal and the stage behaves as if it had infinite input impedance.

A common problem with high impedance circuits is the pick-up of spurious signals. This problem is more acute with the transistor voltage follower than with the valve cathode follower. However this problem can be minimized if a slightly more elaborate circuit, the differential amplifier, is used (Figure 4.3).

In this case none of the input terminals is earthed. The output voltage will then be given by $(V_a - V_b) \times G$. The gain G can have values different from unity if R_x and R_f have values different from zero, i.e. these feedback resistances replace the short circuit of the common voltage follower. The gain will be given by:

$$G = \frac{R_f}{R_g} + \frac{Rf^2}{2R_gR_x} \quad .$$

However in order to have a good voltage follower, i.e.,

one with a high impedance input, the gain has to be close to unity. A typical value of G is ten.

The important point about differential amplifiers is that any spurious signals common to both terminals, e.g., the mains pick-up, will cancel each other out. This characteristic is called the common mode rejection. In spite of this ability to eliminate spurious signals, high impedance probes have to be screened as much as possible. The best way is to use a Faraday cage. The signal, after the voltage follower step, must be fed into an earthed coaxial cable and in turn connected to the recording equipment.

4.3 A.C. Signal Analysis

In previous chapters it has been shown how the membrane parameters can be obtained from D.C. or A.C. studies. In A.C. studies there is the need for the measurement of the phase angle. Most biological materials have time constants of milliseconds or less. This implies very small phase angles at low frequencies and this gives rise to certain experimental difficulties.

Cole (14) tried to determine $R(\omega)$ and $C(\omega)$ from measurements of the impedance magnitude, $|Z|$, alone. He found that it was necessary to use the Kramers-Kronig integral

$$\phi(\omega) = \frac{2}{\pi} \int_0^\infty \frac{|Z(v)|}{v^2 - \omega^2} \, dv$$

where $\phi(\omega)$ is the phase angle. However for the integration to be performed the form of $|Z(v)|$ has to be known for the whole frequency range which makes the method too elaborate.

A more direct method involves feeding the applied current signal and the recorded voltage response into the X and T inputs of an oscilloscope, Kishimoto (15). As a result a family of ellipses, each corresponding to different frequencies, will appear on the oscilloscope screen.

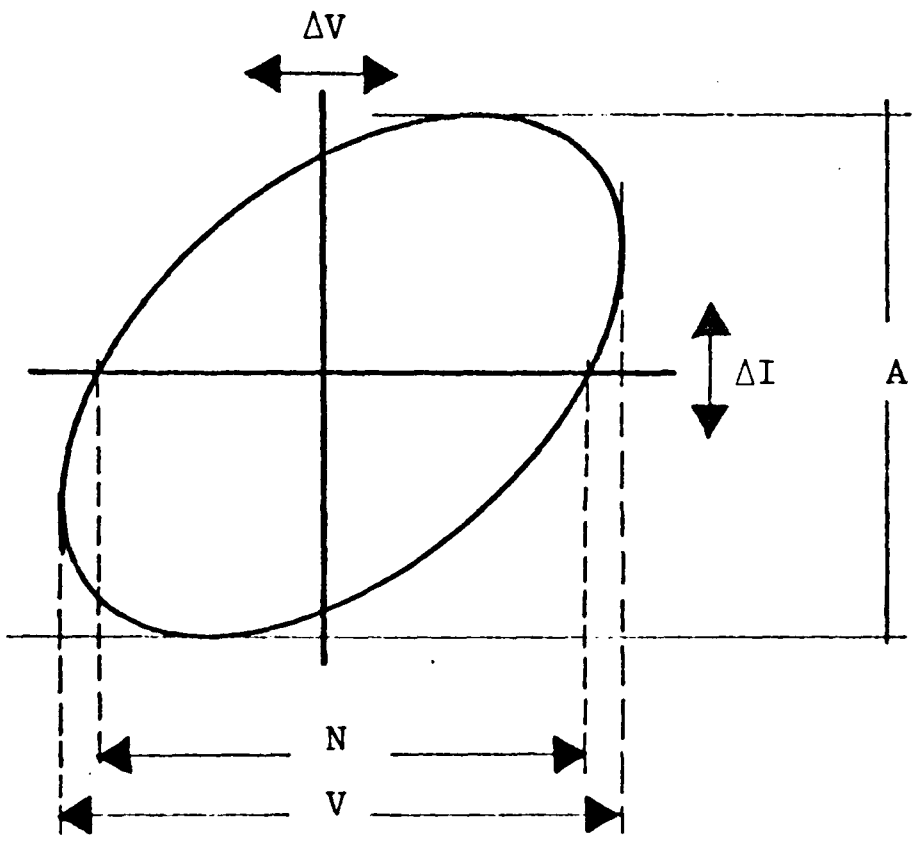

The voltage response has the form $\bar{V} = V \sin(\omega t + \phi)$. and it can be determined from the trace. At zero current $N = V \sin(\phi)$ so the phase angle can be determined from $\phi = \sin^{-1} \frac{N}{V}$.

The system has however two disadvantages:

a) The current and voltage signals have to be fed to the oscilloscope through several electronic steps which have to be carefully calibrated to avoid any additional phase angles being introduced at each step.

b) $N \to 0$ as $f \to 0$. If the oscilloscope sensitivity is increased to measure the small N values the trace becomes diffuse thereby limiting the frequencies at which N can be measured.

As a result of this limitation and the interest in studying the membrane response at very low frequencies more accurate techniques are required. Coster and Smith (16)

developed a highly sophisticated technique which essentially involves the use of a computer. The computer receives, through the corresponding digital-analogue converters, the values of the voltage response and the applied current at particular points. This data is fitted to sinusoidal wave forms by a least squares method and the relative phase angle between the two waveforms is determined.

In the present experiments the measuring of the phase angle involves an altogether different technique. It involves the use of V and N. But in this case the values of N can be determined at low frequencies. The current signal is fed to crossover detectors which trigger markers when zero current occurs. In other words, a train of sharp pulses, of μs duration, occurring at the times of zero current is obtained. This train is then added to the voltage signal, thereby producing a discrete pattern of N Values.

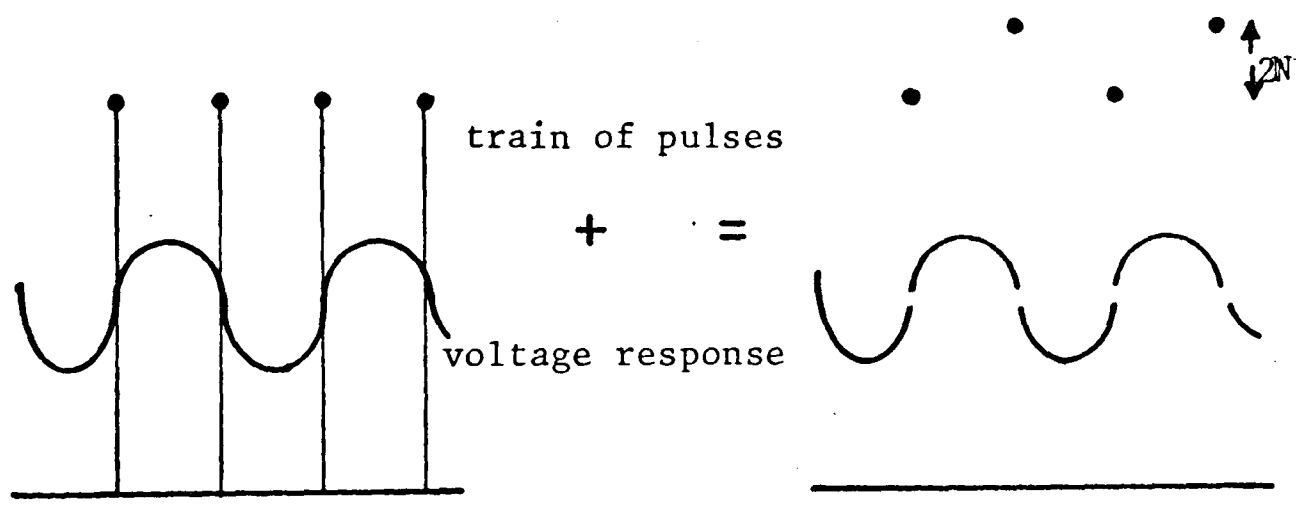

In this case the oscilloscope sensitivity can be increased as N becomes smaller without the continuous trace becoming diffuse. In the actual experiment it was found that a similar treatment for V values was useful at medium frequencies where V also becomes small. A detailed description of the circuit is made in the next chapter.

REFERENCES (CHAPTER IV)

1) Moore, J.W. Operational Amplifiers, Physical Techniques in Biological Research, Vol. VI, Edit. Nastuk, W.L., Academic Press (1963).

2) Frank, K. & Becker, M., Microelectrodes for Recording and Stimulation, Physical Techniques in Biological Research. Vol. V, Edit. Nastuk, W.L., Academic Press (1963).

3) Donaldson, P.E.K. Electronic Apparatus for Biological Research, Butterworth's Scientific Publications (1958).

4) Ives, J.C. & Janz, J., Edit. Reference Electrodes Theory and Practice. Academic Press (1961).

5) Plonsey, R., Bioelectric Phenomena, McGraw-Hill (1969).

6) Bockris, J. O'M. & Reddy, A.K.N. Modern Electrochemistry, Vol. 2, Plenum Rossetta (1970).

7) Sawyer, D.T. & Roberts, J.L., Experimental Electrochemistry for Chemists, Wiley Interscience (1974).

8) Walker, N.A., Aust. J. Biol. Sci. 8, 476 (1955).

9) Adrian, R.H., J. Physiol. (Lond.) 133, 631 (1956).

10) Agin, D. & Holtzman, D. Nature (London) 211, 1194 (1966).

11) Okada, Y. & Inouye, A. Biophys. Struct. Mechanism 2, 31 (1976).

12) Hogg, J., Ph.D. Thesis, Edinburgh University (1966).

13) Young, S. Electronics in the Life Sciences, The MacMillan Press Ltd. (1973).

14) Cole, K.S., Membrane, Ions and Impulses, University of California Press (1968).

15) Kishimoto, U., Plant and Cell Physiol. 7, 429 (1966)

16) Coster H.G.L., & Smith, J.R., The effect of pH on the low frequency capacitance of the membrane of Chara corallina, Membrane Transport in Plants, Edit. Zimmerman, U. and Dainty, J. Springer-Verlag (1974)

17) Chandler, W.K., & Hodgkin A.L., J. Physiol, 181, 594 (1965)

18) Tasaki I, Lurxoro, M & Ruarte, I., Science, 150, 899 (1965)

CHAPTER V

EXPERIMENTAL MATERIALS AND PROCEDURES

In Chapters II and III it was shown that the use of symmetric external stimulation in conjunction with the 0.42L technique is a most convenient method for measuring the membrane electric parameters of Nitella translucens, using either D.C. or A.C. In Chapter IV some of the experimental problems which arise in electrophysiological studies were considered and various means of minimizing such problems were discussed. With these considerations in mind the present experimental arrangement was designed and is now described.

5.1 The Faraday Cage

When very high impedance electrodes, and the corresponding high impedance probes, are used there is a need for some form of Faraday cage to screen them from spurious signals. The cage used in the present experiments was made of mild steel ($\frac{1}{16}$ inch thick) and in the form of a 70 cm. cube closed on all but one side. Located inside the cage were: the micromanipulator, the microscope and its illumination lamp, the high impedance probe heads, the electrode resistance meter and the cell bath.

5.2 The Cell Bath

The cell bath was made by milling channels on a perspex sheet, 1 inch thick, as shown in Figure 5.1. There are three compartments in the bath and separation between the

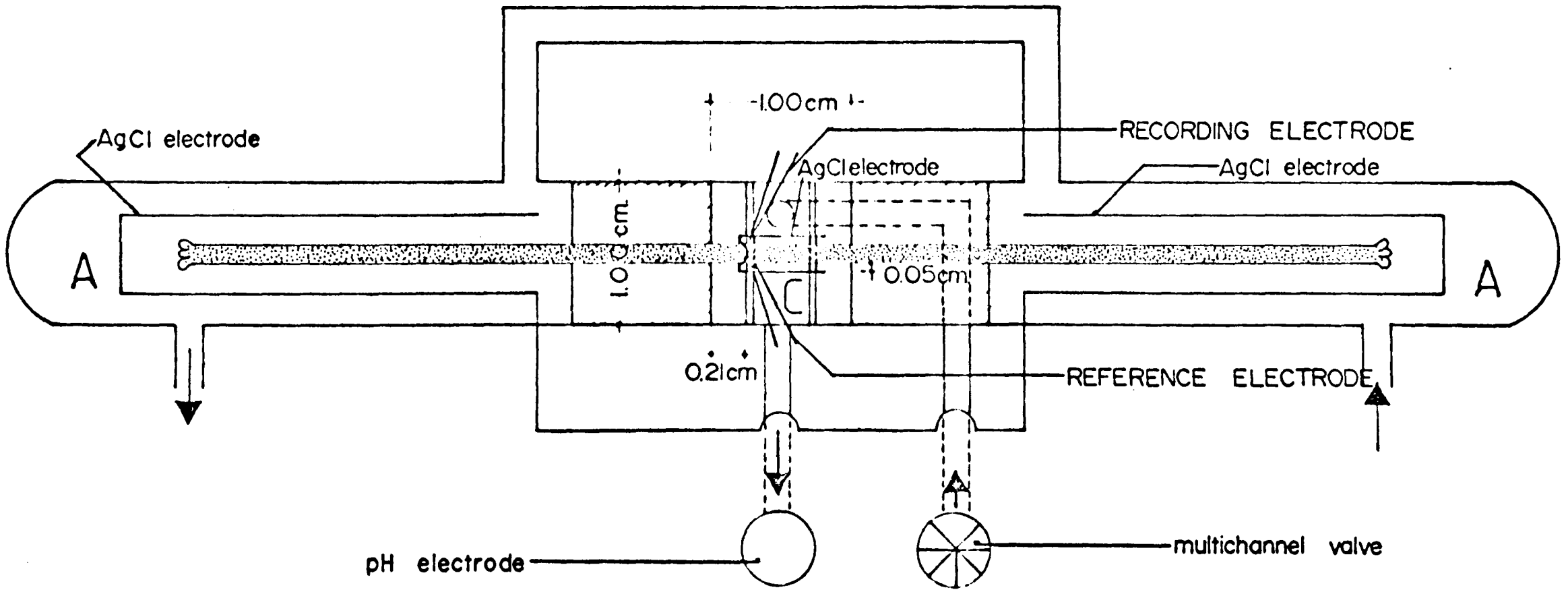

Figure 5.1. The Cell Bath.

compartments is achieved with perspex barriers. Along the centre of these barriers runs a 1 mm. groove into which the cell is mounted. The perspex barriers allow the partition of the cell into three segments.

Good electrical insulation of these segments from each other is of paramount importance because poor insulation would permit current leakage thereby giving an underestimate of R_m. The standard material used by many workers for sealing the barriers has been white vaseline. Whilst vaseline probably provides good sealing there remains the possibility of current leakage along the wet cell wall. Okhawa and Kishimoto (1) measured the resistance of the cell wall of Chara Australis and found that it amounted to $10^6 \Omega$ per cm., considerably greater than the membrane resistance of the short cell segment they used. Thus the leakage current in their experiment was probably negligible. In the present work the resistance of a dried cell wall of Nitella translucens was measured and found to be of the same order of magnitude as that obtained by Okawa and Kishimoto. If the wall was moistened the resistance decreased to $10^4 \Omega$ per cm. Subsequent careful redrying of the cell wall resulted in the resistance value returning to its original high value. These results agree with the more detailed studies of Skierczyńska Śpiewla, Bulanda Zołnierczuk and Sielewiesiuk (2). They measured the longitudinal resistances of Chara Brauni and Nitellopsis Obtusa using the following arrangement

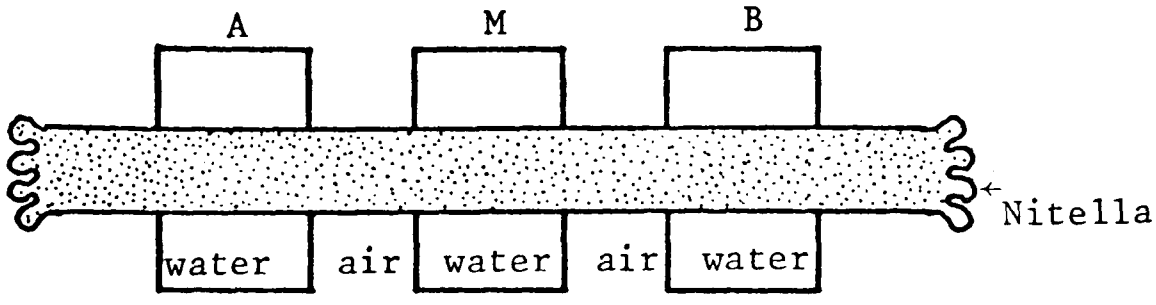

Initially current was fed from compartment A to compartment B and the voltage drop between these two gave the resistance per cm. of the cell interior. However they realized that this resistance value remained constant only if the cell segment exposed to the air remained moist. The addition of compartment M permitted the computation of the change in longitudinal resistance when this section of the cell was immersed in water. A decrease of the longitudinal resistance occurred immediately after immersion in water. With the use of microelectrodes inserted at both extremes of M it was found that the resistance decrease was confined to the moistened region and occurred in an external layer of the cell. They proposed the existence of an immobile layer of the cytoplasm which would have semiconductor characteristics. However the results obtained herein with the cell ghost strongly suggest that this layer is simply the cell wall which increases its conductivity when moistened.

In the first set of experiments (cells 1-12) the isolation of the cell segments was achieved in the following way. After careful drying, the barriers were smeared with white vaseline. The Nitella cell was then dried with filter paper in the regions to be held by the barrier and then mounted into the central groove. The cell segment in the right hand compartment was arranged to be of equal length to that in the

left hand compartment. The barriers were then covered with perspex sheets smeared with vaseline. Finally the cell was vigorously rinsed to remove any loose vaseline.

As a final check that the leakage current had been reduced to negligible proportions, a cell wall was filled with white vaseline and mounted in the same way as the living cell. Thus any current that flows between neighbouring compartments of the cell bath must be a leakage current through the barrier; the leakage resistance can then be estimated. The leakage resistance for each barrier in the present work was found to be of the order of 5 MΩ. Comparison of this value with the value of the cell membrane resistance in the central compartment (∿ 100 kΩ) indicates that any leakage currents were in fact negligible. In spite of this the membrane resistance was sometimes rather low and suggested that some current leakage was taking place, possibly by the water creating pathways through the vaseline. Unfortunately faulty insulation can only be determined after the cell has been impaled and therefore cannot be remedied. Because of these possible leakages and the ease with which vaseline contaminates the APW, it seemed that an alternative sealant to vaseline was desirable. A silicone compound, MS4 (Dow Corning), which has the consistency of vaseline was found to be a better alternative. This compound was used for mounting the cells and silicone rubber (Blue-Tack, Bostik) was used for smearing the perspex sheets that cover the perspex barriers. This combination gave excellent results because it produced a better insulation - the leakage

resistance was 15 MΩ in this case - and never failed to work. This preparation was used in all experiments from cell 12 onwards.

Once the cell has been mounted in the cell bath it could be flushed by means of a continuous flow of solution and this has several advantages:

a) It reduces the contamination produced by the external KCℓ electrode.

b) It is possible to exchange the external solution without disturbing the impaled cell.

c) It reduces the heating of the bath produced by the illumination lamp.

d) It maintains a constant concentration of CO_2 in the external solution. The need for control of the CO_2 concentration has been observed by Spanswick (3) who found that Nitella translucens in stagnant solution does not hold the light produced hyperpolarization. However the flow of solution containing CO_2 restores and maintains this response. A similar effect was also found here in that the initiation of solution flow after a stationary period was usually accompanied by a small increase in the membrane potential.

The continuous flow in the cell bath was supplied to the compartments A and C with the inlet through the bottom and the outlet through the top (Figure 5.1). This arrangement gives a surface outflow which reduces the silicone grease contamination. It also produces a steady flow which is necessary for low pick-up and constant pH.

5.3 Plant Material and External Solutions

In all experiments of the present work the plant material used was Nitella translucens cells. These plants were originally collected from a loch near Dunkeld, Scotland, and transferred to shaded tanks out-of-doors. The plants were rooted in a sand and soil mixture and they grew vigorously after acclimatization. The cells were watered with artificial pond water (APW) of the following composition: 0.1 mM KCl, 0.1 mM $CaCl_2$ and 1 mM NaCl. All external solutions used in the present work were based on this APW. The different solutions consisted of APW having different pH values and in some cases the addition of DNP (2,4-dinitrophenol). In experiments where DNP was used the solutions were prepared by adding 0.2 mM DNP to the APW prior to the setting of pH values. The pH value of the APW was modified by the addition of buffers and adjusted to the required value by the addition of NaOH (pH $\geq$ 5) or HCl (pH = 4).

The selection of the buffers to be used for maintaining a constant pH is important. There are several examples of pH buffers having undesirable effects on biological systems. For instance, Kishimoto (4) found that 10^{-2} M phosphate buffer and 2×10^{-3} M ATP (disodium) produced fluctuations in the resting potential of Chara corallina. Phosphate also produced successive spontaneous action potentials. A more detailed study of the inadequacy of certain buffers in biological systems was made by Good, Winget, Winter, Connolly, Izawa and Singh (5). They found that most buffers have very low buffering capacity at pH below 6. They also

found that commonly used buffers have secondary effects, e.g., Tris-buffer has considerable reactivity and it is often inhibitory. As an alternative they proposed a series of buffers especially useful in biological studies - the zwitterionic buffers or Good buffers. These buffers have pK_a values (the pH at the midpoint of the buffering range) between 6 and 8. They were chosen after satisfying several conditions. Of particular importance in membrane studies is that they have very low membrane permeability and negligible metal binding constant. The latter condition has to be satisfied to ensure that no Ca^{++} sequestration will occur. In the present studies MES(2- (N-morpholino) ethanesulfonic acid) with a pK_a of 6.15 was used for buffering in the range 4-6. Glycylglycine with a pK_a of 8.4 was used for buffering in the range 7-8. In both cases 1 mM concentration in a steady flow were used. Even with the use of buffers the external solutions should be freshly prepared, especially in the alkaline range.

The exchange of solutions was made by first emptying the cell bath and then starting the flow of new solution. The pH of the external solution did not change immediately upon adding the second solution but several minutes of flowing solution were required for it to attain its new value. This was observed by monitoring of the external pH with a direct reading pH meter.(EIL 23A) located at the outflow of the solution.

5.4 Illumination

The microscope illumination was provided by a tungsten lamp (12V, 6W) placed underneath the cell bath and driven by a D.C. supply, one terminal being connected to the common earth to avoid introducing the mains pick-up into the Faraday cage. After insertion of the microelectrode into the Nitella cell the lamp voltage was turned down to 7 volts with the aid of a resistor in the lamp circuit. The fact that this lamp is working below the normal voltage increases its stability and ensures a source of constant illumination, Young (6). It also produces a source with a minimal ultra-violet component, Campbell (7). It has been shown by Doughty and Hope (8, 9, 10) that the ultra-violet radiation affects the membrane electrical characteristics of the characeae and therefore should be maintained at a low constant level during the experiments. The infra-red component has also been shown to affect the membrane electric parameters, e.g. Spanswick (3). Since this component is very considerable when illuminating with a tungsten lamp a combination of glass, air and perspex filters was used to reduce heating of the cell bath to a minimum.

The intensity of the illumination used in the present work was 0.04 mW/cm^2. An intensity of 1 mW/cm^2 was used by Spanswick (3). It is difficult to compare these values with those quoted by other workers because of the common practice of measuring illumination intensity in lux. These units are weighted according to the spectra of the human eye and unless

the wavelength composition of such illumination is given it is not possible to assess the absolute illumination. It should be noted that Brown, Ryan and Barr (11) found that a reduction of the intensity of illumination increases considerably the life span of Nitella clavata cells.

5.5 Electrodes

a) The current electrodes: These consisted of two connected pairs of Ag/AgCℓ wires located in the side compartments and another pair of Ag/AgCℓ wires located in the central compartment. This arrangement ensured symmetric current injection. The wires were arranged to be parallel and close to the cell on each side (see Figure 5.1). The wires were coated with AgCℓ by passing D.C. through the wires when they were immersed in a 100 mM NaCℓ solution. The current, which was controlled by a variable resistance in the circuit, was applied for 1 minute in one direction and then reversed. The procedure was repeated several times until the coating was a dark purple colour. The resistance of these electrodes in APW at 100 mv D.C. was 4 kΩ.

b) The voltage electrodes: These were a pair of glass electrodes, one being a microelectrode which was to be inserted into the cell and the other to be used as a reference electrode placed in the outside solution and close to the former.

The microelectrodes were made by drawing glass tubes

(Jencons H15/3, 1.5 mm. i.d., 2 mm. o.d.) in an electrode puller (Narashige PE-2). These electrodes do not have very large shanks since a short robust electrode is required. The resistances of these electrodes were about 5 MΩ and the tip potentials were less than 10 mv. Immediately after drawing, the electrodes were filled with 3M KCℓ solution. A glass microfibre is used to drive the solution as close as possible to the tip and complete filling of the electrode tip occurs by capillarity. The electrodes were used immediately after preparation.

The electrodes were connected to a stabilized calomel half cell by means of a KCℓ-agar bridge. The bridge was prepared by boiling a plastic cannula (0.5 mm. i.d., 1 mm. o.d.) in a 3M KCℓ solution containing 10% agar. To avoid the common problem of the KCℓ creeping along the bridge a sealant was applied to the open ends of the microelectrode and the calomel half cell. R.T.V. silicone rubber (Radio Spares) was found to be a suitable sealant since at the end of the experiments the rubber can be peeled off and the bridge used again.

In the early experiments a glass microelectrode with smaller resistance than the internal electrode was used as a reference electrode. In later experiments a more robust electrode was used. This was a glass tube (1 mm. o.d., 0.5 mm. i.d.) which had been heated at one end to give a small orifice (∿50μ) and was filled, by boiling, with 3M KCℓ-agar solution. These electrodes have resistance values of ≃ 2 MΩ and tip potentials of a few mv.

The internal electrodes were inserted into the cell

with the aid of a micromanipulator (Leitz or Narishige) and the insertion observed with a stereoscopic microscope (Wild M5). The insertion was made in the central segment at the point $X = -0.58L$. A pH glass electrode was inserted in the symmetric position, i.e. at $x = +0.58L$.

c) pH glass microelectrodes. There are two types of pH glass microelectrodes: Hinke (12) type and the Thomas (13) type. Hinke microelectrodes consist of a tip of pH sensitive glass (Corning 0150) protruding from a truncated pyrex electrode. The pH sensitive tip is joined to the pyrex electrode by a glass-to-glass seal made by blowing the pH glass at its softening point. The Thomas electrode has a recessed tip, i.e. the pH glass tip is inside the pyrex tip. Again both tips are joined by a glass-to-glass seal.

Hinke type electrodes are commercially available with a sensitive tip of 50μ. There are also Hinke electrodes where the sensitive tip is made from Antimony and the insulation consists of a plastic coating. However none of these electrodes are suitable for insertion through the tough cell wall of plant cells. The usual difficulty is breakage of the glass-to-glass seal or the loosening of the plastic coating. Spanswick and Miller (14) overcame these difficulties by making a perforation of the cell wall prior to inserting the pH electrode. Thomas type electrodes appear to be more suitable for plant physiology since they are more robust, but the tips are easily clogged, mainly by cytoplasmic material. Silver (15) suggested that bevelled Thomas electrodes might be more suitable. However such electrodes are not commercially

available and they are very difficult to make. It was therefore considered desirable to develop a suitable electrode for the present studies. The result was essentially a more robust electrode of the Hinke type with a glass-to-glass seal. Such an electrode is very easy to insert into the characeae and produces no more damage to the cell than a conventional glass microelectrode.

The technique for the preparation of these electrodes is similar to that proposed by Thomas (13), with some modifications:

(a) A long pH glass microfibre was drawn in the microelectrode puller. The diameter of the fibre and its wall thickness was determined by the temperature of the heating element and the area of glass tubing being heated. In the present experiments the fibre was ∿20μ diameter and the wall ∿2μ in thickness.

(b) The microfibre was connected to a hypodermic syringe which was then used for blowing the pH glass. The following figure shows the arrangement used.

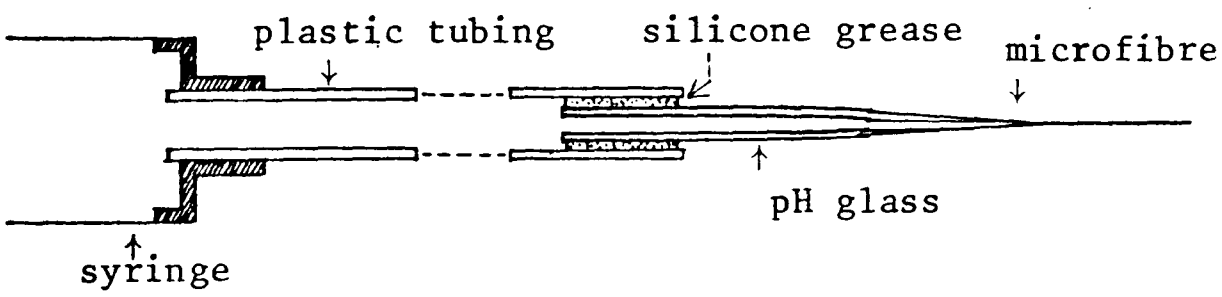

The microfibre and the pyrex electrode were then mounted in the following way:

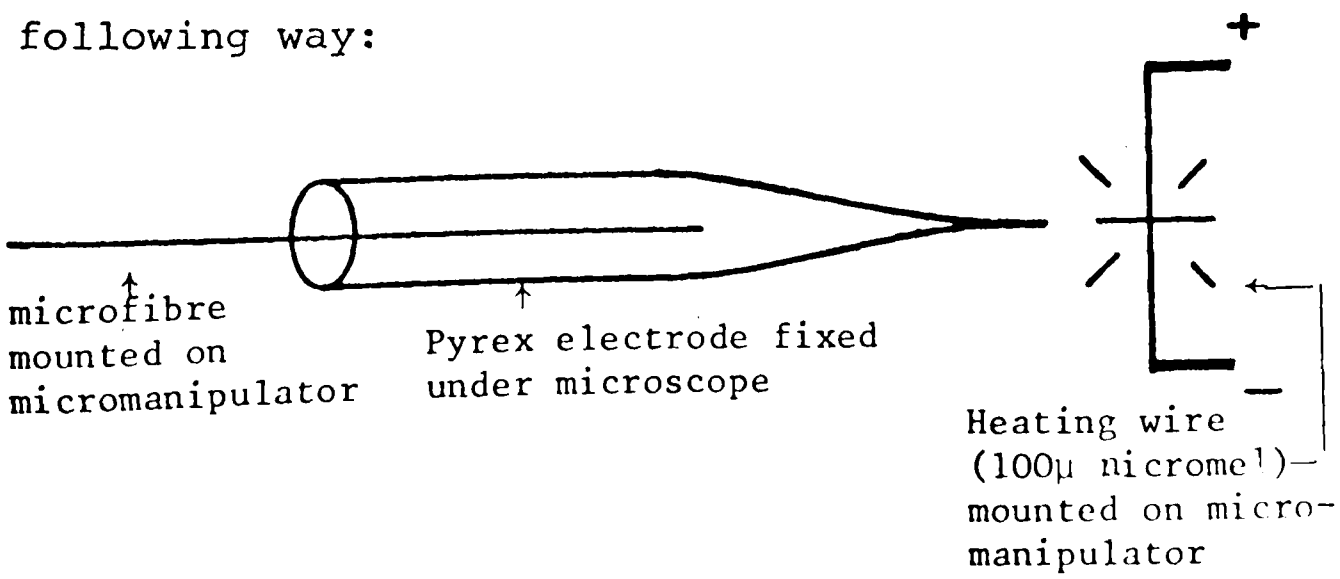

Using the above arrangement the fibre was introduced into the pyrex electrode until it could advance no more into the pyrex tip:

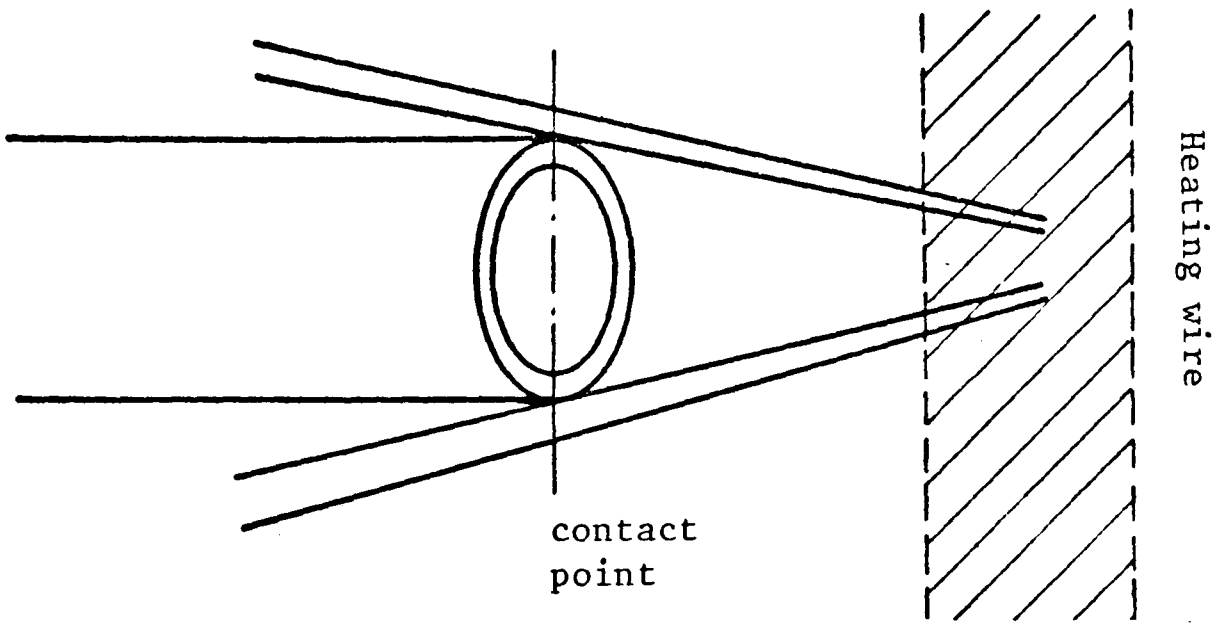

(d) The pyrex tip was broken as close to the contact point as possible. This could be done by bending the pyrex tip with the heating wire until it broke. This is a trial and error procedure and can be repeated as long as the tip breaks ahead of the contact point.

(e) The glass fibre was pulled through the truncated pyrex tip and the heating wire placed close to it. The wire was then heated until the pH glass softened on contact with it. The fibre was brought into contact with the heating wire and when the fibre tip was completely closed it was quickly withdrawn. The extreme tip of the electrode is insensitive to pH and should be kept as short as possible.

(f) The pH glass was pushed out of the pyrex tip until the required sensitive length was exposed. Subsequent heating of the two glasses and simultaneous blowing of the pH glass produced a

a glass-to-glass seal which ran along the pyrex wall. This region should be at least 200μ long to ensure a strong glass-to-glass seal.

(g) The fibre, when pulled, broke at or near the glass-to-glass seal, thus producing a pH tip of the following form.

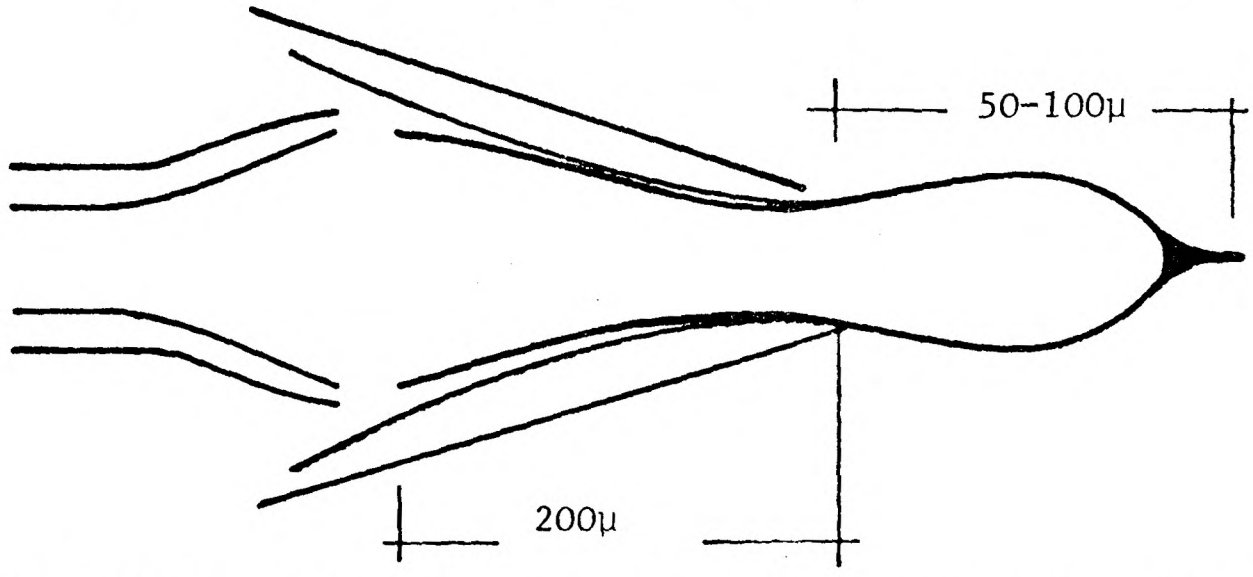

The fibre could then be cut with a pair of scissors and used again for the preparation of another microelectrode.

(h) The pH tips of these microelectrodes have glass walls much thicker than the commercial pH microelectrodes. They had to be boiled in distilled water for several hours to obtain a hydration of the pH glass. The distilled water in the electrodes was then exchanged for a 3M KCℓ solution and the electrodes were connected to the apparatus in the same way as any other glass microelectrodes.

The electrodes used for the determination of the internal pH of the cell had resistances of $10^{10}\Omega$ and gave pH responses per pH unit of between 50 and 58 mv. The electrode response per pH unit should be 58 mv at 18°C. In practice, however, the response is less than the 58 mv and it is therefore necessary to calibrate the electrodes prior to each insertion. This was done by immersing the internal voltage recording electrode and the pH glass electrode in a

calibrating solution at pH 7. The resulting potential between the electrodes was backed off until zero potential was recorded at this pH. The electrodes were then immersed in a pH 4 solution and the response per pH unit determined. A similar procedure was performed with the electrodes immersed in a pH 9.2 solution. The average of these responses was then used for the subsequent determination of the internal pH of the cell. pH glass electrodes, having very high resistance, have a tendency to drift a few mv over a period and it was therefore necessary to check the response at pH 7 after removal from the cell.

5.6 The Electronic Recording

The stabilized calomel half cell interphased the cell with the high impedance probes. These electronic units were described in the previous chapter. The details of the particular circuits used in this work are shown in Figure 5.2. These probes have a head, with FET transistors working as voltage followers, which can be placed close to the preparation and a body made up of a × 10 amplifier and a D.C. balance. The input values of these probes are $R = 10"\Omega$ and $C = 10$ pf. The output is equal to 5 kΩ and the common mode rejection ratio is 1000:1.

The output from the high impedance probes was fed through an earthed 50 kΩ coaxial cable to a storage oscilloscope (Tektronix 564 B). By suitable triggering with a prepulse from a D.C. pulse generator (Advance PE 500 2C) both the injected current and cell response could be recorded

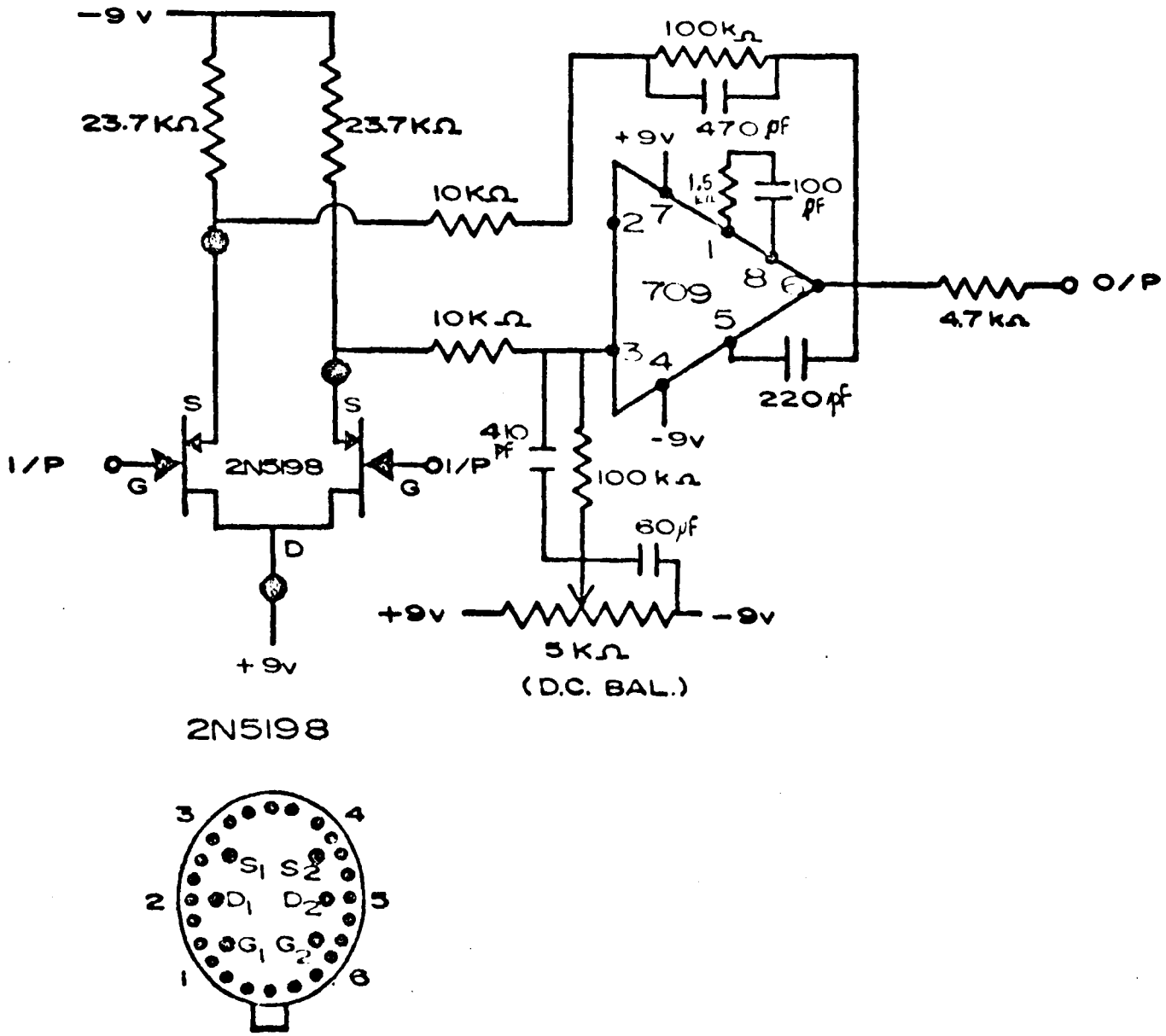

Figure 5.2. The High Impedance Probe.

and stored in a single sweep of the oscilloscope. The image could then be studied at leisure. In the D.C. experiments the current was fed through a 10 MΩ resistor to ensure constant current in the circuit where changes in the membrane resistance occurred. In the A.C. studies the injected current consisted of the summation of the D.C. pulse plus a sine wave from a Muirhead Decade Oscillator D990-A. This composite signal was fed through a 10 MΩ resistor with additional 1.1, 2.5, or 4.2 MΩ resistors. The additional resistors correspond to $10.(^{1}/d)$, where d is the cell diameter (0.9, 0.8, 0.7 mm.). In this way it was possible to apply the same current density (±5%) to cells of different diameter.

The A.C. response from the cell was fed to the A.C. circuit processor mentioned in Chapter IV. This circuit is shown in Figure 5.3. There are several electronic stages between the cell output and the oscilloscope. It is important to ensure that no phase shift additional to the one produced by the cell is introduced by the electronic components. To verify this a cell dummy was used, i.e. an RC parallel circuit with $R = 100\ k\Omega$ and $C = 2.2\ \mu f$. When the capacitor was disconnected no phase shift could be measured. This shows that there is no electronic component contributing appreciably to the measured phase angle. This is true only when the equipment is well calibrated, i.e. when the marking points occur at zero current. It was found that overloading the last amplifier stage before the markers ensured that this condition was met.

It is also important to test the sensitivity of the

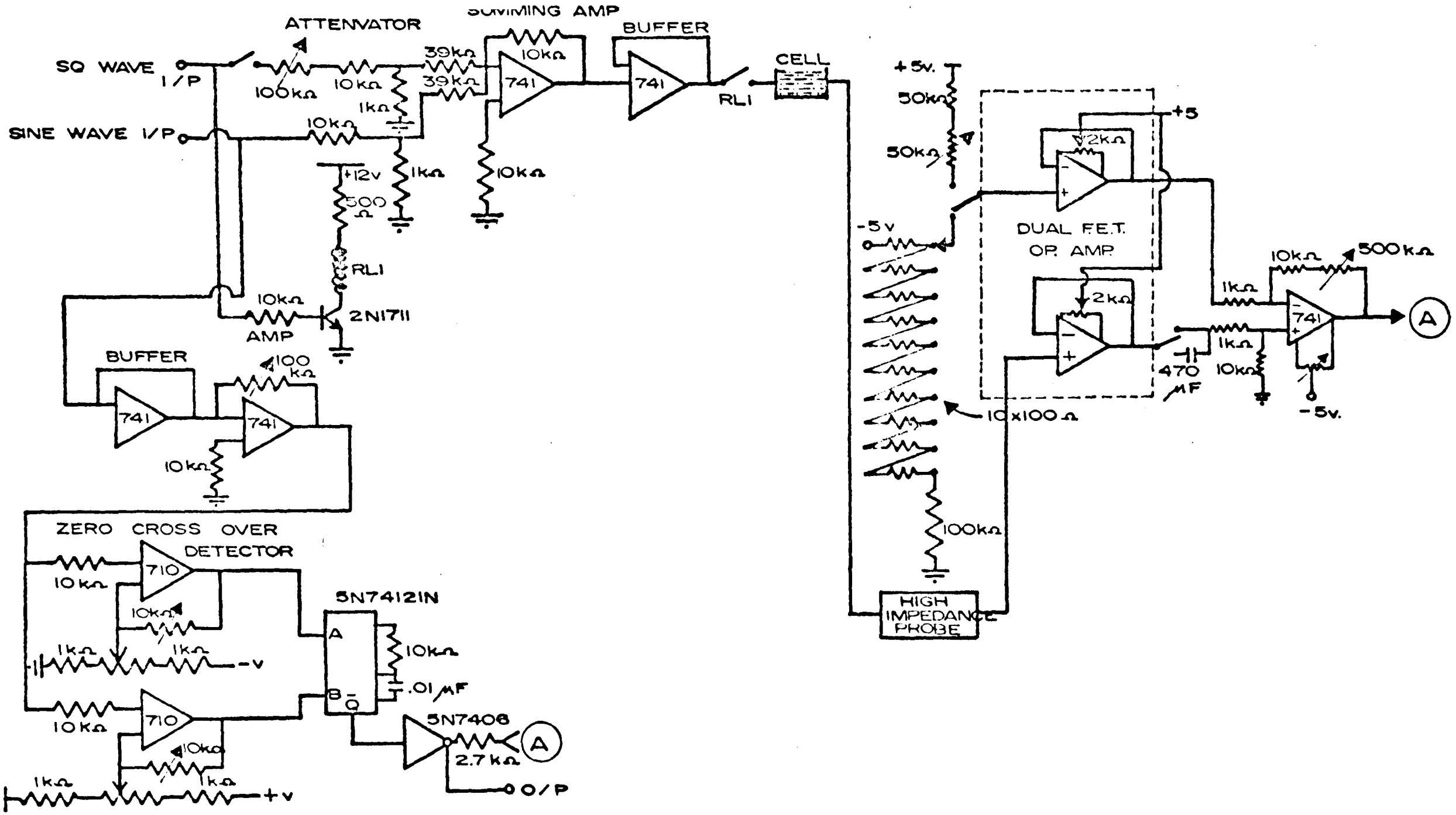

Figure 5.3. A.C. Processor.

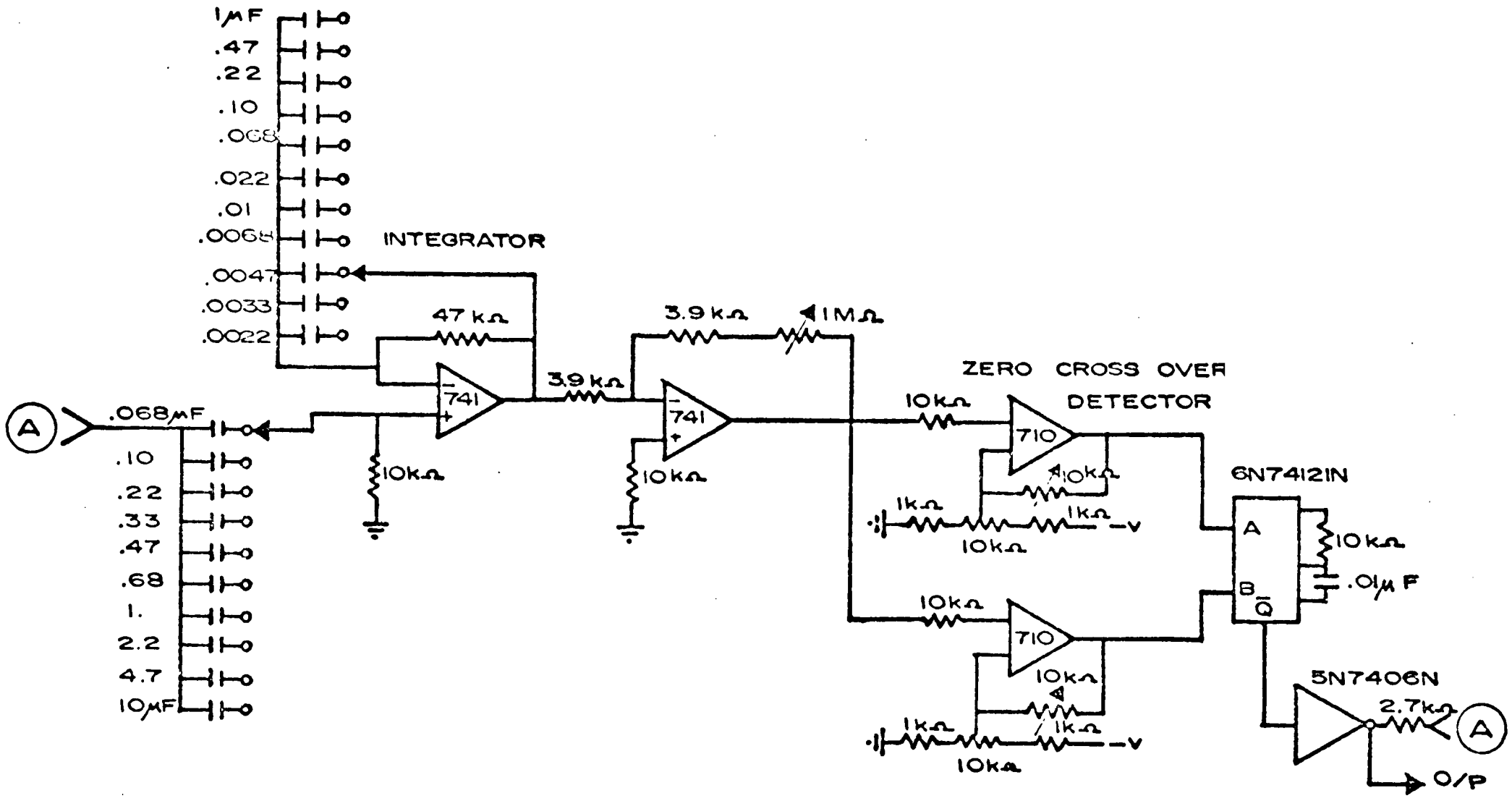

Figure 5.3. A.C. Processor (continuation).

method. For this, the time constant of the cell dummy was measured at different frequencies. The following table shows that the method reproduced the manufacturer's values of the dummy components (τ = 22 ms ± 10%). However, at 100 c.p.s. the method is not very sensitive. The reason for this is that at these frequencies the cell response is of a similar magnitude to the noise introduced by the electrodes. This could have been avoided simply by increasing the applied current at these frequencies.

f (Hz)	τ (ms)
1	20
10	20
50	19
100	14

REFERENCES (CHAPTER V)

1) Okhawa, T & Kishimoto, U. Plant and Cell Physiol. 15, 1039 (1974).

2) Skierczyńska, J., Śpiewla, E, Bulanda, W., Zołnierczuk, R. and Sielewiesiuk, J. J. Expt. Bot. 24, 78, 47 (1973).

3) Spanswick, R.M. Biochim. Biophys. Acta, 332, 387 (1974).

4) Kishimoto, U. Annual Report Sci. Works, Fac. Sci., Osaka Univ. Vol. 7, 115 (1959).

5) Good, N.E., Winget, G.D., Winter, W., Connoly, T.N., Izawa, S. and Raizada, M.M.S., Biochem. 5, 2, 467 (1966).

6) Young, S., Electronics in the Life Sciences, The Macmillan Press, Ltd. (1973).

7) Campbell, F.W. Light sources and detectors. Electronic Apparatus for Biological Research. Edit. Donaldson, P.E.K. Butterworth's Scientific Publications (1958).

8) Doughty, C.J. & Hope, A.B., Aust. J. Plant Physiol. 3, 677 (1976).

9) Doughty, C.J. & Hope, A.B., Aust. J. Plant Physiol. 3, 687 (1976).

10) Doughty, C.J. & Hope, A.B., Aust. J. Plant Physiol. 3, 693, (1976).

11) Brown, D.F., Ryan, T.E. & Barr, C.E., Ion transport in Plants, Edit. Anderson, W.P., Academic Press (1973).

12) Hinke, J.A.M., Nature (London), 184, 1257 (1959).

13) Thomas, R.C., J. Physiol. (London) 210, 55 (1970).

14) Spanswick, R.M. & Miller, A.G., Plant Physiol. 59, 664 (1977).

15) Silver, I.A., Private communication (1976).

16) Donaldson, P.E.K. Electronic Apparatus for Biological Research, Butterworth's Scientific Publications (1958).

CHAPTER VI

EXPERIMENTAL RESULTS

6.1 Control Experiments

(a) Cell recovery after microelectrode insertion.

In order to test the hypothesis of Tazawa, Kikayama and Nagakawa (1) (see section 2.4(b)) that current leakage through the orifice of the electrode perforation is of such a magnitude as to give a serious underestimation of the membrane resistance, the following experiment was performed with the following experimental arrangement:

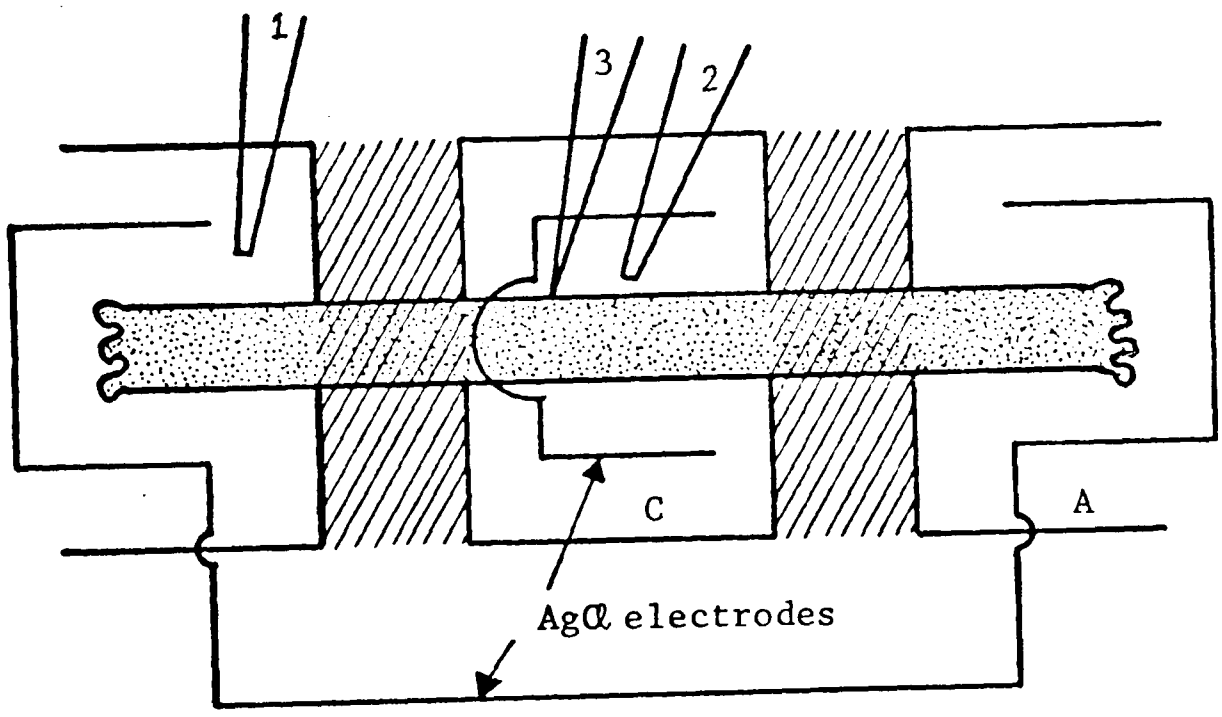

i) A current pulse was applied between electrodes A and C. The resulting voltage response is given by

$$V_{12} = I(R_A + R_C)$$

where R_A and R_C are the resistances of the cell segments A and C and I is the applied current.

ii) Electrode 3 was inserted into the cell and the same current I applied. In this case the voltage responses between electrodes 1 and 2, V'_{12}, and electrodes 1 and 3, V'_{13}, are given by

Table 6.1 .- The Recovery of E and Rm after microelectrode insertion

time (min) / Cell	1 Ra/Rb	1 E	5 Ra/Rb	5 E	15 Ra/Rb	15 E	30 Ra/Rb	30 E	60 Ra/Rb	60 E
18	0.36	-80	0.39	-85	0.75	-112	0.91	-114	1.09	-103
19	0.36	-85	0.44	-90	0.56	-100	1.00	-105	1.05	-107
20	0.23	-70	0.37	-80	0.43	- 94	0.50	- 98	0.71	-104
21	0.48	-83	0.56	-92	0.96	- 99	0.93	-103	0.96	-108
22	0.35	-100	0.27	-80	0.30	-100	0.42	-112	0.72	-118
24	0.23	-75	0.22	-75	0.34	- 75	0.60	- 80	1.02	-100
25	0.33	-80	0.45	-110	0.96	-112	1.04	-115	1.00	-112
26	0.29	-60	0.42	-70	0.97	- 95	1.03	- 95	1.03	- 93
27	0.89	-96	0.88	-112	0.96	-112	0.89	-105	1.04	-110
28	0.57	-100	0.61	-112	0.91	-109	1.06	-112	1.03	-115
29	0.71	-75	0.50	-60	0.67	- 84	0.80	- 90	1.11	- 94
30	0.86	-85	0.87	-84	0.96	- 90	1.04	-100	0.96	-108
31	0.87	-70	0.83	-74	1.04	- 90	1.04	-109	1.04	-115
32	0.94	-74	0.98	-77	0.81	- 79	0.82	- 80	1.03	- 92
33	0.48	-92	0.51	-06	0.62	-108	0.76	-113	1.03	-117
35	0.49	-72	0.56	-75	0.87	-124	0.70	-137	0.89	-140
Av.	0.56	-81	0.59	-81	0.81	- 99	0.90	-104	1.05	-109

Ra/Rb = Rc/Rc' on page 122

$$V'_{12} = I(R_A + R'_C) \quad \text{and} \quad V'_{13} = IR_A,$$

where (') denotes the value after insertion. The ratio between the membrane resistance of the central segment before and after perforation can thus be obtained from

$$V_{12}/V'_{12} = (R_C + R_A)/(R'_C + R_A) .$$

Since $R_A/R'_C = V'_{13}/V'_{23}$

$$\therefore \quad \frac{R_C}{R'_C} = \frac{V_{12}}{V'_{12}} + \frac{V'_{13}}{V'_{12}-V'_{13}} \left(\frac{V_{12}}{V'_{12}} - 1 \right) .$$

This ratio was computed for different times after the electrode insertion and the results are presented in Table 6.1. It can be seen that, with the exception of cell 20, the membrane resistance had recovered after one hour to its value prior to insertion. Similar recovery periods have been reported by Hope and Walker (2). On the other hand, Spanswick (3), reports recovery periods in excess of 4 hours for Nitella translucens. However, Spanswick's experiments were carried out in the dark when the membrane resistance is as much as five times bigger than its value in the light. It is therefore to be expected that the recovery to these very high resistance values would be achieved only over more extended periods.

In the present work it has been shown that the membrane resistance recovers to its original value prior to electrode insertion. However Tazawa et al.(1) claim that their experiments indicate that electrode insertion irreversibly damages the membrane and therefore gives an underestimate of the membrane resistance. In their experiments they compared the resistance

measured by the open vacuole and microelectrode techniques and certainly these comparisons indicate a larger resistance with the former method. However these comparisons may not be entirely valid since the open-vacuole technique requires the presence of osmoticums. Furthermore they fail to mention if the same light regimes were used in the two types of experiments. It should be noted that cell recovery depends ultimately on the amount of damage caused by electrode insertion. In the present work the criteria of a good insertion were that it did not produce migration of the chloroplasts away from the electrode tip or stop the cytoplasmic streaming for more than 1 min.

b) In the measurements of the membrane resistance of single isolated cells Williams, Johnston and Dainty (4) assumed that the nodal terminations acted as infinite impedances. This was apparently confirmed in the later work of Hogg, Williams and Johnston (5). However direct measurements of the nodal resistance between two adjacent cells (see section 2.3) suggest that the resistance is by no means infinite. It would appear to be a relatively simple matter to test the effect of excision on the nodal resistance. This was done in the following way:

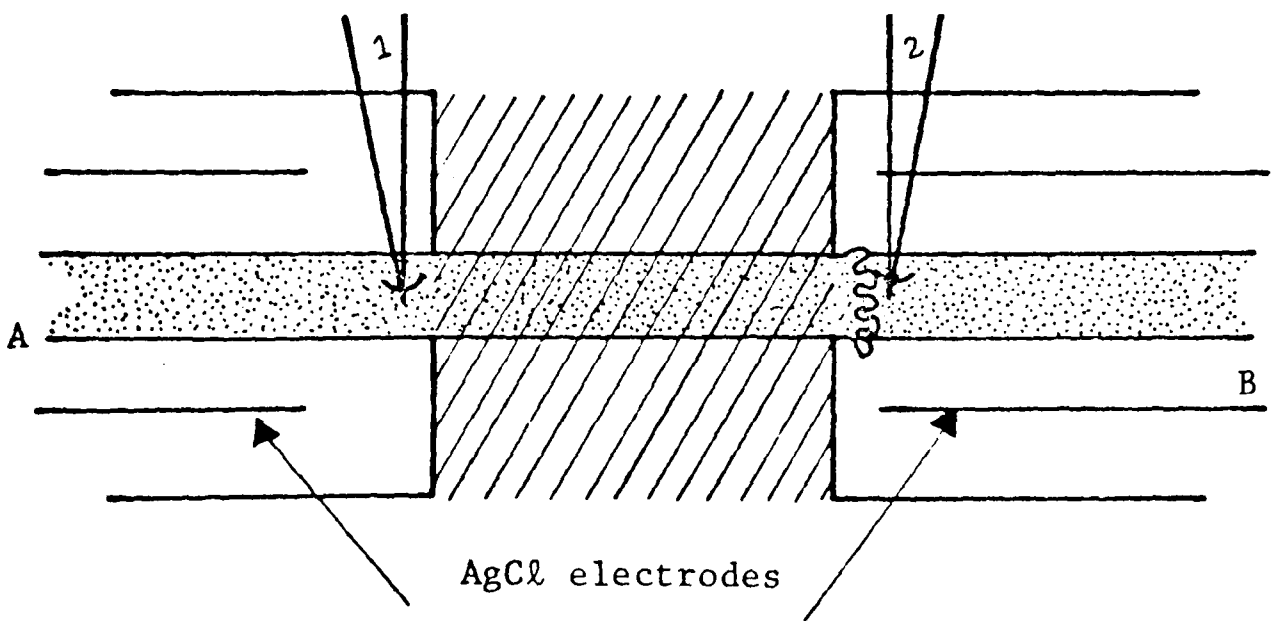

As shown in the above figure the potential across the

node could be recorded by electrodes 1 and 2. When current pulses (.05 μA/cm² of node area) were applied across electrodes A and B the potential response of the node gave a direct recording of the transnodal resistance. Current pulses were applied at regular intervals (by triggering the pulse generator with a Hewlett-Packard function generator) before and after excision of the right hand cell. The nodal response was recorded on a pen-recorder and traces from two experiments are shown in Figure 6.1. It can be seen that in one case the transnodal resistance almost immediately doubles its pre-excision value whereas the other cell required several hours to achieve a similar value. The collected results for 13 cells are shown in Table 6.2. It can be seen that, over a period of a few hours, the average increase in the transnodal resistance is more than 2-fold, though the actual increase varies greatly from cell to cell. It should also be noted that the transnodal resistance between two unexcised cells agrees with that of Spanswick (6).

Even allowing for the average two-fold increase the value of the transnodal resistance, which is the measured ohmic resistance multiplied by the node area, is still small compared with the membrane resistance. However, in making the assumption of infinite impedance for the nodes it is the total resistance of the membrane relative to the total resistance of the node which is important. In the case of a cell of 8 cm length and 1 mm diameter the total resistance of the node is in fact sixteen times bigger than the total resistance of the membrane so that only $^{1}/_{16}$ of the current flows through the node. The assumption of infinite impedance is quite sound

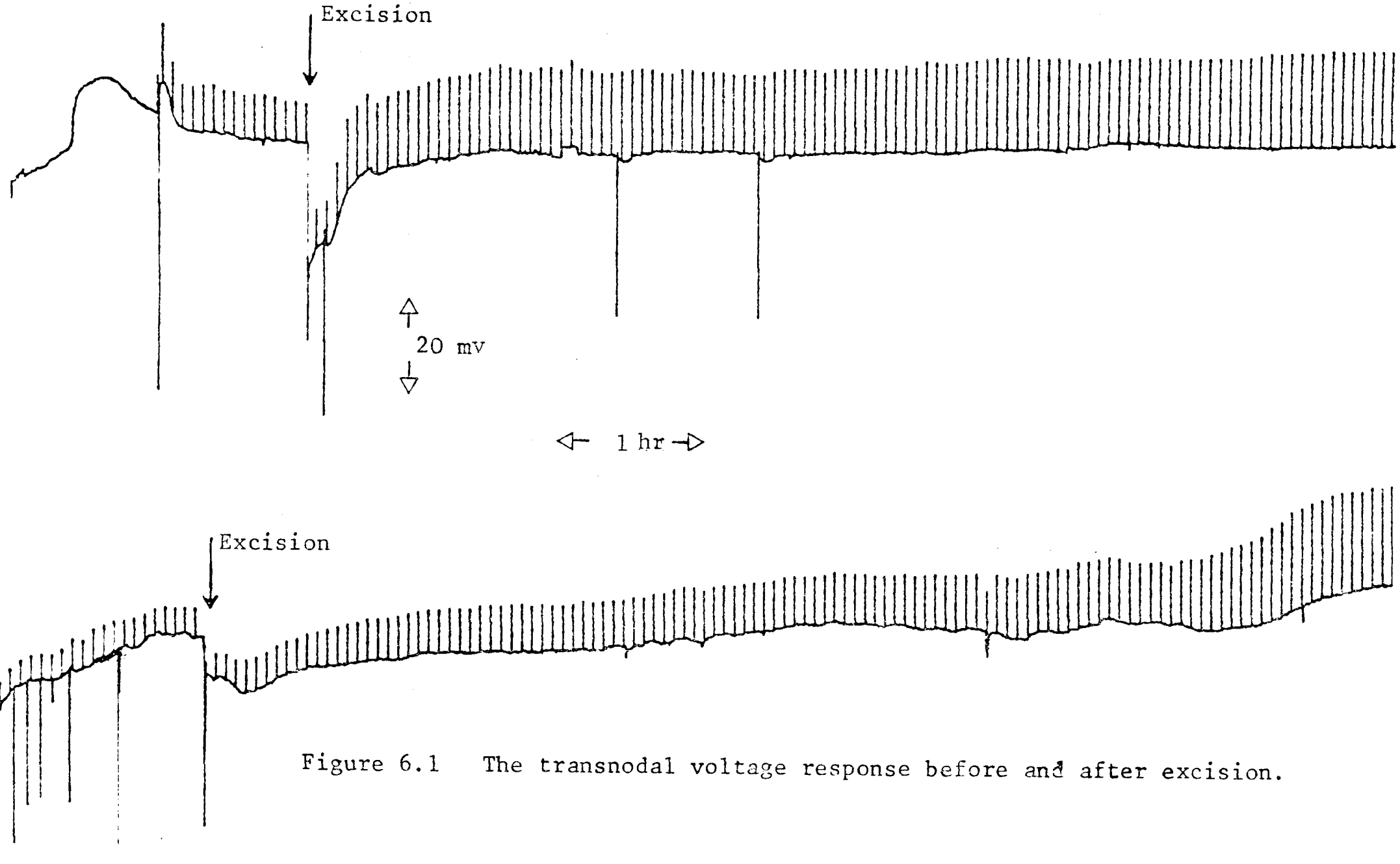

Figure 6.1 The transnodal voltage response before and after excision.

TABLE 6.2. The resistance ($k\Omega.cm^2$) of the cell mode as a function of time after excision of one of the cells.

Cell No. \ Time	0	10 min.	30 min.	1 hr.	2 hrs.	3 hrs.	4 hrs.
100	1.08	1.88	2.20	2.50	2.60	2.50	3.44
101	2.20	3.80	3.80	3.80	3.80	3.80	3.80
102	2.66	2.66	2.66	2.66	3.00	3.44	3.40
103	0.94	1.40	1.40	1.40	1.40	1.40	1.44
104	0.62	0.62	0.62	0.94	1.04	1.08	1.08
105	0.94	1.02	1.02	1.24	1.56	1.64	1.60
106	1.88	2.22	2.66	2.82	3.14	3.36	3.30
107	0.78	1.02	1.10	1.32	2.26	2.66	2.44
108	1.24	1.24	1.98	1.88	2.50	2.58	2.48
109	1.40	2.04	2.66	2.82	2.86	2.90	2.90
110	1.08	2.82	2.82	2.90	2.90	2.90	2.90
111	0.78	0.78	0.86	0.78	1.02	1.02	1.08
112	1.32	1.92	2.50	2.66	2.66	2.66	3.74
Average	1.18	1.78	2.02	2.12	2.36	2.44	2.50

in this case, but it cannot be extended to cases where short cells were used. Such limitations do not apply for external current injection since the insulating barriers ensure effective infinite impedance terminations.

6.2 The Effect of pH on the Membrane Electric Parameters (D.C. Experiments)

The effect of pH on the membrane potential, resistance and capacitance for individual cells are provided in the Appendix. In what follows the average effects for all the cells for each of these parameters are presented in graphical form. In order to attain steady state conditions one and a half hours were allowed to elapse after changing the pH of the external solution and before measuring the electric parameters at the new pH.

a) Membrane potential

The pH dependence of this parameter obtained in the D.C. experiments is shown by the APW batch 1 plot in Figure 6.2. The response is similar to that reported by other authors but it is less marked than that reported by Spanswick (6). This is probably due to the higher illumination used by Spanswick who showed that the pH response is light-dependent.

b) Membrane resistance

The response of the membrane resistance to changes in external pH are shown in Figure 6.3. Again the response is less marked than that reported by Spanswick (1986). This response has been observed in other species of the Characeae and assumed to be produced by changes in external pH. However Vredenberg

Figure 6.2.

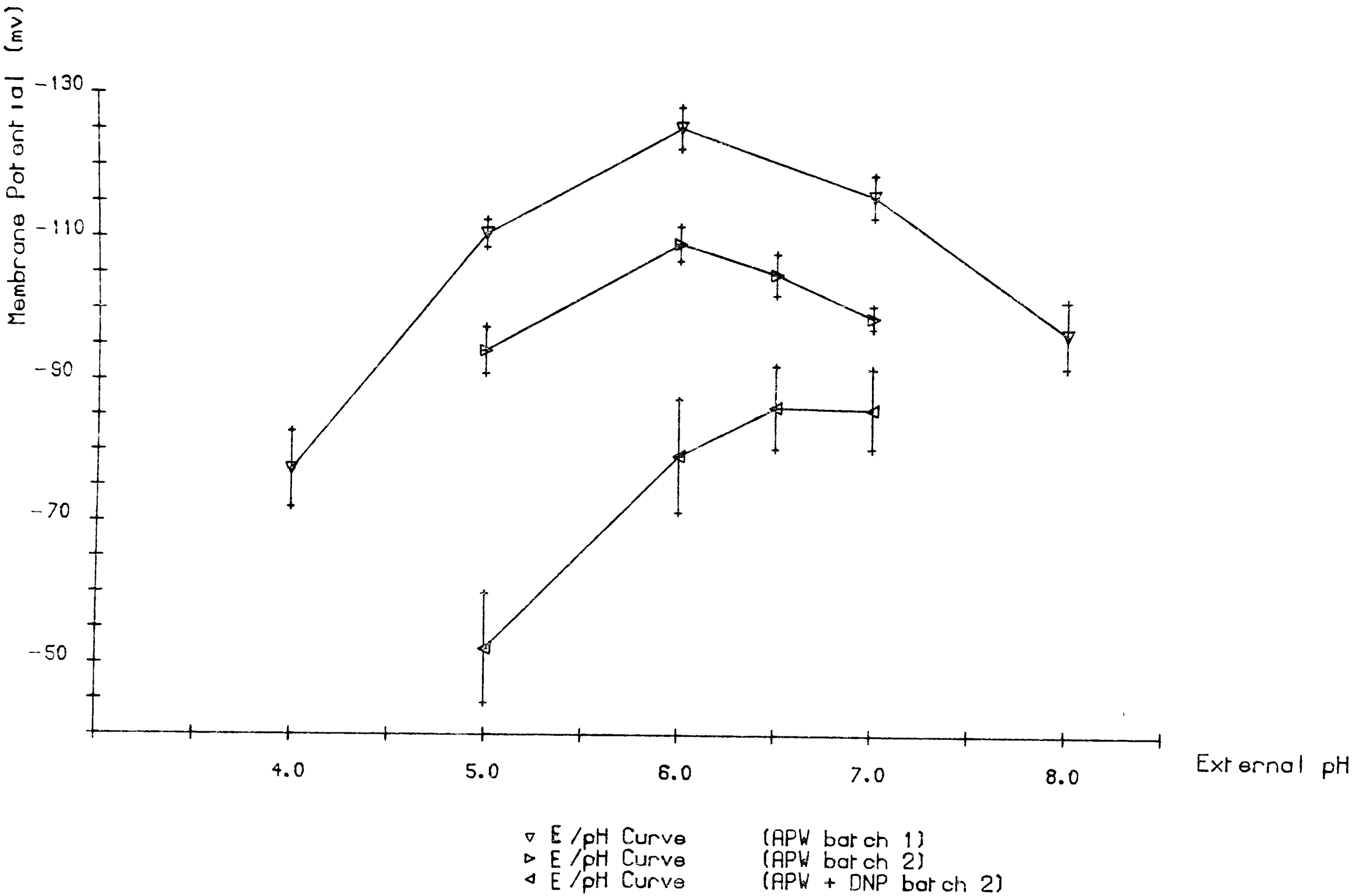
Membrane Potential (mv)
-130
-110
-90
-70
-50
4.0
5.0
6.0
7.0
8.0
External pH
▽ E /pH Curve (APW batch 1)
▷ E /pH Curve (APW batch 2)
◁ E /pH Curve (APW + DNP batch 2)

Figure 6.3. Membrane Resistance Response to pH.

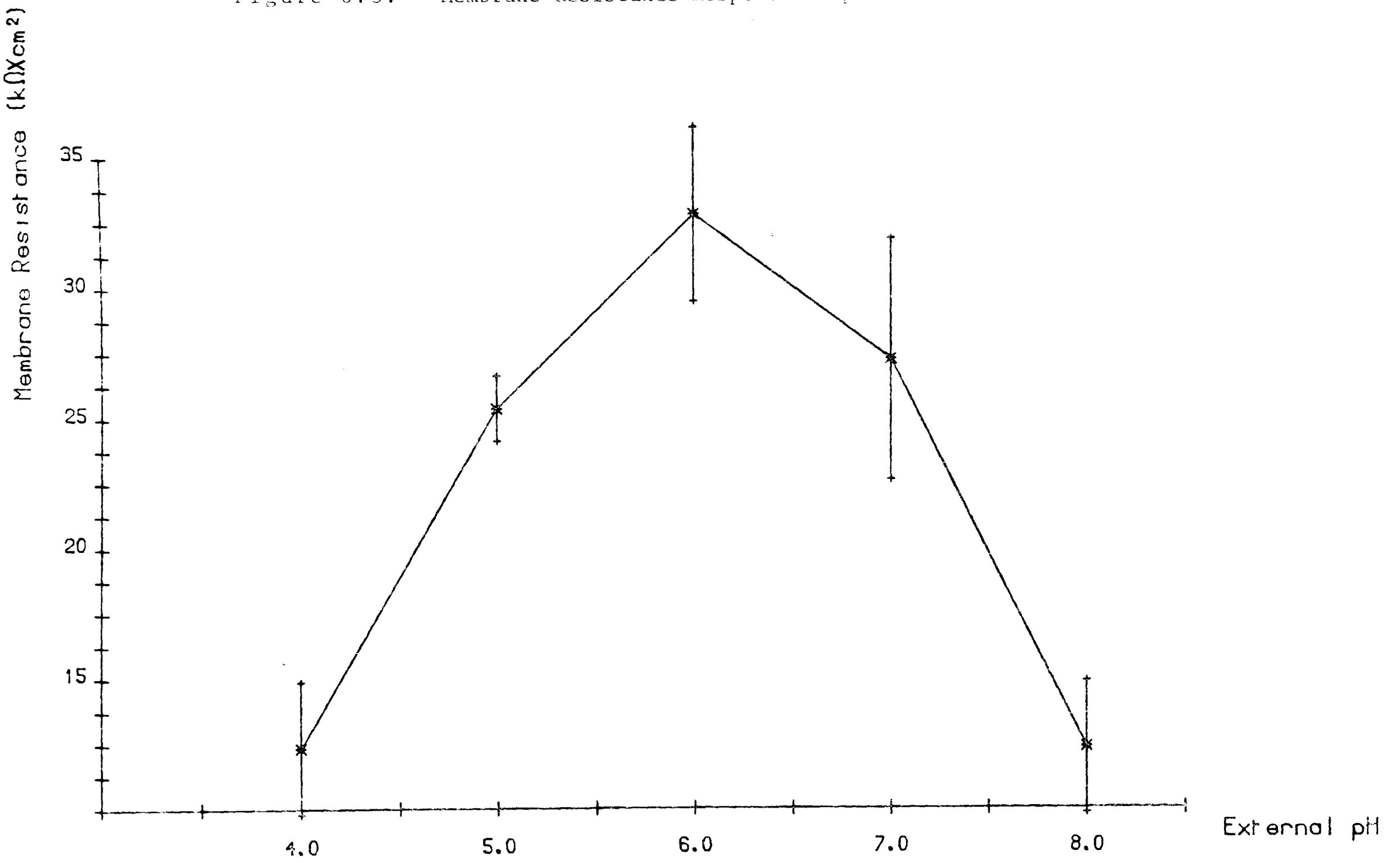

(see Chapter I) proposes that the observed changes in membrane resistance are a result of the pH produced changes in membrane potential. In order to test this hypothesis the membrane rectification curves at different external pH were obtained in the present work.

The rectification curves are limited in the depolarizing direction by the onset of the action potential and in the hyperpolarizing direction by the onset of the hyperpolarizing response. The collected results are presented in Figure 6.4(a). It can be seen that the data for all values of pH cluster around one or probably two rectifying curves.

This is more apparent in Figure 6.4(b) where the standard errors have been omitted. In this plot there appear to be three curves, one of which is firmly associated with pH 8. An examination of the original data for the other two curves shows that the dotted curve was obtained with cells of diameter ≃ 0.8 mm and the solid curve for cells of diameter ≃ 1 mm. These differences in diameter and behaviour could be indicative of differences in the ages of the two groups of cells. This distinction is emphasised in a plot of current density against potential (Figure 6.5) which shows significantly different curves for the two groups at pH 4 and 8. Unfortunately insufficient experiments were carried out with smaller diameter cells at pH 5, 6 and 7 to confirm unequivocally this division, though there are some indications that the division does exist (see, for example, the high resistance values at pH 7 in the tables).

In Figure 6.6 the rectification curves for the two groups are shown. It can be seen that the curve for the larger diameter cells at pH 4 overlaps with the curve for pH 5. This observation will be discussed in the final Chapter.

Figure 6.4(a)

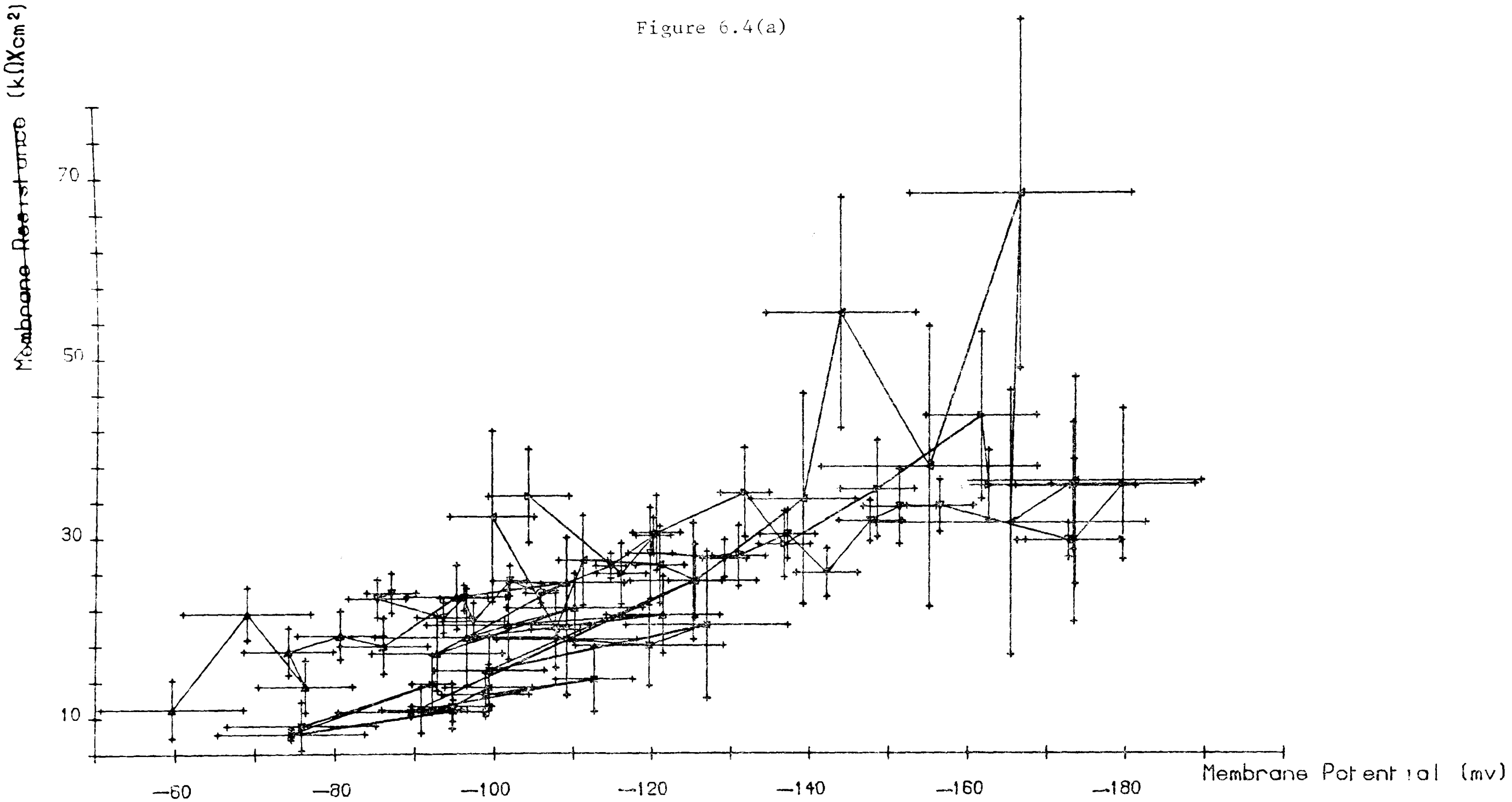
Membrane Resistance (kΩXcm²)
70
50
30
10
−60
−80
−100
−120
−140
−160
−180
Membrane Potential (mv)
△ R/E curve for pH= 4
▽ R/E curve for pH= 5
▷ R/E curve for pH= 6
◁ R/E curve for pH= 7
✱ R/E curve for pH= 8

Figure 6.4(b).

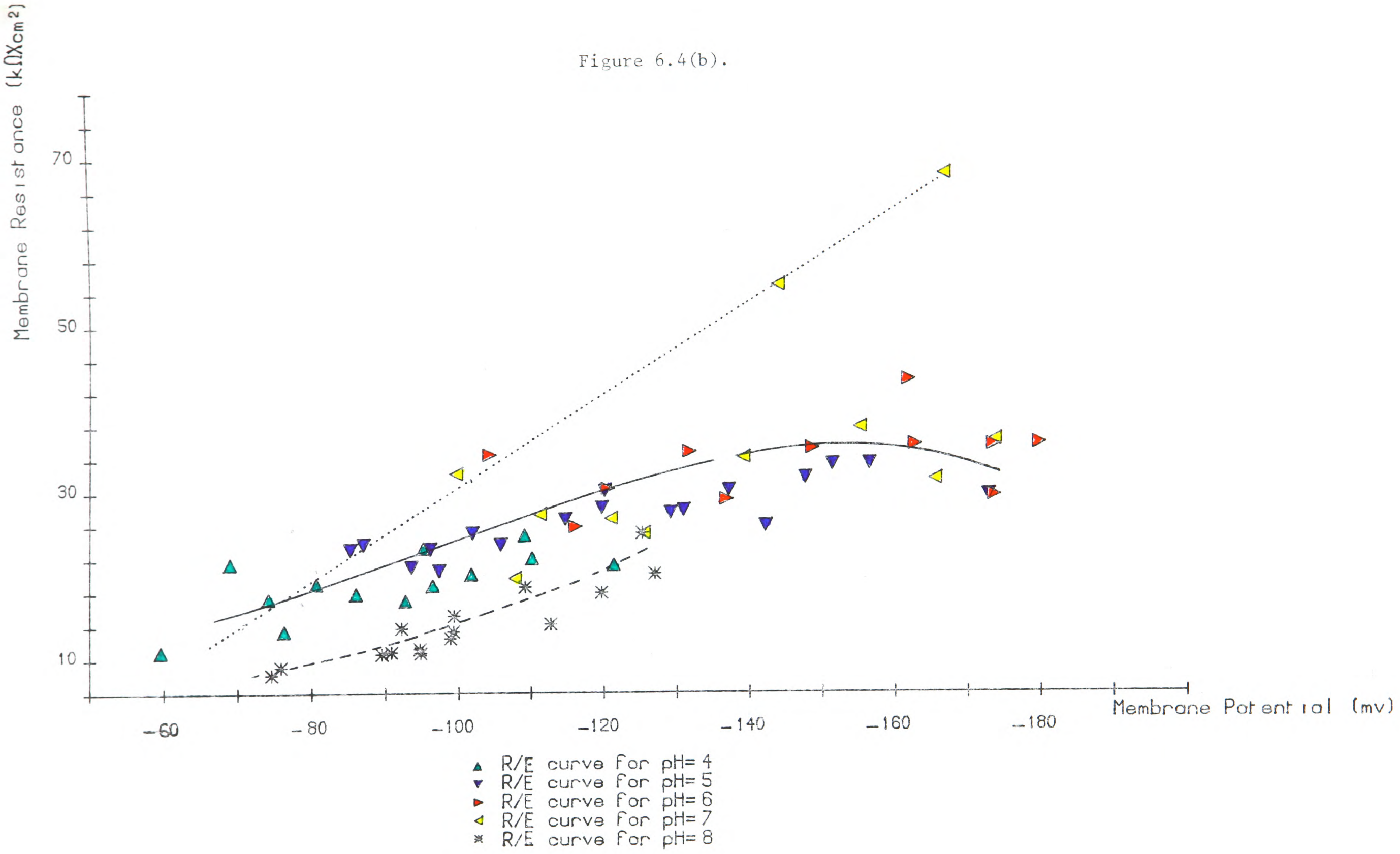
Membrane Resistance (kΩXcm²)
70
50
30
10
−60
−80
−100
−120
−140
−160
−180
Membrane Potential (mv)
R/E curve for pH= 4
R/E curve for pH= 5
R/E curve for pH= 6
R/E curve for pH= 7
R/E curve for pH= 8

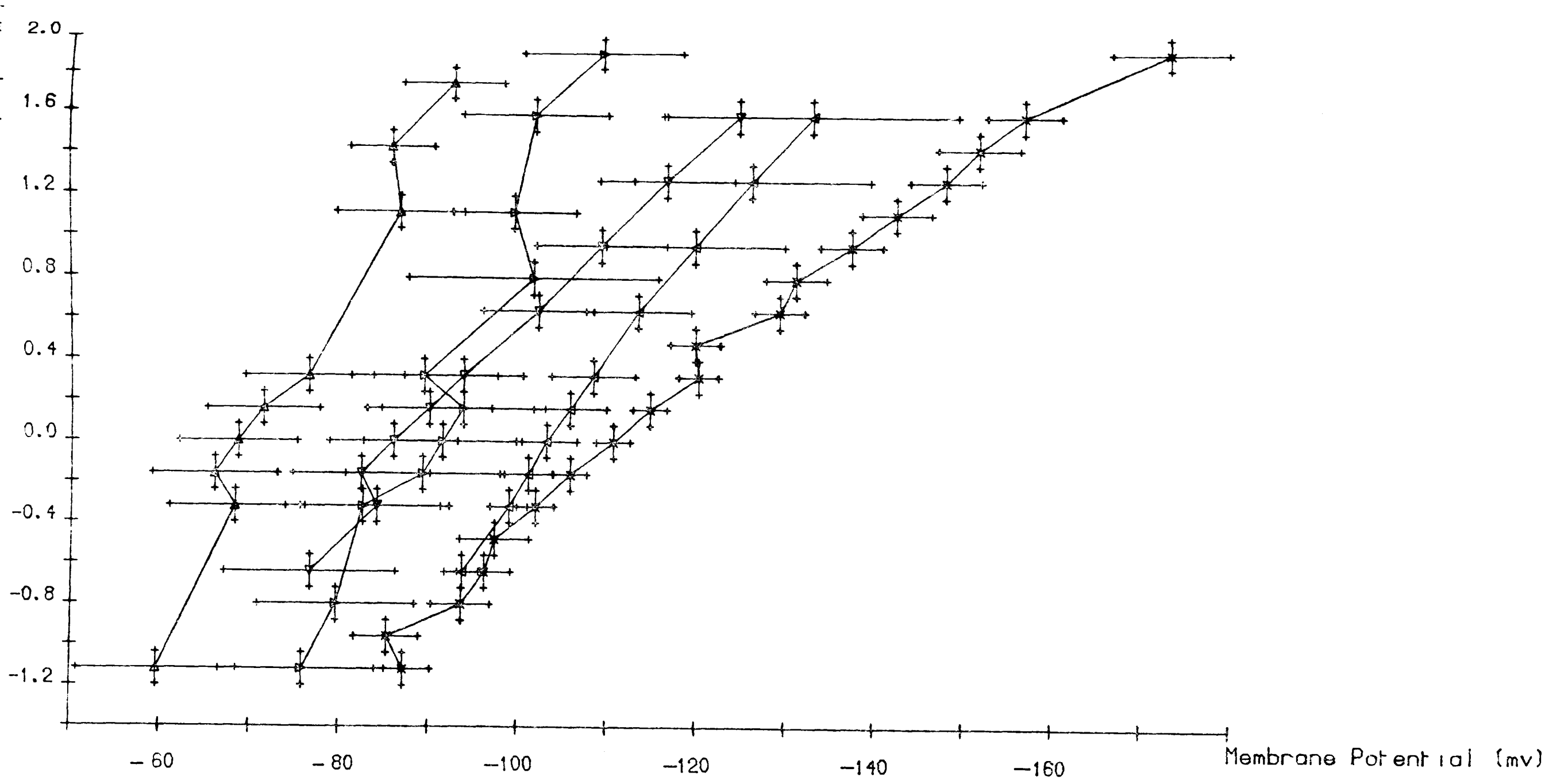
Current Density (μA/cm²)
2.0
1.6
1.2
0.8
0.4
0.0
-0.4
-0.8
-1.2
-60
-80
-100
-120
-140
-160
Membrane Potential (mv)
△ J/E Curve for pH= 4 (d = 0.8 mn)
▽ J/E Curve for pH= 4 (d = 1.0 mn)
▷ J/E Curve for pH= 8 (d = 0.8 mn)
◁ J/E Curve for pH= 8 (d = 1.0 mn)
✱ J/E Curve for pH= 5

Figure 6.5.

Figure 6.6.

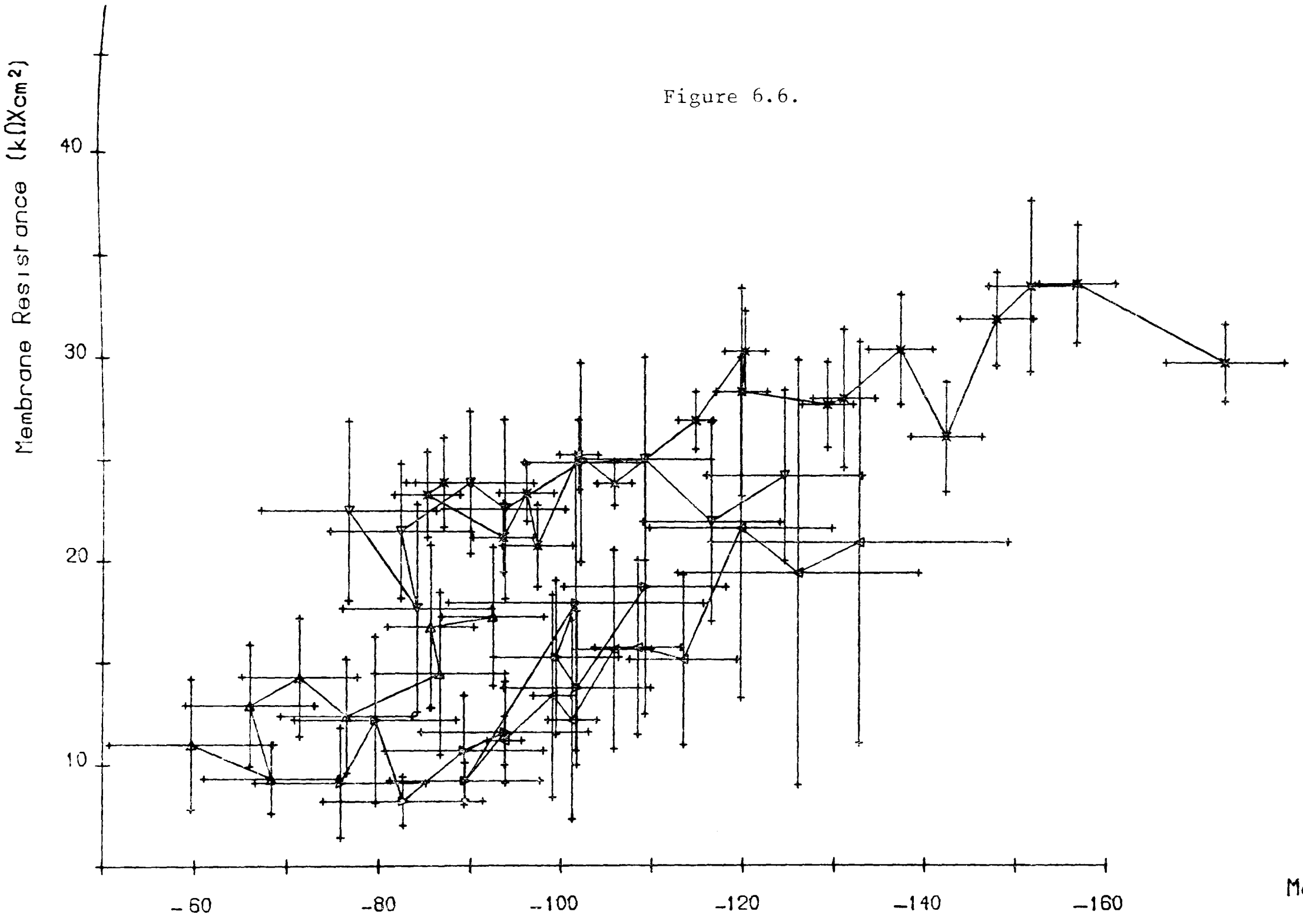

△ R/E curve for pH= 4 (d = 0.8 mn)
▽ R/E curve for pH= 4 (d = 1.0 mn)
▷ R/E curve for pH= 8 (d = 0.8 mn)
◁ R/E curve for pH= 8 (d = 1.0 mn
✱ R/E curve for pH= 5

c) The effect of external pH on the capacitance at different membrane potentials is presented in Figure 6.7(a) and in a simplified form in Figure 6.7(b). It can be seen that the curves corresponding to each pH value overlap in a similar way to that in the rectification curves. The scatter of the capacitance values of pH 8 and pH 4 is again due to the presence of the two groups already discussed. The scatter at high potential is due to the onset of the hyperpolarizing response.

6.3 The Effect of pH on the Excited State Parameters

Kistasato (8) reported that the peak of the action potential of Nitella does not respond to changes in external pH and he therefore suggested that the pH response is not due to changes in the cell wall potential. However, Kishimoto (9) in an earlier work reported that the peak of the action potential of Chara corallina responds to changes in pH in a similar way to the resting potential, though more recently in a private communication he stated that this was not a general observation for all cells. In the present work the response of the action potential of Nitella translucens to changes in external pH was studied. The results for each individual cell are presented in the Appendix and the collected results are shown graphically in Figure 6.8. In this Figure the membrane potential is plotted as a function of time during the action potential. It can be seen that even if there are small differences in the peaks of the action potentials for each pH these differences do not reflect the observed pH response for the resting state.

Figure 6.7(a)

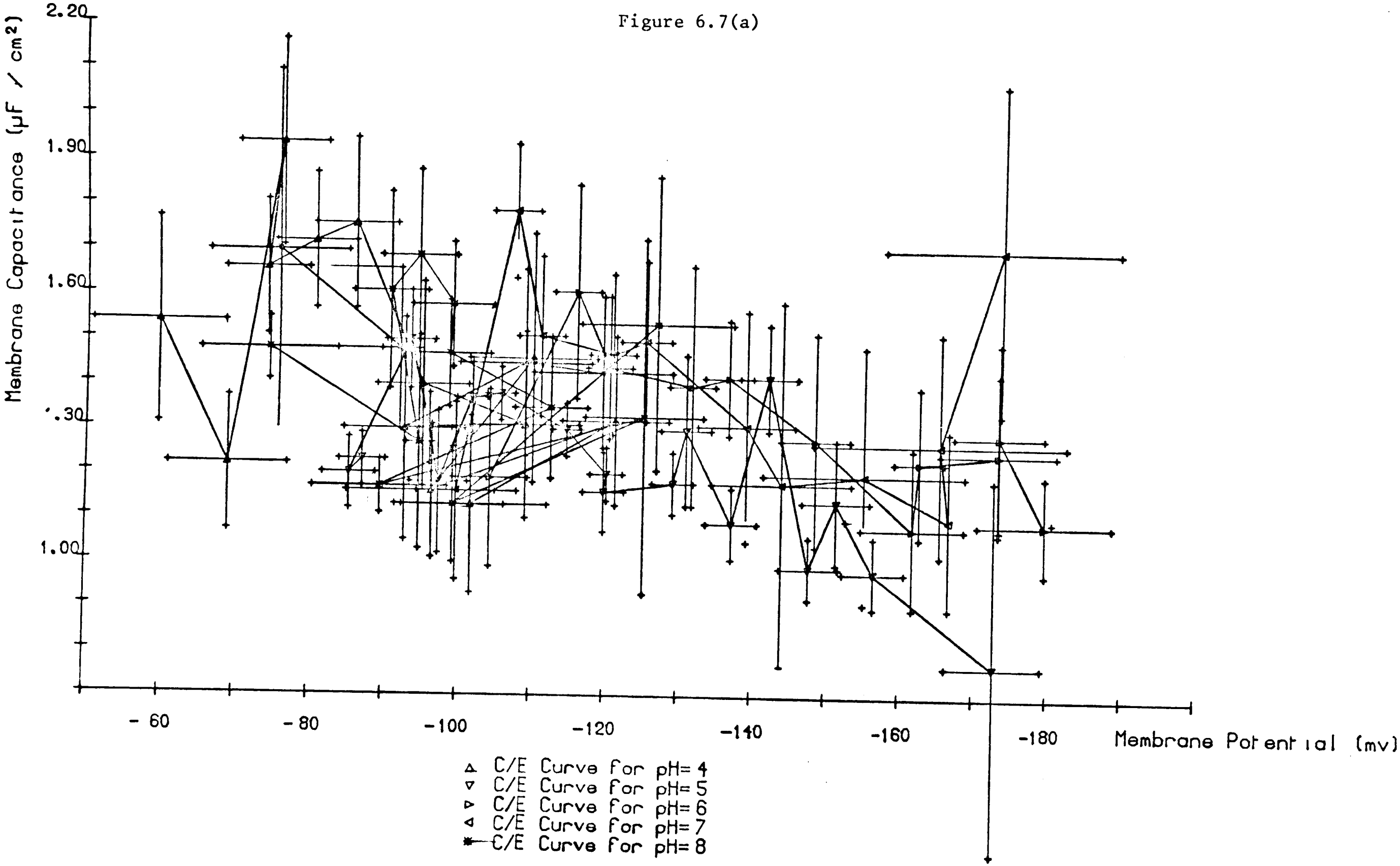
Membrane Capacitance (μF / cm²)
2.20
1.90
1.60
1.30
1.00
- 60
- 80
-100
-120
-140
-160
-180
Membrane Potential (mv)
C/E Curve for pH= 4
C/E Curve for pH= 5
C/E Curve for pH= 6
C/E Curve for pH= 7
C/E Curve for pH= 8

Figure 6.7(b).

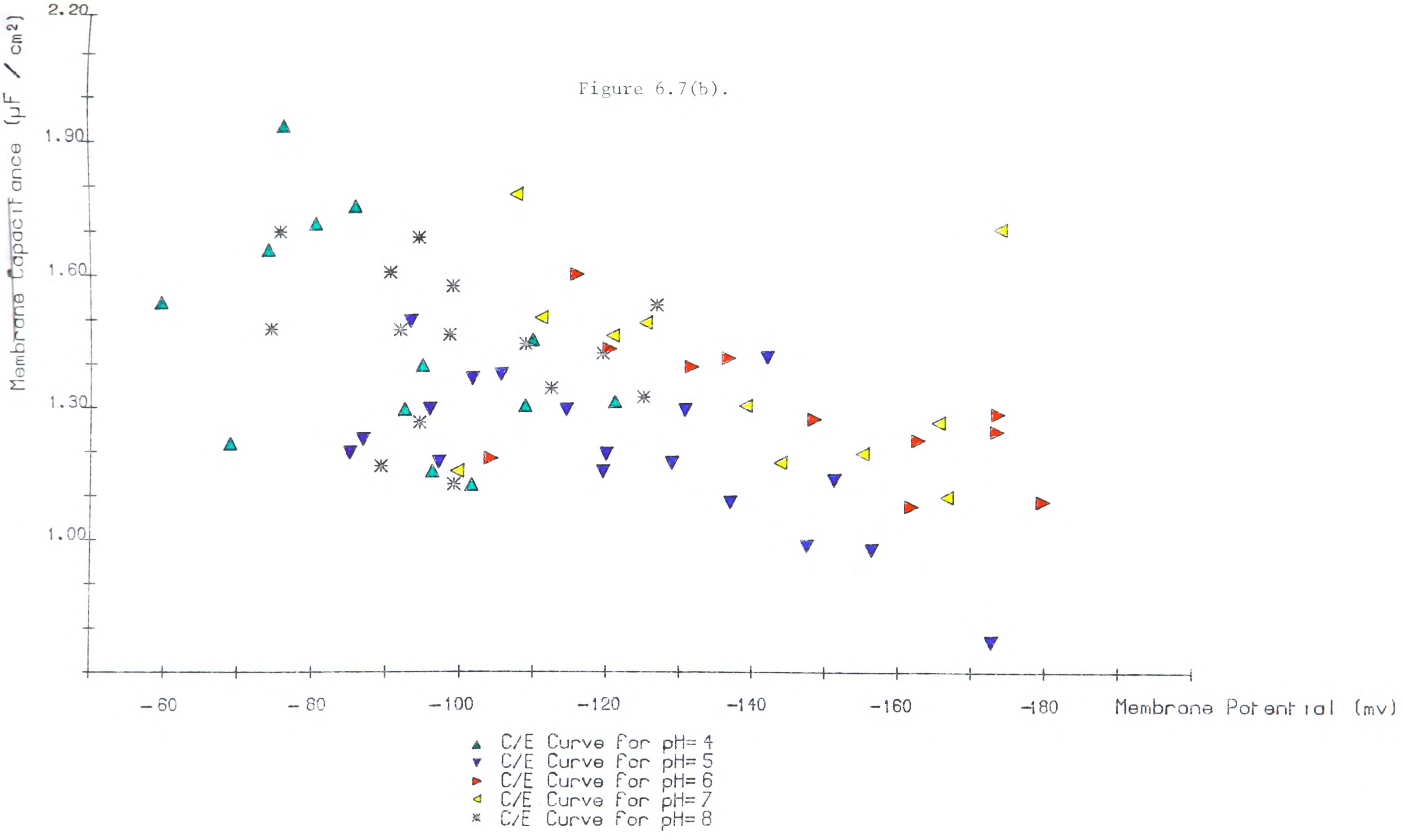
Membrane Capacitance (μF / cm²)
2.20
1.90
1.60
1.30
1.00
-60
-80
-100
-120
-140
-160
-180
Membrane Potential (mv)
C/E Curve for pH= 4
C/E Curve for pH= 5
C/E Curve for pH= 6
C/E Curve for pH= 7
C/E Curve for pH= 8

Figure 6.8.

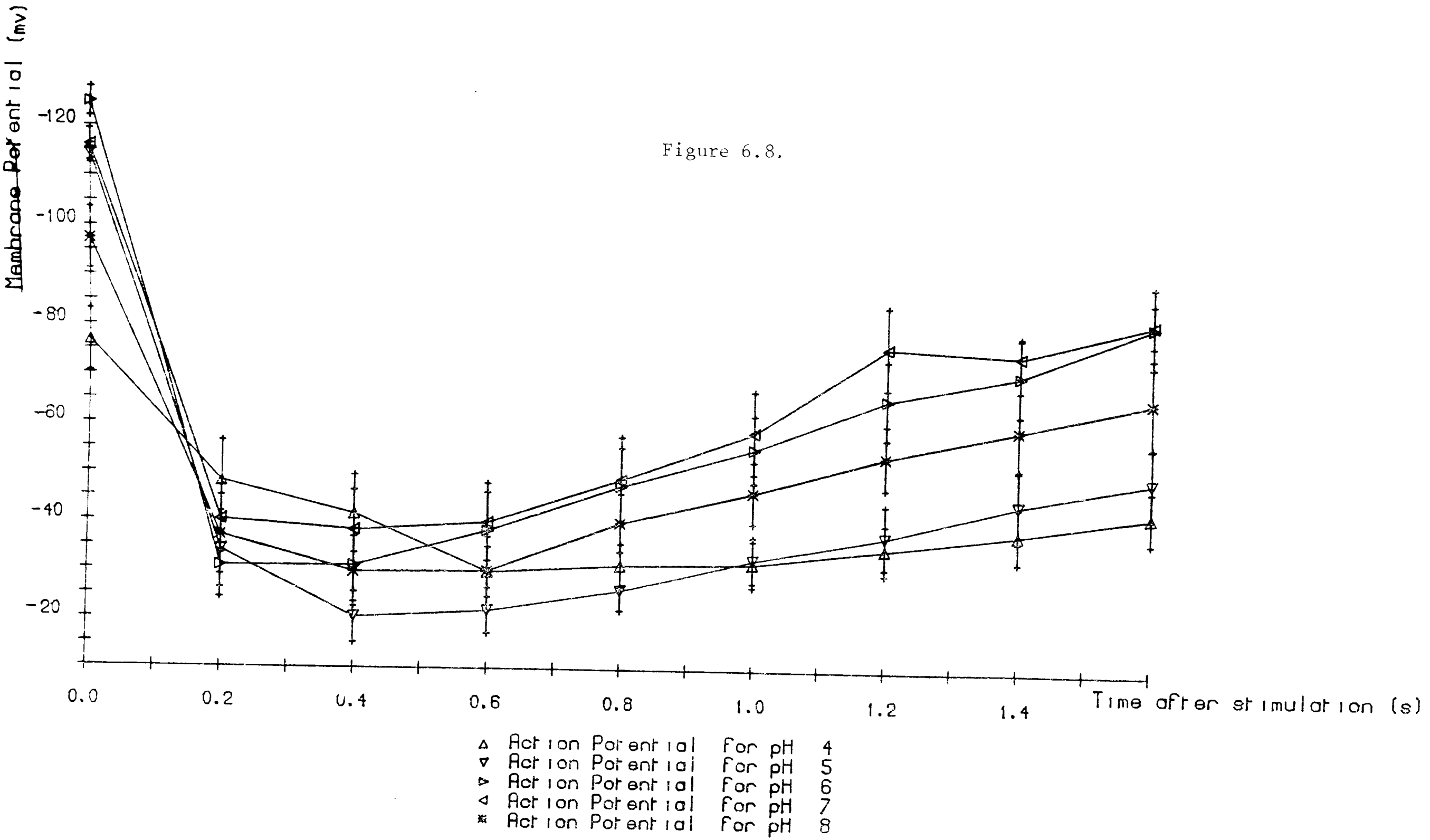
Membrane Potential (mv)
-120
-100
-80
-60
-40
-20
0.0
0.2
0.4
0.6
0.8
1.0
1.2
1.4
Time after stimulation (s)
Action Potential for pH 4
Action Potential for pH 5
Action Potential for pH 6
Action Potential for pH 7
Action Potential for pH 8

Figure 6.8 shows that the effect of pH is on the shape of the action potential. The initial part of the action potential as it rises to its peak appears to be unaffected by pH in the range 5 to 8. However the rate of recovery appears to increase from pH 5 to 7, while at pH 8 the recovery rate is intermediate between the rates for pH 5 and 6. The shape of the action potential at pH 4 is altogether different from that for any other pH, being slower in both the initial phase and in the recovery phase. This can also be seen from Figure 6.9 where the actual recordings of a particular cell are reproduced. The figure also shows the voltage responses to a train of fast current pulses ($1\mu A/cm^2$, 100 ms) superimposed onto the action potential. These responses allow for the determination of the membrane resistance during the excited state.

The membrane resistance during the excited state at different external pHs is shown in Figure 6.10. The values at the peak of the action potential is similar to that reported by Bradley (10) and Kishimoto (11) and appears to be independent of pH except at pH 4. During the recovery period the effect of pH, in the range 5 to 7, on membrane resistance follows the same pattern as for the resting state.

6.4 The Effect of pH and A.C. Frequency on the Membrane Resistance and Capacitance

This section is devoted to the study of the frequency dependence of the membrane resistance and capacitance at different pH. The control of the external pH was different from

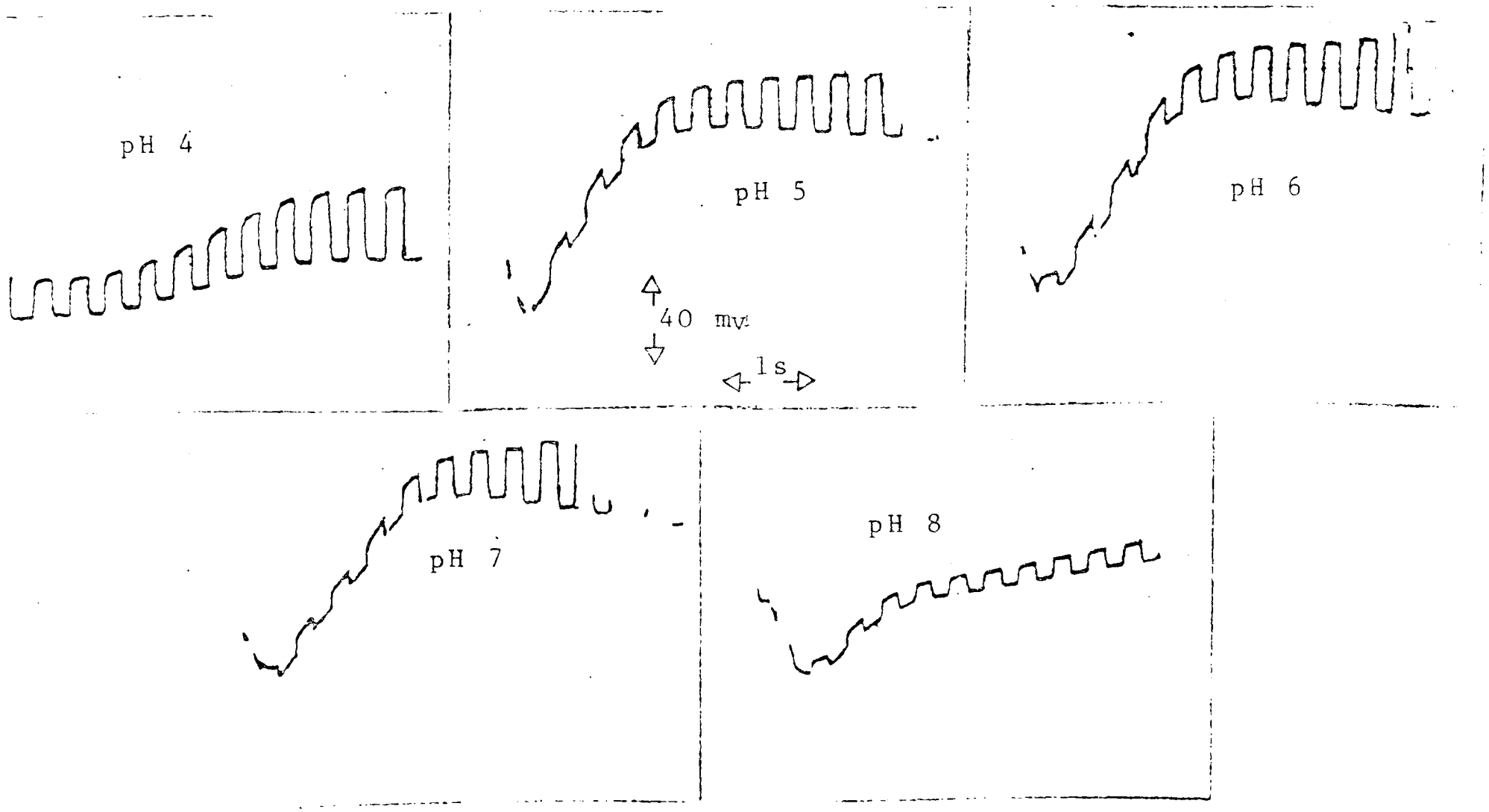

Figure 6.9. The Effect of pH on the Action Potential.

Figure 6.10.

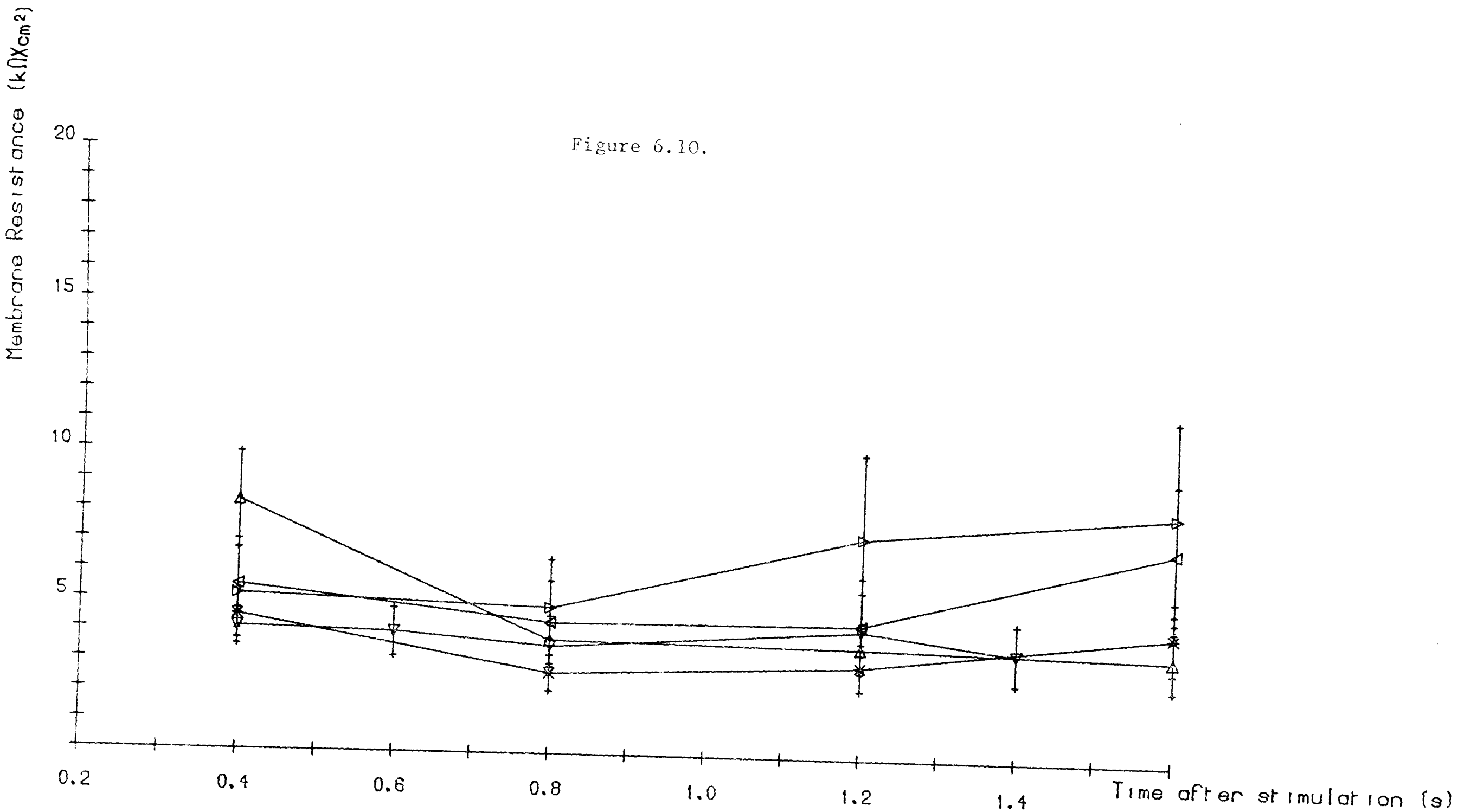
Membrane Resistance (kΩXcm²)
20
15
10
5
0.2
0.4
0.6
0.8
1.0
1.2
1.4
Time after stimulation (s)
Action Potential Resistance for pH4
Action Potential Resistance for pH5
Action Potential Resistance for pH6
Action Potential Resistance for pH7
Action Potential Resistance for pH8

that in the D.C. experiments reported in Section 6.2. In these A.C. experiments the cells were presoaked for more than 12 hours in a solution at a particular pH; the electric parameters were then determined at this pH. This was done in order to allow the vacuolar pH to attain a steady state with respect to the external solution.

As a result of this presoaking procedure the membrane potential was depolarised by about 15 mv but the response to external pH followed the same pattern as for cells soaked for shorter periods (see Figure 6.2). However this meant that at pH 4 and 8 the threshold of the action potential was reached and under these conditions spontaneous action potentials were often observed. The recovery from these was very slow. As a result these A.C. experiments were not extended outside the pH range 5-7.

The parameters determined in these A.C. experiments were the phase angle, the membrane resistance and membrane capacitance. The results for individual cells are given in the Appendix.

The phase angle was determined from the relation

$$\frac{V}{V_{(i=0)}} = \sin\phi \quad . \qquad (6.1)$$

The collected data for the values of the phase angle at different pH and different A.C. frequency are presented in Figure 6.11. It can be seen that the phase angle does not follow the pattern that would be predicted by a simple RC circuit. This anomalous behaviour has also been reported by Kishimoto (12). He found that in the range of frequencies

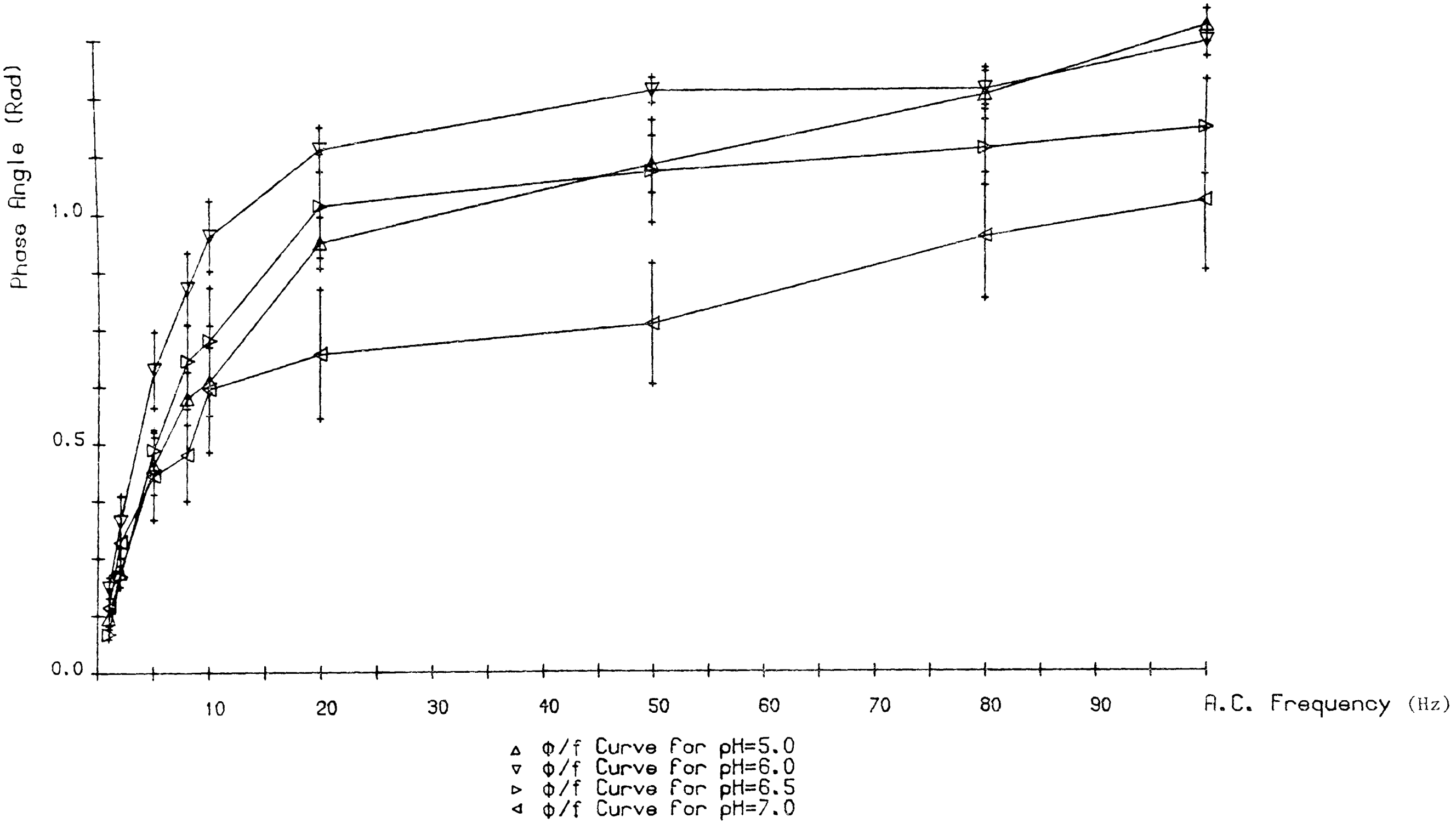
Phase Angle (Rad)
1.0
0.5
0.0
10
20
30
40
50
60
70
80
90
A.C. Frequency (Hz)
Δ Φ/f Curve for pH=5.0
▽ Φ/f Curve for pH=6.0
▷ Φ/f Curve for pH=6.5
◁ Φ/f Curve for pH=7.0

Figure 6.11.

50-100 Hz the phase angle had a constant value of ≈0.86 Radians. This agrees with the curve for pH 6.5 represented in Figure 6.11; this pH was also that used by Kishimoto in his experiments.

From the values of the phase angle the membrane resistance was determined using the following expression

$$R_m = \frac{V}{I}(1 + (\tan\phi)^2)^{\frac{1}{2}} \qquad (6.2)$$

where ϕ is the phase angle, and I the amplitude of the applied current. The resistance values computed in this way are presented in Figure 6.12. It can be seen that R_m shows a frequency dependency which increases with increasing pH.

The capacitance was computed, using these values of resistance and phase angle, from the expression

$$C_m = \frac{\tan(\phi)}{\omega R_m} \quad . \qquad (6.3)$$

The collected results of the capacitance measurements are presented in Figure 6.13 where again a frequency dependency is clearly shown. This dependency on frequency at pH 5 is similar to that observed by Coster and Smith (13). However the resistance dependency reported by these authors is much more marked than the one obtained in this work.

From the last two figures it would appear that both R_m and C_m are frequency dependent as proposed by Coster and Smith. However an alternative explanation has been advanced by Kishimoto (12). He proposed that the membrane, or membranes, in the Characeae cannot be represented by a single RC circuit, but rather by a circuit of the following form:

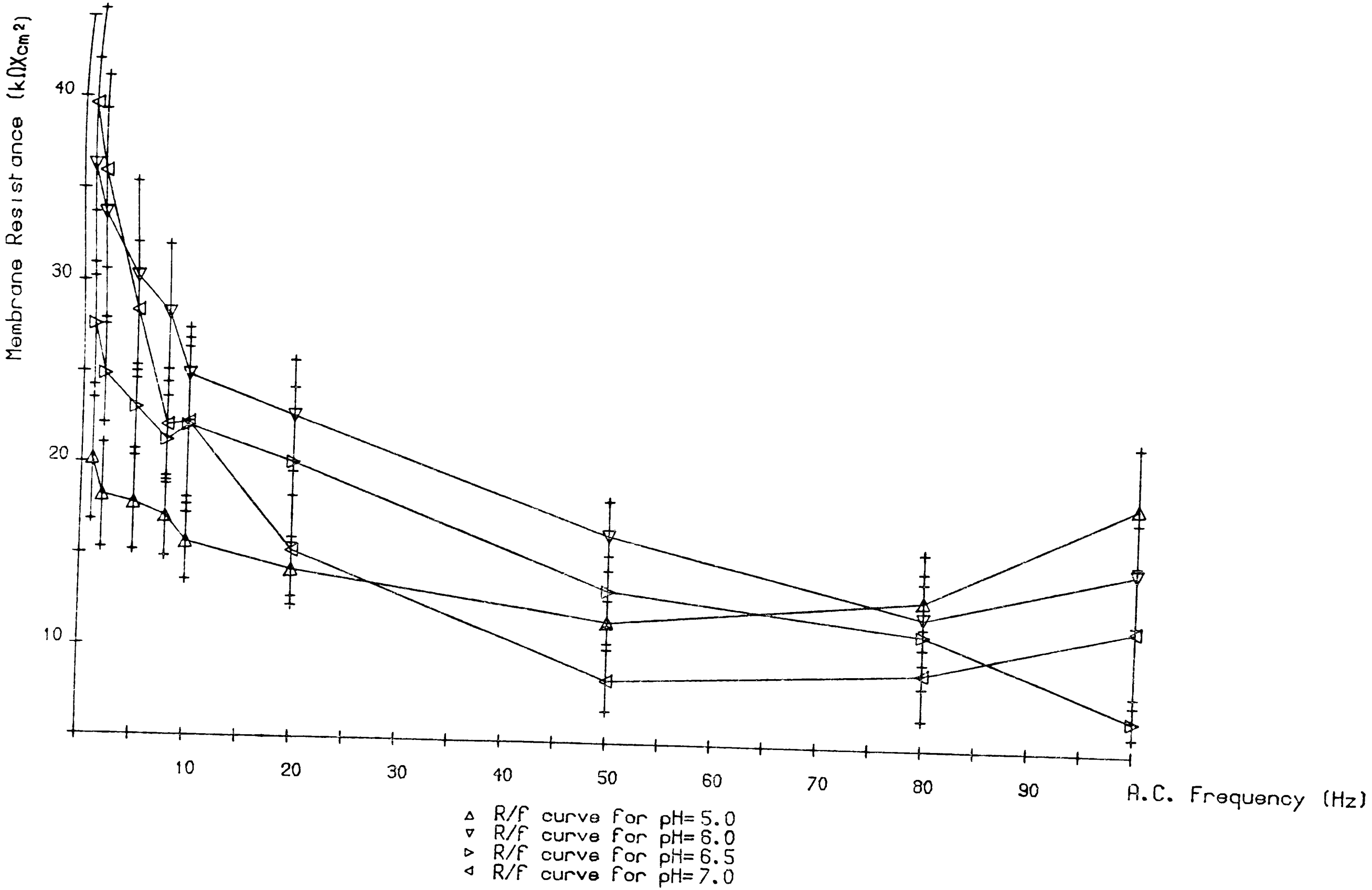
Membrane Resistance (kΩXcm²)
40
30
20
10
10
20
30
40
50
60
70
80
90
A.C. Frequency (Hz)
△ R/f curve for pH=5.0
▽ R/f curve for pH=6.0
▷ R/f curve for pH=6.5
◁ R/f curve for pH=7.0

Figure 6.12.

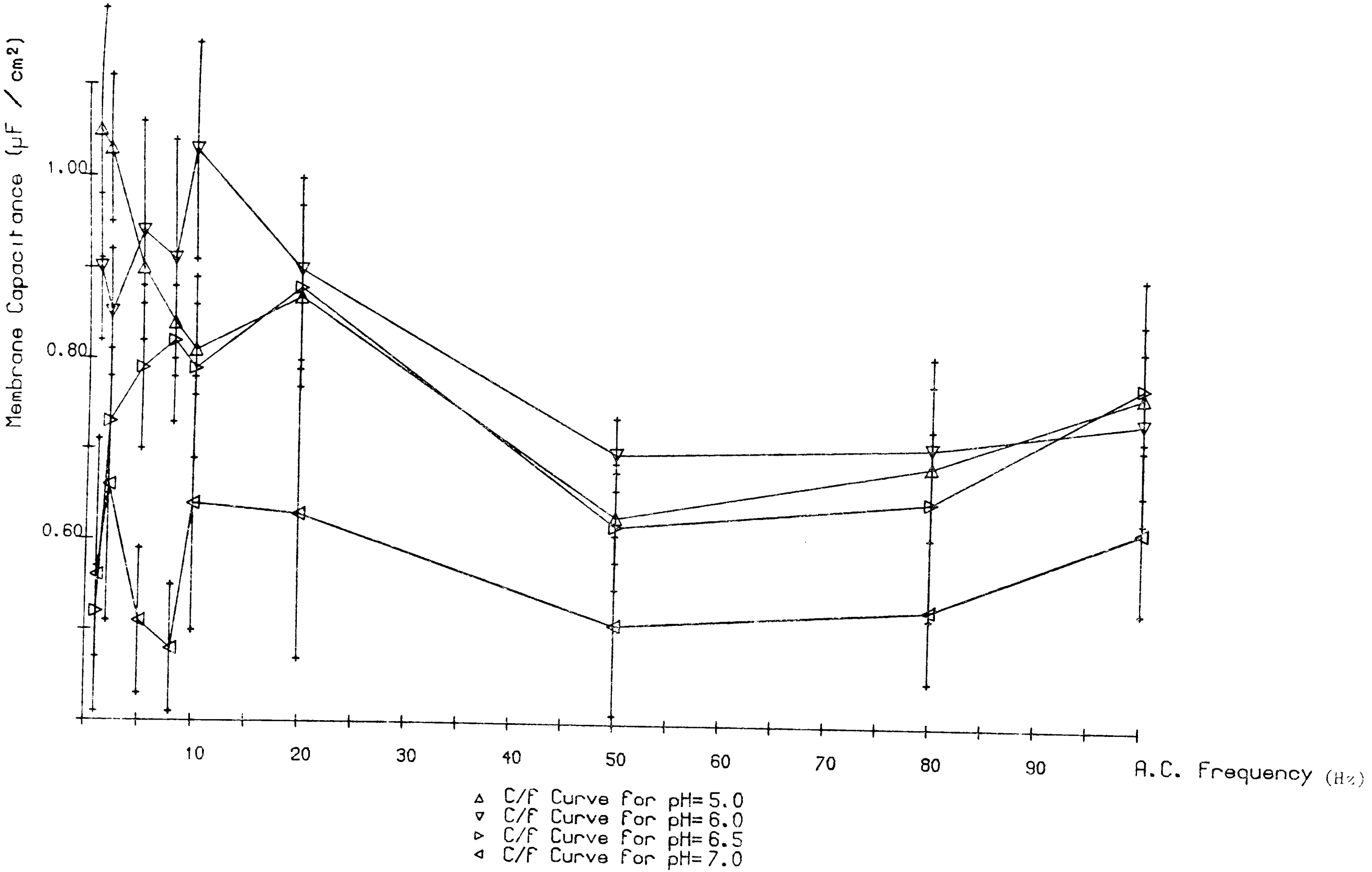
Membrane Capacitance (μF / cm²)
1.00
0.80
0.60
10
20
30
40
50
60
70
80
90
A.C. Frequency (Hz)
C/f Curve for pH= 5.0
C/f Curve for pH= 6.0
C/f Curve for pH= 6.5
C/f Curve for pH= 7.0

Figure 6.13

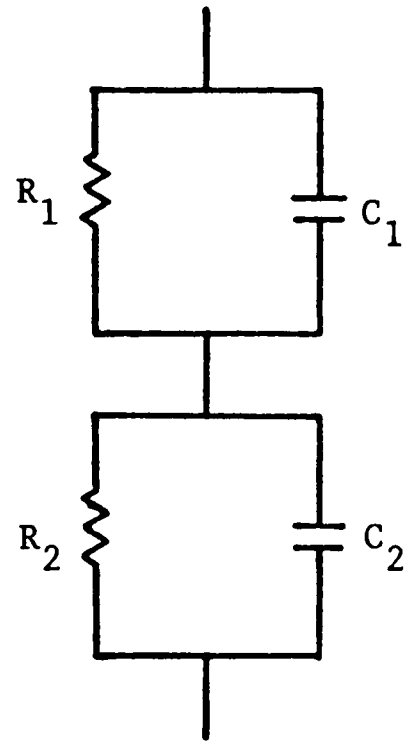

In this case the circuit impedance $z = \frac{R_1}{1+j\omega\tau_1} + \frac{R_2}{1+j\omega\tau_2}$ which can be written as $z = |z|e^{-j\phi}$ where

$$|z| = \left[\frac{(R_1(1+(\omega\tau_2)^2+R_2(1+(\omega\tau_1)^2))^2+(R_1\omega\tau_1(1+(\omega\tau_2)^2)+R_2\omega\tau_1(1+(\omega\tau_1)^2))^2}{(1+(\omega\tau_1)^2)(1+(\omega\tau_2)^2)}\right]^{\frac{1}{2}} \tag{6.4}$$

and

$$\phi = \tan^{-1}\frac{R_1\tau_1(1+(\omega\tau_2)^2) + R_2\tau_2(1+(\omega\tau_1)^2)}{R_1(1+(\omega\tau_2)^2) + R_2(1+(\omega\tau_1)^2)} \tag{6.5}$$

since $V = |z|I$ equations (6.4) and (6.5) can be substituted in equation (6.2) to give

$$R(\omega) = R_1(A'/A)$$

where

$$A' = 1 + \frac{R_2}{R_1}\frac{(1+(\omega\tau_1)^2)}{(1+(\omega\tau_2)^2)} + \frac{2R_2}{R_1}\frac{(1+\omega\tau_1\omega\tau_2)}{1+(\omega\tau_2)^2}$$

and

$$A = 1 + \frac{R_2}{R_1}\frac{(1+(\omega\tau_1)^2)}{(1+(\omega\tau_2)^2)} .$$

Equation (6.5) can be rewritten as

$$\phi(\omega) = \tan^{-1}(\omega\tau_1(B/A))$$

where $$B = 1 + \frac{R_2}{R_1}\,\frac{(1 + (\omega\tau_1)^2)}{(1 + (\omega\tau_2)^2)}\frac{C_1}{C_2}$$

and from equation (6.3):

$$C(\omega) = C_1(B/A') \quad .$$

Using these equations and the values for R_1, R_2, C_1 and C_2 given in Table 6.3, it was possible to obtain the theoretical curves shown in Figures 6.14 and 6.15. The fit to the experimental points is only partially successful. This is in part due to the compromise of fitting both $R_m(\omega)$ and $\phi(\omega)$ and at the same time keeping the values of R_2 and C_2 small enough so that they can be regarded as being only secondary to the main resistance and capacitance values R_1 and C_1.

Table 6.3

R_1 $K\Omega.cm^2$	R_2 $K\Omega.cm^2$	C_1 $\mu f/cm^2$	C_2 $\mu f/cm^2$
16.8	3.0	1.15	1.2
31.4	4.0	1.20	1.35
23.0	4.0	1.0	6.7
31.0	6.5	1.35	0.28

It was not possible to reproduce the behaviour of $C(\omega)$ simultaneously with that of $R(\omega)$ and $\phi(\omega)$ except in the case of pH 5, where a rather poor fit was obtained. The predicted $C(\omega)$ behaviour is always much more marked than the experimental behaviour.

Skiercyńska, Żoknierczuk and Bulanda (14) reported that

Figure 6.14.

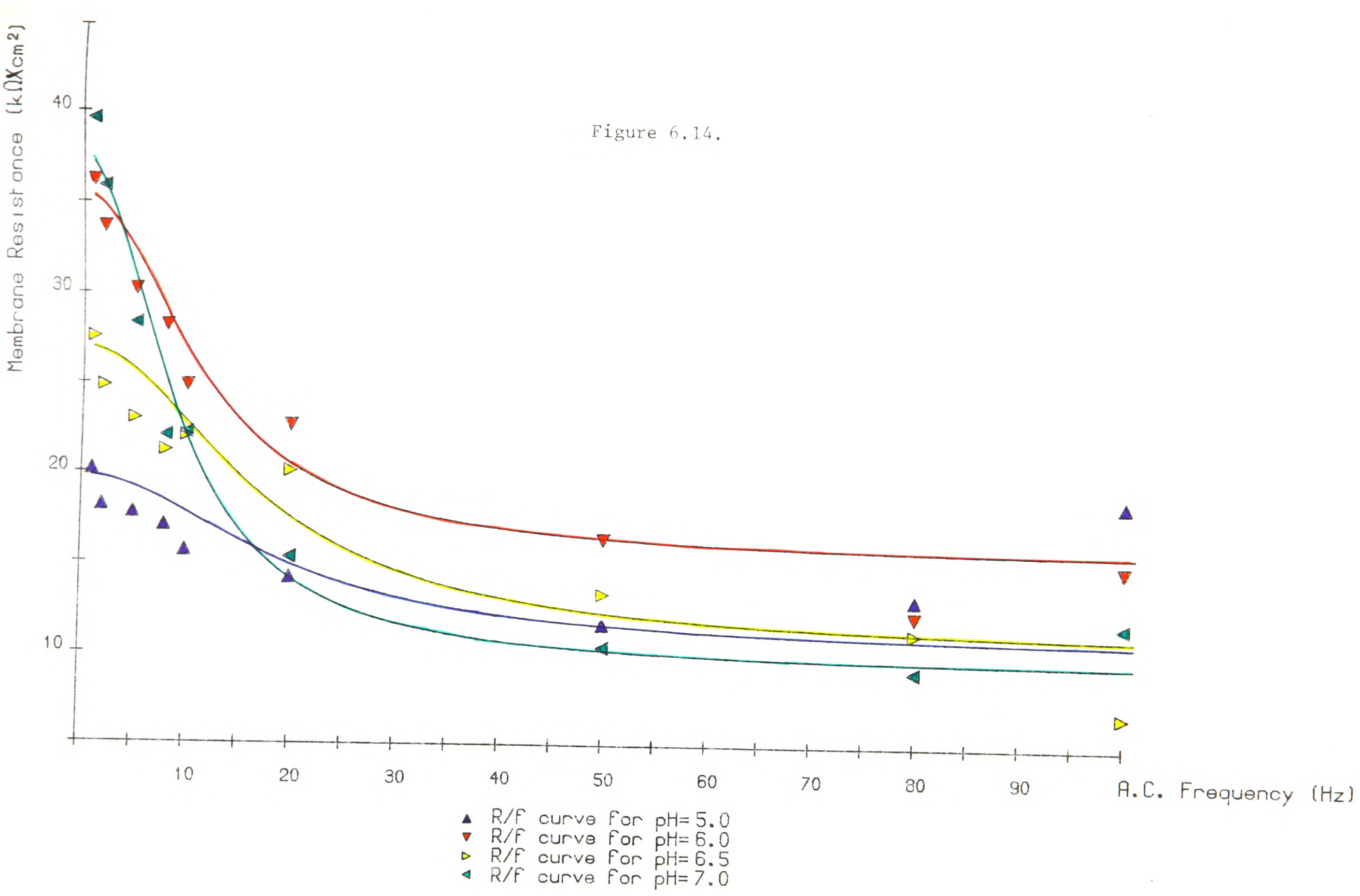
Membrane Resistance (kΩXcm²)
40
30
20
10
10
20
30
40
50
60
70
80
90
A.C. Frequency (Hz)
R/f curve for pH= 5.0
R/f curve for pH= 6.0
R/f curve for pH= 6.5
R/f curve for pH= 7.0

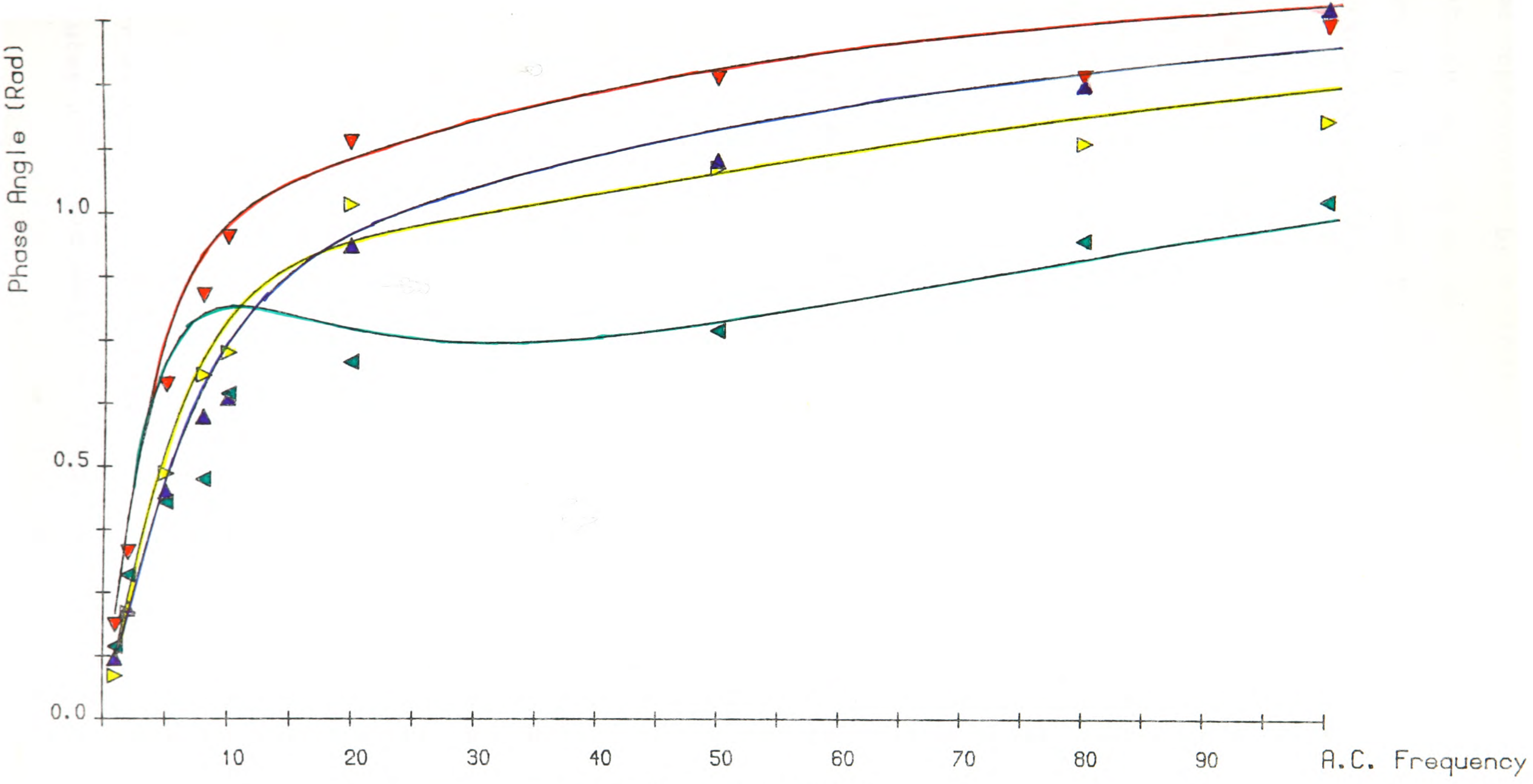
Phase Angle (Rad)
1.0
0.5
0.0
10
20
30
40
50
60
70
80
90
A.C. Frequency
▲ Φ/f Curve for pH=5.0
▼ Φ/f Curve for pH=6.0
▷ Φ/f Curve for pH=6.5
◁ Φ/f Curve for pH=7.0

Figure 6.15.

the measured reactance and resistance of Nitellopsis obtusa can be represented by a single RC circuit in series with a resistance of ≈0.8 $k\Omega.cm^2$, which corresponds to the cell wall resistance. However, the present experimental results cannot be fitted to such a model.

6.5 Internal pH and the Effect of DNP in the Membrane Parameters

In the A.C. experiments described in Section 6.4, the vacuolar pH ($pH_{(i)}$) was monitored by a pH glass microelectrode. The results are shown in Table 6.4(a). These values are comparable with those obtained by other workers using pH glass electrodes (see Hope and Walker (3)). However, the weak acid method used by Smith and Walker (15) gave different results for the vacuolar pH. This is probably due to the inefficacy of this method when used at low pH (see also Spanswick and Miller (16)).

After the completion of an A.C. experiment on a particular cell, the external solution was replaced by one of the same composition and pH but with the addition of 0.2 mM DNP. This concentration of DNP was the same as that used by Kitasato (8) for the inhibition of the H^+ pump. He found that a steady state was reached after 30 minutes and that recovery after DNP removal took between 2 and 4 hours. It should be mentioned that Kitasato used K^+ concentrations of 1 mM and this must also have affected the period of recovery. In the present experiments it was observed that the DNP effects were always reversible, the recovery period being shorter at higher pH. The effects on the membrame parameters 30 minutes after the addition of DNP are shown in Table 6.4(a).

TABLE 6.4(a)

	pH(o)	pH(i)	E (mv)	R_m (1 Hz) (kΩ.cm^2)	R_m (10 Hz) (kΩ.cm^2)	C_m (1 Hz) (μf/cm^2)	C_m (10 Hz) (μf/cm^2)
APW	5	4.91±0.07 (11)	-94.2±3.2		15.7±2.1		0.81±0.05
+DNP	5	4.56±0.10 (6)	-52.2±7.8		26.9±4.3		0.89±0.06
APW	6	5.06±0.08 (10)	-109.5±2.4	36.2 ±6.0	24.9±2.6	0.90±0.08	1.03±0.12
+DNP	6	5.49±0.12 (10)	-79.5±8.0	57.9 ±27.7	31.6±3.7*	0.79±0.18	0.99±0.15*
APW	6.5		-105.2±2.9	27.6 ±3.3	22.1±4.8	0.52±0.05	0.79±0.10
+DNP	6.5		-86.4±5.8	41.73±6.0	28.3±4.6	0.66±0.14	1.02±0.11
APW	7	4.94±0.07 (10)	-99.1±2.0	39.6 ±5.9	22.2±4.1	0.56±0.15	0.52±0.05
+DNP	7	5.23±0.10 (10)	-86.1±6.1	55.0 ±7.8	25.7±7.8	0.46±0.08	0.66±0.14

The quoted errors are standard errors. Figures in parenthesis denote number of cells.
*The number of cells is 4.

TABLE 6.4(b) The ratios of the various parameters in APW and DNP (denoted by ')

pH(o)	$\frac{pH'(i)}{pH(i)}$	$\frac{E}{E'}$	$\frac{R'_m}{R_m}$(10 Hz)	$\frac{R'_m}{R_m}$(1 Hz)	$\frac{C'_m}{C_m}$(10 Hz)	$\frac{C'_m}{C_m}$(1 Hz)
5	1.11	1.8		1.71	1.09	
6	1.08	1.37	1.26	1.60	0.96	0.78
6.5		1.21	1.20	1.51	1.29	1.26
7	1.05	1.15	1.15	1.38	0.78	0.82

The responses for the individual cells are given in the Appendix. One immediate effect of the addition of DNP was sometimes a small hyperpolarization, probably due to an increase in the CO_2 level in the solution adjacent to the cell. With the exceptions of cell 91 (pH 6.5) and cell 89 (pH 7), a depolarized steady state was reached after 30 minutes in the DNP solution. The membrane potentials of cells 78 (pH ~~5~~ 6) and 84 (pH ~~6.5~~ 7) did not respond to DNP. The average response of E to DNP is presented in Figure 6.1 as APW + DNP batch 2. It can be seen that the depolarization produced by DNP decreases with increasing pH.

The membrane resistance also responded to DNP. In many cases the resistance increased to a steady value during the 30 minutes after addition of DNP in agreement with the observations of Kitasato (8), (though there were instances in which it did not respond and it even decreased in the case of cell 78 (pH 6)). The membrane capacitance also responded to the addition of DNP but to a lesser degree than the resistance. The vacuolar pH increased with the addition of DNP. This and other responses to DNP are better represented in Table 6.4(b) where the ratios of the values of the parameters before and after DNP addition are presented. It can be seen that all parameters except the capacitance have a decreasing response to DNP with increasing pH. It can also be seen that the resistance ratio is higher at 1 Hz than at 10 Hz.

6.6 The Hyperpolarizing Response

The rectification curves obtained in Section 6.2 were limited in the hyperpolarizing direction by the onset of the hyperpolarizing response; this response occurs at hyperpolarizations of 60 mv. In other words the D.C. method with short-duration current pulses can not be used to measure the resistance and capacitance in this region. A resistance value can however be obtained by using a longer current pulse and recording the voltage response after the peak of the hyperpolarizing response has subsided. These resistance values can be very low and sometimes negative (see Figure 1.1). This resistance (the slope resistance) was computed here for cells in APW at pH 6.5. From Figure 6.16 it can be seen that a second resistance value (the point resistance) can be determined from the response of the membrane to an A.C. signal superimposed on the current pulse. This point resistance is constant during the length of the current pulse in contrast with the slope resistance which changes along the pulse length.

In Table 6.5 the average values of the slope resistance, at the end of a 1 second current pulse, are presented together with the values of the point resistance and the membrane capacitance.

From this table it can be seen that whilst the slope resistance is very small at these hyperpolarized levels the point resistance has a value slightly smaller than the resting resistance value observed at this frequency in APW at 6.5 (Figure 6.12). The membrane capacitance also has a value close to that of the resting value (Figure 6.13).

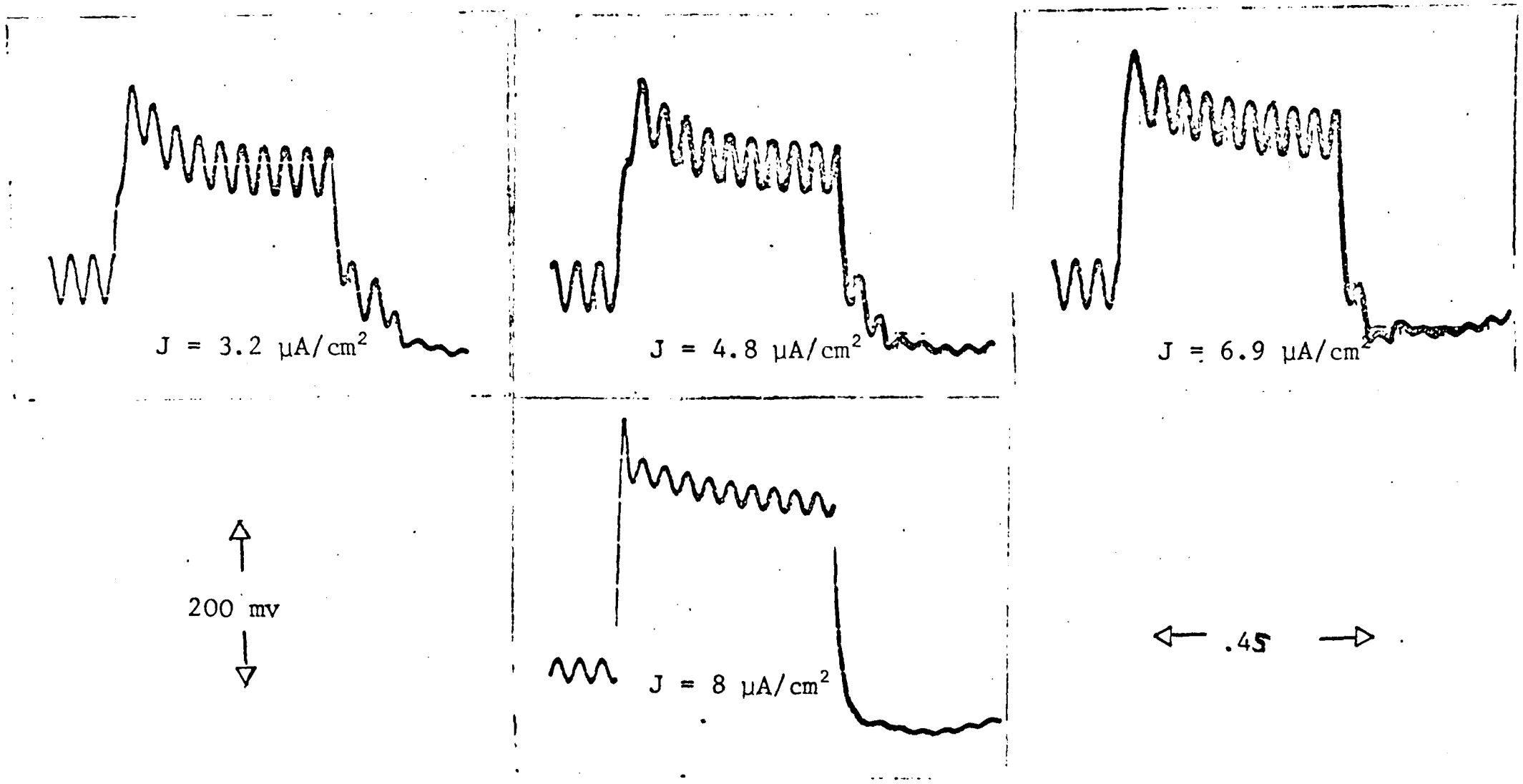

Figure 6.16. The hyperpolarizing response with an A.C. (25 Hz) superimposed. Note that at $J = 8\ \mu A/cm^2$ the A.C. superimposed has half the value than in the previous three curves. This emphasises the distinction between the A.C. response and the peak of the hyperpolarizing response.

TABLE 6.5

Current Density ($\mu A/cm^2$)	E (mv)	Slope Resistance ($k\Omega.cm^2$)	Point Resistance ($k\Omega.cm^2$)	C_m ($\mu f/cm^2$)
3.18	-119 ± 11 (10)	5.1 ± 0.7	17 ± 2	0.69 ± 0.03
4.77	-136 ± 11 (10)	5.5 ± 0.6	18 ± 2	0.77 ± 0.08
6.36	-153 ± 11 (10)	3.8 ± 1.2	15 ± 1	0.73 ± 0.08
7.95	-166 ± 11 (10)		18 ± 2	0.80 ± 0.08

6.7 The Punch-through Region

A negative slope resistance region at high hyperpolarized potentials, the punch-through effect, has been reported in Chara and Nitella, Coster (17). However Bradley (10) did not observe this type of response in Nitella translucens despite the fact that he hyperpolarized the membrane to the same levels, i.e. ≈250 mv. In this work the possible existence of such a region in Nitella translucens was re-examined. Current ramps of different rates from a Hewlett-Packard function generator were applied to the cell and the response recorded on the oscilloscope (Figure 6.17). The limit to the hyperpolarizing level to which the cell can respond is almost 250 mv and from Figure 6.17 there appears to be no evidence of a punch-through effect. It should be noted that in all the cases presented in Figure 6.17 the maximum current density applied was 4.7 $\mu A/cm^2$, which is a smaller value than the current densities at which punch-through was observed in Chara ($\sim 50 \mu A/cm^2$) or Nitella ($\sim 40 \mu A/cm^2$), Coster (17). The reason why such big currents are required to reach the 250 mv hyperpolarizations is because these species have smaller resistances than Nitella translucens (Chara ≈ 4 $k\Omega.cm^2$ and Nitella ≈ 17.1 $k\Omega.cm^2$, Hope and Walker (3)).

When the applied current to Nitella translucens is increased it can be observed that the potential does not hyperpolarize by more than 250 mv (Figures 6.18, 6.19, 6.20). A region of negative resistance is observed in the first curve of Figure 6.18 which resembles the hyperpolarizing response both in form and time of occurrence. Decreasing the rate of the current ramp however shows a negative slope region at hyperpolarisations

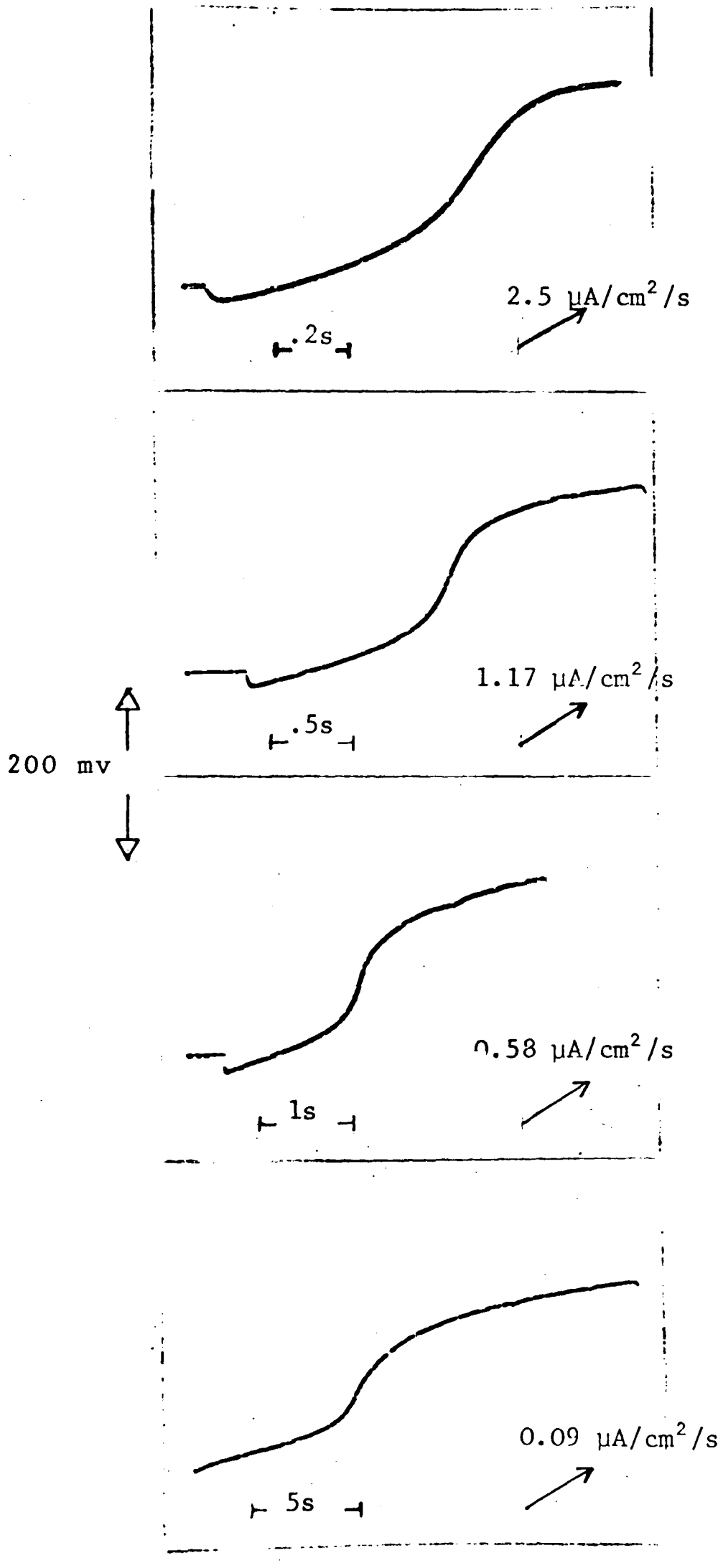

Figure 6.17. The voltage response to a current ramp with a maximum value of 4.7 μA/cm².

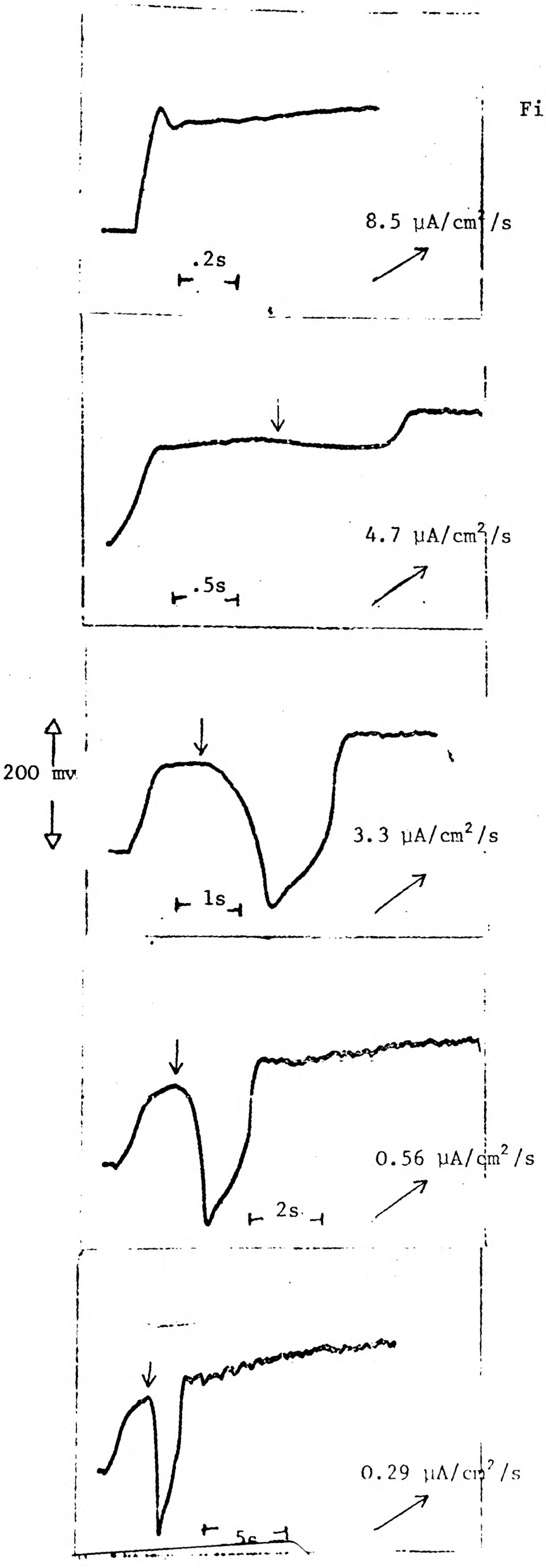

Figure 6.18. The voltage response to a current ramp with a maximum value of 11.9 $\mu a/cm^2$.

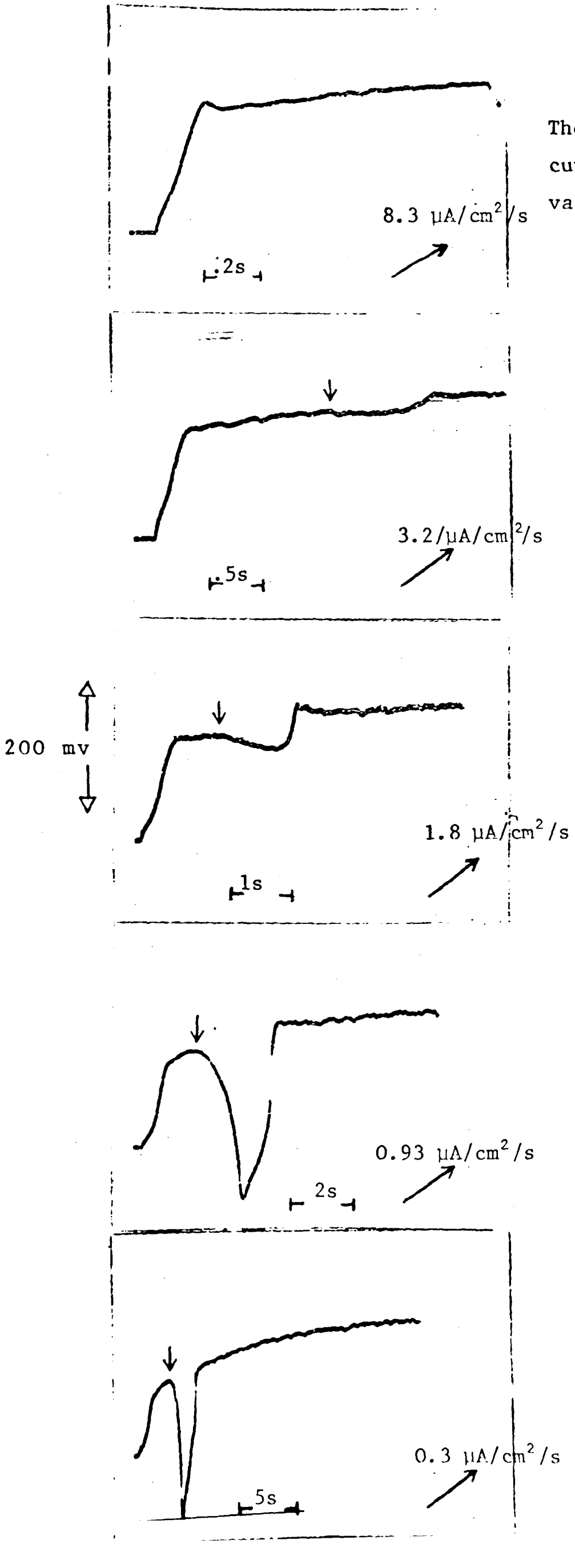

Figure 6.19

The voltage response to a current ramp with a maximum value of 16.9 µA/cm^2.

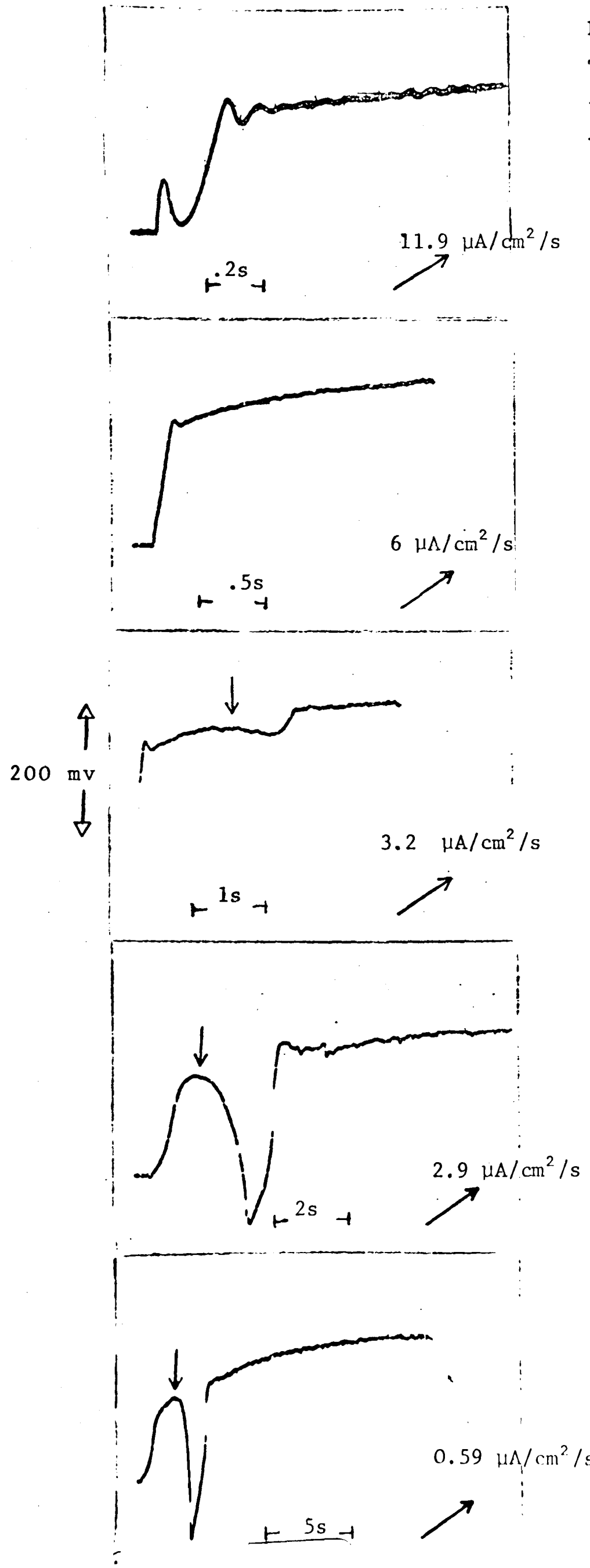

Figure 6.20.

The voltage response to a current ramp of a maximum value of 23.8 $\mu A/cm^2$.

of 250 mV which can definitely be associated with the punch-through region. The excursion in the depolarizing direction increases with decreasing rate of the current ramp. At very slow rates ($<2.4\ \mu A/cm^2/s$) the punch-through degenerates into an action potential. Decreasing ramp rate decreases the current densities at which the negative slope region is observed, but it increases the time after the initiation of the ramp at which these regions appear.

The effects of even higher current densities are shown in Figure 6.20. It can be seen that with a fast ramp rate multiple hyperpolarizing responses appear. At slow rates the negative slope appears at a higher current density than in the cases shown in Figures 6.18, 6.19, but the time after ramp initiation at which this response occurs is the same in all cases. It seems that the negative resistance region cannot occur earlier than 2 seconds after initiating the current ramp and this requires a minimum current density. The punch-through effect can also be observed with current densities lower than this minimum, but they have to be applied for longer times and the effect is observed at later times.

REFERENCES (CHAPTER VI)

1) Tazawa, M., Kikayama, M. & Nagakawa, S., Plant & Cell Physiol. 16, 611 (1975).

2) Spanswick, R.M., J. Expt. Bot. 21, 68, 617 (1970).

3) Hope, A.B. & Walker, N.A., The Physiology of the Giant Algal Cells, Cambridge University Press (1975).

4) Williams, E.J., Johnston, R.J. & Dainty, J., J. Expt. Bot. 15, 1 (1964).

5) Hogg, J., Williams, E.J. & Johnston, R.J., J. Theoret. Biol. 24, 317 (1969).

6) Spanswick, R.M., Symplasmic Transport in Plants, Symposia of the Society for Experimental Biology XXVIII, Cambridge University Press (1974).

7) Spanswick, R.M., Biochim. Biophys. Acta 288, 73 (1972).

8) Kitasato, H., J. Gen. Physiol. 52, 60 (1968).

9) Kishimoto, U., Ann. Rep. Scient. Works, Fac. Sci. Osaka University 7, 115 (1959).

10) Bradley, J., Ph.D. Thesis, University of Edinburgh (1966).

11) Kishimoto, U., Plant & Cell Physiol. 9, 539 (1968).

12) Kishimoto, U., Jap. J. Physiol. 24, 403 (1974).

13) Coster, H.G.L. & Smith, J.R., The effect of pH on the low frequency capacitance of the membrane of Chara corallina, Membrane Transport in Plants, Edit. Zimmermann, U. & Dainty, J., Springer-Verlag (1974).

14) Skierczyńska, J., Żoknierczнk, R. & Bulanda, W.J., Expt. Bot. 24 78, 38 (1973).

15) Smith, F.A. & Walker, N.A., Plant Sc. Lett. 4, 125 (1975).

16) Spanswick, R.M. & Miller, A.G., Plant Physiol. 59, 664 (1977).

17) Coster, H.G.L., Biophys. J. 5, 669 (1965).

CHAPTER VII

DISCUSSION

The membrane characteristics of the cells of the Characeae have been studied by many workers and in many cases marked discrepancies have been observed. To some extent these discrepancies have arisen because of the lack of control of external pH and light intensity. Even when these factors are controlled, differences in the age of the cell or its prehistory, e.g. dark preconditioning, will still produce considerable variations in the values for individual cells. This difficulty in controlling all variables is reflected by the relatively large standard errors observed in the present work, which makes for difficulties in the interpretation of the experimental results. On the other hand, the use of 'typical' cells is probably less advantageous because of the difficulty in choosing such a cell and the danger of making generalized conclusions from a particular behaviour. For this reason the conclusions and the discussion to follow were generally made from observations of the average responses from a number of cells.

7.1 The Membrane Response to External pH

(a) The resting state

Whilst Vredenberg (1) and Spanswick (2) are agreed that the effect of pH is on the H^+ pump they differ widely as to the degree of involvement of pH and the membrane characteristics. Spanswick contends that pH affects both membrane potential and resistance and that the resting resistance of the membrane is

determined by the pump resistance. Thus his observation of the large increase in the membrane resistance and the hyperpolarized state of the membrane in the dark is interpreted as being due to the almost complete inactivation of the pump. Vredenberg claims that the pH affects only the potential and that observations of a high resistance at a high potential are simply observations of the rectifying properties of the membrane. He obtained the current-voltage curves using a current ramp arrangement and apparently found a correlation between high resistance and high potential in the light.

Spanswick (3) challenged this by suggesting that Vredenberg's resistance values at the higher levels of hyperpolarization were overestimates since by the very nature of the current ramp he was only measuring the hyperpolarizing response. Support for the Spanswick viewpoint comes from the present experiments in which the membrane resistance actually decreases at large negative potentials (see Section 6). Further evidence can be found in the work of Brown, Ryan and Barr (4). They found that at external K^+ concentrations of 1 mM the membrane potential in the dark was only -120 mv yet the membrane resistance was larger than the membrane resistance in the light at the same potential.

Vredenberg[1] also claimed that his current-voltage curves at different pH could be superimposed after suitable translation which would mean that the passive rectifying properties of the membrane are independent of pH. This was apparently confirmed in the present work where, in the pH range 4 to 7, the rectifying curves overlap (see Figure 6.4(b)). However, this observation can also be explained by the Spanswick model

if it is assumed that the observed rectification corresponds to the rectifying properties of R_p. This assumption cannot be tested directly from the Spanswick expression for the pump resistance. It can, however, be tested indirectly by examining whether the experimental curves can be fitted by any theoretical rectification relationship for passive, independent, univalent transport. A lack of fit would support the Spanswick model.

The equation for the chord resistance $(R(E') = (E'-E)/I)$ based on the constant field assumption was obtained by Hope (5) and can be written as:

$$R(E') = \frac{RT}{F^2} \frac{(E'-E)}{E' A} \left(\frac{1 - e^{FE'/RT}}{1 - e^{F(E'-E)/RT}} \right) \qquad (7.1)$$

where E' is the new membrane potential resulting from the flow of current and A is defined by equation (1.22). The corresponding equation for the Kimizuka-Koketzu membrane was obtained by Kimizuka (6):

$$R(E') = \frac{RT}{F^2 \sqrt{A'B'}} \sinh \frac{(F(E' - E)/2RT)}{(F(E' - E)/2RT)} \qquad (7.2)$$

where A' and B' are defined by equation (1.23) and are potential-dependent. The expression for the slope resistance $(R = dE'/dI)$, based in the Kimizuka-Koketzu membrane, can be obtained by differentiating the expression of membrane current (Kimizuka and Koketzu (7)):

$$I = -2F\sqrt{A'B'} \sinh F(E' - E)/2RT \quad . \qquad (7.3)$$

Using equation (1.20), equation (7.3) can be expressed as

$$I = \frac{-F^2}{RT}\sqrt{A\,B}\;E\;\frac{\sinh(F(E'-E)/2RT)}{\sinh(FE/2RT)} .$$

Thus $R(E')$ can be obtained from $R(E') = 1/(dI/dE')$, i.e.

$$R(E') = \frac{RT}{F^2\sqrt{A'B'}}\left[\cosh F(E'-E)/2RT + \frac{\sinh F(E'-E)/2RT}{FE/2RT} - \frac{\sinh(F(E'-E)/2RT)\cosh(FE/2RT)}{\sinh(FE/2RT)}\right]^{-1} \quad (7.4)$$

Since the H^+ permeability values, and therefore the constants A and B, have not been determined by other than electric measurements, Kitasato (8), it is necessary to compute the constants in equations (7.1), (7.2) and (7.4) from one experimental point. Using the constants so obtained comparisons can then be made between the predicted and experimental rectifying curves. This comparison is shown in Figure 7.1 where the solid line represents equation (7.1), the dotted line equation (7.2) and the broken line represents equation (7.4). The constants were computed from the point -110 mv, 25.45 $k\Omega.cm^2$, i.e. from the resting value at pH 5. The experimental points correspond to the group of cells of diameter ≃ 1 mm.

It can be seen that none of these equations predict the observed rectification. This is perhaps to be expected for equation (7.1) because of the severe constraint of the constant field assumption. However poor fits are also obtained with equations (7.2) and (7.4) which are valid for any passive, independent, univalent transport process. Thus it appears that the present work confirms the Spanswick[2] proposition that the measured resistance corresponds to R_p, i.e. the

Figure 7.1.

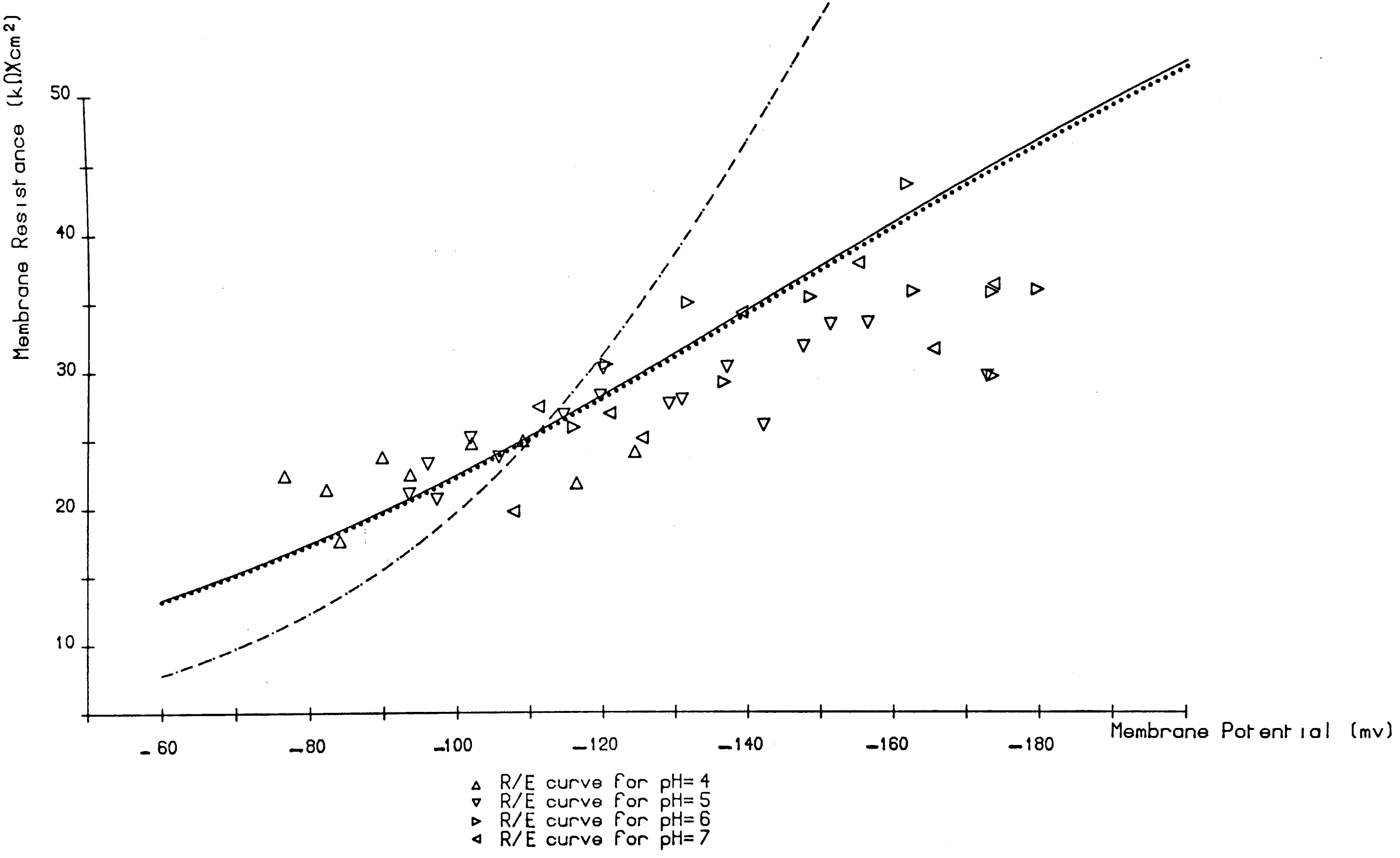
Membrane Resistance (kΩXcm²)
50
40
30
20
10
-60
-80
-100
-120
-140
-160
-180
Membrane Potential (mv)
R/E curve for pH=4
R/E curve for pH=5
R/E curve for pH=6
R/E curve for pH=7

resistance associated with the active transport of H^+. A further test of this hypothesis would come from the measurement of the rectification curves in the dark where the passive membrane resistance should dominate and the curves should be reproduced by the Kimisuka-Koketzu equations.

As a final observation it should be noted that the pH response is more marked in the cells of diameter 0.8 mm than in the cells of diameter 1 mm. If the diameter is a measure of the age of a cell then this might suggest that the H^+ pump is more active in younger cells.

b) The excited state

The action potentials recorded in the pH range 5 - 7 do not show any marked differences. However at pH 8 a faster recovery phase than at ph 4 or 5 is observed even though the excited state resistances are comparable. An increased potassium permeability at the high pH could account for this observation (see Gillet and Lefebvre, 9). Support for this comes from Kitasato's findings (8) that at high pH the K^+ efflux shows a slight increase from that observed when the membrane is clamped at the same potential and at a lower pH. An increased K^+ permeability produced by pH 8 would also explain the observed departure of the rectification curve at pH 8 from the general rectification curve at pH 4 to 7.

The form of the action potential at pH 4 is more difficult to explain. The very slow recovery could be explained by an increased $C\ell^-$ permeability at low pH but this would not explain the slow initial phase of the action potential at this pH. It should be mentioned that Doughty and Hope (10) found a similar form for the action potential in Chara

corallina when the Cl^- permeability was increased by ultraviolet radiation. A high Cl^- conductance at low pH has also been proposed by Lannoye, Tarr and Dainty (11) and by Richards and Hope (12).

7.2 The Frequency Dependence of the Membrane Resistance and Capacitance

The frequency dependence of the resistance observed in the present work can be represented, though not with complete success, by a circuit having two time constants. The experimental curves are more faithfully reproduced if it is assumed that C_2 (see Section 6.4) is frequency dependent, i.e. if it increases with increasing frequency. However for each pH curve an ad hoc behaviour of C_2 has to be assumed which casts doubts on the validity of this assumption. It should be mentioned that most of the discrepancy between the theoretical and the experimental curves occurs at high frequencies. This could be due to the greater experimental inaccuracies at these frequencies (see Section 5.6).

This two time constant circuit fails completely to describe the frequency dependence of the membrane capacitance. It is possible to speculate that this discrepancy arises because of the existence of an inductance associated with the membrane. The existence of such an element was suggested for nerve by Cole (13) and for Nitella translucens by Bradley and Williams (14). The response of the membrane to the application of a fast ramp of high current density also suggests the existence of a membrane inductance (see Figure 6.20)

In this case ringing, characteristic of an RLC circuit, can be observed. Clearly this circuit model should be rigorously tested.

Coster and Smith (15) have proposed a single RC circuit model in which both R_m and C_m are frequency dependent. However the present work with DNP conflicts with this hypothesis. In those experiments it was shown that the DNP induced increase in resistance was larger at 1 Hz than at 10 Hz. This is inconsistent with the proposition of a single frequency dependent resistance, R_m. It could, however, be explained by assuming a model in which the RC circuit for the membrane is in series with the RC circuit for the cell wall and in which the membrane time constant is bigger than that for the cell wall. Then at high frequencies R_m would be shunted through the capacitor so that the resistance being measured is that of the cell wall, i.e. R_2. The lack of response of the cell wall to DNP is then only to be expected.

7.3 Internal pH and the Effect of DNP on the Membrane Parameters

The present measurement of the vacuolar pH ($pH_{(i)}$) indicate that, even after prolonged presoaking of the cells, its response to variations of external pH, $pH_{(o)}$, is small. Smith and Walker (16) showed that the cytoplasmic pH is more sensitive to variations in $pH_{(o)}$. They reported that with short presoaking periods the cytoplasmic pH increases 0.22 pH units per unit increase in $pH_{(o)}$. The increase in pH(i), observed here, between $pH_{(o)} = 5$ and $pH_{(o)} = 6$ could be due to the vacuolar response to the change in cytoplasmic pH, attenuated by a low H^+ permeability of the

tonoplast. However this explanation cannot be extended to the observed value of $pH_{(i)}$ at $pH_{(o)} = 7$. In this case $pH_{(i)}$ was actually less than its value at $pH_{(o)} = 6$. This behaviour could be the result of the long presoaking periods during which the tonoplast potential may have been affected. This calls for the separate determination of the plasmalema and the tonoplast pH responses as well as the monitoring of cytoplasmic and vacuolar pH for different presoaking periods.

The DNP effects on the membrane parameters obtained in the present work are very similar to those found by Kitasato (8). The observed depolarization of the membrane potential led Kitasato to propose the DNP inhibition of the H^+ pump and, because of the high proton permeability, the membrane potential would then move to the H^+ Nernst potential (E_H). This interpretation was challenged by Spanswick (2) who drew attention to high external K^+ concentration used by Kitasato and suggested that the membrane potential would move to the K^+ Nernst potential (E_K) rather than to E_H. This proposition has been supported by observations on the membrane potential when the pump is inhibited in the dark, Spanswick (2) and ~~Barr~~ Brown et al. (4), or by uncoupling agents, Spanswick (17).

The results of the present work do not support either Kitasato's or Spanswick's hypothesis since the membrane potential moved to a value intermediate between E_H and E_K. A similar result was obtained by Spanswick (17) when he used 1 mM Azide as an inhibitor. Furthermore, ~~in~~ for the depolarizations observed by Spanswick when he added 50 µM DCCD* or 1 µM CCCP†

---

* dicyclohexylcarbodiimide ; † carbonylcyanide m-chlorophenylhydrazone.

to a pH 6 solution, the ratio E/E'_t (where E' is the depolarized level) has the values 1.37 and 1.30 respectively. These values are similar to the value of E/E' obtained in this work for the DNP produced depolarization at pH 6, thus suggesting that the move of E to E_K in Spanswick's experiments was fortuitous. Spanswick does not mention if in his experiments the external pH was established prior to the addition of the inhibitors. If this was the case the addition of 50 µM DCCD or 1 µM CCCP would have little effect on the external pH, but the addition of 1 mM Azide (a weak acid) would certainly decrease it. The ratio E/E' corresponding to the Azide experiments reported by Spanswick is 1.7, a value similar to the ratio observed here for the DNP produced depolarization at pH 5.

Hope and Walker (18) state that uncoupling agents increase the proton permeability of artificial membranes. Such an effect, leading to an influx of H^+, would certainly explain the observed depolarisation in the Characeae (Spanswick (17), Kitasato (8), and herein). The reduction in the ratio E/E' with increasing pH, observed herein, would then be the result of a reduction in the H^+ concentration gradient. However an increase in proton permeability in Nitella translucens seems unlikely since the resistance increases with the addition of DNP, though Spanswick would explain this as being due to an increase in the pump resistance. The hypothesis is made further untenable by the observation that R'/R, where R' is the resistance in DNP solution, decreases with increasing pH.

An alternative explanation of the effect of DNP has been advanced by Duncan and Croghan (19) from their observations on the toad lens membrane. They proposed that DNP diffuses through the membrane only in its undissociated form (HP), where P^- is the dinitrophenate radical. The diminishing effect of DNP with increasing alkalinity of the external solution is thus a consequence of the dissociated form (H^+,P^-) being favoured at high pH values. This mechanism would account for the observed DNP effects on the membrane parameters of Nitella translucens. HP will permeate through the membrane and dissociate in the cytoplasm leading to its acidification and a depolarisation of the membrane. Since there would be less undissociated DNP at higher pH then the observed decrease in R'/R and E/E' is only to be expected. Furthermore Spanswick's hypothesis would still be correct.

The observed response of vacuolar pH to DNP is difficult to explain. If there is an acidification of the cytoplasm a similar response would be expected for the vacuolar pH. A possible explanation of the observed rise in vacuolar pH would be that DNP increases the H^+ permeability of the tonoplast, as distinct from the plasmalema, thus producing an equilibration of vacuolar and cytoplasmic pH at an intermediate value. Alternatively it could be assumed that the tonoplast, as distinct from the plasmalema, is permeable to P^-. Migration of P^- from the cytoplasm to the vacuole would produce the observed alkalinization of vacuolar pH. Clarification for the effect of DNP and other inhibitors calls for the monitoring of the membrane potential and internal pH of both phases, the vacuole and the cytoplasm.

7.4 The Punch-through Region

The results of the present work on the punch-through region show that contrary to the Coster theory (see Chapter I), this response is not simply a consequence of applying large negative potentials across the membrane. The observations relating the size of the current density required for the appearance of a negative slope region and the time of appearance of this region can be fitted into a strength-duration curve (Figure 7.2). The existence of a strength-duration curve for the action potential of the Characeae, Oda (20), suggests that the punch-through effect and the action potential are closely related. This assumption is supported by the observations in this work and those of Kishimoto (21) that the punch-through degenerates into an action potential with long lasting applications of large hyperpolarizing currents. Coster and Hope (22) found a large increase in the effect of Cl^- in the punch-through region and interpreted this efflux as the avalanche current produced in a double fixed charge membrane. However Kishimoto (23) interpreted the punch-through as being due to an increase in both Cl^- and K^+ conductance in a similar way to the action potential. Further evidence showing the close relation between the action potential and the punch-through region is presented in Figure 7.3. It can be seen that the punch-through effect cannot be elicited during the refractory period of an action potential. In conclusion the results of the present experiments studying the membrane response to A.C. frequency and to large hyperpolarizing currents are inconsistent with a double fixed-charge membrane model.

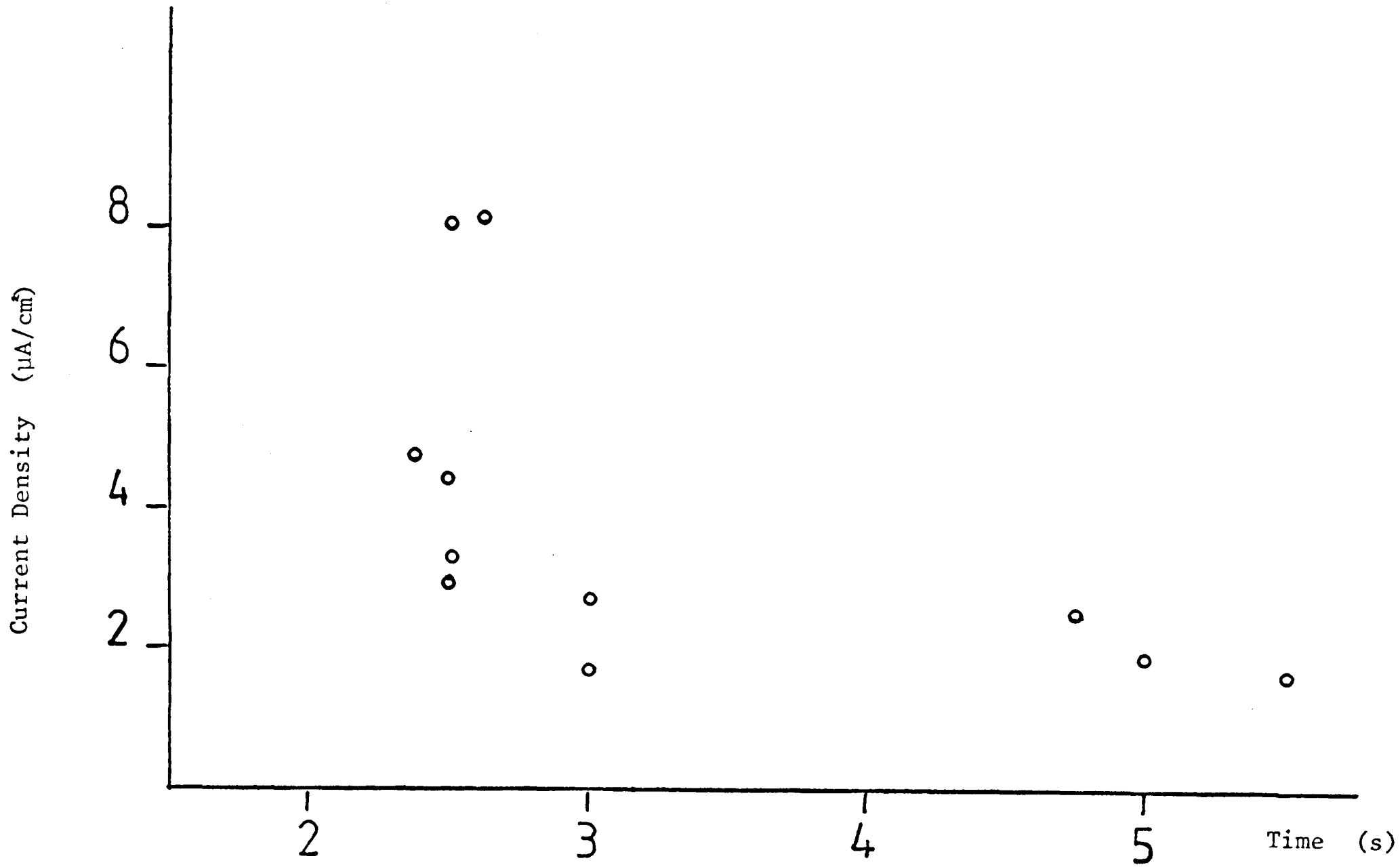

Figure 7.2 Strength-Duration Curve for the Punch-through Effect.

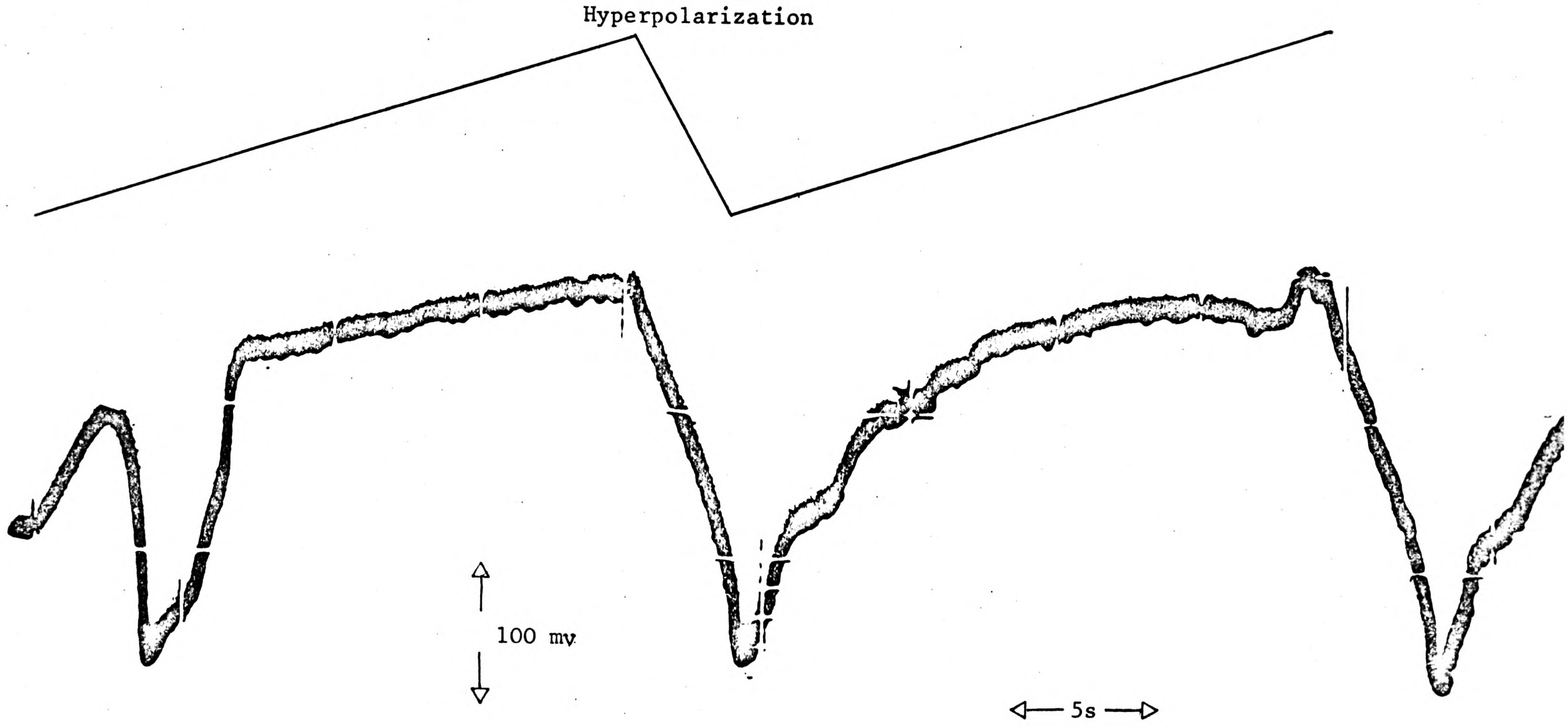

Figure 7.3. The voltage response to a current ramp showing that no punch-through is elicited during the refractory period of the action potential. The upper line represents the form of the applied current.

REFERENCES (CHAPTER VII)

1) Vredenberg, W.J., Energy control of Ion fluxes, Ion Transport in Plants, Edit. Anderson, W.P., Academic Press (1973).

2) Spanswick, R.M., Biochim. Biophys. Acta 288, 73 (1972).

3) Spanswick, R.M., Discussion pp. 183, Ion Transport in Plants, Edit. Anderson, W.P., Academic Press (1973).

4) Brown, D.F., Ryan, T.E. & Barr, C.E., The effect of light and darkness in relation to the external pH on calculated H^+ fluxes in Nitella, Ion Transport in Plants, Edit. Anderson, W.P., Academic Press (1973).

5) Hope, A.B., Ion Transport and Membranes, Butterworth's London (1971).

6) Kimizuka, H., J. Theoret. Biol. 13, 145 (1966).

7) Kimizuka, H. & Koketzu, K., J. Theoret. Biol. 6, 290 (1964).

8) Kitasato, H., J. Gen. Physiol. 52, 60 (1968).

9) Gillet, C. & Lefebvre, J., Combined Effect of Potassium and Bicarbonate Ions on the Membrane Potential and Electric Conductance of Nitella Flexilis. Ion Transport in Plants. Edit. Anderson, W.P., Academic Press (1973).

10) Doughty, C.J. & Hope, A.B., Aust. J. Plant Physiol., 3, 687 (1976).

11) Lannoye, R.J., Tarr, S.E. & Dainty, J., J. Expt. Bot. 21, 543 (1970).

12) Richards, J.L. & Hope, A.B., J. Memb. Biol. 16, 121 (1974).

13) Cole, K.S., J. Gen. Physiol., 25, 29 (1941).

14) Bradley, J. & Williams, E.J., Biochim. Biophys. Acta 135, 1078 (1967).

15) Coster, H.G.L. & Smith, J.R., The effect of pH on the low frequency capacitance of the membrane of Chara corallina, Membrane Transport in Plants, Edit. Zimmermann, U. and Dainty, J., Springer-Verlag (1974).

16) Smith, F.A. & Walker, N.A., J. Expt. Bot. 27, 98, 451 (1976).

17) Spanwick, R.M., Biochim. Biophys. Acta, 332, 384 (1974).

18) Hope, A.B. & Walker, N.A., The Physiology of Giant Algal Cells. Cambridge University Press (1975).

19) Duncan, G. & Croghan, P.C., Exptl. Eye Res. 10, 192 (1970).

20) Oda, K., Sci. Rep. Tohoku Univ. Ser. IV (Biol.) 28, 1 (1962).

21) Kishimoto, U., Plant & Cell Physiol. 16, 83 (1975).

22) Coster, H.G.L. & Hope A.B., Aust. J. Biol. Sci. 21, 243 (1968).

23) Kishimoto, U., Plant & Cell Physiol. 18, 67 (1977).

ACKNOWLEDGEMENTS

I wish to thank my supervisors, Dr. E.J. Williams and Dr. J. Hogg, for their encouragement and advice. I would also like to thank other members of the Physics Department for their assistance, in particular to Mr. L.W. Kennedy and Mr. C. Inglis (ret.).

I am indebted to Mr. R. McCluskey from the Botany Greenhouse for all his help and to Mrs. R.W. Chester for her typing of this thesis.

The author held a British Council grant during the years 1974-76, and a Conacyt (México) grant during the years 1976-7.

APPENDIX

Current Density rounding error= 0.080 pH(o)= 4.0
J= Current Density ($\mu A/cm^2$) , in the form of a step pulse of .4 s duration
E= Membrane Potential (mv)
R= Memorane Resistance ($k\Omega \cdot cm^2$)
C= Membrane Capacitance ($\mu f/cm^2$)

	Cell 39 d= 0.95 T= 23.0			Cell 41 d= 1.00 T= 22.0			Cell 42 d= 1.00 T= 23.0			Cell 43 d= 0.90 T= 22.0			Cell 44 d= 0.95 T= 22.0			Cell 45 d= 0.75 T= 22.0			Cell 47 d= 0.80 T= 23.0		
J	E	R	C	E	R	C	E	R	C	E	R	C	E	R	C	E	R	C	E	R	C
-1.28																-25	23.6	1.06			
-1.12																			-83	7.5	2.12
-0.96				-56	12.6	2.39	-96	12.6	1.51												
-0.80																-35	23.6	1.27	-86	7.5	1.99
-0.64				-60	31.4	0.70	-100	12.6	1.75	-62	28.3	1.41	-85	17.9	1.40						
-0.48																-45	23.6	0.85			
-0.32				-70	12.6	2.39	-104	6.3	3.18	-72	28.3	1.31	-91	23.9	1.68				-89	10.1	1.49
-0.16	-63	29.8	1.01	-72	18.8	1.59	-105	12.6	2.39	-77	28.3	1.24	-95	17.9	2.23	-50	23.6	1.06	-91	10.1	1.99
0.00	-68			-75			-107			-82			-98			-55			-93		
0.16	-73	29.8	1.34	-78	18.8	1.59	-109	12.6	2.39	-87	28.3	1.41	-103	29.8	1.51	-60	23.6	1.10	-95	10.1	2.49
0.32	-78	29.8	1.17	-80	12.6	2.39	-111	12.6	2.39	-93	33.9	1.03	-107	23.9	1.88				-97	10.1	1.99
0.48																-65	23.6	1.27			
0.64	-88	29.8	1.17	-87	22.0	1.14	-114	9.4	2.55	-107	39.6	0.88	-115	23.9	1.88						
0.80																-75	23.6	1.49	-101	10.1	1.79
0.96	-100	35.8	0.98	-94	22.0	1.18	-118	12.6	1.91				-125	29.8	1.17						
1.12										-117	28.3	0.88							-105	10.1	1.99
1.28	-110	29.8	1.17	-100	18.8	1.33	-121	9.4	2.55				-135	29.8	1.01	-85	23.6	1.27			
1.44										-128	31.1	0.80									
1.60	-118	23.9	1.26	-107	22.0	1.23	-126	15.7	1.27				-147	35.8	0.84				-109	10.1	1.99
1.76										-139	31.1	0.80				-96	25.9	0.96			
1.92																			-113	10.1	1.99
2.08																-108	28.3	1.24			

	Cell 50 d= 0.90 T= 23.0			Cell 51 d= 0.87 T= 23.0			Cell 52 d= 0.90 T= 22.0		
J	E	R	C	E	R	C	E	R	C
-1.28									
-1.12	-56	11.3	1.68	-59	5.5	1.10	-40	19.8	1.26
-0.96									
-0.80				-61	5.5	1.65			
-0.64	-60	17.0	0.94				-47	22.6	1.11
-0.48									
-0.32	-66	11.3	1.86	-63	4.4	2.29	-55	11.3	1.33
-0.16	-68	11.3	1.77	-64	4.4	1.83	-57	17.0	1.47
0.00	-70			-65			-60		
0.16	-73	17.0	1.77	-66	5.5	2.20	-63	17.0	1.41
0.32	-76	17.0	1.41	-67	5.5	2.38	-66	17.0	1.24
0.48									
0.64	-82	17.0	1.18				-74	22.6	0.97
0.80				-69	5.5	2.20			
0.96									
1.12	-89	19.8	0.81	-71	5.5	1.83	-82	22.6	0.97
1.28									
1.44	-95	17.0	1.06	-73	5.5	1.46	-90	22.6	1.33
1.60									
1.76	-101	17.0	0.88	-76	8.2	1.10	-97	19.8	1.92
1.92									

F	s.e.	R	s.e.	C	s.e.	
-25.0		23.6		1.06		(1)
-59.6	8.9	11.0	3.2	1.54	0.23	(4)
-76.0	20.0	12.6	0.0	1.95	0.44	(2)
-60.8	14.7	12.2	5.7	1.64	0.21	(3)
-69.0	8.0	21.6	2.9	1.22	0.15	(6)
-45.0		23.6		0.85		(1)
-76.3	5.9	13.5	2.9	1.94	0.23	(8)
-74.2	5.6	17.4	2.6	1.66	0.15	(10)
-77.3	5.4					(10)
-80.7	5.4	19.2	2.7	1.72	0.15	(10)
-86.1	5.5	18.0	3.1	1.76	0.19	(9)
-65.0		23.6		1.27		(1)
-95.3	6.2	23.5	3.6	1.40	0.23	(7)
-81.7	9.8	13.0	5.4	1.82	0.21	(3)
-109.2	7.3	25.1	5.0	1.31	0.21	(4)
-92.8	8.2	17.2	4.2	1.30	0.25	(5)
-110.2	8.6	22.3	3.8	1.46	0.28	(5)
-96.5	11.5	19.0	5.4	1.16	0.15	(4)
-121.4	7.2	21.5	4.3	1.32	0.19	(5)
-101.8	10.3	20.4	3.9	1.13	0.20	(5)
-113.0		10.1		1.99		(1)

Current Density rounding error= 0.080 pH(o)= 5.0
J= Current Density ($\mu A/cm^2$) , in the form of a pulse of .4s duration
E= Membrane Potential (mv)
R= Membrane Resistance ($K\Omega.cm^2$)
C= Membrane Capacitance ($\mu f/cm^2$)

	Cell 1 d= 1.00 T= 21.0			Cell 11 d= 1.00 T= 22.0			Cell 10 d= 1.00 T= 22.0			Cell 2 d= 1.00 T= 21.0			Cell 3 d= 1.00 T= 21.0			Cell 4 d= 1.00 T= 21.0			Cell 5 d= 1.00 T= 22.0		
J	E	R	C	E	R	C	E	R	C	E	R	C	E	R	C	E	R	C	E	R	C
-1.28																					
-1.12																					
-0.96				-74	22.0	1.23	-73	22.0	1.36	-81	40.8	0.98	-64	31.4	1.27				-93	28.3	0.71
-0.80																					
-0.64				-81	25.1	0.99	-80	22.0	1.36	-94	37.7	1.19	-74	40.8	0.98				-102	25.1	0.76
-0.48																					
-0.32	-125	31.4	1.43	-89	25.1	0.99	-87	25.1	1.39	-106	44.0	0.91	-87	50.3	0.90						
-0.16	-130	31.4	1.27	-93	25.1	1.19	-91	31.4	1.27	-113	44.0	1.02	-95	31.4	0.95						
0.00	-135			-97			-96			-120			-100			-110			-110		
0.16	-142	44.0	1.25	-102	31.4	1.91	-101	31.4	1.11	-126	37.7	0.80	-105	31.4	0.80	-118	50.3	0.99			
0.32	-149	44.0	1.02	-107	31.4	1.43	-106	31.4	0.80	-135	44.0	0.68	-112	44.0	0.68	-126	50.3	0.99			
0.48																					
0.64	-162	40.8	1.35	-117	31.4	0.95	-114	25.1	0.99	-148	47.1	0.85	-124	37.7	0.80	-140	44.0	0.80	-120	31.4	1.11
0.80																					
0.96	-176	44.0	1.02	-127	31.4	0.95	-121	22.0	0.91	-170	69.1	0.58	-134	31.4	1.11	-154	44.0	0.80	-130	31.4	0.95
1.12																					
1.28	-189	40.8	0.98	-140	40.8	0.86	-131	31.4	0.64	-187	53.4	0.75	-148	44.0	0.80	-169	47.1	0.85	-140	31.4	1.11
1.44																					
1.60	-202	40.8	0.73	-153	40.8	0.86	-139	25.1	0.60				-165	53.4	0.66	-186	53.4	0.75	-156	50.3	0.60
1.76																					
1.92																					
2.08																					
2.24																					

	Cell 6 d= 1.00 T= 22.0			Cell 7 d= 0.90 T= 22.0			Cell 8 d= 0.80 T= 22.0			Cell 9 d= 1.00 T= 22.0			Cell 12 d= 1.00 T= 24.0			Cell 13 d= 0.70 T= 23.0			Cell 14 d= 0.90 T= 20.0		
J	E	R	C	E	R	C	E	R	C	E	R	C	E	R	C	E	R	C	E	R	C
-1.28																					
-1.12				-84	25.4	1.18	-98	22.6	1.11												
-0.96	-114	22.0	0.91							-102	18.8	1.33									
-0.80							107	25.1	1.19												
-0.64	-121	22.0	1.05	-93	31.1	1.29				-108	15.7	1.59	-134	18.8	1.06				-104	22.6	0.88
-0.48																-107	22.0	1.00			
-0.32	-128	25.1	0.99	-104	28.3	1.41	-117	30.2	0.99	-113	18.8	1.59							-112	22.6	0.88
-0.16	-132	25.1	1.19	-109	33.9	1.33	-123	25.1	1.39	-116	25.1	1.19				-112	17.6	1.02	-116	22.6	0.80
0.00	-136			-115			-128			-120			-140			-116			-120		
0.16	-141	31.4	1.75	-121	33.9	1.18	-134	30.2	0.83	-123	18.8	1.33				-120	17.6	1.02	-124	22.6	0.71
0.32	-146	31.4	1.27	-131	56.5	0.88	-141	35.2	0.85	-126	18.8	1.33							-129	28.3	0.71
0.48																-125	22.0	0.91			
0.64	-155	28.3	1.24	-151	56.5	0.62				-132	18.8	1.06	-146	18.8	1.17				-139	28.3	0.71
0.80							-150	22.6	1.11												
0.96	-161	18.8	1.33							-138	18.8	1.06				-136	24.2	1.24			
1.12				-168	48.1	1.25	-157	17.6	1.71												
1.28	-171	31.4	0.80							-145	22.0	0.91	-153	22.0	0.91						
1.44				-193	70.7	1.06										-150	30.8	1.30			
1.60	-181	31.4	0.80				-167	25.1	0.99	-152	22.0	0.91									
1.76				-218	70.7	0.99															

Continuation.

	Cell 15 d= 0.81 T= 20.0			Cell 16 d= 0.70 T= 20.0			Cell 17 d= 0.90 T= 20.0			Cell 18 d= 0.85 T= 20.0			Cell 19 d= 0.63 T= 20.0			Cell 20 d= 0.80 T= 21.0			Cell 21 d= 0.78 T= 21.0		
J	E	R	C	E	R	C	E	R	C	E	R	C	E	R	C	E	R	C	E	R	C
-1.28																					
-1.12							-94	17.0	1.36										-89	17.2	1.46
-0.96				-87	17.6																
-0.80	-103	17.8	1.40																-96	17.2	1.46
-0.64							-100	22.6	1.19												
-0.48				-95	17.6	1.14													-103	14.7	1.70
-0.32	-110	25.4	0.79				-108	17.0	1.77	-86	26.7	1.12	-93	47.5	1.05	-91	15.1	1.66			
-0.16	-115	25.4	0.79	-99	22.0	1.59	-111	22.6	1.77	-91	26.7	1.50				-94	15.1	1.66	-106	19.6	1.53
0.00	-120			-104			-115			-96			-105			-97			-110		
0.16	-124	20.4	1.23	-109	22.0	1.36	-119	22.6	1.77	-102	32.0	1.09				-101	20.1	1.24	-114	19.6	1.28
0.32	-129	25.4	0.86				-123	22.6	1.77	-110	42.7	0.59	-117	47.5	1.58	-104	15.1	1.66			
0.48				-114	22.0	0.91							-130	51.5	1.36				-119	24.5	1.43
0.64							-131	22.6	1.33												
0.80	-141	30.5	0.98							-128	48.1	0.52				-112	20.1	1.24	-127	19.6	1.53
0.96				-127	28.6	0.87							-148	35.6	2.11						
1.12	-153	30.5	0.98				-141	28.3	0.88	-142	37.4	0.80				-118	15.1	1.66			
1.28																			-134	17.2	1.46
1.44				-143	35.2	0.71	-157	45.2	0.55	-162	53.4	0.66	-166	35.6	1.40						
1.60																-124	15.1	1.99	-144	24.5	1.02
1.76																					
1.92																					
2.08													-176	19.8							
2.24																					

	Cell 22 d= 0.90 T= 20.0			Cell 23 d= 0.69 T= 21.0			Cell 24 d= 0.90 T= 20.0			Cell 25 d= 0.85 T= 20.0			Cell 26 d= 1.00 T= 21.0			Cell 27 d= 0.81 T= 21.0			Cell 28 d= 0.95 T= 23.0		
J	E	R	C	E	R	C	E	R	C	E	R	C	E	R	C	E	R	C	E	R	C
-1.28																					
-1.12							-92	17.0	1.47	-80	32.0	1.09				-75	22.9	1.09			
-0.96				-88	21.7	0.69							-79	12.6	1.19				-94	17.9	1.12
-0.80										-92	26.7	1.12				-84	22.9	1.44			
-0.64	-101	17.0	2.06				-98	19.8	1.52				-83	18.8	0.80				-100	20.9	1.20
-0.48				-98	26.0	0.77															
-0.32	-107	22.6	1.77				-105	22.6	1.11	-102	21.4	0.94	-89	18.8	1.06	-93	20.4	1.72	-107	23.9	1.05
-0.16	-111	22.6	1.77	-104	26.0	0.96	-109	17.0	1.47	-106	21.4	0.70	-92	12.6	1.59	-97	25.4	1.57	-111	17.9	1.68
0.00	-115			-110			-112			-110			-94			-102			-114		
0.16	-118	17.0	1.47	-116	26.0	0.77	-116	22.6	1.33	-116	32.0	0.47	-98	25.1	1.39	-107	25.4	1.57	-117	17.9	1.68
0.32	-122	22.6	1.11				-121	28.3	1.24	-124	42.7	0.70	-101	18.8	1.33	-112	25.4	1.18	-120	17.9	1.40
0.48				-120	17.3	1.15															
0.64	-130	22.6	1.55				-131	28.3	1.24				-110	28.3	1.24				-126	17.9	1.28
0.80										-134	26.7	0.94				-126	35.6	0.98			
0.96				-130	21.7	0.92							-118	25.1					-133	20.9	0.96
1.12	-138	22.6	1.77				-139	22.6	1.33	-142	21.4	1.17				-140	35.6				
1.28													-126	25.1					-141	23.9	0.84
1.44	-147	25.4	1.57	-140	21.7	0.69	-149	28.3	1.41	-154	32.0	0.56									
1.60													-133	22.0		-164	61.1		-149	23.9	0.96
1.76																					
1.92				-152	26.0	0.35				-166	32.0					-178	35.6				
2.08																					
2.24				-166	30.3																

Continuation.

	Cell 31 d= 0.80 T= 23.0			Cell 36 d= 1.00 T= 23.0			Cell 37 d= 1.00 T= 22.0			Cell 38 d= .90 T= 24.0			Cell 39 d= 0.95 T= 23.0			Cell 40 d= 1.00 T= 23.0			Cell 41 d= 1.00 T= 22.0		
J	E	R	C	E	R	C	E	R	C	E	R	C	E	R	C	E	R	C	E	R	C
-1.28																					
-1.12	-87	30.2	1.33																		
-0.96										-84	31.4	1.43	-61	32.8	1.37						
-0.80	-99	27.6	1.45	-96	20.7	2.41										-101	10.4	1.74	-85	17.3	1.45
-0.64				-102	24.2	2.07				-94	25.1	0.99	-72	29.8	1.34	-104	13.8	2.17	-90	17.3	1.16
-0.48																					
-0.32	-110	25.1	1.59	-109	20.7	2.89	-98	37.7	0.93	-102	18.8	1.59	-82	29.8	1.51	-108	13.8	1.81	-95	13.8	1.45
-0.16	-115	25.1	1.39	-112	27.6	2.17	-104	31.4	1.59	-105	18.8	1.33	-87	23.9	1.47	-110	13.8	1.81	-97	20.7	1.21
0.00	-120			-116			-109			-108			-91			-112			-100		
0.16	-127	35.2	1.28	-120	27.6	1.81	-115	37.7	1.33	-113	31.4	1.27	-96	29.8	1.34	-114	13.8	2.53	-102	13.8	1.45
0.32	-133	30.2	1.49	-124	27.6	1.81	-120	31.4	1.43	-116	18.8	1.59	-102	35.8	1.26	-117	20.7	1.69	-105	20.7	0.96
0.48																					
0.64				-131	24.2	2.07	-130	31.4	0.83	-124	25.1	1.19	-112	29.8	1.27	-120	10.4	1.93	-110	17.3	1.16
0.80	-149	40.2	1.12	-136	17.3	2.89										-124	13.8	1.81	-115	17.3	1.45
0.96							-140	31.4	0.80	-131	22.0	1.59	-121	26.9	1.49						
1.12	-163	35.2	1.28	-142	20.7	2.41										-128	13.8	1.81	-120	17.3	1.45
1.28							-150	31.4	0.89	-136	15.7	1.91	-133	35.8	0.98						
1.44				-148	20.7	2.17										-133	17.3	1.45	-126	20.7	1.30
1.60	-179	40.2					-162	37.7	0.66	-142	18.8	1.59	-142	26.9	1.12						
1.76																					
1.92	-191	30.2																			
2.08																					
2.24																					

	Cell 42 d= 1.00 T= 23.0			Cell 44 d= 0.95 T= 22.0			Cell 45 d= 0.75 T= 22.0			Cell 47 d= 1.00 T= 23.0		
J	E	R	C	E	R	C	E	R	C	E	R	C
-1.28							-59	33.0	1.12			
-1.12												
-0.96	-96	15.7	1.59	-90	14.9	1.68						
-0.80							-73	25.9	1.35			
-0.64	-101	15.7	1.59	-95	29.8	1.51				-82	22.0	1.05
-0.48							-84	23.6	1.27			
-0.32	-106	18.8	1.86	-105	29.8	1.34				-89	12.6	1.99
-0.16	-109	12.6	2.39	-110	23.9	1.55	-89	33.0	1.21	-91	18.8	1.06
0.00	-111			-114			-96			-94		
0.16	-114	18.8	1.33	-118	23.9	1.47	-104	37.7	1.19	-97	18.8	1.59
0.32	-116	12.6	1.75	-122	23.9	1.05				-101	25.1	1.39
0.48							-111	33.0	1.21			
0.64	-121	15.7	1.27	-127	14.9	1.68				-109	25.1	0.99
0.80							-130	44.8	1.01			
0.96	-126	15.7	1.27	-137	29.8	1.17				-124	47.1	0.74
1.12												
1.28	-132	18.8	1.33	-148	32.8	0.76	-146	37.7	0.93	-156	37.7	1.19
1.44												
1.60	-138	18.8	1.22	-159	32.8	1.22				-150	44.0	1.02
1.76							-158	28.3	1.06			
1.92												
2.08												
2.24												

E	s.e.	R	s.e.	C	s.e.	
-74.0	15.0	25.1	7.9	1.29	0.17	(2)
-87.1	3.1	23.9	2.2	1.23	0.06	(7)
-85.3	3.6	23.3	2.1	1.20	0.08	(15)
-93.6	3.3	21.2	1.7	1.50	0.11	(10)
-96.2	3.0	23.4	1.4	1.30	0.08	(23)
-97.4	3.9	20.8	2.0	1.18	0.16	(5)
-102.0	2.1	25.3	1.7	1.37	0.08	(31)
-105.9	1.9	23.9	1.1	1.38	0.06	(35)
-110.7	1.9					(39)
-114.8	1.9	27.0	1.4	1.30	0.06	(35)
-120.2	2.2	30.4	2.0	1.20	0.06	(32)
-119.8	2.8	28.4	5.1	1.16	0.09	(6)
-129.2	2.8	27.8	2.1	1.18	0.07	(26)
-131.0	3.4	28.1	3.4	1.30	0.17	(12)
-137.2	3.5	30.5	2.7	1.09	0.08	(21)
-142.2	3.9	26.2	2.7	1.42	0.12	(14)
-147.7	4.0	32.0	2.3	0.99	0.07	(20)
-151.4	4.6	33.6	4.2	1.14	0.14	(13)
-156.5	4.2	33.7	2.9	0.98	0.08	(21)
-188.0	30.0	49.5	21.2	1.03	0.04	(2)
-172.8	6.5	29.8	1.9	0.77	0.42	(5)
-176.0		19.8		0.00		(1)
-166.0		30.3		0.00		(1)

Current Density rounding error= 0.080 pH(o)= 6.0
J= Current Density (μA/cm²) , in the form of step pulse of .4 s duration
E= Membrane Potential (mv)
R= Membrane Resistance (kΩ×cm²)
C= Membrane Capacitance (μf/cm²)

	Cell 36 d= 1.00 T= 23.0			Cell 38 d= 0.90 T= 24.0			Cell 40 d= 1.00 T= 23.0			Cell 48 d= 1.00 T= 23.0			Cell 49 d= 0.90 T= 23.0			Cell 51 d= 0.87 T= 23.0			Cell 53 d= 0.98 T= 21.0		
J	E	R	C	E	R	C	E	R	C	E	R	C	E	R	C	E	R	C	E	R	C
-1.12													-91	28.3	1.06	-101	30.1	1.00			
-0.96	-109	31.4	1.59				-124	9.4	3.18	-79	44.0	1.36									
-0.80																-112	16.4	0.79			
-0.64	-119	31.4	1.27	-95	48.1	1.46	-127	15.7	2.23	-93	56.5	0.71	-101	28.3	1.06				-103	36.9	0.84
-0.32	-129	31.4	1.11	-112	33.9	1.92	-132	12.6	3.18	-111	44.0	1.14	-111	28.3	0.85	-118	16.4	1.22	-115	18.5	1.68
-0.16	-134	31.4	1.59	-118	50.9	1.57	-134	18.8	2.39	-118	50.3	0.80	-116	28.3	0.88	-121	16.4	1.46	-118	18.5	1.68
0.00	-139			-127			-137			-126			-121			-124			-121		
0.16	-146	44.0	1.14	-136	50.9	1.08	-139	12.6	3.58	-135	56.5	1.15	-126	28.3	1.06	-128	21.9	1.10	-126	30.8	1.01
0.32	-151	31.4	1.43	-142	33.9	1.62	-141	12.6	1.99	-143	50.3	0.99	-131	28.3	0.88	-131	16.4	1.46	-131	30.8	1.04
0.64	-161	31.4	1.27	-157	42.4	1.18	-145	12.6	2.39	-161	56.5	0.88	-145	39.6					-145	43.1	0.77
0.80																-140	24.6	1.06			
0.96	-171	31.4	1.43				-150	15.7	1.59	-183	69.1	0.72							-161	49.3	0.91
1.12				-169	33.9	1.47							-161	45.2		-154	38.3	0.91			
1.28	-181	31.4	1.34				-156	18.8	1.59	-195	37.7								-181	61.6	0.73
1.44				-189	56.5	0.88							-167	17.0		-161	19.1	1.57			
1.60	-191	31.4	1.11				-161	15.7	1.27										-199	55.4	0.78
1.76				-199	28.3	1.77							-175	22.6		-170	24.6	0.81			
1.92																					

	Cell 55 d= 0.80 T= 21.0			Cell 58 d= 0.95 T= 22.0								
J	E	R	C	E	R	C	E	s.e.	R	s.e.	C	s.e.	
-1.12	-87	26.7	1.50				-93.0	4.2	28.3	1.0	1.19	0.16	(3)
-0.96							-104.0	13.2	28.3	10.1	2.05	0.57	(3)
-0.80	-97	48.1	1.04				-104.5	7.5	32.2	15.8	0.92	0.12	(2)
-0.64				-93	26.9	0.74	-104.4	5.1	34.8	5.2	1.19	0.20	(7)
-0.32	-115	32.0	2.03	-102	17.9	1.34	-116.1	3.1	26.1	3.4	1.61	0.24	(9)
-0.16	-121	32.0	1.56	-105	29.8	1.04	-120.6	3.0	30.7	4.2	1.44	0.16	(9)
0.00	-127			-110			-125.8	2.9					(9)
0.16	-136	48.1	1.25	-114	23.9	1.26	-131.8	3.1	35.2	5.0	1.40	0.27	(9)
0.32	-143	37.4	1.87	-118	23.9	1.47	-136.8	3.3	29.4	3.7	1.42	0.13	(9)
0.64				-126	23.9	1.17	-148.6	4.7	35.6	5.4	1.28	0.24	(7)
0.80	-157	37.4	1.20				-148.5	8.5	31.0	6.4	1.13	0.07	(2)
0.96				-144	53.7	0.74	-161.8	7.0	43.8	9.3	1.08	0.18	(5)
1.12	-167	26.7	1.31				-162.7	3.4	36.0	3.9	1.23	0.17	(4)
1.28				-154	29.8	1.34	-173.4	7.9	35.9	7.1	1.25	0.18	(5)
1.44	-177	26.7	1.42				-173.5	6.1	29.8	9.1	1.29	0.21	(4)
1.60				-168	41.8	1.20	-179.7	9.1	36.1	8.4	1.09	0.11	(4)
1.76							-181.3	9.0	25.2	1.7	1.29	0.48	(3)
1.92	-185	21.4	1.17				-185.0		21.4		1.17		(1)

62 LINES PRINTED

Current Density rounding error= 0.080 pH(o)= 7.0
J= Current Density ($\mu f/cm^2$) , in the form of a step pulse of .4 s duration
E= Membrane Potential (mv)
R= Membrane Resistance ($k\Omega X cm^2$)
C= Membrane Capacitance ($\mu f/cm^2$)

	Cell 38 d= 0.90 T= 24.0			Cell 40 d= 1.00 T= 23.0			Cell 42 d= 1.00 T= 23.0			Cell 47 d= 0.80 T= 23.0			Cell 48 d= 1.00 T= 23.0			Cell 49 d= 0.90 T= 23.0			Cell 53 d= 0.98 T= 21.0		
J	E	R	C	E	R	C	E	R	C	E	R	C	E	R	C	E	R	C	E	R	C
-1.12																-89	17.0	1.24			
-0.96				-114	9.4	2.12	-106	6.3	3.18												
-0.80										-76	25.1	1.27									
-0.64	-104	22.6	1.33	-117	12.6	1.59	-108	15.7	1.72				-79	66.0	0.91	-95	19.8	1.01	-96	58.5	0.43
-0.32	-112	22.6	1.77	-121	12.6	1.59	-113	12.6	1.99	-86	10.1	2.98	-100	56.5	1.15	-102	11.3	1.77	-115	18.5	1.41
-0.16	-115	22.6	1.99	-123	12.6	2.39	-115	12.6	2.19	-88	25.1	1.91	-109	69.1	1.09	-104	22.6	0.88	-118	30.8	0.78
0.00	-120			-125			-117			-93			-120			-108			-123		
0.16	-125	28.3	1.77	-127	12.6	2.39	-120	18.8	1.59	-98	25.1	1.39	-130	62.8	0.91	-111	17.0	1.18	-128	30.8	0.81
0.32	-130	28.3	1.59	-129	12.6	1.99	-122	12.6	2.39	-101	15.1	1.99	-139	56.5	1.24	-114	17.0	1.06	-133	30.8	0.78
0.64	-140	28.3	1.38	-132	9.4	1.59	-126	12.6	2.39				-167	88.0	0.83	-123	25.4	0.98	-147	43.1	0.70
0.80										-118	42.7	1.01									
0.96				-135	9.4	1.59	-130	12.6	1.75				-187	62.8	0.95				-169	67.7	0.49
1.12	-152	33.9	1.62							-137	47.8	1.05				-133	28.3	0.85			
1.28				-139	12.6	1.43	-133	9.4	1.59				-197	31.4	1.53				-193	73.9	0.54
1.44	-163	31.1	1.77													-142	25.4	0.75			
1.60				-142	9.4	2.02	-137	12.6	1.83	-149	30.2	1.66							-213	61.6	0.57
1.76	-175	33.9	1.68													-153	31.1	0.80			
1.92										-169	50.3	1.03									

	Cell 54 d= 0.80 T= 22.0			Cell 55 d= 0.80 T= 21.0			Cell 57 d= 0.75 T= 22.0		
J	E	R	C	E	R	C	E	R	C
-1.12				-92	25.1	2.86			
-0.96									
-0.80				-102	27.6	2.68	-95	35.2	0.99
-0.64									
-0.32	-107	20.1	1.64	-113	20.1	1.99	-109	15.1	1.66
-0.16	-111	30.2	1.09	-117	25.1	1.39	-112	25.1	1.39
0.00	-117			-122			-117		
0.16	-122	25.1	0.92	-127	25.1	2.39	-122	25.1	1.39
0.32	-128	30.2	1.03	-132	25.1	1.99	-127	25.1	0.95
0.64									
0.80	-157	72.9	0.75	-142	25.1	2.39	-159	80.4	0.56
0.96									
1.12	-197	100.5	0.75	-162	50.3	1.79	-219	150.8	0.56
1.28									
1.44									
1.60	-229	80.4	0.99	-172	25.1	3.18			
1.76									
1.92	-255	65.3	1.24	-186	35.2	2.27			

E	s.e.	R	s.e.	C	s.e.	
-90.5	1.5	21.0	4.1	2.05	0.81	(2)
-110.0	4.0	7.9	1.6	2.65	0.53	(2)
-91.0	7.8	29.3	3.0	1.65	0.52	(3)
-99.8	5.3	32.5	9.5	1.16	0.20	(6)
-107.8	3.1	19.9	4.3	1.79	0.15	(10)
-111.3	3.1	27.6	5.0	1.51	0.18	(10)
-116.2	3.0					(10)
-121.0	3.1	27.1	4.3	1.47	0.18	(10)
-125.5	3.4	25.3	4.1	1.50	0.18	(10)
-139.2	6.6	34.5	11.8	1.31	0.26	(6)
-144.0	9.5	55.3	12.9	1.18	0.41	(4)
-155.2	13.7	38.1	15.7	1.20	0.29	(4)
-166.7	14.0	68.6	19.5	1.10	0.20	(6)
-165.5	17.1	31.8	14.8	1.27	0.25	(4)
-152.5	10.5	28.3	2.8	1.26	0.51	(2)
-173.7	15.9	36.5	11.6	1.71	0.37	(6)
-164.0	11.0	32.5	1.4	1.24	0.44	(2)
-203.3	26.3	50.3	8.7	1.52	0.38	(3)

W#9198

62 LINES PRINTED

Current Density rounding error= 0.080 pH(o)= 8.0
J= Current Density ($\mu A/cm^2$) , in the form of a step pulse of .4 s duration
E= Membrane Potential (mv)
R= Membrane Resistance ($k\Omega.cm^2$)
C= Membrane Capacitance ($\mu f/cm^2$)

	Cell 38 d= 0.95 T= 24.0			Cell 40 d= 1.00 T= 23.0			Cell 42 d= 1.00 T= 23.0			Cell 46 d= 0.80 T= 23.0			Cell 49 d= 0.90 T= 23.0			Cell 53 d= 0.98 T= 21.0			Cell 54 d= 0.80 T= 22.0		
J	E	R	C	E	R	C	E	R	C	E	R	C	E	R	C	E	R	C	E	R	C
-1.12										-62	17.6	0.85	-98	2.8	3.18				-95	5.0	1.79
-0.96	-90	11.9	1.51				-88	9.4	2.12							-87	12.3	1.46			
-0.80										-69	7.5	1.59							-97	7.5	1.46
-0.64	-94	14.9	1.27				-91	9.4	2.12				-99	8.5	1.06	-91	12.3	0.65			
-0.48																					
-0.32	-99	17.9	1.06	-105	31.4	1.66	-94	6.3	3.18	-72	10.1	1.69	-102	5.7	1.77	-95	6.2	0.97	-100	10.1	0.99
-0.16	-102	11.9	2.18	-110	31.4	1.59	-95	6.3	3.18	-74	10.1	1.99	-103	5.7	1.77	-96	6.2	1.30	-102	10.1	1.09
0.00	-104			-115			-96			-76			-104			-97			-104		
0.16	-108	23.9	1.47	-120	31.4	1.43	-97	6.3	2.86	-78	10.1	1.49	-105	5.7	1.77	-99	12.3	1.46	-106	10.1	1.49
0.32	-111	17.9	1.79	-125	31.4	1.62	-99	12.6	1.59	-80	10.1	1.19	-106	5.7	1.77	-100	6.2	1.62	-108	10.1	1.29
0.48																					
0.64	-116	14.9	1.14	-135	31.4	1.59	-102	9.4	1.59				-109	8.5	1.89	-104	12.3	0.89			
0.80										-85	12.6	1.19							-112	10.1	1.19
0.96	-123	20.9	1.68	-149	44.0	0.91	-104	6.3	3.18							-112	24.6	0.49			
1.12										-96	27.6	0.90	-112	8.5					-115	7.5	1.46
1.28	-131	23.9	1.47	-165	50.3	0.90	-106	6.3	2.23							-117	15.4	0.78			
1.44													-115	8.5							
1.60	-139	23.9	1.42	-181	50.3	0.80	-109	9.4	1.59	-106	25.1	1.47				-122	15.4	0.84	-119	10.1	1.09
1.76													-118	8.5							
1.92										-121	37.7	1.19							-124	12.6	1.03
2.24																					

	Cell 55 d= 0.80 T= 21.0			Cell 56 d= 0.80 T= 22.0			Cell 57 d= 0.75 T= 22.0			Cell 57 d= 0.95 T= 22.0		
J	E	R	C	E	R	C	E	R	C	E	R	C
-1.12	-74	12.6	1.19	-50	7.5	1.46						
-0.96							-100	26.4	1.06	-96	9.0	1.23
-0.80	-79	10.1	1.29	-53	7.5	1.59						
-0.64										-99	9.0	1.23
-0.48							-112	13.2	1.74			
-0.32	-83	5.0	2.19	-56	10.1	1.19				-102	6.0	1.34
-0.16	-84	5.0	1.79	-58	10.1	1.19	-115	22.0	1.14	-103	6.0	1.34
0.00	-85			-60			-120			-104		
0.16	-87	10.1	1.79	-62	10.1	1.19	-125	22.0	1.09	-105	6.0	1.34
0.32	-89	10.1	1.99	-64	10.1	1.19				-107	11.9	0.67
0.48							-130	22.0	1.14			
0.64										-110	9.0	1.01
0.80	-93	10.1	0.99	-68	10.1	1.29						
0.96							-150	44.0	0.91	-114	11.9	0.84
1.12	-98	12.6	1.19	-76	20.1	0.94						
1.28										-116	6.0	2.35
1.44							-180	66.0	0.91			
1.60	-102	10.1	1.99	-80	10.1	2.39				-119	9.0	1.23
1.76							-210	66.0	0.91			
1.92	-107	12.6	1.99	-85	12.6	1.59						
2.24							-230	44.0				

E	s.e.	R	s.e.	C	s.e.	
-75.8	9.3	9.1	2.7	1.70	0.40	(5)
-92.2	2.5	13.8	3.2	1.48	0.18	(5)
-74.5	9.2	8.2	0.6	1.48	0.07	(4)
-94.8	1.8	10.8	1.2	1.27	0.24	(5)
-112.0		13.2		1.74		(1)
-90.8	5.0	10.9	2.6	1.61	0.22	(10)
-94.7	5.0	11.3	2.5	1.69	0.19	(11)
-96.8	5.2					(11)
-99.3	5.5	13.4	2.6	1.58	0.14	(11)
-98.9	5.5	12.6	2.4	1.47	0.12	(10)
-130.0		22.0		1.14		(1)
-112.7	4.9	14.3	3.6	1.35	0.16	(6)
-89.5	9.1	10.7	0.6	1.17	0.06	(4)
-125.3	8.0	25.3	6.5	1.33	0.40	(6)
-99.4	6.9	15.3	3.8	1.13	0.13	(5)
-127.0	10.3	20.4	8.2	1.54	0.33	(5)
-147.5	32.5	37.2	28.7	0.91		(2)
-119.7	9.4	18.1	4.5	1.43	0.17	(9)
-164.0	46.0	37.2	28.7	0.91		(2)
-109.2	8.9	18.8	6.3	1.45	0.21	(4)
-230.0		44.0		0.00		(1)

pH(o) 4
T time after stimulation (s)
E Memorane Potential (mv)
R Membrane Resistance(kΩ.cm²)

T(s)	Cell 39 d= 0.95 E	R	Cell 41 d= 1.00 E	R	Cell 42 d= 1.00 E	R	Cell 43 d= 0.90 E	R	Cell 44 d= 0.95 E	R	Cell 46 d= 0.80 E	R
0.0	-70.0	2.01	- 75.0	11.78	- 107.0	23.24	- 82.0		- 98.0	14.74	-60.0	7.96
0.2	-24.0	6.70	- 73.0		- 85.0		- 22.0	9.90	- 50.0		-40.0	9.15
0.4	-20.0	6.70	- 71.0	12.73	- 67.0	12.10	- 10.0	3.89	- 36.0	2.68	-40.0	
0.6	-20.0	4.69	- 41.0		- 33.0		- 12.0		- 32.0		-40.0	9.55
0.8	-26.0		- 35.0	3.82	- 29.0	0.64	- 22.0	3.54	- 35.0	3.02	-48.0	
1.0			- 27.0		- 41.0		- 26.0		- 33.0		-50.0	11.94
1.2			- 26.0	2.86	- 45.0	2.55	- 36.0	4.95	- 38.0	1.34	-54.0	
1.4			- 25.0		- 55.0		- 42.0		- 44.0		-54.0	13.53
1.6			- 31.0	2.55	- 57.0	1.27	- 48.0	5.66	- 48.0	0.67	-56.0	

T(s)	Cell 51 d= 0.87 E	R	Cell 52 d= 0.90 E	R	E	s.e.	R	s.e.
0.0	- 62.0	16.46	- 60.0		-76.7	6.3	12.70	2.98
0.2	- 62.0		- 30.0		-48.2	8.3	8.59	
0.4	- 62.0	7.32	- 28.0	12.73	-41.7	8.0	8.31	1.61
0.6	- 52.0		- 10.0	5.31	-30.0	5.2	6.52	
0.8	- 48.0	6.59	- 10.0	4.95	-31.6	4.5	3.76	0.81
1.0	- 38.0		- 10.0		-32.1	4.8	11.94	
1.2	- 36.0	5.12	- 12.0	5.66	-35.3	5.1	3.75	0.71
1.4	- 36.0		- 14.0	6.37	-38.6	5.7	9.95	
1.6	- 40.0	4.02	- 18.0	7.07	-42.6	5.3	3.54	1.03

W#9218

42 LINES PRINTED

pH(o) 5
T time after stimulation (s)
E Memorane Potential (mv)
R Membrane Resistance (kΩ.cm^2)

	Cell 13 d= 0.07		Cell 15 d= 0.81		Cell 17 d= 0.90		Cell 18 d= 0.90		Cell 19 d= 0.63		Cell 20 d= 0.80	
T(s)	E	R	E	R	E	R	E	R	E	R	E	R
0.0	-116.0	127.32	-120.0	5.89	-115.0		-115.0	8.84	-105.0	6.57	- 97.0	
0.2	- 32.0	63.66	- 20.0		- 35.0	6.37	- 31.0		- 25.0	10.11	- 27.0	7.96
0.4	- 24.0	9.09	- 20.0	2.36	- 35.0		- 5.0		- 13.0		- 13.0	3.18
0.6	- 32.0		- 22.0	0.79	- 37.0	3.54	- 5.0	3.54	- 5.0	3.03	- 11.0	1.59
0.8	- 40.0		- 29.0	1.18	- 45.0	2.83	- 5.0	2.12	- 6.0	2.53	- 13.0	1.99
1.0	- 54.0		- 30.0		- 55.0		- 7.0		- 11.0		- 13.0	
1.2			- 38.0	2.36	- 65.0	4.24	- 13.0	0.71	- 13.0	4.04		
1.4			- 40.0	1.18	- 75.0	4.24	- 21.0		- 15.0	3.03		
1.6			- 36.0		- 85.0		- 31.0		- 23.0			

	Cell 22 d= 0.81		Cell 23 d= 0.69		Cell 24 d= 0.90		Cell 25 d= 0.85		Cell 27 d= 0.81	
T(s)	E	R	E	R	E	R	E	R	E	R
0.0	-115.0		-130.0		- 112.0	22.64	- 110.0	32.21	- 112.0	
0.2	- 40.0	12.58	- 2.0	3.69	- 106.0	16.27	- 98.0		- 8.0	2.36
0.4	- 12.0	2.36	- 2.0	3.69	- 82.0		- 18.0	1.50	- 18.0	4.72
0.6	- 16.0	3.93	- 18.0	3.69	- 72.0	10.61	- 17.0	1.12	- 26.0	7.07
0.8	- 29.0	4.32	- 36.0		- 48.0	5.66	- 20.0		- 42.0	10.22
1.0	- 48.0		- 46.0		- 40.0	2.83	- 42.0	0.75	- 46.0	
1.2					- 40.0		- 48.0		- 52.0	11.79
1.4					- 47.0	3.54	- 64.0	1.50	- 62.0	7.86
1.6					- 48.0	2.12	- 68.0		- 68.0	

	Cell 28 d= 0.95		Cell 31 d= 0.80		Cell 36 d= 1.00		Cell 38 d= 0.90					
T(s)	E	R	E	R	E	R	E	R	E	s.e.	R	s.e.
0.0	-114.0		-120.0		- 114.0		-120.0		- 114.3	1.9	33.91	19.16
0.2	- 24.0	2.01	0.0	7.96	- 20.0		- 42.0		- 34.0	7.8	13.30	5.77
0.4	- 14.0	3.35	+2.0	5.17	- 12.0	5.73	- 40.0	3.54	- 20.4	5.2	4.06	0.63
0.6	- 14.0	3.35	- 9.0	5.17	- 4.0		- 42.0		- 22.0	4.7	3.95	0.78
0.8	- 15.0	2.35	- 18.0	3.98	- 5.0	2.55	- 45.0	3.18	- 26.4	4.1	3.57	0.70
1.0	- 18.0		- 26.0		- 6.0		- 52.0		- 32.9	4.7	1.79	
1.2					- 16.0	2.55	- 56.0	4.24	- 37.9	6.5	4.28	1.34
1.4					- 18.0		- 60.0		- 44.7	7.5	3.56	0.99
1.6					- 26.0	3.50	- 62.0	3.54	- 49.7	7.3	3.05	

pH (o) 6
T time after stimulation (s)
E Membrane Potential (mv)
R Membrane Resistance ($k\Omega.cm^2$)

	Cell 36 d= 1.00		Cell 38 d= 0.90		Cell 40 d= 1.00		Cell 48 d= 1.00		Cell 51 d= 0.87		Cell 53 d= 0.98	
T(s)	E	R	E	R	E	R	E	R	E	R	E	R
0.0	−139.0		−120.0		−137.0		−126.0		−124.0		−121.0	
0.2	− 37.0		− 44.0		− 31.0		− 8.0		− 10.0		− 23.0	
0.4	− 21.0	3.82	− 43.0	4.60	− 33.0	2.55	− 1.0	3.50	− 11.0	1.46	− 24.0	0.97
0.6	− 20.0		− 42.0		− 53.0		− 6.0		− 20.0		− 37.0	
0.8	− 21.0	2.55	− 44.0	2.83	− 59.0	2.55	− 30.0	1.91	− 28.0	1.46	− 43.0	0.65
1.0	− 29.0		− 54.0		− 67.0		− 42.0		− 36.0		− 57.0	
1.2	− 35.0	2.23	− 56.0	3.89	− 79.0	3.82	− 60.0	3.82	− 44.0	3.66	− 65.0	0.65
1.4	− 40.0		− 60.0		− 86.0		− 65.0		− 48.0		− 75.0	
1.6	− 47.0	2.23	− 62.0	3.54	− 97.0	3.82	− 88.0	6.37	− 56.0	2.93	− 89.0	0.65

	Cell 55 d= 0.80		Cell 57 d= 0.75		Cell 58 d= 0.95					
T(s)	E	R	E	R	E	R	E	s.e.	R	s.e.
0.0	−127.0	6.76	−120.0	4.24	−110.0		−124.9	3.0	5.50	
0.2	− 55.0		− 60.0		− 10.0		− 30.9	6.6		
0.4	− 53.0	13.53	− 74.0	12.73	− 20.0	4.02	− 31.1	7.5	5.24	1.54
0.6	− 55.0		− 84.0		− 30.0		− 38.6	7.8		
0.8	− 57.0	13.53	−100.0	12.73	− 50.0	6.03	− 48.0	7.8	4.92	1.63
1.0	− 63.0		−100.0		− 54.0		− 55.8	6.9		
1.2	− 71.0	17.51	−120.0	25.46	− 66.0	5.36	− 66.2	8.1	7.38	2.78
1.4	− 69.0		−124.0		− 76.0		− 71.4	8.1		
1.6	− 83.0	19.89	−129.0	29.28	− 86.0	6.03	− 81.9	8.2	8.30	3.23

pH(o) 7
T time after stimulation (s)
E Membrane Potential (mv)
R Membrane Resistance ($k\Omega.cm^2$)

	Cell 38 d= 0.90		Cell 40 d= 1.00		Cell 42 d= 1.00		Cell 47 d= 0.80		Cell 48 d= 1.00		Cell 53 d= 0.98	
T(s)	E	R	E	R	E	R	E	R	E	R	E	R
0.0	−120.0		−125.0		−117.0		− 93.0	1.19	−120.0		−123.0	
0.2	− 60.0		− 55.0		− 55.0		− 23.0	6.37	− 2.0		− 31.0	
0.4	− 60.0	4.95	− 19.0	4.46	− 51.0	4.46	− 21.0	3.98	− 5.0	1.59	− 27.0	1.30
0.6	− 55.0		− 11.0		− 45.0		− 23.0		− 9.0		− 43.0	
0.8	− 57.0	3.18	− 10.0	1.59	− 47.0	1.27	− 23.0	7.96	− 44.0	1.91	− 53.0	0.65
1.0	− 59.0		− 15.0		− 56.0		− 53.0		− 50.0		− 67.0	
1.2	− 64.0	3.54			− 62.0	1.59	−81.0	7.16	− 66.0	3.50	− 73.0	0.65
1.4	− 66.0				− 69.0		− 93.0		− 70.0		− 85.0	
1.6	− 70.0	3.54			− 73.0	6.05	−102.0	15.52	− 80.0	5.73	− 93.0	0.65

	Cell 54 d= 0.80		Cell 55 d= 0.80		Cell 57 d= 0.75					
T(s)	E	R	E	R	E	R	E	s.e.	R	s.e.
0.0	−117.0		−110.0	11.94	−120.0	8.49	−116.1	3.2	7.21	
0.2	− 23.0		− 64.0		− 50.0		− 40.3	7.1	6.37	
0.4	− 23.0	2.39	− 64.0	13.53	− 76.0	12.73	− 38.4	8.2	5.49	1.51
0.6	− 33.0		− 62.0		− 82.0		− 40.3	8.0		
0.8	− 43.0	1.59	− 66.0	11.94	− 102.0	9.34	− 49.4	8.7	4.38	1.40
1.0	− 53.0		− 66.0		− 114.0		− 59.2	8.5		
1.2	− 63.0	2.39	− 72.0	12.73	− 134.0		− 76.9	8.5	4.51	1.58
1.4	− 71.0		− 74.0				− 75.4	3.7		
1.6	− 79.0	2.39	− 80.0	15.92			− 82.4	4.3	7.11	2.33

pH(o) 8
T time after stimulation (s)
E Membrane Potential (mv)
R Membrane Resistance ($k\Omega.cm^2$)

	Cell 38 d= 0.90		Cell 40 d= 1.00		Cell 42 d= 1.00		Cell 47 d= 0.80		Cell 53 d= 0.98		Cell 54 d= 0.80	
T(s)	E	R	E	R	E	R	E	R	E	R	E	R
0.0	-104.0		-115.0		-96.0		-76.0		-97.0		-104.0	
0.2	- 56.0		- 51.0	3.82	-52.0		- 0.0		-61.0		- 34.0	
0.4	- 54.0	4.95	- 45.0	1.91	-44.0	3.82	+2.0	4.77	-43.0	6.50	- 24.0	
0.6	- 48.0		- 51.0		-40.0		0.0		-31.0		- 34.0	
0.8	- 50.0	3.54	- 63.0	1.91	-46.0	1.27	-10.0	3.18	-35.0	1.95	- 44.0	0.80
1.0	- 50.0		- 69.0		-51.0		-14.0		-43.0		- 54.0	
1.2	- 54.0	3.54			-64.0	2.55	-22.0	0.80	-47.0	3.25	- 64.0	0.80
1.4	- 55.0				-68.0		-25.0		-51.0		- 66.0	
1.6	- 54.0	3.54			-74.0	1.91	-28.0	1.59	-53.0	3.25	- 72.0	2.39

	Cell 56 d= 0.80		Cell 57 d= 0.75		Cell 58 d= 0.95					
T(s)	E	R	E	R	E	R	E	s.e.	R	s.e.
0.0	- 60.0		-120.0		-104.0		- 97.3	6.2		
0.2	+6.0		- 48.0		- 38.0		- 37.1	8.1	3.82	
0.4	+6.0	7.56	- 42.0	5.94	- 24.0	0.67	- 29.8	7.2	4.52	0.82
0.6	+10.0		- 46.0		- 32.0		- 30.2	7.1		
0.8	- 16.0	6.37	- 60.0	4.24	- 40.0	1.34	- 40.4	6.0	2.73	0.59
1.0	- 20.0		- 70.0		- 50.0		- 46.8	6.4		
1.2	- 40.0	7.96	- 84.0	4.24	- 60.0	2.01	- 54.4	6.6	3.14	0.82
1.4	- 40.0		-102.0		- 74.0		- 60.1	8.2		
1.6	- 50.0	11.94	-116.0	6.79	- 82.0	2.68	- 66.1	9.3	4.26	1.24

APW pH(o) 5.0

Cell	d	T	E(mv)	pH(i)
60.0	0.83	22.5	-115	5.07
61.0	0.80	23.0	-95	4.86
62.0	0.80	23.0	-90	4.72
63.0	0.90	24.0	-90	5.01
64.0	0.90	23.0	-95	4.63
65.0	0.90	23.5	-90	4.87
66.0	0.80	23.0	-96	5.04
67.0	0.80	23.0	-111	4.65
68.0	0.80	2.2	-90	5.23
69.0	0.90	22.0	-90	4.51
70.0	0.80	22.0	-75	5.22

APW +DNP pH(o) 5.0

E(mv)	pH(i)
-36.0	5.54
-26.0	5.62
-75.0	5.28
-70.0	5.35
-50.0	5.16
-56.0	5.81

A.C. Frequency (Hz)

	1	2	5	8	10	20	50	80	100
60.0	0.141	0.152	0.287	0.446	0.427	0.947	1.110	0.841	1.485
61.0	0.151	0.183	0.220	0.389	0.407	0.526	0.575	1.120	1.434
62.0	0.088	0.147	0.383	0.451	0.332	0.796	1.278	1.468	1.515
63.0	0.070	0.134	0.368	0.535	0.560	0.842	1.210	1.426	1.493
64.0	0.093	0.170	0.376	0.595	0.533	0.906	0.968	1.160	1.422
65.0	0.132	0.195	0.446	0.666	0.694	1.025	1.259	1.413	1.205
66.0	0.120	0.365	0.873	0.941	1.057	1.099	1.073	1.245	1.407
67.0	0.273	0.477	0.821	0.955	1.092	1.168	1.275	1.482	1.158
68.0	0.105	0.232	0.493	0.595	0.718	1.155	1.081	1.156	1.456
69.0	0.104	0.176	0.417	0.576	0.659	0.991	1.133	1.312	1.430
70.0	0.061	0.184	0.287	0.453	0.531	0.875	1.261	1.268	1.501

A.C. Frequency (Hz)

10

Phase Angle (Rad)

0.923
1.000
1.169
0.683
1.160
0.644

Membrane Resistance (kΩ.cm²)

60.0	11.5	9.5	9.8	10.1	8.3	6.1	8.1	4.7	19.9
61.0	10.8	9.7	9.8	9.8	9.1	8.2	7.3	7.2	17.3
62.0	16.2	14.0	14.1	13.8	11.6	11.0	18.0	29.4	36.8
63.0	18.7	17.9	16.8	16.3	15.0	14.9	13.8	20.6	26.4
64.0	14.7	14.0	13.3	12.5	11.9	12.0	5.8	4.7	9.7
65.0	20.6	19.1	16.5	17.8	15.3	16.6	14.8	16.1	6.6
66.0	31.7	33.5	34.5	32.0	29.7	22.1	10.9	9.3	14.5
67.0	49.0	38.9	34.3	29.7	27.3	20.0	12.4	26.6	5.1
68.0	18.3	17.5	16.9	17.3	16.5	18.3	11.4	6.4	20.7
69.0	15.2	14.7	14.6	14.8	13.3	14.1	9.4	9.2	11.3
70.0	15.4	11.3	15.1	14.0	14.8	13.7	17.3	11.6	37.3

22.4
34.9
35.4
13.2
37.7
17.7

Membrane Capacitance (μf/cm²)

60.0	1.971	1.283	0.957	0.941	0.878	1.802	0.789	0.472	0.929
61.0	1.949	1.511	0.724	0.828	0.757	0.565	0.282	0.570	0.669
62.0	0.869	0.841	0.912	0.698	0.471	0.758	0.588	0.659	0.778
63.0	0.594	0.599	0.729	0.726	0.564	0.600	0.611	0.654	0.771
64.0	1.007	0.974	0.941	1.075	0.791	0.848	0.795	0.967	1.101
65.0	1.025	0.825	0.920	0.879	0.864	0.787	0.665	0.777	0.626
66.0	0.608	0.708	1.100	0.853	0.949	0.705	0.539	0.631	0.666
67.0	0.912	1.057	0.995	0.948	1.124	0.932	0.842	0.835	0.708
68.0	0.911	1.073	1.010	0.780	0.844	0.986	0.526	0.702	0.666
69.0	1.099	0.963	0.964	0.872	0.925	0.865	0.722	0.816	0.993
70.0	0.633	1.306	0.622	0.692	0.633	0.694	0.574	0.549	0.612

0.939
0.710
1.059
0.983
0.967
0.675

f	Ph.A.	s.e.	P	s.e.	C	s.e.
1	0.120	0.017	20.19	3.53	1.05	0.14
2	0.219	0.032	18.20	2.87	1.03	0.08
5	0.452	0.063	17.81	2.58	0.90	0.04
8	0.600	0.058	17.10	2.20	0.84	0.04
10	0.637	0.075	15.70	2.07	0.81	0.05
20	0.939	0.056	14.28	1.47	0.87	0.10
50	1.111	0.062	11.75	1.20	0.63	0.05
80	1.263	0.057	13.27	2.64	0.69	0.04
100	1.410	0.036	18.68	3.33	0.77	0.05

f	Ph.A.	s.e.	R	s.e.	C	s.e.
1						
10	0.930	0.093	26.88	4.27	0.89	0.06

E = -94.27 s.e.= 3.27 pH(i) = 4.91 s.e.= 0.07

E = -52.17 S.E.= 7.76 pH(i)= 5.46 S.E.= 0.10

APW pH(o) 6.0

Cell	d	T	E(mv)	pH(i)
71.0	0.80	22.5	-120	5.16
72.0	0.80	22.0	-120	5.42
73.0	0.70	23.0	-108	5.19
74.0	0.70	23.0	-112	5.25
75.0	0.70	23.0	-115	5.12
76.0	0.80	22.5	-105	4.93
77.0	0.80	21.0	-106	4.70
78.0	0.90	22.0	-110	4.77
79.0	0.80	22.0	-95	5.26
80.0	0.80	23.0	-104	4.77

APW +DNP pH(o) 6.0

E(mv)	pH(i)
-40.0	6.26
-110.0	5.48
-70.0	5.80
-106.0	5.31
-89.0	5.32
-50.0	5.36
-60.0	5.31
-110.0	4.88
-70.0	5.91
-90.0	5.29

A.C. Frequency (Hz)

	1	2	5	8	10	20	50	80	100
71.0	0.134	0.175	0.343	0.583	0.537	0.956	1.226	1.245	1.324
72.0	0.170	0.217	0.392	1.013	1.149	1.208	1.261	1.204	1.442
73.0	0.149	0.191	0.317	0.484	0.620	0.950	1.211	1.108	1.451
74.0	0.152	0.376	0.867	1.108	1.175	1.191	1.281	1.413	1.429
75.0	0.208	0.383	0.751	0.968	1.224	1.163	1.439	1.130	1.246
76.0	0.262	0.652	1.022	1.009	1.160	1.316	1.312	1.465	1.489
77.0	0.516	0.604	0.949	1.065	0.931	1.160	1.243	1.253	1.462
78.0	0.170	0.224	0.660	0.931	1.030	1.249	1.338	1.234	1.176
79.0	0.065	0.158	0.490	0.430	0.796	0.898	1.312	1.380	1.320
80.0	0.236	0.318	0.759	0.793	0.918	1.316	1.104	1.323	1.407

	1	10
Phase Angle (Rad.)		
71.0	0.943	
72.0	0.958	
73.0	0.872	
74.0	1.360	
75.0	1.095	
76.0	1.120	
77.0	0.589	1.172
78.0	0.143	0.885
79.0	0.068	0.816
80.0	0.213	1.068

Membrane Resistance (kΩ.cm²)

71.0	20.0	18.4	17.4	17.6	16.1	16.3	15.8	9.3	10.6
72.0	36.7	32.2	22.3	29.4	30.7	20.3	10.8	6.6	14.8
73.0	16.0	16.0	15.4	15.3	14.3	15.9	11.2	6.7	18.4
74.0	23.1	23.5	19.4	20.1	19.0	11.9	13.2	8.0	6.7
75.0	46.6	39.0	32.4	33.0	38.8	24.2	27.8	8.1	10.3
76.0	55.3	55.4	51.2	38.3	33.0	38.7	18.4	26.9	34.7
77.0	74.4	70.6	63.9	51.9	26.6	28.3	14.6	10.1	24.7
78.0	36.7	27.0	28.3	26.6	25.6	19.4	25.2	7.6	5.3
79.0	14.5	14.2	15.1	14.5	17.3	13.9	18.4	27.3	10.1
80.0	38.8	38.1	36.8	35.8	27.7	38.7	9.8	12.5	14.5

71.0	29.4	
72.0	24.1	
73.0	27.1	
74.0	33.7	
75.0	30.9	
76.0	43.3	
77.0	136.1	56.6
78.0	17.8	15.4
79.0	23.3	21.1
80.0	54.7	34.2

Membrane Capacitance (μf/cm²)

71.0	1.072	0.766	0.656	0.761	0.583	0.689	0.561	0.631	0.595
72.0	0.747	0.544	0.509	1.085	1.155	1.029	0.919	0.788	0.830
73.0	1.489	0.962	0.679	0.685	0.795	0.698	0.756	0.596	0.718
74.0	1.060	1.337	1.931	1.987	2.006	1.679	0.809	1.563	1.671
75.0	0.723	0.823	0.915	0.876	1.134	0.762	0.866	0.521	0.457
76.0	0.771	1.098	1.016	0.824	1.105	0.790	0.653	0.699	0.561
77.0	0.700	0.777	0.774	0.692	0.804	0.645	0.639	0.601	0.592
78.0	0.747	0.625	0.910	1.005	1.034	1.232	0.533	0.747	0.719
79.0	0.716	0.895	1.122	0.628	0.940	0.720	0.603	0.377	0.613
80.0	0.985	0.689	0.820	0.564	0.752	0.790	0.646	0.626	0.666

71.0	0.745					
72.0	0.942					
73.0	0.699					
74.0	2.201					
75.0	1.000					
76.0	0.760					
77.0	0.782	0.667				
78.0	1.292	1.265				
79.0	0.462	0.802				
80.0	0.631	0.845				

f	Ph.A.	s.e.	R	s.e.	C	s.e.
1	0.186	0.023	36.20	6.01	0.90	0.08
2	0.330	0.056	33.62	5.71	0.85	0.07
5	0.662	0.083	30.22	5.18	0.94	0.12
8	0.839	0.079	28.25	3.78	0.91	0.13
10	0.954	0.076	24.91	2.56	1.03	0.12
20	1.141	0.048	22.75	3.06	0.90	0.10
50	1.273	0.028	16.52	1.92	0.70	0.04
80	1.275	0.037	12.31	2.53	0.71	0.10
100	1.375	0.033	15.01	2.83	0.74	0.11

E =-109.50 s.e.= 2.43 pH(i) = 5.06 S.E.= 0.08

f	Ph.A.	s.e.	R	s.e.	C	s.e.
1	0.253	0.116	57.96	27.27	0.79	0.18
10	1.029	0.052	31.58	3.69	0.99	0.15

E = -79.50 S.E.= 8.00 pH(i)= 5.49 S.E.= 0.12

APW pH(o) 6.5

Cell	d	T	E(-v)
91.0	0.75	23.0	-110
92.0	0.80	23.0	-110
93.0	1.00	23.0	-120
94.0	1.00	24.0	-100
95.0	1.00	25.0	-100
96.0	0.80	24.0	-111
97.0	0.80	24.0	-100
98.0	0.80	25.0	-106
99.0	0.80	23.0	-90

APW +DNP pH(o) 6.5

E(mv)
-120.0
-90.0
-89.0
-60.0
-92.0
-72.0
-96.0
-89.0
-70.0

A.C. Frequency (Hz)

Phase Angle (Rad)

	1	2	5	8	10	20	50	80	100
91.0	0.064	0.153	0.316	0.298	0.336	0.491	0.461	0.558	0.395
92.0	0.087	0.276	0.650	0.811	0.863	1.272	1.298	1.030	1.268
93.0	0.153	0.293	0.567	0.977	1.315	1.378	1.503	1.335	1.176
94.0	0.111	0.270	0.586	0.773	0.458	1.102	1.343	1.253	1.148
95.0	0.054	0.118	0.318	0.435	0.507	0.895	1.176	1.236	1.295
96.0	0.080	0.263	0.589	0.955	1.117	1.204	1.172	1.341	1.303
97.0	0.043	0.171	0.481	0.673	0.675	0.970	1.275	1.030	1.398
98.0	0.087	0.233	0.545	0.782	0.889	1.357	1.268	1.312	1.322
99.0	0.088	0.125	0.331	0.436	0.384	0.500	0.572	1.215	1.303

	1	10
91.0	0.124	0.921
92.0	0.465	0.502
93.0	0.355	1.214
94.0	0.184	1.048
95.0	0.074	1.253
96.0	0.072	1.160
97.0	0.179	1.160
98.0	0.050	0.605
99.0	0.082	0.848

Membrane Resistance ($k\Omega.cm^2$)

91.0	39.4	36.6	31.4	17.9	14.6	9.4	3.2	3.1	2.2
92.0	21.8	22.2	21.5	20.8	19.1	24.0	15.7	4.3	5.8
93.0	33.4	29.5	29.8	31.2	57.1	44.3	16.6	24.2	5.3
94.0	42.7	34.2	30.4	29.9	18.2	12.9	21.6	10.1	6.5
95.0	14.5	15.3	13.2	13.2	12.6	12.6	10.6	8.6	11.7
96.0	31.5	27.5	27.2	29.7	31.9	26.3	20.6	26.2	8.3
97.0	14.5	14.0	14.2	13.9	12.9	11.1	12.4	2.1	5.2
98.0	23.7	21.0	19.8	19.5	18.9	32.6	11.6	9.2	8.3
99.0	26.8	25.3	19.9	15.6	15.6	8.6	9.0	14.4	8.3

91.0	45.9	12.7
92.0	51.0	19.4
93.0	77.1	49.9
94.0	55.9	37.8
95.0	19.2	40.3
96.0	39.4	37.7
97.0	28.7	28.3
98.0	31.5	9.7
99.0	26.8	19.0

Membrane Capacitance ($\mu f/cm^2$)

91.0	0.259	0.335	0.331	0.341	0.379	0.451	0.500	0.394	0.300
92.0	0.638	1.013	1.125	1.009	0.974	1.075	0.722	0.775	0.879
93.0	0.735	0.813	0.681	0.945	1.065	0.920	0.698	0.342	0.719
94.0	0.417	0.643	0.696	0.650	0.431	1.221	0.657	0.601	0.543
95.0	0.598	0.711	0.791	0.701	0.703	0.790	0.719	0.664	0.767
96.0	0.405	0.783	0.782	0.948	1.023	0.788	0.366	0.324	0.698
97.0	0.479	0.981	1.171	1.143	0.989	1.045	0.842	1.550	1.660
98.0	0.585	0.893	0.973	1.014	1.035	1.125	0.879	0.816	0.755
99.0	0.525	0.396	0.549	0.594	0.475	0.506	0.229	0.371	0.698

	1	10
91.0	0.434	1.645
92.0	1.566	0.452
93.0	0.766	0.855
94.0	0.529	0.732
95.0	0.612	1.203
96.0	0.292	0.967
97.0	1.000	1.290
98.0	0.253	1.129
99.0	0.491	0.950

f	Ph.A.	s.e.	R	s.e.	C	s.e.
1	0.085	0.011	27.57	3.35	0.52	0.05
2	0.211	0.023	24.86	2.71	0.73	0.08
5	0.487	0.044	23.06	2.31	0.79	0.09
8	0.682	0.080	21.28	2.39	0.82	0.09
10	0.727	0.114	22.10	4.80	0.79	0.10
20	1.019	0.113	20.19	4.13	0.88	0.09
50	1.096	0.112	15.48	1.94	0.62	0.07
80	1.145	0.083	11.36	2.91	0.65	0.13
100	1.189	0.103	6.85	0.89	0.78	0.12

E =-105.22 s.e.= 2.91

f	Ph.A.	s.e.	R	s.e.	C	s.e.
1	0.176	0.048	41.73	5.97	0.66	0.14
10	0.968	0.090	28.32	4.63	1.02	0.11

E = -86.44 s.e.= 5.84

APW pH(o) 7.0

Cell	c	T	E(mv)	pH(i)
A1.0	0.80	22.0	-100	4.85
A2.0	0.90	21.0	-101	5.11
B3.0	0.90	21.0	-97	4.80
B4.0	0.90	21.0	-90	5.22
B5.0	1.00	21.0	-102	5.00
B6.0	1.00	21.0	-110	4.95
B7.0	0.80	21.0	-90	4.77
B8.0	0.80	24.0	-95	4.49
B9.0	0.90	24.0	-105	5.06
90.0	0.80	23.0	-101	5.17

APW +DNP pH(o) 7.0

E(mv)	pH(i)
-76.0	5.21
-88.0	5.36
-86.0	4.96
-90.0	5.32
-90.0	5.21
-90.0	5.00
-86.0	4.83
-40.0	5.95
-115.0	5.26
-100.0	5.22

A.C. Frequency (Hz)

	1	2	5	8	10	20	50	80	100
Phase Angle (Rad)									
A1.0	0.256	0.439	0.447	0.488	0.631	0.866	1.065	1.160	1.466
A2.0	0.435	0.504	0.910	0.890	1.086	1.210	1.257	1.405	1.516
B3.0	0.046	0.064	0.133	0.181	0.221	0.290	0.350	0.391	0.629
B4.0	0.071	0.084	0.227	0.269	0.306	0.288	0.308	0.424	0.365
B5.0	0.182	0.468	0.349	0.351	1.086	1.030	1.086	1.338	1.451
B6.0	0.037	0.449	0.611	0.996	1.048	1.221	1.293	1.341	1.415
B7.0	0.086	0.412	0.784	0.866	1.208	1.204	1.054	1.413	1.447
B8.0	0.221	0.281	0.361	0.310	0.198	0.279	0.453	0.948	1.016
B9.0	0.021	0.073	0.159	0.231	0.229	0.319	0.372	0.424	0.384
90.0	0.016	0.067	0.117	0.177	0.192	0.253	0.395	0.690	0.623
Membrane Resistance (kΩ.cm²)									
A1.0	26.1	20.8	20.6	14.4	7.6	5.1	5.2	4.7	16.6
A2.0	65.8	52.0	48.6	32.4	35.0	27.6	20.9	27.5	37.3
B3.0	20.4	19.7	17.9	16.0	13.2	10.3	5.9	3.6	3.3
B4.0	26.8	25.2	20.8	17.8	15.3	9.5	4.9	2.9	2.4
B5.0	57.5	56.9	31.8	21.9	35.0	17.1	8.8	12.6	18.4
B6.0	52.1	50.6	45.6	41.3	37.6	30.2	14.9	13.1	16.7
B7.0	34.7	34.3	35.5	31.5	40.7	26.3	7.3	16.0	16.5
B8.0	66.0	58.9	28.6	15.7	10.6	4.7	2.8	4.3	2.4
B9.0	22.6	21.7	19.1	16.9	14.2	9.6	5.6	2.9	2.7
90.0	23.9	18.9	15.2	13.1	13.4	13.0	8.9	4.5	2.3
Membrane Capacitance (μf/cm²)									
A1.0	1.652	1.794	0.742	0.733	1.532	1.837	1.108	0.967	0.916
A2.0	1.122	0.443	0.842	0.757	0.862	0.764	0.470	0.431	0.772
B3.0	0.360	0.259	0.238	0.228	0.271	0.230	0.198	0.230	0.350
B4.0	0.421	0.267	0.353	0.309	0.328	0.248	0.205	0.307	0.258
B5.0	0.506	0.742	0.365	0.332	0.862	0.775	0.689	0.866	0.718
B6.0	0.298	0.759	0.734	0.743	0.752	0.721	0.749	0.649	0.606
B7.0	0.398	1.013	0.894	0.742	1.029	0.788	0.766	0.781	0.773
B8.0	0.542	0.391	0.421	0.407	0.302	0.482	0.554	0.643	1.076
B9.0	0.147	0.266	0.267	0.276	0.262	0.274	0.223	0.307	0.237
90.0	0.105	0.281	0.246	0.271	0.230	0.158	0.190	0.366	0.492

f	Ph.A.	s.e.	R	s.e.	C	s.e.
1	0.144	0.042	39.60	5.90	0.56	0.15
2	0.286	0.061	35.91	5.32	0.66	0.15
5	0.430	0.095	28.37	3.74	0.51	0.08
8	0.476	0.101	22.11	3.04	0.48	0.07
10	0.620	0.139	22.29	4.13	0.64	0.14
20	0.696	0.141	15.34	3.00	0.63	0.16
50	0.763	0.132	8.50	1.72	0.51	0.10
80	0.953	0.137	9.21	2.55	0.53	0.08
100	1.031	0.153	11.86	3.63	0.62	0.09

E = -99.10 s.e.= 1.99 pH(i) = 4.94 s.e.= 0.07

f	Ph.A.	s.e.	R	s.e.	C	s.e.
1	0.171	0.044	55.05	7.80	0.46	0.08
10	0.608	0.136	25.71	3.94	0.50	0.09

E = -86.10 s.e.= 6.06 pH(i)= 5.23 s.e.= 0.10